

HEXANE: Architecting Manned Space Exploration Missions beyond
Low-Earth Orbit

by

Alexander August Rudat

B.S. Mechanical Engineering
Georgia Institute of Technology, 2011

SUBMITTED TO THE DEPARTMENT OF AERONAUTICS AND ASTRONAUTICS
IN PARTIAL FULFILLMENT OF THE REQUIREMENTS FOR THE DEGREE OF

MASTER OF SCIENCE IN AERONAUTICS AND ASTRONAUTICS
AT THE
MASSACHUSETTS INSTITUTE OF TECHNOLOGY

JUNE 2013

© 2013 Massachusetts Institute of Technology. All Rights Reserved.

Signature of Author: _____
Department of Aeronautics and Astronautics
May 23, 2013

Certified by: _____
Prof. Edward F. Crawley
Ford Professor of Aeronautics and Astronautics and Engineering Systems
Thesis Supervisor

Accepted by: _____
Prof. Eytan H. Modiano
Professor of Aeronautics and Astronautics
Chair, Graduate Program Committee

[page intentionally left blank]



Architecting Manned Space Exploration Missions beyond Low-Earth Orbit

by

Alexander August Rudat

Submitted to the Department of Aeronautics and Astronautics
on May 23, 2013 in Partial Fulfillment of the Requirements for the
Degree of Master of Science in Aeronautics and Astronautics

Abstract

With the end of the Space Shuttle Program and the cancellation of the Constellation Program, NASA's long-term designs for manned spaceflight beyond Earth orbit remain indefinite. Although progress has been made in plans for operations on orbit, the capabilities gap for manned spaceflight beyond orbit has grown. Gaining an understanding of the trade-offs inherent in future system architectures for manned missions aids decision support for long-term planning of the spaceflight infrastructure. Assessments of such manned missions are particularly difficult due to the quantity of applicable technologies and potential component, sub-system, and system-level elements. Complex interactions between these technologies and elements lead to the need for high-fidelity analysis, requiring significant resource investments. NASA has typically turned to expert opinion and detailed point design studies to assess possible mission architectures, but recent developments in the field of systems architecture and computer science allow for the assessment of these architectures through system modeling techniques.

This thesis presents a tool for the enumeration and analysis of system architectures for future manned missions to the Moon, Mars, and Near-Earth Asteroids (NEAs). An abstracted, solution-neutral formulation of the system allows for the analysis of the in-space transportation infrastructure portion of potential mission architectures through a unique functional decomposition and use of a decision formulation. Cost-based metrics are derived for the evaluation of architectures, representing both mass-based operations costs as well as development and procurement costs. The full combinatorial enumeration of the architecture tradespace generates a

large data set on which to perform analysis. Rigorous techniques are used to derive decision influence information from this data. In-depth evaluation of Mars conjunction-class missions, with an emphasis on the assessment of highly influential architectural decisions, is presented, along with a more superficial treatment of lunar and NEA architectures.

Mission architectures to these destinations are likely to require many new technologies and large-scale mission elements. In order to build confidence in these technologies and elements, precursor demonstration sub-missions (missions performed prior to the final surface mission) are often required. A tool is presented to leverage the results from the mission enumeration and evaluation model, exploring the tradespace of demonstration sub-mission sequences. In particular, this tool analyzes the grouping of technologies and mission elements to demonstrate. It also examines the use of Lagrange points as destinations for precursor sub-missions. Results from this tool are presented for lunar and low-energy NEA missions using metrics representing both individual sub-mission properties as well as sequence-level properties.

Finally, a framework is presented for the construction of architecture-level complex system models. The development of this framework is based in knowledge gained from building the previously described tools as well as an academic background in system architecting. The framework directs professionals and academics in the process of designing complex system models with the intent of reducing gratuitous and modeling-induced complexity while retaining essential complexity. A brief case study is used to demonstrate the benefits gained from the use of the framework in comparison to unguided model creation.

Thesis Supervisor: Edward F. Crawley

Title: Ford Professor of Engineering

[page intentionally left blank]

Acknowledgements

To my many friends and colleagues, both at M.I.T. and elsewhere, you have my everlasting thanks for your support both during the process of working toward my Master's degree and during the years before it. I could not have come this far without you. To my close friend and roommate, Tamas, thank you for putting up with my late night rants, both good and bad. You, Vishnu, Michael, and my other supporters in the M.I.T. community have kept my days lively and my love of space strong.

To my colleagues, both here and far away, thank you for your understanding and encouragement in coming from a mechanical engineering background with little knowledge of spacecraft to this point. Jon and Alessandro, HEXANE would never have been produced without your help. Dani, my thesis would certainly have never been completed without your tireless hours of editing and very helpful feedback. You have always been an excellent resource. And I also thank your wife and my friend, Ana, who put up with you editing my thesis and also gave me support in this process. Morgan, Peter, Francisco, Marc, Wen, and Andreas, you have all been great friends and supporters through my time here, and I have always been impressed with all of your passions and capabilities. And, of course, to my friends across the office, Narek, Sydney, Koki, Andrew, Margaret, Ioana, and Amanda, thank you for putting up with our conversations over on our side and keeping our enthusiasm strong.

Bruce, this thesis and this degree would never have been completed without your support. Your insights have created much of this research, and for that I thank you.

To my advisor, Ed Crawley, your enthusiasm has never waned as your time sometimes did. It has been an honor and a pleasure.

And finally, to my family, my parents and my sisters as well as my relatives and relatives in-law, without your wisdom and your guidance, your support in all things, I would not be at M.I.T., nor would I have such a fruitful life. As always, you have my thanks and my love.

And thank you, space, because you're awesome.

Table of Contents

ACKNOWLEDGEMENTS.....	6
LIST OF FIGURES.....	11
LIST OF TABLES.....	14
ACRONYMS AND ABBREVIATIONS.....	16
1. INTRODUCTION.....	19
1.1 MOTIVATION.....	19
1.1.1 <i>Current State of Manned Space Exploration</i>	19
1.1.2 <i>Infrastructure Development and Long-Term Planning</i>	20
1.2 THE ROLE OF SYSTEM ARCHITECTURE AND ARCHITECTING.....	21
1.3 DECISION ANALYSIS IN SYSTEM ARCHITECTURE.....	22
1.4 EXHAUSTIVE TRADESPACE EXPLORATION.....	23
1.5 PRIOR MANNED SPACEFLIGHT MODELS.....	23
1.5.1 <i>Hofstetter Manned Spaceflight Tradespace Model</i>	23
1.5.2 <i>Simmons Manned Spaceflight Tradespace Model</i>	25
1.5.3 <i>Design Reference Architecture 5.0</i>	28
1.5.4 <i>Austere</i>	34
1.5.5 <i>Mars-Oz</i>	36
1.5.6 <i>Additional Point Design Studies</i>	38
1.5.7 <i>The Design of Complex System Models</i>	38
1.6 OBJECTIVES.....	39
1.7 THESIS OVERVIEW.....	40
2. HEXANE: HUMAN EXPLORATION ARCHITECTURE NETWORK EVALUATOR.....	42
2.1 SCOPING AND PROBLEM STATEMENT.....	42
2.1.1 <i>Infrastructure Downscoping</i>	43
2.1.2 <i>Destination Selection</i>	44
2.1.3 <i>Sortie-Like Mission Design</i>	46
2.1.4 <i>Abstraction</i>	47
2.2 HABITATION AND TRANSPORTATION FUNCTIONAL DECOMPOSITION.....	47
2.2.1 <i>Primal Functions</i>	49
2.2.2 <i>Temporal- & Requirement-based Sub-Functions</i>	50
2.2.3 <i>Representation in an Exploration Mission Context</i>	53
2.2.4 <i>Invariant Functions and Set Partitioning</i>	54
2.3 ARCHITECTURE-LEVEL TECHNOLOGIES.....	56
2.4 FORMULATION AS AN ASSIGNMENT PROBLEM.....	57
2.5 PARAMETRICS.....	59
2.5.1 <i>The Need for Parametrics</i>	59
2.5.2 <i>Assumptions</i>	61
2.5.3 <i>Metrics</i>	63
2.6 MODEL STRUCTURE.....	65
2.7 VALIDATION.....	68
2.7.1 <i>Mars Validation</i>	69

2.7.2	<i>Lunar Validation</i>	72
2.7.3	<i>NEA Validation</i>	73
2.8	CHAPTER SUMMARY	73
3.	PRIMARY FINDINGS: MARS	74
3.1	ANALYSIS GOALS AND SUMMARY.....	74
3.2	CONSTRAINED TRADESPACE ANALYSIS	76
3.2.1	<i>Mass Feasibility Constraint</i>	76
3.2.2	<i>Orion Multi-Purpose Crew Vehicle Constraint</i>	77
3.2.3	<i>General Tradespace Characteristics</i>	80
3.3	OPTIMAL ARCHITECTURES	85
3.3.1	<i>Minimum IMLEO Architecture</i>	86
3.3.2	<i>Minimum LCC Architecture</i>	89
3.3.3	<i>All Non-Dominated Architectures</i>	93
3.4	ARCHITECTURAL DECISIONS AND COUPLING.....	96
3.4.1	<i>IMLEO-Minimal Decision “Switches”</i>	97
3.4.2	<i>Fixed Architecture Decision Switches</i>	100
3.4.3	<i>Technology Influence Measure</i>	103
3.4.4	<i>Cryogenic Propellant Usage</i>	105
3.4.5	<i>Boil-Off Control</i>	107
3.4.6	<i>Nuclear Thermal Rockets</i>	109
3.4.7	<i>Pre-Deployment using Solar-Electric Propulsion</i>	110
3.4.8	<i>Ablative Aerocapture</i>	112
3.4.9	<i>In-Space LOX/LCH₄ Stages</i>	114
3.4.10	<i>Capsules and the MPCV</i>	115
3.4.11	<i>Monolithic and Semi-Monolithic Habitats</i>	116
3.4.12	<i>Decision Coupling</i>	118
3.5	CONCLUSIONS AND RECOMMENDATIONS.....	122
3.6	A BRIEF DISCUSSION OF LUNAR AND NEA RESULTS.....	123
3.6.1	<i>Lunar Architecture Results</i>	123
3.6.2	<i>Low-Energy NEA Results</i>	124
3.6.3	<i>High-Energy NEA Results</i>	125
3.6.4	<i>Combined Results Analysis</i>	125
3.7	SUMMARY.....	127
4.	STEPPING STONES: PROGRESSION TOWARD LOW-ENERGY DESTINATIONS	128
4.1	MOTIVATION AND PROBLEM STATEMENT	128
4.2	LOW-E AS A BACKEND TO HEXANE.....	131
4.2.1	<i>Demonstrable Technologies & Capabilities</i>	131
4.2.2	<i>Demonstration Destinations</i>	136
4.2.3	<i>Assumptions</i>	136
4.2.4	<i>Metrics</i>	137
4.3	RESULTS AND FINDINGS.....	138
4.3.1	<i>Lunar Results</i>	139
4.3.2	<i>Low-Energy NEAs</i>	149
4.4	CONCLUSIONS AND RECOMMENDATIONS.....	154
4.5	CHAPTER SUMMARY	155

5.	A FRAMEWORK FOR THE MODELING OF COMPLEX SYSTEMS	156
5.1	INTRODUCTION	156
5.1.1	<i>Motivation: Modeling of Complex Systems as a General Challenge</i>	<i>156</i>
5.1.2	<i>Lessons Learned from HEXANE</i>	<i>157</i>
5.1.3	<i>Gratuitous & Modeling-Induced Complexity vs. Essential Complexity</i>	<i>158</i>
5.1.4	<i>Objectives</i>	<i>159</i>
5.2	IDEOLOGICAL VS. PHYSICAL MODELS AND THE FUNNEL FRAMEWORK	161
5.2.1	<i>Ideological Model</i>	<i>162</i>
5.2.2	<i>Physical Model</i>	<i>165</i>
5.2.3	<i>Funnel Framework</i>	<i>166</i>
5.3	THE EXPANDED FRAMEWORK	167
5.3.1	<i>Classification of Coupling Relationships</i>	<i>168</i>
5.3.2	<i>Separability</i>	<i>169</i>
5.3.3	<i>Reducible vs. Irreducible Coupling</i>	<i>170</i>
5.3.4	<i>Parallel vs. Serial Sub-problems</i>	<i>172</i>
5.3.5	<i>The Role of Cognitive Psychology</i>	<i>175</i>
5.3.6	<i>Expanded Ideological Model</i>	<i>175</i>
5.3.7	<i>Expanded Physical Model</i>	<i>178</i>
5.3.8	<i>Integrated Expanded Models</i>	<i>180</i>
5.3.9	<i>Topics for Further Consideration</i>	<i>181</i>
5.4	COMPARISON WITH PREVIOUS CONCEPTS	181
5.4.1	<i>Simon's Four Steps to Decision Making</i>	<i>182</i>
5.4.2	<i>Simmons' Four Steps</i>	<i>183</i>
5.5	ASSUMPTIONS AND LIMITATIONS	186
5.6	CASE STUDY IN BRIEF: HOFSTETTER MANNED SPACEFLIGHT MODEL	187
5.7	FUTURE WORK	190
5.8	CHAPTER SUMMARY	192
6.	CONCLUSION	194
6.1	THESIS SUMMARY	194
6.2	PRIMARY CONTRIBUTIONS	195
6.2.1	<i>Methodology and Tool Contributions</i>	<i>195</i>
6.2.2	<i>Analysis Findings</i>	<i>196</i>
6.3	FUTURE WORK	197
6.3.1	<i>HEXANE Refinement</i>	<i>198</i>
6.3.2	<i>Low-E Refinement</i>	<i>201</i>
6.3.3	<i>Funnel Framework Development</i>	<i>201</i>
	BIBLIOGRAPHY	203
	APPENDIX A: ADDITIONAL HEXANE INFORMATION	212
A-1:	PARAMETER DATABASE	212
A-2:	EXPANDED FUNCTIONAL BLOCK DIAGRAM	214
A-3:	ASSUMPTIONS LIST	215
A-4:	ΔV MATRICES	217
A-5:	TOF MATRIX	219
A-6:	LOW-THRUST ΔV ESTIMATION METHOD	220

A-7:	LOW-THRUST ΔV MATRIX.....	222
A-8:	LOW-THRUST TOF MATRIX.....	223
A-9:	MATRIX METHOD FOR SIMULTANEOUS PROPULSION ELEMENT SIZING	224
A-10:	ALTERNATIVE ITERATIVE SOLVER FOR NESTED PROPULSION ELEMENTS.....	226
A-11:	CHEMICAL PROPULSION ELEMENT SIZING METHOD	227
A-12:	SEP ELEMENT SIZING METHOD.....	228
A-13:	PROPELLANT DATA.....	230
A-14:	AEROCAPTURE SHIELD SIZING AND EDL RESPONSE SURFACE	230
A-15:	ISRU	234
A-16:	HABITAT SIZING PARAMETRICS.....	235
A-17:	LOGISTICS SIZING PARAMETRIC	237
APPENDIX B: LUNAR AND NEA HEXANE RESULTS.....		239
B-1:	LUNAR RESULTS.....	239
B-2:	LOW-ENERGY NEA RESULTS.....	245
B-3:	HIGH ENERGY NEA RESULTS.....	250

List of Figures

FIGURE 1: MANNED SPACE EXPLORATION FLEXIBLE PATH.....	20
FIGURE 2: HOFSTETTER TRADESPACE MODEL MORPHOLOGICAL MATRIX	24
FIGURE 3: SIMMONS APOLLO PROGRAM MORPHOLOGICAL MATRIX	26
FIGURE 4: SIMMONS APOLLO PROGRAM MODEL OPN.....	28
FIGURE 5: DRA 5.0 MISSION PHASING	29
FIGURE 6: DRA 5.0 BAT CHART	30
FIGURE 7: DRA 5.0 SURFACE HABITAT OPTION SUMMARY	33
FIGURE 8: AUSTERE AND DRA 5.0 DECISION TRADE TREE	35
FIGURE 9: MARS-OZ SEMI-DIRECT MISSION MODE DESCRIPTION	36
FIGURE 10: MANNED EXPLORATION MISSION SEGMENTS	43
FIGURE 11: ISECG MULTIPLE PATHS TO MARS	44
FIGURE 12: HEXANE DESTINATIONS AND PATHWAYS	46
FIGURE 13: ELEVATOR SUB-SYSTEM DECOMPOSITION	48
FIGURE 14: ISS ECLSS DECOMPOSITION AND FLOW DIAGRAM.....	51
FIGURE 15: SUB-FUNCTION DECOMPOSITION OF IN-SPACE INFRASTRUCTURE PRIMAL FUNCTIONS.....	52
FIGURE 16: HABITATION SUB-FUNCTIONS IN MARS CONJUNCTION-CLASS MISSION CONTEXT.....	54
FIGURE 17: TRANSPORTATION SUB-FUNCTIONS IN MARS CONJUNCTION-CLASS MISSION CONTEXT.....	54
FIGURE 18: LUNAR ORBIT RENDEZVOUS SET PARTITIONING EXAMPLE	55
FIGURE 19: HEXANE ASSIGNMENT PROBLEM MORPHOLOGICAL MATRIX	58
FIGURE 20: HABITAT PARAMETRIC BETWEEN TOTAL MASS AND TOTAL VOLUME.....	60
FIGURE 21: NASA HABITABLE VOLUME WORKSHOP PARAMETRIC.....	61
FIGURE 22: HEXANE KEY STEPS	66
FIGURE 23: HEXANE FUNCTIONAL BLOCK DIAGRAM	67
FIGURE 24: NESTED PROPULSION EXAMPLE.....	68
FIGURE 25: VALIDATION WITH DRA 5.0.....	71
FIGURE 26: APOLLO VALIDATION.....	72
FIGURE 27: ORION MPCV QUICK FACT SHEET	78
FIGURE 28: MPCV PARAMETRIC TRADESPACES (8.6MT, PARAMETRIC, AND 15MT, RESPECTIVELY)	79
FIGURE 29: CONSTRAINED MARS TRADESPACE	80
FIGURE 30: MARS ARCHITECTURE UNCONSTRAINED TRADESPACE.....	81
FIGURE 31: EXAMPLE MARS TRADESPACE FEATURES	82
FIGURE 32: CONSTRAINED TRADESPACE FEATURE DRIVERS.....	83
FIGURE 33: MARS CONSTRAINED TRADESPACE PARETO FRONTIER	86
FIGURE 34: MARS MINIMUM IMLEO BAT CHART	87
FIGURE 35: MARS MINIMUM IMLEO ARCHITECTURE MASS BAR CHART	88
FIGURE 36: MARS MINIMUM IMLEO ARCHITECTURE MASS PIE CHART	88
FIGURE 37: MARS MINIMUM LCC ARCHITECTURE BAT CHART	90
FIGURE 38: MARS MINIMUM LCC ARCHITECTURE MASS BAR CHART	91
FIGURE 39: MARS MINIMUM LCC ARCHITECTURE MASS PIE CHART.....	92
FIGURE 40: MARS NON-DOMINATED ARCHITECTURE TECHNOLOGY STOPLIGHT CHART	94
FIGURE 41: MARS TRADESPACE MPCV CAPSULE PARETO FRONTIER COVERAGE	94
FIGURE 42: MARS TRADESPACE MONOLITHIC AND SEMI-MONOLITHIC HABITAT PARETO FRONTIER COVERAGE.....	95
FIGURE 43: MARS MINIMUM IMLEO DECISION SWITCH ARCHITECTURES.....	98

FIGURE 44: MARS FIXED ARCHITECTURE DECISION SWITCH BOX PLOTS	101
FIGURE 45: MARS DECISION TIM BAR CHART.....	103
FIGURE 46: MARS CRYOGENIC PROPELLANT IMLEO INFLUENCE BOX PLOT	106
FIGURE 47: MARS CRYOGENIC PROPELLANT TIM BAR CHART.....	106
FIGURE 48: MARS BOIL-OFF CONTROL TRADESPACE COVERAGE	108
FIGURE 49: MARS NTR OVERLAP WITH FULL TRADESPACE.....	109
FIGURE 50: MARS SEP PRE-DEPLOYMENT TRADESPACE COVERAGE.....	111
FIGURE 51: MARS SEP PRE-DEPLOYMENT TRADESPACE COMPLEMENT.....	112
FIGURE 52: MARS AEROCAPTURE TRADESPACE COVERAGE	113
FIGURE 53: MARS IN-SPACE CH ₄ STAGE TRADESPACE COVERAGE	114
FIGURE 54: MARS CAPSULE OVERLAP WITH FULL TRADESPACE	116
FIGURE 55: MARS MONOLITHIC AND SEMI-MONOLITHIC HABITAT OVERLAP WITH THE FULL TRADESPACE	118
FIGURE 56: MARS DECISION TCIM.....	120
FIGURE 57: LONG-TERM MISSION STRATEGY BREAKDOWN	129
FIGURE 58: SEV CHARACTERISTICS FROM NASA FACTS SHEET.....	133
FIGURE 59: LUNAR MINIMUM IMLEO MISSION BAT CHART	140
FIGURE 60: LUNAR CUMULATIVE IMLEO VS. CUMULATIVE LCC	142
FIGURE 61: LUNAR PEAK IMLEO VS. PEAK LCC	143
FIGURE 62: LUNAR PEAK IMLEO VS. CUMULATIVE LCC	145
FIGURE 63: LUNAR CUMULATIVE IMLEO VS. PEAK LCC	146
FIGURE 64: LUNAR CUMULATIVE IMLEO VS. PEAK LCC WITH PARETO FRONTIER	147
FIGURE 65: LOW-ENERGY NEA MINIMUM IMLEO MISSION BAT CHART.....	150
FIGURE 66: LOW-ENERGY NEA PEAK IMLEO VS. CUMULATIVE LCC.....	151
FIGURE 67: LOW-ENERGY NEA CUMULATIVE IMLEO VS. PEAK LCC.....	152
FIGURE 68: LOW-ENERGY NEA CUMULATIVE IMLEO VS. PEAK LCC WITH PARETO FRONTIER	153
FIGURE 69: IDEOLOGICAL MODEL FUNDAMENTAL STEPS	162
FIGURE 70: SYSTEMS ARCHITECTING FLOW	164
FIGURE 71: PHYSICAL MODEL FUNDAMENTAL STEPS	165
FIGURE 72: FUNNEL FRAMEWORK	166
FIGURE 73: REDUCIBLE COUPLING EXAMPLE.....	171
FIGURE 74: SUB-PROBLEM CLASSIFICATION	174
FIGURE 75: EXPANDED IDEOLOGICAL MODEL BUILDING PROCESS	176
FIGURE 76: EXPANDED PHYSICAL MODEL BUILDING PROCESS.....	179
FIGURE 77: INTEGRATED EXPANDED IDEOLOGICAL AND PHYSICAL MODELS.....	180
FIGURE 78: COMPARISON BETWEEN IDEOLOGICAL MODEL BUILDING PROCESS AND SIMON’S FOUR STAGES TO DECISION-MAKING.....	182
FIGURE 79: COMPARISON BETWEEN THE IDEOLOGICAL MODEL BUILDING PROCESS AND SIMMONS’ FOUR STEPS TO MODEL BUILDING.....	184
FIGURE 80: HOFSTETTER MANNED SPACEFLIGHT MODEL MORPHOLOGICAL MATRIX.....	188
FIGURE 81: ESCAPE ΔV PARAMETRIC FOR LOW-THRUST.....	221
FIGURE 82: PROPULSION ITERATIVE SOLVER	226
FIGURE 83: HIDH SITTING VOLUME	236
FIGURE 84: HIDH SUIT DONNING VOLUME	236
FIGURE 85: LUNAR TRADESPACE	239
FIGURE 86: LUNAR MINIMUM IMLEO BAT CHART	240
FIGURE 87: LUNAR MINIMUM LCC BAT CHART	240

FIGURE 88: LUNAR FEATURE TIM CHART	241
FIGURE 89: LUNAR CAPSULE TRADESPACE COVERAGE	242
FIGURE 90: LUNAR SEMI-MONOLITHIC HABITAT COVERAGE	242
FIGURE 91: LUNAR NTR COVERAGE.....	243
FIGURE 92: LUNAR SEP PRE-DEPLOYMENT COVERAGE COMPLEMENT	243
FIGURE 93: LUNAR FEATURE TCIM	244
FIGURE 94: LOW-ENERGY NEA TRADESPACE	245
FIGURE 95: LOW-ENERGY NEA MINIMUM IMLEO BAT CHART	246
FIGURE 96: LOW-ENERGY NEA MINIMUM LCC BAT CHART.....	246
FIGURE 97: LOW-ENERGY NEA FEATURE SWITCH BOX PLOTS.....	247
FIGURE 98: LOW-ENERGY NEA FEATURE TIM CHART	247
FIGURE 99: LOW-ENERGY NEA CAPSULE TRADESPACE COVERAGE	248
FIGURE 100: LOW-ENERGY NEA SEMI-MONOLITHIC HABITAT COVERAGE	248
FIGURE 101: LOW-ENERGY NEA TCIM	249
FIGURE 102: HIGH-ENERGY NEA TRADESPACE	250
FIGURE 103: HIGH-ENERGY NEA MINIMUM IMLEO BAT CHART	251
FIGURE 104: HIGH-ENERGY NEA MINIMUM LCC BAT CHART	251
FIGURE 105: HIGH-ENERGY NEA FEATURE SWITCH BOX PLOTS	252
FIGURE 106: HIGH-ENERGY NEA FEATURE TIM CHART	252
FIGURE 107: HIGH-ENERGY NEA CAPSULE COVERAGE.....	253
FIGURE 108: HIGH-ENERGY NEA SEMI-MONOLITHIC HABITAT COVERAGE.....	253
FIGURE 109: HIGH-ENERGY NEA NTR COVERAGE.....	254
FIGURE 110: HIGH-ENERGY NEA SEP PRE-DEPLOYMENT COVERAGE.....	254
FIGURE 111: HIGH-ENERGY NEA FEATURE TCIM	255

List of Tables

TABLE 1: SIMMONS APOLLO PROGRAM MODEL LOGICAL CONSTRAINTS	26
TABLE 2: SIMMONS APOLLO PROGRAM MODEL LOGICAL CONSTRAINT TABLES.....	27
TABLE 3: DRA 5.0 NTR MISSION VEHICLE SUMMARY	31
TABLE 4: DRA 5.0 NTR MISSION VEHICLE ASSEMBLY TIMELINE AND ETO DELIVERY MANIFEST.....	31
TABLE 5: DRA 5.0 CHEMICAL MISSION VEHICLE SUMMARY	32
TABLE 6: DRA 5.0 CHEMICAL MISSION VEHICLE ASSEMBLY TIMELINE AND ETO DELIVERY MANIFEST..	32
TABLE 7: AUSTERE ELEMENT MASSES BREAKDOWN	35
TABLE 8: MARS-OZ VEHICLE DESCRIPTIONS	37
TABLE 9: MARS-OZ MISSION MASS BREAKDOWN	38
TABLE 10: HIGH AND LOW ENERGY DESTINATION ΔV COMPARISON.....	45
TABLE 11: HABITAT PARAMETRIC DATA	60
TABLE 12: COST COEFFICIENT INFORMATION.....	65
TABLE 13: MARS VALIDATION STUDY MODEL ADJUSTMENT EFFECTS ON MASS	70
TABLE 14: MARS VALIDATION STUDY MODEL ADJUSTMENTS ON MASS AS A PERCENT OF THE DRA 5.0 BASELINE	71
TABLE 15: CAPSULE MASS SIZING PARAMETRIC SENSITIVITY TO METHODS.....	78
TABLE 16: MARS NON-DOMINATED ARCHITECTURE METRICS AND PRIMARY TECHNOLOGY PRESENCE ...	93
TABLE 17: MARS MINIMUM IMLEO DECISION SWITCH RESULTS.....	98
TABLE 18: MARS FIXED ARCHITECTURE DECISION SWITCH IMPACT MEAN VALUES	101
TABLE 19: DECISION TIM VALUES.....	104
TABLE 20: MARS DECISIONS - GENERAL ANALYSIS SUMMARY	105
TABLE 21: MARS CRYOGENIC PROPELLANT ANALYSIS SUMMARY	107
TABLE 22: MARS BOIL-OFF CONTROL ANALYSIS SUMMARY.....	108
TABLE 23: MARS NTR ANALYSIS SUMMARY	110
TABLE 24: MARS SEP PRE-DEPLOYMENT ANALYSIS SUMMARY	112
TABLE 25: MARS AEROCAPTURE ANALYSIS SUMMARY	113
TABLE 26: MARS IN-SPACE CH ₄ ANALYSIS SUMMARY.....	115
TABLE 27: MARS MPCV ANALYSIS SUMMARY	115
TABLE 28: MARS MONOLITHIC AND SEMI-MONOLITHIC HABITAT ANALYSIS SUMMARY	117
TABLE 29: TCIE VARIABLES	119
TABLE 30: DECISION SUMMARY AND RECOMMENDATIONS	122
TABLE 31: DEMONSTRATION MISSION SET EXAMPLE	131
TABLE 32: HABITAT AND PROPULSION ELEMENT HIERARCHY	132
TABLE 33: LUNAR FINAL SURFACE MISSION PROPERTIES.....	139
TABLE 34: LUNAR CUMULATIVE IMLEO VS. CUMULATIVE LCC PROXY TRADESPACE EXAMPLES	141
TABLE 35: LUNAR PEAK IMLEO VS. CUMULATIVE LCC TRADESPACE EXAMPLES	144
TABLE 36: NON-DOMINATED LUNAR SUB-MISSION SEQUENCE PROPERTIES FOR THE PEAK IMLEO VS. CUMULATIVE LCC TRADESPACE.....	148
TABLE 37: LOW-ENERGY NEA BASE MISSION PROPERTIES	149
TABLE 38: LOW-ENERGY NEA PEAK IMLEO VS. CUMULATIVE LCC TRADESPACE EXAMPLES	151
TABLE 39: NON-DOMINATED LOW-ENERGY NEA SUB-MISSION ARCHITECTURE SEQUENCE PROPERTIES	153
TABLE 40: PROPELLANT DATA	230
TABLE 41: SRP RESPONSE SURFACE WITH NO PRE-ENTRY JETTISON	233

TABLE 42: MARS SURFACE HABITAT REGRESSION DATA.....	237
TABLE 43: LUNAR NON-DOMINATED ARCHITECTURE PROPERTIES	239
TABLE 44: LOW-ENERGY NEA NON-DOMINATED ARCHITECTURE PROPERTIES	245
TABLE 45: HIGH-ENERGY NEA NON-DOMINATED ARCHITECTURE FEATURES.....	250

Acronyms and Abbreviations

ADG	Architecture Decision Graph
AOS	Algebra of Systems
CER	Cost Estimating Relationship
CM	Command Module
ConOps	Concept of Operations
DAV	Descent and Ascent Vehicle
DOE	Design of Experiments
DRA	Design Reference Architecture
DRM	Design Reference Mission
DSH	Deep Space Habitat
EDL	Entry, Descent, and Landing
EDS	Earth Departure Stage
EELV	Evolved Expendable Launch Vehicle
EM	Earth-Moon
EOR	Earth Orbit Rendezvous
ESAS	Exploration Systems Architecture Study
EVA	Extravehicular Activity
FOM	Figure of Merit
GA	Genetic Algorithm
HAT	Human Spaceflight Architecture Team
HEO	Earth Highly Elliptical Orbit
HEOMD	NASA Human Exploration and Operations Mission Directorate
HIDH	NASA Human Integration Design Handbook (NASA-STD-3000)
HSF	Human Spaceflight
IMLEO	Initial Mass in Low-Earth Orbit
INCOSE	International Council on Systems Engineering
ISECG	International Space Exploration Coordination Group
ISRU	<i>In-Situ</i> Resource Utilization
ISS	International Space Station
JPL	NASA Jet Propulsion Laboratory
JSC	NASA Johnson Space Center
KSC	NASA Kennedy Space Center
LCC	Lifecycle Cost
LEM	Lunar Excursion Module

LLO	Low Lunar Orbit
LMO	Low Mars Orbit
LOI	Lunar Orbit Insertion
LOR	Lunar Orbit Rendezvous
LOX/LCH ₄	Liquid Oxygen and Liquid Methane Propellant
LOX/LH ₂	Liquid Oxygen and Liquid Hydrogen Propellant
LSR	Lunar Surface Rendezvous
MIT	Massachusetts Institute of Technology
MOI	Mars Orbit Insertion
MPCV	Multi-Purpose Crew Vehicle
MPLM	Multi-Purpose Logistics Module
MSDO	Multi-Disciplinary Systems Design and Optimization
mt	Metric Ton
MTV	Mars Transfer Vehicle
NASA	National Aeronautics and Space Administration
NATO	North Atlantic Treaty Organization
NEA	Near-Earth Asteroid
NERVA	Nuclear Engine for Rocket Vehicle Application
NP	Non-Polynomial
NRC	National Research Council
NTO/MMH	Nitrogen Tetroxide and Monomethylhydrazine Propellant
NTR	Nuclear-Thermal Rocket
OPM	Object Process Methodology
OPN	Object Process Network
PICA	Phenolic Impregnated Carbon Ablator
PVS	Property Variable Sensitivity
RCS	Reaction Control System
R&D	Research and Development
SAP	Systems Architecting Problem
SEP	Solar-Electric Propulsion
SEV	Space Exploration Vehicle
SHAB	Mars Surface Habitat
SLS	Space Launch System
SM	Service Module
SRP	Supersonic Rocket Propulsion
TCIM	Technology Coupling Interaction Matrix

TDI	Trans-Destination Injection
TEI	Trans-Earth Injection
TICE	Technology Interaction Coupling Effects
TIM	Technology Influence Measure
TMI	Trans-Mars Injection
TOF	Time of Flight
TPM	Technology Performance Measure
TPS	Thermal Protection System
TRL	Technology Readiness Level
T/W	Thrust to Weight Ratio
UPM	Unique Propulsive Maneuver

1. INTRODUCTION

During the final phases of the Apollo program, grand schemes were developed by NASA, the U.S. space community, and its global counterparts for the exploration of the Martian surface and beyond for mission dates as early as the 1980s. Since that point, such plans have been remade in cycles of reference architectures, allocated funding, and cancelled funding. While technologies for manned space exploration have significantly improved since that time, the long-term planning and funding requirements for the successful execution of a Mars exploration program have prevented the implementation of human spaceflight schemes beyond Earth orbit. However, a current void in exploration infrastructure affords the opportunity to lay the groundwork for these long term goals without some of the prior constraints imposed by heritage systems now discarded. Furthermore, developments in computational resources and analysis techniques have enabled the evaluation of a range of exploration mission designs in order to inform early decisions for the future of the manned exploration infrastructure.

1.1 MOTIVATION

1.1.1 Current State of Manned Space Exploration

The current void in infrastructure grew out of the recent reduction in major areas of manned space exploration. The final flight of the Space Shuttle Program occurred on July 8, 2011, ending manned space launches on U.S. vehicles [1]. This followed at the heels of the cancellation of the U.S. Constellation Program by President Obama in 2010 [2], often attributed to the 2009 final report of the Review of U.S. Human Spaceflight Plans Committee [3]. In place of the large-scale program, President Obama announced a new National Space Policy, which focuses on the near-term goals of increased use of commercial space capabilities, the mid-term goal of asteroid exploration, and the long-term goal of Mars surface exploration [4]. Although this policy draws heavily on the “Flexible Path” concept proposed in the U.S. Human Spaceflight Plans Committee Report, the goals outlined in the new policy are non-specific in terms of the pathways to these destinations.

With the exceptions of the continued development of the Orion Multi-Purpose Crew Vehicle (MPCV) [5], the recent extension of the operation of the International Space Station (ISS) to 2020 [6], and development of the Space Launch System (SLS) [7], the infrastructure of NASA for manned exploration is not being utilized on a large scale. The underutilization can be attributed to the ambiguity of the appropriate path forward and the series of program cancellations. Some of the U.S. space capabilities have been handed off to the commercial sector with the Commercial Crew

Development funding [8]. This includes many of the small and medium-sized cargo missions for satellite missions as well as ISS cargo and manned missions, such as the ISS servicing by the SpaceX Falcon vehicle and Dragon capsule [9]. Furthermore, there is, in general, a lack of sufficient dedicated funding for the progression of manned space exploration to new destinations. Constellation was canceled primarily due to this lack of funding, as the program was “pursuing goals that do not match allocated resources” [3]. A combination of underutilized infrastructure and shortage of funding has emerged.

1.1.2 Infrastructure Development and Long-Term Planning

Although enthusiasm for manned exploration missions is not lacking in the space community [10], the current deficiency of resources and U.S. space launch and support capabilities have created a lack of definitive goals and infrastructure development in human spaceflight for the United States. This is partially due to the ambiguity of how the next steps for surface missions should be pursued. Assuming that a Mars surface mission is the end goal of manned space exploration, there are a myriad of paths to follow in order to accomplish this goal. Figure 1 demonstrates the variety of pathways as shown in [3]. There are a variety of trade-offs between the pathway options, and experts around the world have yet to agree on the best way forward.

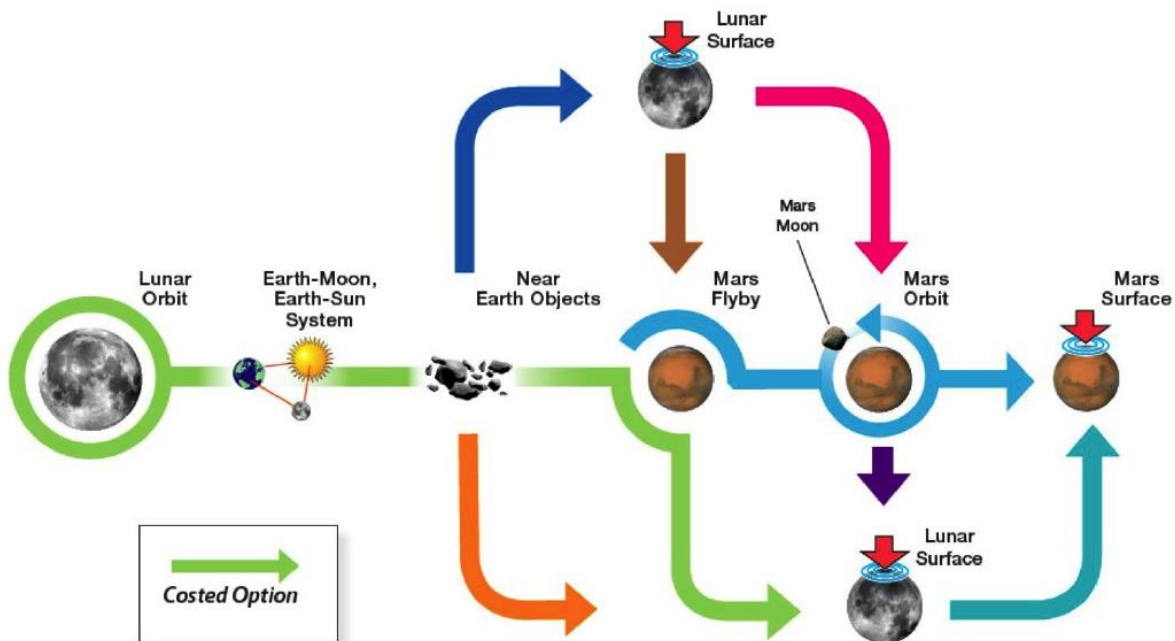


Figure 1: Manned Space Exploration Flexible Path

Final selection of the destinations for a long-term human spaceflight program will need to be

the result of extensive analysis involving technical, social, economic, and political factors. In addition, the architectures for each specific mission will require complex trades in similar regimes, ultimately being defined by layers of increasingly detailed designs. For now, with the recent void in manned spaceflight capabilities and resources, long-term planning must take place to build the infrastructure for the set of future missions. In particular, these decisions include not only the set of destinations, but also the investment in technologies to aid in these missions, the development of long-term facilities for the production of mission elements, and the underlying science infrastructure for utilizing the outputs of these missions.

In order to begin making these decisions, the trade in the underlying resource requirements (*e.g.* allocated operation budgets, launch resources, etc.) versus mission properties (*e.g.* *in-situ* science, surface stay time, crew mobility, etc.) must be established. Information must be gained regarding which destinations to design missions toward, how should those missions be accomplished, and what investments in technology are necessary to accomplish those objectives. This thesis presents a method for the comparison of high-level options for mission elements to facilitate in the decision-making process.

1.2 THE ROLE OF SYSTEM ARCHITECTURE AND ARCHITECTING

In order to tackle the complexity of such decisions, a useful field is the study of system architecture and system architecting. The application of concepts from civil architecture and civil engineering to large, complex systems was first practiced during the late 1980's, particularly in the creation of lead systems engineering roles, namely the system architect [11]. Given the responsibility of interfacing between the client and the design team, the system architect is not only interested in the specific technical design but also in holistic, value-centered design. Rechtin was arguably the first to formalize the concept, coining the phrase "system architecting" [12].

The system architecture of any given entity is fundamentally the highest level design, encompassing not only technical factors but also value delivery functions and full lifecycle impacts. The inclusion of non-technical factors and consideration of both upstream and downstream effects separates the system architecture from more traditional design views. Furthermore, because of the ambiguity associated with systems at this level, the descriptions are often abstracted beyond the level of system design models. Crawley *et al* define system architecture as "an abstract description of the entities of a system and the relationships between those entities" [13]. The entities described in a system architecture include the elements of function (*i.e.* what the system does) as well as the elements of form (*i.e.* what the system is). The mapping between the form and function constitutes the system *concept*. The concept is then used for further, more detailed design.

The process of creating the system architecture, referred to as system architecting, is concerned

with the earliest decisions to define the elements of function and form for the final concept. These decisions are both important and difficult because they are considered in an ambiguous context that has an impact on lifecycle cost and system capabilities. Once the concept is defined, the bulk of the necessary investments are defined, as well as the core technologies and mechanisms in the system.

With the deficiency of infrastructure development and long-term planning for manned space exploration, it is at this time that the system architecture for human spaceflight infrastructures is being developed. System architecting tools and methods can and should therefore be used to determine the most appropriate forward progression for the human spaceflight program. Most notably, the system functions are well understood (*i.e.* the functions performed during any given space exploration mission) while the form is yet to be defined. Decades of research into the structure of manned space exploration, particularly to the Marian surface, have clarified the needs for the performance of the elements in an exploration mission. However, the elements themselves have not been defined. In order to move forward with the development of assets for future use, the functions must be mapped to form to create the base concepts for manned space exploration missions.

1.3 DECISION ANALYSIS IN SYSTEM ARCHITECTURE

Because system architectures are concerned with the upfront system decisions, the analysis tools associated with decision analysis are relevant. More importantly, any analysis to support these upfront decisions needs to be formulated in such a way as to easily translate between the technical setting and the decision support environment. Willard Simmons describes in his dissertation a method for both describing a system for architectural analysis and retaining understandability for decision support [14]. Most importantly, he showed that the architecture of complex systems may be described by a set of high level decisions. By choosing among the various options for each decision, a system architecture may be defined. He went on to describe how this may be encoded in an Object Process Network (OPN) and analyzed with the associated tools. In his thesis, he stated that the specific objectives of the research presented were “to develop an explicit representation of architecture as a set of decisions and show that, through using this representation, an architect can gain useful insight into the architectural candidate space.” He also showed that many complex systems which were traditionally believed to be “non-programmable” (*i.e.* non-routine, weakly-defined, imprecise models), such as complex socio-political decisions like “Should the nation go to war?” or highly complex technical decisions like the mission mode for Apollo, could be encoded using a decision formulation. From this information, it can be understood that the problem at hand, namely the architecting of future manned exploration missions, can be understood and programmed in a manner that is conducive to aiding in the real-world decision-making process

through the use of Simmons' formulation.

1.4 EXHAUSTIVE TRADESPACE EXPLORATION

Exhaustive tradespace exploration is a rigorous method that combines a decision formulation with full tradespace coverage. This is the concept of enumerating the full set of architectural options and exploring how each interrelates with the set and other architectures, as seen in Simmons' ADG model. In order to address the problem of designing the architecture for manned exploration missions, however, a large set of decisions may be necessary. The full combination of architectures grows rapidly with the set of decisions. This effect is often referred to as combinatorial explosion [15]. Full combinatorial exploration increases rigor from heuristic optimization methods by guaranteeing optimality, since all information is known for discernible architectures. Furthermore, quantitative analysis may be performed to allow insight into the impact of decisions on the architectures as they relate to the broader tradespace.

Recent advancements in computing technology, namely parallel processing, allow for the increase in allowable computational requirements for the analysis of combinatorial tradespace exploration models. By taking advantage of these capabilities, a more detailed exploration of the tradespace of manned exploration infrastructures may be accomplished at a level of fidelity not previously possible due to computational resource constraints.

1.5 PRIOR MANNED SPACEFLIGHT MODELS

Much of the work presented draws off prior models developed to analyze manned spaceflight missions. These include several tradespace exploration models as well as many point designs developed by NASA and the global space community. Prior tradespace exploration models have inherent limitations, produced either by the severe scoping of the model to a small portion of the architecture or by the manner of implementation. Prior point designs have explored the details of specific missions but do not inform decisions for trades with alternative exploration schemes or technologies.

1.5.1 Hofstetter Manned Spaceflight Tradespace Model

Wilfried Hofstetter described a manned spaceflight tradespace generation model in his Master's thesis conducted at M.I.T. [16]. He attempted to describe the high level architecture for both lunar and Mars missions through a breakdown of the crew operations. Specifically, his model uses a set of decisions to describe the number of crew transfers, the number of vehicles, and the types of maneuvers that each vehicle may accomplish. Figure 2 shows the morphological matrix that he

created for these decisions, with an example mission highlighted.

Number of crew transfers between vehicles	0	1	2	3	4
Number of vehicles	1	2	3		
Event 1	O	L	T		
Event 2	S	O	L	T	N
Event 3	S	O	L	T	N
Event 4	S	O	L	T	N
Event 5	S	O	L	T	N

Figure 2: Hofstetter Tradespace Model Morphological Matrix

Hofstetter described the vehicle maneuvers as one of a set of five possible actions. “O” refers to vehicles on orbit, “L” refers to landing on the surface of a destination, “T” stands for crew transfers in transit, “S” describes crew transfers on the surface, and “N” is non-applicable. This set of decisions successfully describes the set of vehicles and crew operations, in terms of transfers, for a given mission. Specifically, Hofstetter sought to describe a set of four variables:

1. The number of vehicles inserted toward the destination
2. The number of crew transfers between these vehicles
3. The sequence of changes and their location (surface/orbit)
4. The position of the crew landing in the sequence of events

However, it does require a set of additional constraints, since the decisions are coupled in such a way as to disallow certain combinations. These constraints required a set of twelve rules, which cover both the restriction of what is present on the morphological matrix as well as the constraints on their combinations:

Rule 1: Only manned vehicles are modeled (*i.e.* vehicles with both crew and propulsion stages)

Rule 2: Every manned vehicle must be used at least once

Rule 3: For n crew transfers, the number of vehicles must be below $n+1$

Rule 4: A vehicle that the crew has used and then abandoned rests at the location where the crew last used it

Rule 5: Crew transfers on the surface can only occur after landing

Rule 6: The crew goes to the surface only once per mission and does not return

Rule 7: The vehicles are numbered in sequence of crew occupancy

Rule 8: The entire crew always stays together

Rule 9: No dedicated destination orbital space stations exist

Rule 10: No dedicated space stations in transit exist

Rule 11: Only one dedicated surface habitat is provided in every mission

Rule 12: Crew transfers in transit can only be the first and/or last crew transfer in an architecture

When unconstrained, the morphological matrix in Figure 2 produces $5^3 \times 3^3 = 28,125$ variants. Only 30 unique design vectors comply with the rules. This indicates that the model produces only a limited variety of architectures to trade. Furthermore, these architectures lack a great deal of information that is useful at the architectural level. Specifically, Hofstetter points out the lack of the description of a set of four characteristics, although there are many more technical details not described by the model. He includes the following as important characteristics:

1. No information about whether vehicles travel together or separately
2. No propellant usage information
3. The use of ISRU is not addressed
4. The use of aerocapture at Mars is not addressed

Because this model is primarily used by Hofstetter to describe landing vehicles, much of the general information about the system architecture is not, in fact, necessary for his results. However, the need for a large set of rules indicates a lack of appropriate description of the decisions, which could be reformulated to reduce the number of necessary constraints. The small size of the tradespace and limited number of decisions in the model made the enumeration and exploration of the set of architectures simple enough to not necessitate a radical change in the description.

In general, Hofstetter was one of the first researchers to attempt to describe the architecture of manned exploration vehicles in an enumeration model, which was successfully performed for a limited set in a unique fashion. Hofstetter's Excel-based model, however, is insufficient to describe the majority of manned exploration architectures at the high level of design needed for early decisions about major infrastructure elements. This concept laid the foundation for the creation of future, more advanced tradespace models.

1.5.2 Simmons Manned Spaceflight Tradespace Model

Like Hofstetter, Willard Simmons used system architecture techniques to describe specific cases for specific goals related to manned space exploration missions. In this case, Simmons sought to validate the use of the Architecture Decision Graph (ADG) framework presented in his

dissertation by using the Apollo Program as a case study [14]. The formulation was therefore dependent on historical information as a retrospective case study. Under the ADG formulation, Simmons developed a set of nine decision variables for the Apollo Program. His formulation of the corresponding morphological matrix is shown in Figure 3.

shortID	Decision	units	alt A	alt B	alt C	alt D
EOR	Earth Orbit Rendezvous	none	no	yes		
earthLaunch	Earth Launch Type	none	orbit	direct		
LOR	Lunar Orbit Rendezvous	none	no	yes		
moonArrival	Arrival at Moon	none	orbit	direct		
moonDeparture	Departure from Moon	none	orbit	direct		
cmCrew	Command Module Crew	people	2	3		
lmCrew	Lunar Module Crew	people	0	1	2	3
smFuel	service module fuel	none	cryogenic	storable		
lmFuel	lunar module fuel	none	NA	cryogenic	storable	

Figure 3: Simmons Apollo Program Morphological Matrix

The decision variables focus on the “mission mode,” or the method for the decomposition of the vehicle and crew transfers. This is a significantly different approach from Hofstetter, given that the decisions are more explicit in nature rather than generic. This set of decisions also assumes the use of a service module and a lunar module. For the purposes of describing the mission mode decision for Apollo, this is logical. However, it does not capture the alternative vehicle arrangements that were decided prior to this point in the Apollo Program but are critical to the overall system architecture.

Like the Hofstetter model, Simmons’ model also required a set of what he called “logical constraints,” shown in Table 1 and Table 2. These are the constraints placed on the combinations of architectural decisions based on both logic and physics, and their specifics are described below.

Table 1: Simmons Apollo Program Model Logical Constraints

name	scope	equation
EORconstraint	EOR,earthLaunch	(EOR == yes && earthLaunch == orbit) (EOR == no)
LORconstraint	LOR,moonArrival	(LOR == yes && moonArrival == orbit) (LOR == no)
moonLeaving	LOR,moonDeparture	(LOR == yes && moonDeparture == orbit) (LOR == no)
lmcncrew	cmCrew,lmCrew	(cmCrew >= lmCrew)
lmexists	LOR,lmCrew	(LOR == no && lmCrew == 0) (LOR == yes && lmCrew >0)
lmFuelConstraint	LOR,lmFuel	(LOR == no && lmFuel == NA) (LOR == yes && lmFuel != NA)

Table 2: Simmons Apollo Program Model Logical Constraint Tables

EORConstraint		EOR	
earthLaunch	no	yes	
orbit	1	1	
direct	1	0	

Imcmcrew		cmCrew	
ImCrew	2	3	
0	1	1	
1	1	1	
2	1	1	
3	0	1	

LORConstraint		LOR	
moonArrival	no	yes	
orbit	1	1	
direct	1	0	

Imexists		LOR	
ImCrew	no	yes	
0	1	0	
1	0	1	
2	0	1	
3	0	1	

moonLeaving		LOR	
moonDeparture	no	yes	
orbit	1	1	
direct	1	0	

ImFuelConstraint		LOR	
ImFuel	no	yes	
NA	1	0	
cryogenic	0	1	
storable	0	1	

EORConstraint: If there is an Earth orbit rendezvous, then this implies that the earthLaunch decision must be equal to orbit, since it is impossible to rendezvous without entering Earth orbit first.

LORConstraint: If there is a lunar orbit rendezvous in the mission mode, this implies that the moonArrival decision must be equal to orbit, since it is impossible to complete the rendezvous maneuver without entering lunar orbit before descending to the lunar surface.

moonLeaving: If there is a lunar orbit rendezvous in the mission mode, this implies that the moonDeparture decision must be equal to orbit, since it is impossible to complete the rendezvous maneuver without entering lunar orbit after ascending from the lunar surface.

Imcmcrew: This constraint restricts the crew size of the lunar module to be less than or equal to the crew size of the command module.

Imexists: This constraint forces ImCrew to be zero if there is no lunar orbit rendezvous.

ImFuelConstraint: This constraint forces ImFuel to be NA if there is no lunar orbit rendezvous.

The reduced number of constraints implies that this formulation is more efficient in application than Hofstetter's model, although they describe different portions of the architecture. However, the need for constraints may imply that some inefficiencies exist in the decision formulation.

As part of the ADG framework, this set of decisions was encoded in an Object Process Network (OPN), shown in Figure 4.

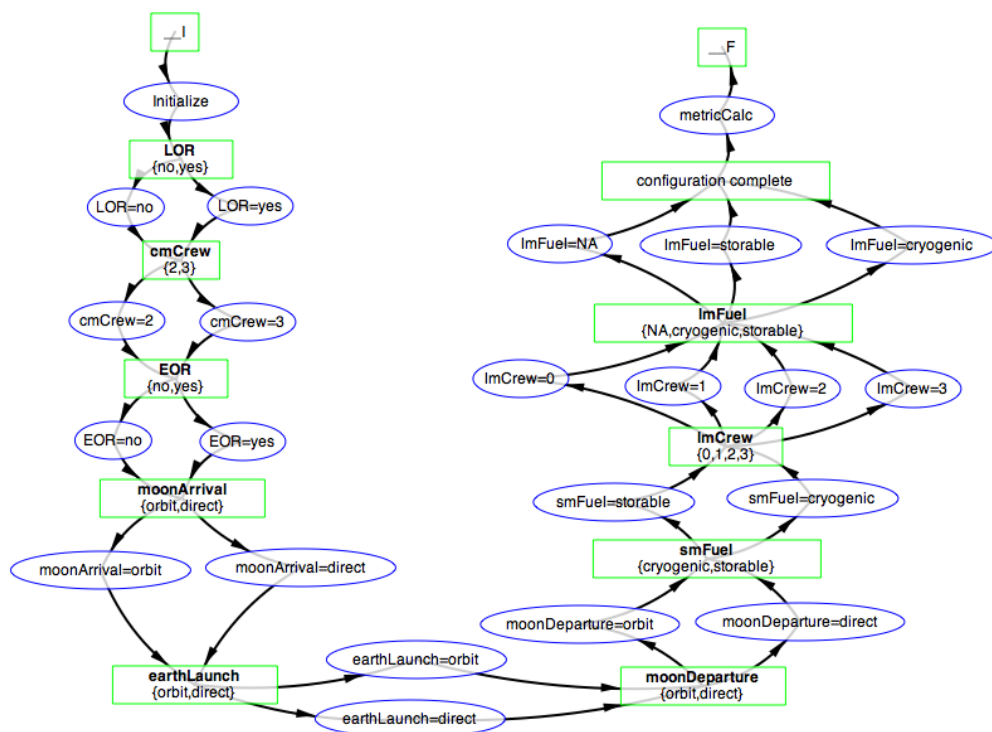


Figure 4: Simmons Apollo Program Model OPN

Because of the nature of the implementation, this model is restricted to a set of decisions that are linear in nature (*i.e.* the set of decisions must be able to be made in a predetermined sequence). The implementation in an Object Process Network also is limited by the capabilities of the base program. A large set of decision options is generally difficult to encode in this method.

Overall, Simmons' model is highly capable of describing the decisions centered on the Apollo Program's mission mode decision, with limited variables and option sets. However, it does not provide enough flexibility to encode all of the architecture-level decisions necessary to inform early architecture definition in full.

1.5.3 Design Reference Architecture 5.0

In order to have a deep technical understanding of the requirements for manned spaceflight missions, NASA and many international space agencies typically use point design studies. These studies allow for an in-depth look at a particular mission architecture by going through the process of engineering design. Engineering design differs from system architecting in that it is the process of transforming the concept into a detailed design, while architecting creates the concept. Much of this is preceded by larger tradespace studies in order to select the architecture for the final point design. However, that work often is not publically available and is typically more reliant on expert

opinion rather than rigorous analysis. NASA’s most recent publicly available point design is referred to as Design Reference Architecture (DRA) 5.0, published in 2009 [17]. This has followed a line of prior Design Reference Missions, each looking at point designs for Mars surface exploration missions. Because of the component-up design of many of the architecture’s elements, this study has been used as a baseline for understanding the technical requirements of Mars surface missions and the sizing of certain architectural elements as presented in this thesis.

DRA 5.0 describes a mission architecture for a conjunction-class Mars surface mission, with approximately 500 days of surface time and 6 crew members. The final report recommends a set of three consecutive missions performed over a 10 year period, each exploring a different region of the Martian surface. In addition, each mission would be split between two launch stacks, one of which is unmanned and pre-deploys cargo to the Martian surface and another which carries the crew to the surface. An example of the mission phasing is given in Figure 5. This shows that there would be overlap between multiple missions in terms of cargo delivered to the surface during the operations of the previous crew.

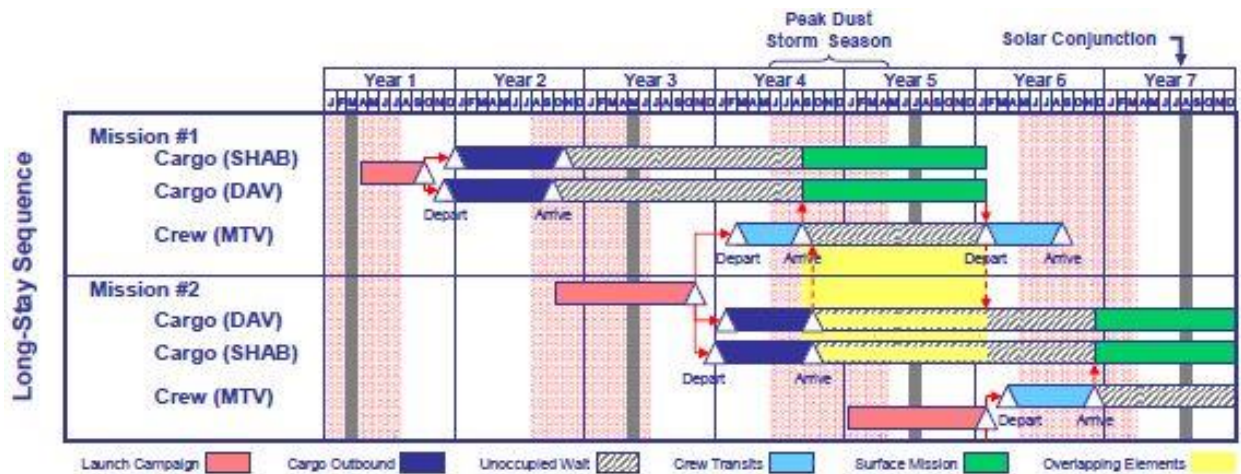


Figure 5: DRA 5.0 Mission Phasing

The base mission design is reliant on the development of nuclear thermal rockets (NTR) with liquid hydrogen as propellant, as well as advanced entry, descent, and landing systems for a combined descent and ascent vehicle (DAV); a long-duration Mars Transfer Vehicle (MTV); the Mars surface habitat (SHAB); and heavily-lift launch vehicles for raising these elements to orbit. Additionally, the architecture assumes the development of ISRU capabilities, nuclear fission surface power, and the use of large pressurized rovers on the surface. Figure 6 shows the concept of operations (ConOps) for the base reference mission in the form of a BAT chart. This describes the major elements and the timeline for the use of these elements.

In addition to the NTR-based mission architecture, NASA also developed an alternative

chemical propulsion option. This was found to be much more massive than the baseline NTR option, but it provided a trade with mass for ease of development and political survivability. The manifest for the NTR reference mission can be found in Table 3 and Table 4, while the manifest of the chemical propulsion option is given in Table 5 and Table 6. These tables give specific masses for both propulsion elements and other cargo, including habitat elements.

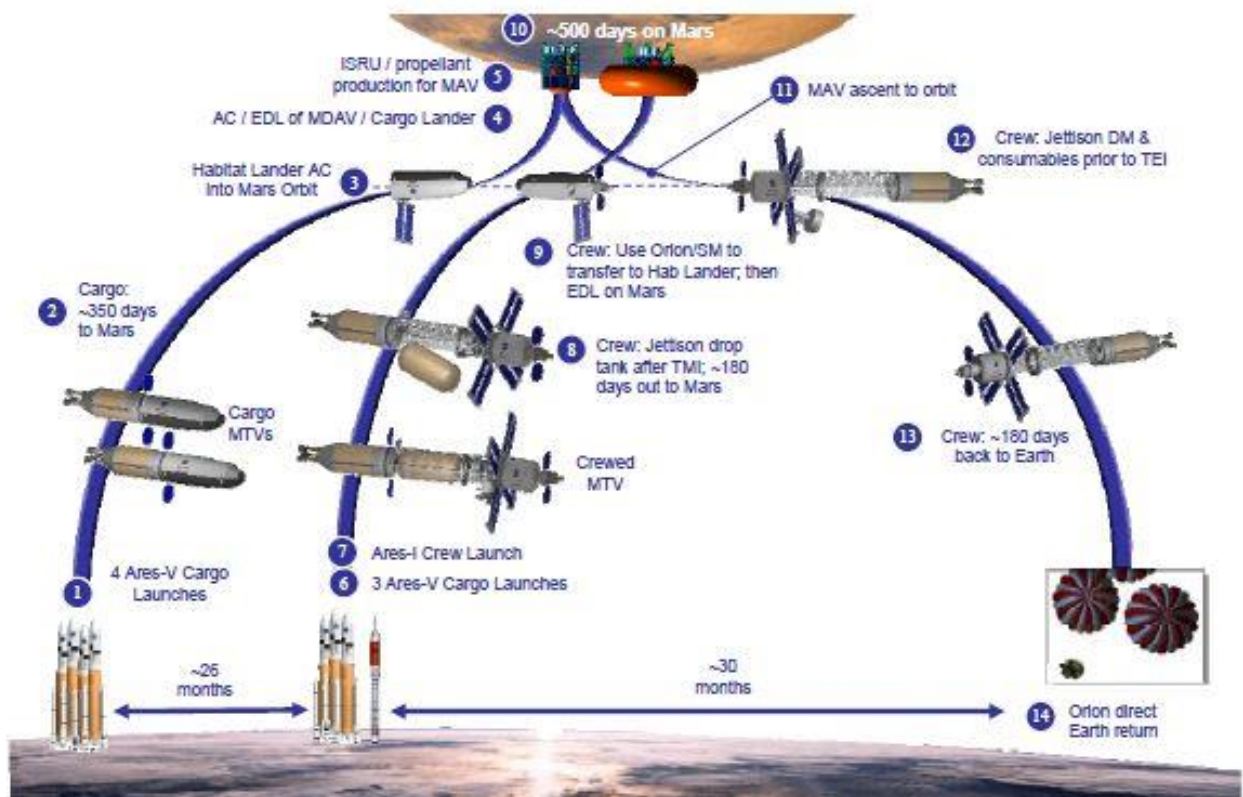


Figure 6: DRA 5.0 BAT Chart

Table 3: DRA 5.0 NTR Mission Vehicle Summary

Cargo Mission (Single Vehicle, 1 of 2)			Crewed Mission		
Vehicle Elements		Mass (t)	Vehicle Elements		Mass (t)
NTR "Core" Stage	Core Stage Dry Mass	33.7	NTR "Core" Stage w/Ext. Rad. Shield	Core Stage Dry Mass	41.7
	LH2 Propellant Load	59.4		LH2 Propellant Load	59.7
	RCS Propellant Load	3.6		RCS Propellant Load	4.9
	Total Core Stage Mass	96.6		Total Core Stage Mass	106.2
	Number of Core Stage	1.0		Number of Core Stage	1.0
	Total Stage Mass	96.6		Total Stage Mass	106.2
In-Line LH2 Tank	In-Line Tank Dry Mass	10.8	In-Line LH2 Tank	In-Line Tank Dry Mass	21.5
	LH2 Propellant Load	34.1		LH2 Propellant Load	69.9
	RCS Propellant Load	1.7		RCS Propellant Load	
	Total In-Line Mass	46.6		Total In-Line Mass	91.4
	Number of Tanks	1.0		Number of Tanks	1.0
	Total In-Line Mass	46.6		Total In-Line Mass	91.4
			Long Saddle Truss & LH2 Drop Tank	Saddle Truss Mass	8.9
				Drop Tank Dry Mass	14.0
				LH2 Propellant Load	73.1
Payload			Payload Elements	Short Saddle Truss	4.7
				Conting. Food Canister	9.8
				2nd Docking Module	1.8
				Fwd RCS Prop Load	3.2
				Transit Habitat	32.8
				CEV/SM + Crew	10.6
				Total Payload Mass	62.8
Total Cargo Lander	103.0				
(Aeroshell, PL & Lander)					
Total Cargo Vehicle Mass		246.2	Total Crewed Vehicle Mass		356.4

Table 4: DRA 5.0 NTR Mission Vehicle Assembly Timeline and ETO Delivery Manifest

	Launch Number	Launch Time Before TMI (days)	Launch Manifest	Shroud Length (m)	Launch Mass (t)
Cargo Mission (Two Vehicles)	Ares V Launches				
	1	-180	NTR TMI Core Stage 1	30.0	96.6
	2	-150	NTR TMI Core Stage 2	30.0	96.6
	3	-120	Twin In-Line LH2 Tank	30.0	93.2
	4	-90	Payload 1 (Cargo Lander)	30.0	103.0
	5	-60	Payload 2 (Hab Lander)	30.0	103.0
		-60	TMI Window Allowance		
Total MTV Mass Delivered to Orbit					492.3
Crewed Mission	1	-150	NTR Core Stage	30.00	106.2
	2	-120	In-Line LH2 Tank	30.00	91.4
	3	-90	Truss & Drop Tank	30.00	96.0
	4	-60	Crew Payload Element	30.00	62.2
		-60	TMI Window Allowance		
	Ares I Launch (delivers astronauts to orbiting crew MTV)				
1	-5	6 Mars Crew	n/a	0.6	
Total MTV Mass Delivered to Orbit					356.4
Ares V launches:		9	Total IMLEO (t):		848.7

Table 5: DRA 5.0 Chemical Mission Vehicle Summary

Cargo Missions (Both Vehicles)			Crew Mission		
Veh. Element		Mass (t)	Veh. Element		Mass (t)
TMI Stage 1	Mbo (Module)	15.1	TMI Stage 1	Mbo (Module)	15.1
	M prop (Module)	86.2		M prop (Module)	91.1
	RCS (Module)	2.3		RCS (Module)	2.3
	Total Module Mass	103.6		Total Module Mass	108.5
	Number of Modules	1.0		Number of Modules	2.0
Total Stage Mass		103.6	Total Stage Mass		217.0
TMI Stage 2	Mbo	15.1	TMI Stage 2	Mbo	15.1
	M prop	86.2		M prop	91.1
	RCS (Module)	2.2		RCS (Module)	2.3
	Total Module Mass	103.6		Total Module Mass	108.5
	Number of Modules	1.0		Number of Modules	1.0
Total Stage Mass		103.6	Total Stage Mass		108.5
			MOI Stage	Mbo	10.3
				M prop	50.2
				RCS	5.3
				Total Stage Mass	65.8
			TEI Stage	Mbo	11.4
				M prop	24.1
				RCS	7.3
				Total Stage Mass	42.7
Payload	Surface hab	103.0	Payload	Transit Habitat	41.3
				CM + Crew	10.6
Total Vehicle Mass		310.2	Total Vehicle Mass		486.0

Table 6: DRA 5.0 Chemical Mission Vehicle Assembly Timeline and ETO Delivery Manifest

	Launch Number	Launch Time Before TMI (days)	Launch Manifest	Shroud Length (m)	Launch Mass (t)			
Cargo Mission (Both Vehicles)	Ares V Launches							
	1	-270	Reboost Module 1 Reboost Module 2	14.00	96.9			
	2	-240	Payload 1 (Surf. Hab)	30.00	103.0			
	3	-210	Payload 2 (Lander)	30.00	103.0			
	4	-180	TMI Module 1a	16.26	103.6			
	5	-150	TMI Module 2a	16.26	103.6			
	6	-120	TMI Module 1b	16.26	103.6			
	7	-90	TMI Module 2b	16.26	103.6			
					-60	TMI Window		
Total Mass Delivered to Orbit					717.3			
Crew Mission	8	-210	Transit Hab/CEV Reboost Module	17.00	99.9			
	9	-180	MOI & TEI Stages	22.30	108.5			
	10	-150	TMI Module 1a	16.26	108.5			
	11	-120	TMI Module 1b	16.26	108.5			
	12	-90	TMI Module 1c	16.26	108.5			
						-60	TMI Window	
Ares I Launches								
	1	-5	6 Mars Crew	n/a	0.6			
Total Mass Delivered to Orbit					534.5			
Ares V launches:		12	Total IMLEO (mt):		1,251.8			

Figure 7 describes another important sizing trade described in the final report for DRA 5.0 – the trade between two surface habitats, both developed based on prior work on lunar habitat designs. Both of these designs are used for sizing parametrics described in this thesis.

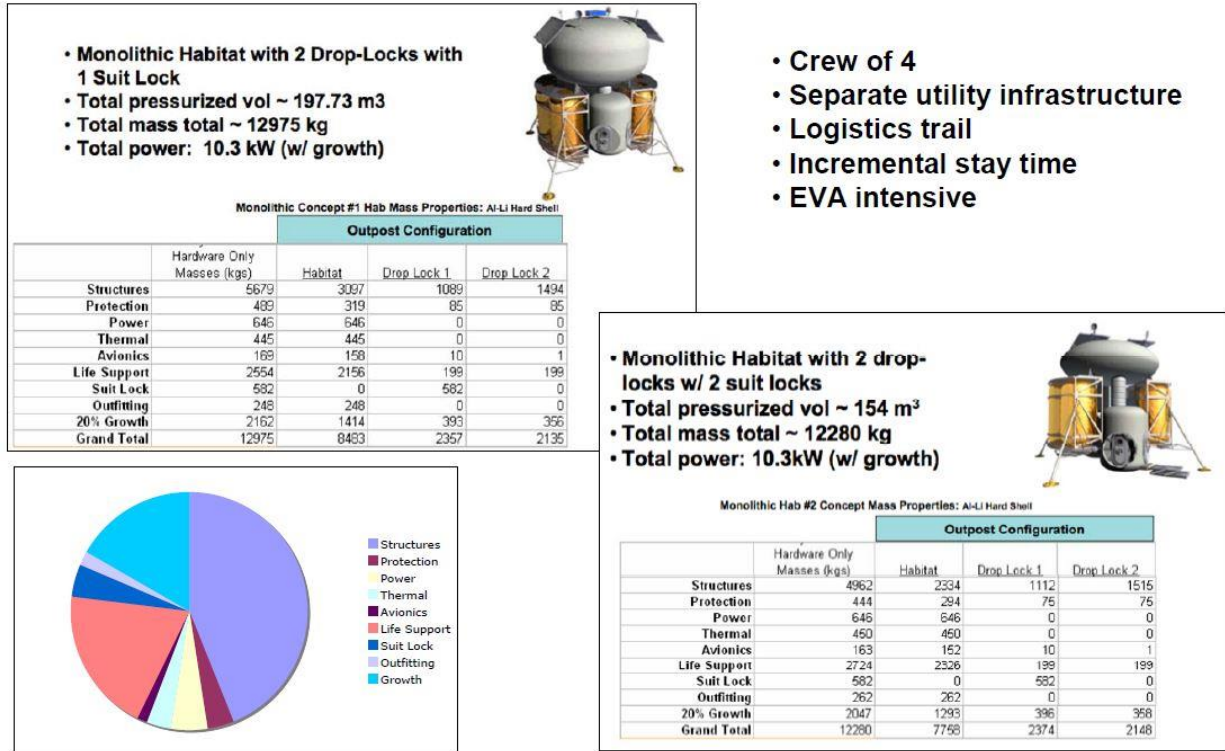


Figure 7: DRA 5.0 Surface Habitat Option Summary

The final report goes on to describe a set of five decisions that the designers believe are foundational for the creation of the mission described in the report. These include:

Decision 1: Mission Type – This describes the choice between an opposition class short-stay mission and a conjunction class long-stay mission.

Decision 2: All-up vs. Pre-Deploy Cargo – This is the decision between the use of a single launch stack to deliver both crew and cargo or the use of a prior launch stack to deliver a portion of the mission cargo to the surface.

Decision 3: Aerocapture vs. Propulsive Mars Orbit Capture of Cargo – For only the cargo, the option between aerocapture and propulsive capture was considered. Aerocapture was concluded to be infeasible for the manned stack.

Decision 4: ISRU for Mars Ascent – This represents the option to use *in-situ* resources to produce ascent propellant. Use of ISRU requires significant time and energy, along with an increased risk corresponding to the possibility of mission failure if the propellant cannot be generated.

Decision 5: Mars Surface Power – Correlated with Decision 4 is the use of different technologies for surface power. DRA 5.0 considered the use of solar power, large-scale radioisotope power systems, and nuclear fission plants.

Overall, DRA 5.0 represents the latest and most vetted point design produced by NASA that is publically available. The Human Spaceflight Architecture Team (HAT) out of NASA Johnson Space Center (JSC) is currently finalizing new reference architecture studies for public release. Information from these studies has also been integrated into this thesis. DRA 5.0 represents a baseline to assess the need for large-scale technologies and provides a validation case for the tradespace analysis model described in this thesis.

1.5.4 Austere

Members of the NASA Jet Propulsion Laboratory (JPL) and Aerospace Corporation responded to the publication of Design Reference Architecture 5.0 by producing a minimalist mission that they called Austere [18]. Specifically, the goal of the mission design was to provide an alternative architecture that “might lower development cost, lower flight cost, and lower development risk.” However, the majority of the components are still heavily based on DRA 5.0 elements. Figure 8 shows how Austere differentiated itself from DRA 5.0 by identifying the decision differences from the list of five described in Section 1.5.3 in a trade tree. The differences in the decisions focus on the use of chemical propellants rather than NTR and the decision not to employ ISRU. Austere also avoids the use of hydrogen-based propulsion in order to limit the need for development of cryogenic boil-off control. The individual vehicles developed for Austere, although providing many of the same functions as those in DRA 5.0, are also sized much differently. Table 7 gives a breakdown of the element masses as well as properties of these elements. The overall mission mode, a long-stay conjunction class mission, the set of vehicles in terms of functionality, and much of the Earth-based infrastructure requirements remain the same between Austere and DRA 5.0.

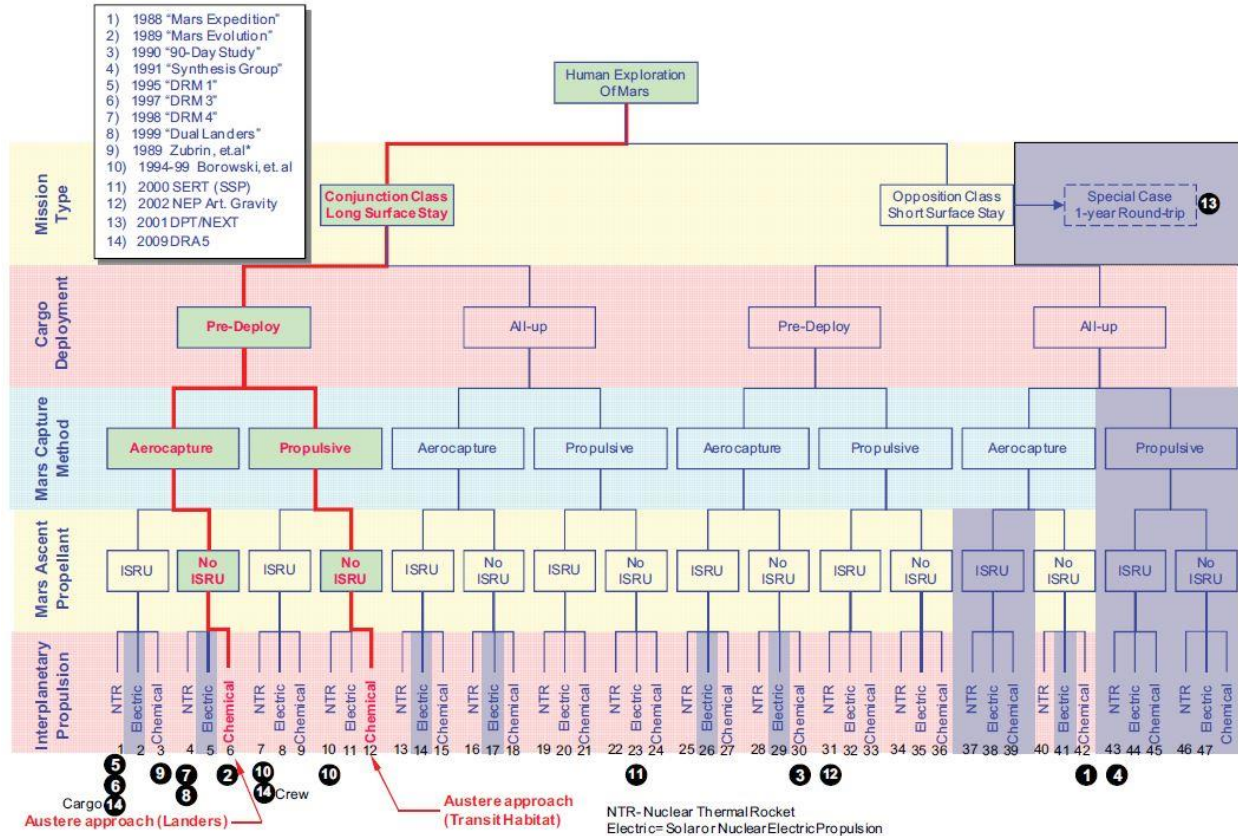


Figure 8: Austere and DRA 5.0 Decision Trade Tree

Table 7: Austere Element Masses Breakdown

Element	Mass (T)	"Gear Ratio"	Prop. type	Ares V	Ares I	Comments
MAV Cabin	6.2					2.9 times Apollo Ascent Module dry mass
MAV Total	45.9	7.4	NTO/MMH			Includes ascent propulsion and structure
Lander Descent Stage	119.3	3.6	NTO/MMH			Includes separate aerocapture heat shield
Lander/MAV Total	165.2			1		
MAV EDS's	330.3	3.0	LOX/LH ₂	2		Two stage assembly requiring two Ares V launches
Cargo Lander payload	52.0					Can be Habitat, or Surface Power and Logistics Module
Cargo Descent Stage	114.4	3.2	NTO/MMH			
Cargo Total	166.4			1		
Cargo EDS's	332.8	3.0	LOX/LH ₂	2		Two stage assembly requiring two Ares V launches
CEV	10.0				1	Current Orion CM mass
Transit Habitat	35.0					For comparison, Mir Core Module mass = 21 T
Contingency Module	7.0					Emergency supplies for Mars abort to orbit (jettisonable)
Subtotal	52.0					
MOI/TEI Module	114.4	3.2	LOX/LCH ₄			Assumes 1.2 km/s MOI followed by aerobraking
Subtotal (w/o CEV)	156.4			1		A single Ares V launches MOI/TEI module plus Habitat
EDS Stages	332.8	3.0	LOX/LH ₂	2		Two stage assembly requiring two Ares V launches
Grand Total	1,983.1			12	1	Incl. 2 Cargo Landers (Surf. Hab., Power & Logistics)

What Austere showed was that a Mars mission could be accomplished with far less technology

development, although at a much higher mass cost. This indicates that the first and third goal were accomplished, *i.e.* the reduction of development cost and development risk. However, the drastic increase of mass on a per-mission basis indicates that the flight cost may very well be increased by this approach. In this thesis, the fundamentally different approaches represented by DRA 5.0 and Austere are used in comparison charts for tradespace analysis to show how these approaches are reflected in the metrics.

1.5.5 Mars-Oz

Prior to the development of DRA 5.0 and Austere, the Mars Society Australia designed a reference mission for a Mars surface mission based on the “Semi-Direct” approach originally conceived by Zubrin and Weaver [19][20]. They emphasized four points:

1. Providing the lowest cost mission to encourage funding
2. Maximizing safety
3. Minimizing mission complexity in order to optimize reliability
4. Providing the best science return given the remaining constraints

For this “Mars-Oz” mission, the designers chose the “Semi-Direct” option described in Figure 9 in order to match with the remaining decisions about vehicles and employed technologies. As the authors describe, “the first [decision] set the need for a minimum number of vehicles, adopting proven technology where possible.” The second revolves around the decision to use solar power on the surface rather than a nuclear source. The third describes the use of ISRU for ascent propellant production. In addition to this set, the authors also chose to use aerocapture to insert into Mars orbit and limited the LEO launch payload to 130mt.

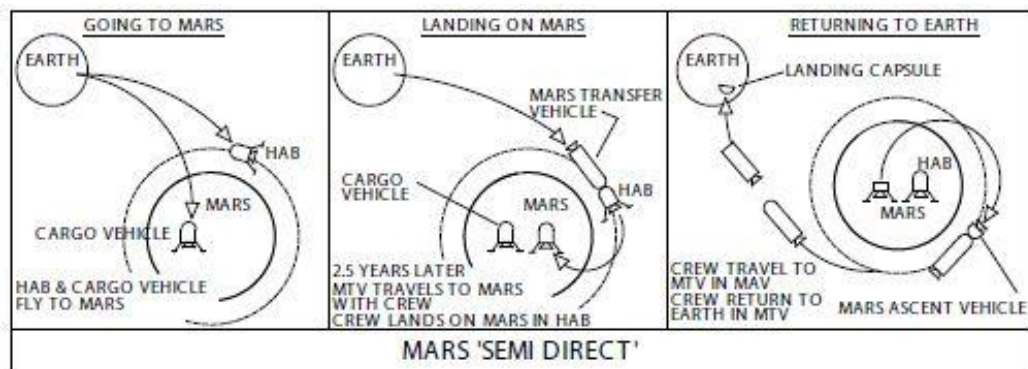


Figure 9: Mars-Oz Semi-Direct Mission Mode Description

The overall mission concept requires the use of five separate elements: a surface habitat, an ascent vehicle, a transfer vehicle, a cargo vehicle, and the trans-Mars stage. A description of each can be found in Table 8.

Table 8: Mars-Oz Vehicle Descriptions

Vehicle	Function Detail
Habitat (Hab) LEO mass: 62 tonnes	<p>It travels to Mars low orbit and waits for the crew to arrive in the MTV.</p> <p>It lands on the Martian surface with crew and becomes the core of the Mars station for a minimum of 4 people.</p> <p>It consists of a cabin, propulsion module, heat shield, landing engines and parachutes.</p> <p>The propulsion module is removed after landing enabling other structures to be mated with the HAB forming a larger station.</p>
Cargo Vehicle LEO mass: 62 tonnes	<p>It transports equipment to the Martian surface direct from earth 2 years prior to the arrival of the crew.</p> <p>The vehicle is in two parts.</p> <p>The first forward section consists of a Mars Ascent Vehicle (MAV), hydrogen stock fuel and an in-situ resource utilization processing plant.</p> <p>The second rear section is a detachable garage carrying a pressurized rover and surface supplies for the crew.</p> <p>It also has a propulsion module, heat shield, landing engines and parachutes.</p> <p>The Cargo section of the vehicle can be detached, towed to the Hab and connected together to form the Mars station</p>
Mars Ascent Vehicle (MAV) Dry mass: 4 tonnes	<p>It lifts the crew from the Mars Surface to low Mars orbit. It is located in the forward section of the cargo vehicle It has room for 4 –6 crew with a 2 day flight duration.</p>
Mars Transfer Vehicle (MTV) LEO mass: 130 tonnes	<p>It transports the crew from low Earth orbit to low Mars orbit with the crew. Capture into Mars orbit is by aerobrake and meets the Hab in low Mars orbit.</p> <p>The crew transfer to the Hab for landing. The MTV remains in low Mars orbit while the crew are on the surface.</p> <p>It transports the crew back to Earth from low Mars orbit. The crew land on direct earth in a capsule</p> <p>It consists of a cabin, water lined storm shelter, landing capsule, heat shield, a science and supply module to be jettison in Mars orbit and propulsion module for Mars escape.</p> <p>It has supplies for 400 days for a minimum of 4 people.</p>
Trans-Mars Stage (TMS) LEO mass: nominally 110 tonnes	<p>It boosts the payloads on a trajectory from low earth orbit to Mars. The TMS propellant is assumed to be liquid Hydrogen and Liquid Oxygen. The tanks would require insulation on the to enable long periods of loitering in LEO.</p> <p>One TMS would be required for boosting the HAB and Cargo vehicles to Mars.</p> <p>Two TMSs would be required for boosting the MAV to Mars.</p>

Mass estimates for the complete mission are given in Table 9. This shows that the Mars Society Australia believed that a manned Mars mission was possible on an even smaller mass budget than DRA 5.0 even without NTR.

Table 9: Mars-Oz Mission Mass Breakdown

Payload Lifted into Low Earth Orbit	TMS(s) required for the Trans-Mars burn
Hab, 62 tonnes	1 TMS, 110 tonnes
Cargo vehicle, 62 tonnes	1 TMS, 110 tonnes
MTV, 130 tonnes	2 TMSs, 220 tonnes
Total mass in LEO	694 tonnes

Mars-Oz provides a reference Mars surface mission from a source distinctly outside of the U.S. space program, therefore providing additional prospective for element estimations and overall architectural thinking.

1.5.6 Additional Point Design Studies

Beyond those mentioned in the preceding sections, several point design studies are relevant to the development of Martian and lunar mission architectures. These include NASA’s Design Reference Mission [21], NASA Design Reference Mission 3.0 [22], NASA’s Exploration Systems Architecture Study [23], the European Mars Missions Architecture Study [24], the European Space Agency’s recent report on human missions to Mars [25], reports from NASA’s Concepts Exploration and Refinement Contract [26], and designs from the Constellation Program [2].

1.5.7 The Design of Complex System Models

Models of complex systems, like manned exploration infrastructures, are difficult to design in a way that captures the system behavior of interest while retaining computational efficiency. Such models are typically designed in an iterative fashion, developing from expert training in modeling techniques and knowledge from previous iterations. The process also draws on many dispersed tools and methods that have been developed for system architecture and model design, each of which is limited in its abilities. Currently, very little guidance exists on the use of different modeling methods and tools for such systems, and the burden of understanding appropriate applications rests on the model builder.

Some architectural frameworks exist, but these are designed explicitly to create common architecture-level system descriptions rather than aid in creating well-formulated models. Rather,

they strive for consistency in model formulation. These include but are not limited to the Department of Defense Architecture Framework (DoDAF); Command, Control, Communications, Computers, Intelligence, Surveillance, Reconnaissance Architecture Framework (C4ISRAF); NATO Architecture Framework (NAF); the Federal Enterprise Architecture Framework (FEAF); and the British Ministry of Defense Architecture Framework (MODAF).

There is therefore a need for a framework that: 1) aims to create well-formulated architectures, and 2) provides guidance for the use of system architecture tools and methods. This would reduce the burden on system architects to be familiar with all tools and methods in the field and their limitations as well as helping to create better complex system models.

1.6 OBJECTIVES

This thesis has three objectives, one primary and two secondary. The primary objective is to describe a tool for the evaluation of arbitrary manned exploration missions beyond Low-Earth Orbit (LEO). This tool is developed to inform near-term decisions about long-term manned spaceflight infrastructures. A secondary objective is to present a tool for the exploration of precursor demonstration missions for the development of technologies and capabilities leading to the ability to successfully perform the arbitrary exploration missions described by the previous model. Another secondary objective is to describe a framework for the creation of architecture-level models of complex systems with the goal of reducing gratuitous and modeling-induced complexity.

These general objectives further decompose into a set of specific objectives. These specific objectives are grouped by their relation to the tools developed in this thesis.

HEXANE-Related Specific Objectives

Create a model that describes the in-space infrastructure architecture tradespace for manned exploration missions beyond LEO.

Evaluate and explore the tradespace of architectures in depth for Mars surface missions.

Evaluate and explore the tradespace of architectures for Lunar and Asteroid missions.

Determine and evaluate specific decisions at the architectural level that have the greatest influence on the overall mission architectures for Mars surface missions.

Determine and evaluate coupling relationships between architecture-level decisions that have the greatest influence on the mission architectures for Mars surface missions.

Low-E-Related Specific Objectives

Create a model that produces and explores the tradespace of demonstration sub-mission sequences as precursors to final science missions described by HEXANE.

Generate and evaluate the tradespace of demonstration sub-mission sequences for Lunar and low-energy NEA minimum-IMLEO final science missions.

Modeling Framework-Related Specific Objectives

Formulate a framework for the production of architecture-level complex system models with the goal of reducing gratuitous and modeling-induced complexity.

Compare the formulated framework with previously generated concepts to describe the benefits of a revised framework.

1.7 THESIS OVERVIEW

Chapter 2 of this thesis describes the methodology behind the creation of HEXANE, a model for the description and evaluation of the in-space infrastructure for manned exploration missions beyond Earth orbit. The scoping of the model from the more general problem is discussed, followed by a description of the system decomposition method, information about the inclusion of architecture-level technologies, the overall formulation of the model, and the structure of the model implementation. Validation of the model is also presented, along with a general summary.

Chapter 3 describes the evaluation of Mars surface missions in HEXANE, focusing on the determination and evaluation of architecture-level decisions that influence the properties of the architectures to the greatest degree. Eight decisions are identified along with a set of decision couplings as having potentially significant impact on the architectures. These are each studied in further detail, concluding with a set of recommendations for the timing of the associated decisions based on these results and levels of robustness against changes in the architectures.

Chapter 4 presents the modeling methodology and set of results for Low-E, a tool to enumerate and analyze the sequence of precursor demonstration missions for the development of

technologies and capabilities for the successful execution of surface science missions. The model leverages the results of HEXANE by integrating the outputs and expanding the optimal results to understand the precursor mission options and resulting tradespaces. Additional metrics are presented for the appropriate evaluation of these sub-missions as they relate to the overall campaign of missions. Chapter 4 also presents the results for Lunar and low-energy NEA IMLEO-optimal final science missions. General trends are identified, leading to a set of conclusions regarding commonality between demonstration mission sequences for these destinations and possible impacts on launch vehicle infrastructures, leading to recommendations for decision makers.

Chapter 5 formulates the concept behind a modeling framework for building architecture-level complex system models with the explicit goal of reducing gratuitous and modeling-induced complexity. A general framework is given, along with a more directed, specific framework for the integration of specific methods and tools.

Chapter 6 summarizes the findings and contributions of the thesis and highlights opportunities for further research.

Appendix A provides further technical details on the operation of HEXANE. Appendix B covers results from HEXANE for lunar, low-energy NEA, and high-energy NEA missions. Attached electronically is the code for HEXANE and Low-E.

2. HEXANE: HUMAN EXPLORATION ARCHITECTURE NETWORK EVALUATOR

Chapter 1 has given a brief introduction to the field of systems architecture, its application to manned exploration systems, and the need for the development of a model to deliver quantitative analysis of architecture-level elements to support decisions for future manned exploration systems. Chapter 2 describes the methodology used in the creation of such a model, HEXANE, focusing on the unique functional decomposition that allows for the broad exploration of a rich tradespace of potential exploration architectures. The scoping of the general problem to a tractable sub-problem is addressed, followed by a discussion of the functional decomposition, infused and optional technologies, the enabling of analysis through parametric relationships, the general model structure, and a set of validation cases. The chapter presents sufficient information for the recreation of the model, along with a complete understanding of its breadth and limitations. As the most encompassing case, Mars architectures will be used as the foundation for the description of the methodology as well as the base case for the results presented in Chapter 3.

Several efforts have been made to analyze manned space exploration architectures through systems architecting techniques over the last 10 years. Typically, these models have been developed specifically to validate a method as a case study or to explore a very specific set of architectural elements [14][16]. HEXANE has been developed as a tool explicitly designed to explore the relevant tradespace of architectures for manned exploration beyond low-Earth orbit (LEO). This has several implications. First, the methods for the development of the tool have been chosen explicitly to aid in efficiently exploring the tradespace while maintaining necessary rigor. Second, the program has been shaped to allow for dynamic definition of parameters for flexibility in future use. Third, HEXANE is designed to explore the complete tradespace, beyond the capabilities of previous models.

2.1 SCOPING AND PROBLEM STATEMENT

Given that HEXANE is designed to quantitatively explore a tradespace of architectures for a highly complex technical system, appropriate scoping of the system is necessary to allow for computation. This section presents the methods for the scoping of the system, which will be followed by a discussion of the modeling method. As a description of the full tradespace of human exploration systems infrastructures is far too broad, downscoping of the problem at hand is necessary in order to create a comprehensible set of analysis. The two methods of scoping are: a limitation on the *infrastructure elements* and a selection of *destinations*. The latter restricts the analysis

to overall missions of interest to NASA and its global counterparts, while the former reduces the complexity of the system by bounding around portions of the infrastructure that do not have set designs and are still able to be quantified given current ambiguities. Further, lower level assumptions that potentially influence the architectures at the modeling level of fidelity will also be addressed, along with the choice of overall abstraction for the model (*i.e.* how much to simplify).

2.1.1 Infrastructure Downscoping

HEXANE limits the design tradespace to the in-space portion of manned exploration architectures. In general, the overall infrastructure for such missions can be divided into three segments, as shown in Figure 10: Earth-based and launch operations, the in-space infrastructure, and surface operations.

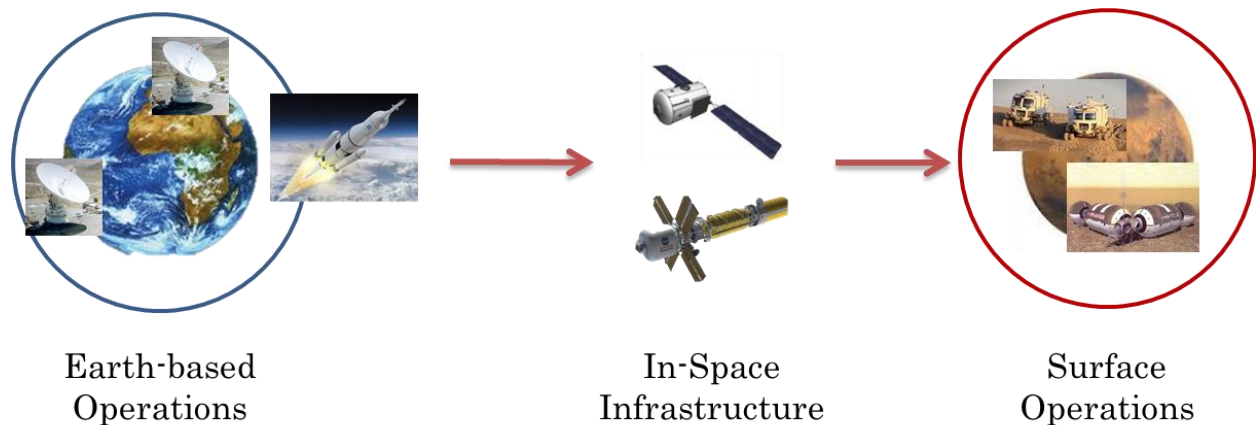


Figure 10: Manned Exploration Mission Segments

Earth-based resources, such as mission operations centers and data relay sites, have traditionally been set by heritage due to the expense of rebuilding and cross-usage among other programs. The new phase of launch vehicles, the Space Launch System [7], also currently has a set design, although production has not yet begun. These systems are unlikely to be redefined by high-level analysis, given the ingrained system heritage and/or the state of the system development. Surface operations are also unlikely to be defined by current analysis, as they are the least defined portion of mission architectures. Typically, the elements involved in surface operations are determined from the science requirements as coupled with the environmental requirements. There is a wide range of possible science missions for all of the destinations explored with HEXANE, and the inclusion of this breadth would add a considerable amount of complexity. Furthermore, these science missions are likely to change with time, both in the definition of specific science objectives as well as the

addition of new objectives. The exploration breadth of HEXANE is therefore limited to only include the in-space infrastructure portion of manned exploration missions in order to avoid the additional complexity and uncertainty associated with the science mission as well as to avoid the redefinition of developed resources for Earth-based operations and the launch infrastructure. Specifically, the model simulates the mission segments between low-Earth orbit (LEO) and destination orbit, descent to the destination, ascent from the destination, and return to Earth.

2.1.2 Destination Selection

In order to limit the set of possible exploration destinations, HEXANE includes lunar return, Mars missions, and a set of two representative asteroid missions as the baseline for all science missions. NASA and its international counterparts have debated the set of destinations appropriate for human exploration missions for many years, culminating in deliberations revolving around the concept of the “Flexible Path” [27][2][3] within the last ten years, such as the set proposed by the International Space Exploration Coordination Group (ISECG), shown in Figure 11 [28]. The three destinations described in such a path, regardless of the order in which they are explored or not explored, are generally the Moon, Mars, and Near Earth Asteroids (NEAs). In theory, these destinations allow for incremental technology development, building up mission elements for requirement-intensive surface missions by conducting a series of missions targeted at these destinations. NASA HAT is currently exploring detailed point designs for missions to these destinations [29]. The model reflects these location choices, both in deference to the foremost U.S. authority and in order to better coordinate result comparisons with NASA.

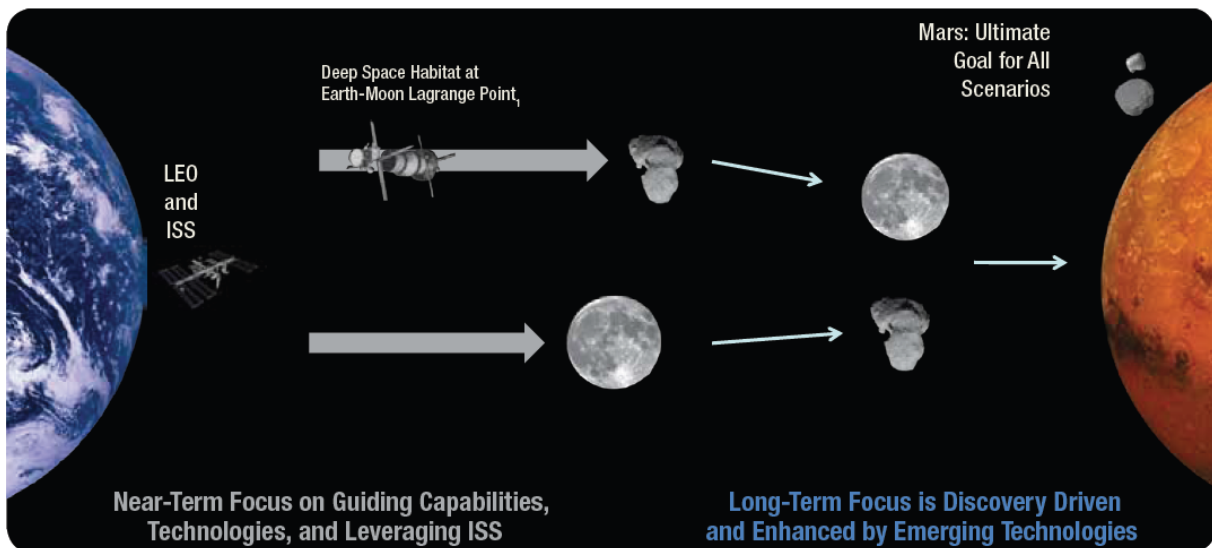


Figure 11: ISECG Multiple Paths to Mars

Of the three destinations, the NEAs involve the most ambiguity in terms of specific mission requirements. As there are many asteroids with a wide range of characteristics that may be classified as NEAs, two asteroids that represent the widest breadth of possibilities, one “High Energy NEA” and one “Low Energy NEA”, are included. Table 10 gives a comparison with Mars and Moon flyby missions in terms of energetic requirements. Since energetic requirements drive propellant mass, which has a compounding nature (*i.e.* an extra kilogram of propellant requires additional propellant to push that propellant and so forth), the NEAs are differentiated into these two classes based on this property. “High energy” NEAs have energetic requirements similar to Mars flyby missions, while “low energy” NEAs have energetic requirements similar to lunar flyby missions. Although these in theory represent a set of possible destinations, the specific numerical values used to model these generic destinations come from specific asteroids also being studied by NASA HAT, namely 2000SG344 [30] and 2008EV5 [31]. Although a variety of other asteroids could and should be considered as real mission destinations, they are not sufficiently different from the representative asteroids to necessitate their inclusion as separate destination choices.

Table 10: High and Low Energy Destination ΔV Comparison

Destination:	High Energy		Low Energy	
	Low Mars Orbit	High Energy NEA	Low Lunar Orbit	Low Energy NEA
LEO to Orbit Departure ΔV (m/s):	4272	4208	3150	3400

The “Flexible Path” often also includes other “non-solid” destinations, usually Earth-Moon or Earth-Sun Lagrange points. Typically these low-energy points are used for intermediate missions in campaigns that build toward other final destinations or as intermediate staging points during larger mission schemes. In this model these points are not included as distinct destinations for much the same reason. They are, however, included as intermediate staging locations, meaning that they can be used as points to pre-deploy elements that are “picked up” as a crew progresses toward the final mission destination.

Figure 12 gives a pictorial representation of the set of destinations and pathways. In summary, this study includes the evaluation of round-trip missions to the Moon, Mars, and a set of two representative NEAs. Each of these missions may also use one of several intermediate rendezvous points, including the most favorable Earth-Moon and Earth-Sun Lagrange points [32].

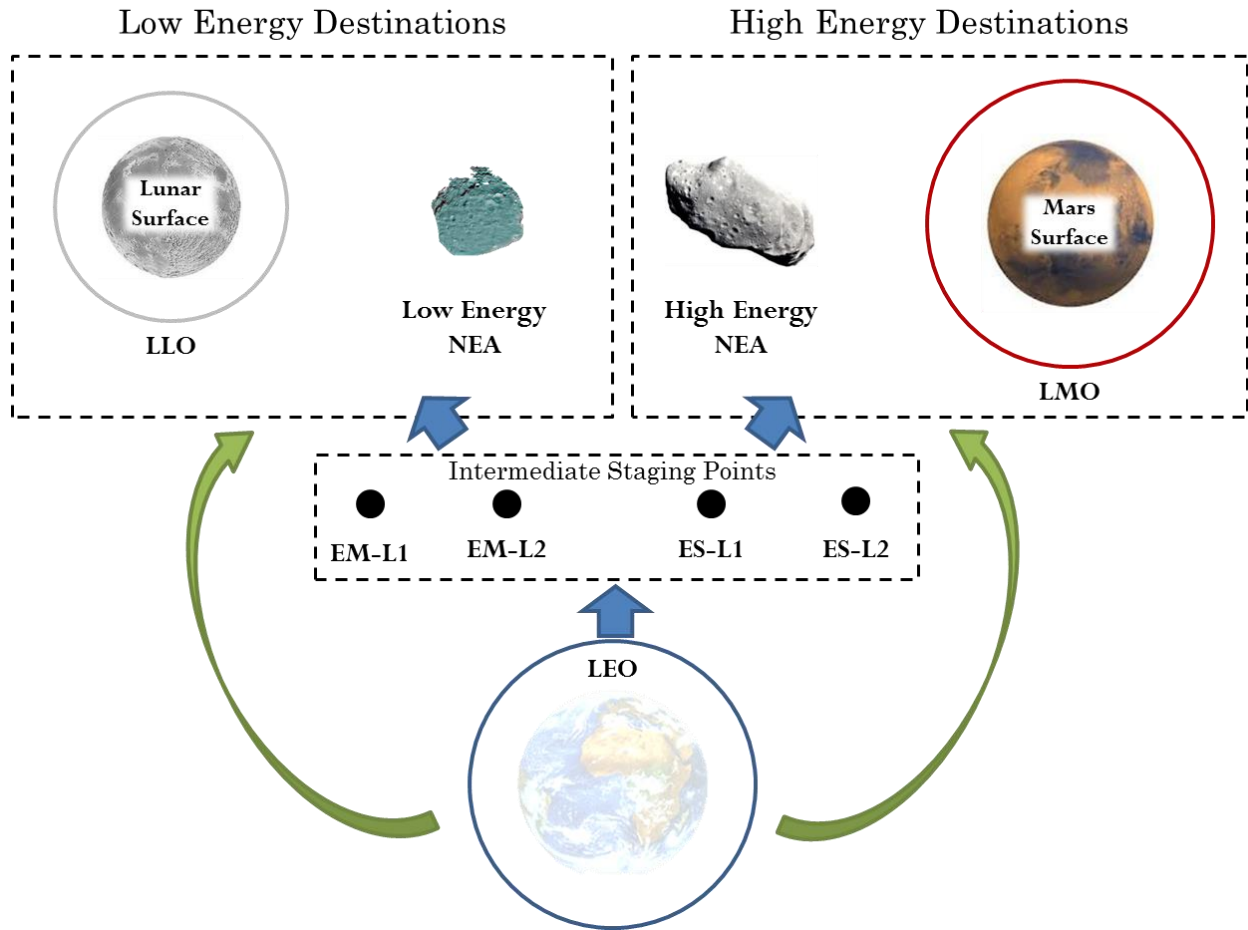


Figure 12: HEXANE Destinations and Pathways

2.1.3 Sortie-Like Mission Design

In order to limit the complexity of the analysis, the model applies some further assumptions about the nature of the manned exploration missions. A significant reduction of complexity is accomplished by limiting each mission to be “sortie-like” only. This means that each individual mission is assumed to be stand-alone, outside of the context of a larger campaign of missions. This has several implications. During the given mission, each element is discarded at the end of its functional use. For example, if a deep-space habitat is only used to get to Mars in a particular mission, it is discarded at Mars orbit after the crew transfers to a descent module. In some mission architectures, this habitat would instead be sent back to a staging point to be re-used in a later mission. This architecture would require additional propellant to transfer the habitat to such a location as well as imposing additional requirements on the habitat for extended use. In order to define those additional requirements, knowledge of the overall campaign would be necessary.

Because this would require significant additional analysis for each mission architecture, it is therefore assumed that no such greater campaign exists. Future work should integrate these missions into a larger campaign structure.

2.1.4 Abstraction

Under the constraints listed, the problem of interest has been scoped to the in-space portion of the transportation infrastructure, specifically as it relates to a set of solid solar system destinations that have been deemed feasible and interesting by NASA and the global space community. The overall fidelity of a model, however, is set by two variables: the scoping of the context of the problem and the level of abstraction at which the problem is analyzed. NASA’s traditional point designs, such as DRA 5.0, look at both a larger context and analyze missions at fine detail (*i.e.* a low level of abstraction). Typically, this detail will either be at the subsystem or component level. This, in turn, necessitates the use of significant man-power and the reduction of the tradespace to one or a few architectures. HEXANE looks to complement this type of analysis by analyzing a significantly larger set of mission architectures at the cost of the fidelity of the analysis in order to remain within reasonable resource requirements. Specifically, only architecture-level elements are analyzed.

The issue therefore becomes a question of what constitutes an “architecture-level element.” This term is ambiguous outside the context of a specific problem and desired tradespace. For this model, these elements are defined as system components that require large (billion dollar or more) investments for the development of the system and have the potential to change the mass of the total system on the order of metric tons or more. This includes both large physical elements as well as near- and mid-term large-scale technologies. Section 2.3 presents a listing of these technologies. Such a threshold for inclusion in the system is not absolute – it requires the use of expert knowledge and experience in order to decide which features are considered “architecture-level,” and it is not a claim that this model includes all such features, either present or future. However, the functional decomposition of the in-space mission infrastructure aids in understanding the definition of architecture-level elements for this model.

2.2 HABITATION AND TRANSPORTATION FUNCTIONAL DECOMPOSITION

Although the problem at hand has been scoped to allow for quantitative analysis under given resource constraints, an understanding of the elements of the system (*i.e.* the parts of the system that drive the emergent behavior of interest) is necessary in order to accurately model such a complex system. A decomposition from the highest level to one that retains enough complexity to model interesting behavior while creating diversity in the design space allows for this further insight

into the system. Typically, the clearest way to decompose a complex technical system is to cleave upon obvious groupings of physical system elements. This is most directly reflected in traditional systems engineering, where design teams are broken into groups focused on the primary subsystems. However, this requires prior knowledge of where these subsystems cleave. Figure 13 gives an example of a well-understood system that has been cleaved along physical sub-systems [33]. This elevator system has three elements at the first layer of decomposition, separating the people, elevator car, and controls system. The elevator car is further decomposed in the second layer into four sub-systems. These are well-established groups because designers understand intuitively, given their experience, that the interfaces between these sub-systems have minimal interactions.

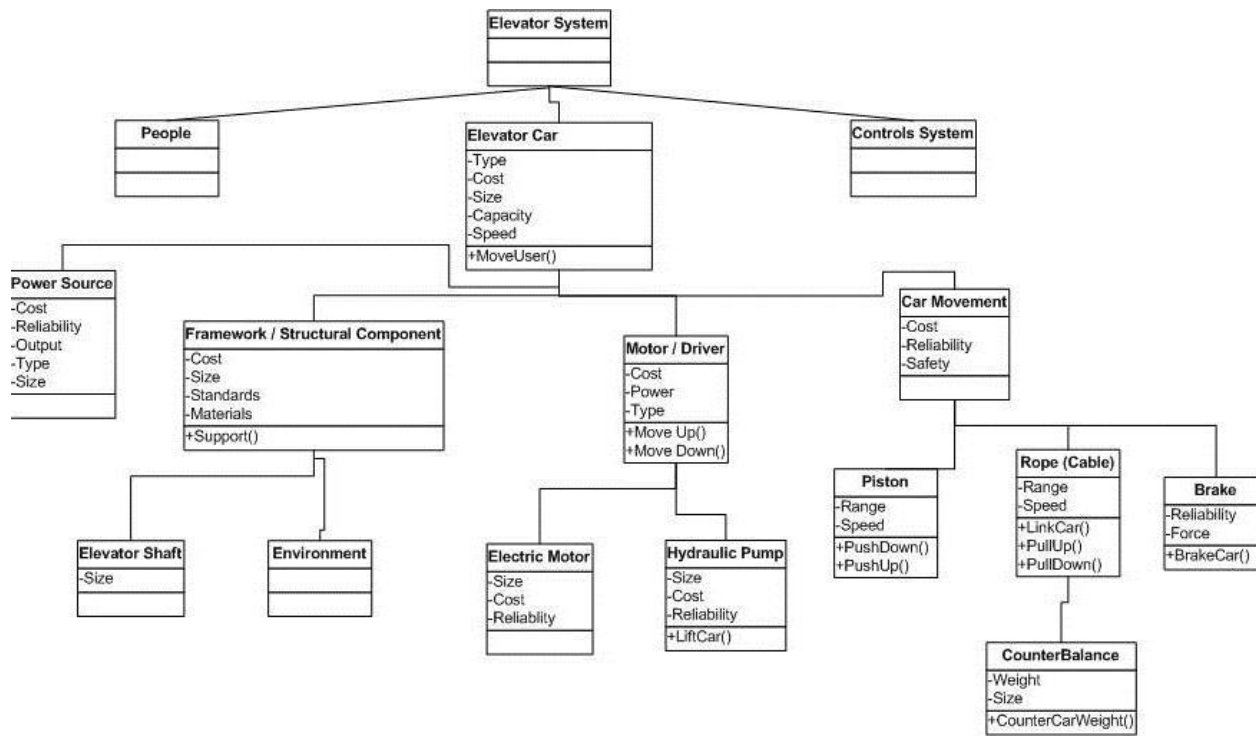


Figure 13: Elevator Sub-System Decomposition

Although there are rigorous methods for determining where such sub-systems cleave from each other [34][35][36], complex systems with significant heritage often have relevant experts who are able to determine the best or near-best points of cleavage. This experiential knowledge has served well for decades in systems like automobiles, but it tends to fail with new and complex systems.

This ability to decompose a system by experience is directly contrasted by new or unusual systems that lack the same level of system heritage. New and simple systems often decompose easily enough that formal methods are unnecessary. Highly complex systems, on the other hand,

often are convoluted enough to necessitate more rigorous formal methods. These methods fall into two general categories. The first is data intensive, requiring large amounts of data on the internal structure and flow of the system. Algorithms group the system elements to create minimal interaction interfaces [35]. The second set of methods seeks to generalize the decomposition approach. This involves the abstraction of the system to a point where there is sufficient knowledge to draw conclusions about the relationships between the abstracted elements or functions. Such methods are necessary when insufficient knowledge of the coupling between elements exists. Abstracting upwards tends to generalize the system decomposition. This second method set is appropriate for the system at hand for two reasons. Firstly, there is minimal system heritage from which to draw information, and the level of detailed knowledge for advanced modern systems is insufficient for the first approach. Secondly, it is desired to abstract the system to a point at which a larger tradespace can be analyzed, and therefore the second method accomplishes this while providing a more rigorous decomposition.

2.2.1 Primal Functions

A generalized functional decomposition falls into the second of the two categories described above. For a given system, it is sought to determine the basic or “primal” functions that are necessary for the success of the system. These primal functions help determine the fundamental drivers of the value delivery for the system. The success of the system is determined by its value proposition to the beneficiary of the system [37] and therefore the value delivery mechanism. In the case of in-space transportation infrastructures for manned exploration missions, the value takes two forms. First, it is absolutely necessary to **keep the astronauts alive and return them to Earth’s surface** under the constraints imposed by NASA’s relevant regulations [38], [39]. Second, the overall purpose of the mission is to **gather knowledge**. This can take the form of various types of **science knowledge**, such as planetary information gathered on the surface, or it may include **technical knowledge** about the performance of the mission elements. This technical information is the primary focus of demonstration missions, where the main purpose is to test and gather performance information for newly-developed elements for use in later missions. As the model here presented assumes missions are “sortie-like” only, demonstration missions are not included in the analysis, and therefore the technical knowledge is not the focus for value delivery. The sequence of demonstration missions will, however, be addressed by a different tool described in Chapter 4.

The knowledge gathered from exploration missions derives primarily from surface operations, although some knowledge may be gained during the transfer from Earth to the destination. Due to the decoupling of the model from this portion of mission architectures, this value delivery mechanism is not directly addressed. This leaves only one main value delivery pathway for manned

exploration missions to be addressed by the model.

In order to deliver value through successful transportation of the astronauts, they must be transported from the Earth to the destination surface and back in a safe manner. This means that all successful mission architectures must include the mechanisms to transport the astronauts from Earth to the destination and back in a safe manner as determined by the relevant regulations. Due to the functional nature of this requirement, it is most easily mapped to functions performed by the in-space architecture itself. In combination with the lack of detailed coupling information leading away from a decomposition of form, it becomes clear that a generalized functional decomposition of the system is the most appropriate method for decomposition at the architectural level. To satisfy the value delivery mechanism described, there are two primal functions present. The first comes directly from the statement: the astronauts must be *transported* from Earth to the destination and back. The second reflects the need to do this in a safe manner for the astronauts, or the need to provide appropriate *habitation*. Therefore the primal functions for the system of interest are *transportation* and *habitation*. **These are considered primal because they are the most highly abstracted versions of the basic requirements for the value delivery mechanism and are mutually exclusive.**

2.2.2 Temporal- & Requirement-based Sub-Functions

With the primal functions for the in-space infrastructure defined, the space of sub-functions can be determined from this set. Understanding the next level of function granularity allows for the creation of a richer tradespace of architectures, given that the primal functions alone do not drive the complex behavior of interest. It will be shown that the forms mapped to the sub-functions also meet the outlined criteria to be considered architectural elements in this context. A variety of methods exist to further decompose these primal functions. For the habitation function, a traditional decomposition would determine the subset of requirements for retaining the astronauts' health, such as air revitalization and waste management, like that shown in Figure 14 for the ISS [40]. However, this necessitates the decomposition to a subsystem or component level, which requires analysis at a higher fidelity than the architectural level and therefore increased computational resources. An alternative method **decomposes along sets of integrated requirements**. This is distinctive for the in-space transportation architecture system, as the astronauts must pass through multiple unique environments requiring fundamentally different types of habitable environments. For example, the zero-g space environment is very different from the descent through the Mars atmosphere, making the fundamental requirements of the habitats for these environments significantly different. In each of these environments, the more traditional functional decomposition still applies, but the decomposition remains constant through these environmental changes. This consistency is desirable for other purposes but does not allow for a

decomposition that is not dependent on high-fidelity information. By grouping with environment and therefore major requirements changes, a set of sub-functions can be derived that creates a rich tradespace without the need for higher fidelity.



Space Station Regenerative ECLSS Flow Diagram (Current Baseline)

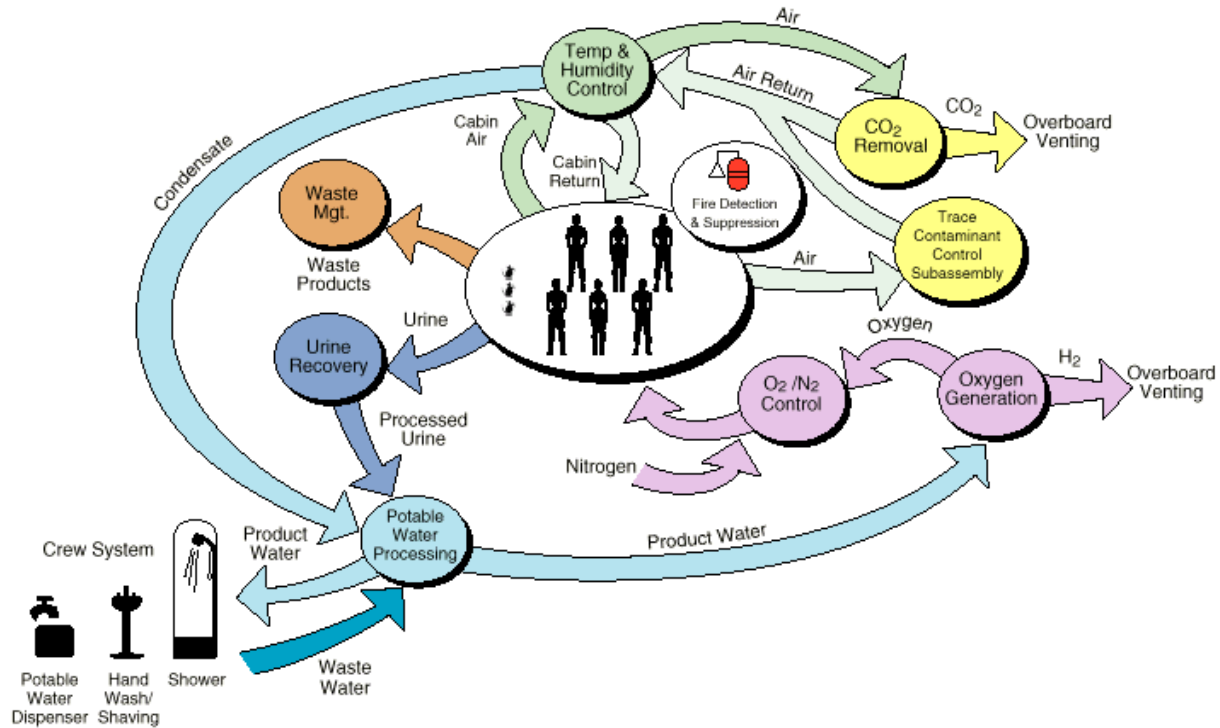


Figure 14: ISS ECLSS Decomposition and Flow Diagram

Due to the nature of the environmental changes, this grouping of fundamental requirements also corresponds to a **temporal decomposition**, *i.e.* the sub-functions corresponding to the groups of requirements are also sequential with time throughout the exploration mission. As can be seen in Figure 15, this decomposition method leads to seven habitation sub-functions: the launch segment, deep space habitation (outbound), descent, surface habitation, ascent, deep space habitation (inbound), and Earth re-entry. There are several features of importance in this sub-function set. The first is the inclusion of two deep space habitation phases. Both of these phases have very similar fundamental requirements, as the environment in which they operate is the same. They are separated for two reasons. Firstly, this retains the concept of temporal separation. These phases are separated from each other by mission segments. Secondly, it may be advantageous to separate the habitat into two segments with shorter lifetime requirements.

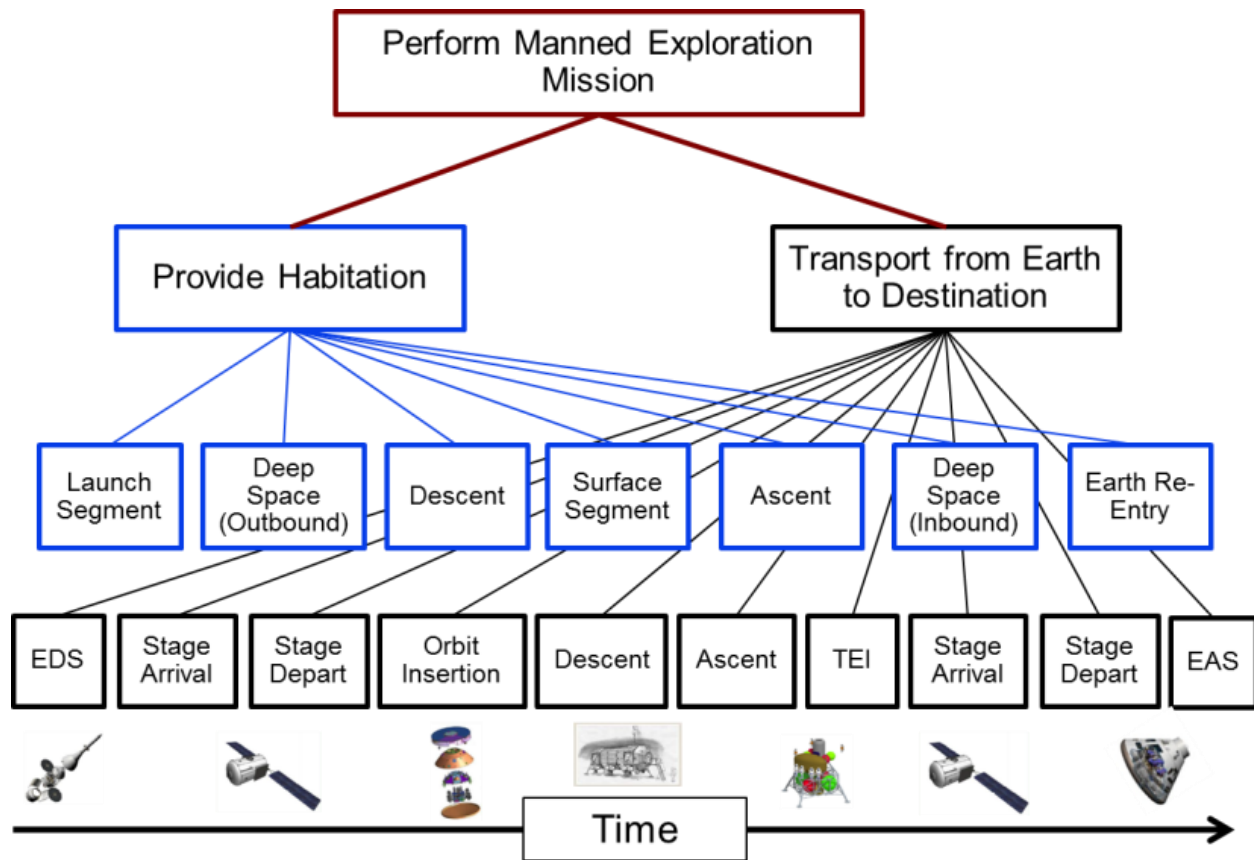


Figure 15: Sub-Function Decomposition of In-Space Infrastructure Primal Functions

The second feature in the sub-function set is the inclusion of the launch segment, surface segment, and Earth re-entry segment, which were previously explicitly decoupled from the tradespace. These sub-functions represent only the specific living environments for the astronauts and therefore remain decoupled from the remainder of the elements present in launch and surface operations. For man-rated launch vehicles, the manned capsule is treated much the same as other cargo in the fact that it does not contribute to the performance of the vehicle. There are considerations for the integration of the manned capsule as well as launch abort systems that may drive further analysis beyond this model. However, these considerations are minor in comparison to the considerations that drive the decoupling of the launch system in general. The same is true for the surface habitat. In this case, the habitat provides the living environment for the astronauts during surface operations and therefore is decoupled from the remainder of the surface operations. Again, there are further considerations, such as the inclusion of pressurized rovers in which some astronauts could live for several days, as is present in some reference architectures [17]. However, it is assumed that all astronauts must use the surface habitat for the duration of the surface operations and that the majority of the design of said habitat is not heavily influenced by other

portions of the surface operations. Furthermore, it is desired to investigate the combination of this sort of habitat with other habitats, and therefore it is desired to be included in the list of sub-functions.

A similar decomposition can be performed for the transportation functions. The transportation sub-functions are **grouped by major ΔV operations**. These include stages such as the Earth Departure Stage (EDS), orbit insertion, descent, and ascent. This also includes the arrival and departure burns from the intermediate staging locations, as these may require maneuvers on the order of km/s in ΔV . Like the habitation sub-functions, this method also corresponds to a temporal decomposition, with ten segments throughout the mission, as seen in Figure 15. With the exception of the intermediate staging location burns, the remainder of the ten are self-evident in their necessity in the set. It should be noted that small burns, such as the de-orbit burn prior to descent, are typically included in the following major burn, although they have only minor impacts on the architectures, and therefore are excluded from the sub-function set.

In conclusion, the primal functions of habitation and transportation are decomposed into seven and ten sub-functions, respectively. The cleavage points for this decomposition are based on a combination of requirements grouping and temporal segmentation, with environmental changes driving habitation sub-functions and ΔV requirements driving transportation sub-functions.

2.2.3 Representation in an Exploration Mission Context

The set of seven and ten habitation and transportation sub-functions, respectively, are more easily visualized in the context of a specific destination. Of the set of destinations previously described, Mars is the most exhaustive in terms of requirements. Therefore a Mars conjunction class mission will be used to describe the context of the sub-functions. An opposition class mission is not described for clarity, given that the mission has increased complexity due to the Venus flyby necessary in opposition class missions. Furthermore, long-stay conjunction class missions are the baseline for the majority of point designs studied by NASA and its global counterparts. In Figure 16 and Figure 17, Earth and Mars are represented, along with Earth orbit (in black, left curve), intermediate staging locations (center line in black, given as Earth-Moon L2), and Mars orbit (in black, right curve). The red arrows represent the mission path for the astronauts, leaving Earth's surface, going to Mars surface, and returning. Figure 16 shows the habitation sub-functions, while Figure 17 shows the transportation sub-functions. Examples of corresponding hardware are also shown for the habitation functions, although these do not correspond to the formal mapping of every architecture. The matching between the temporal and requirement-based decompositions becomes clearer in this mission context.

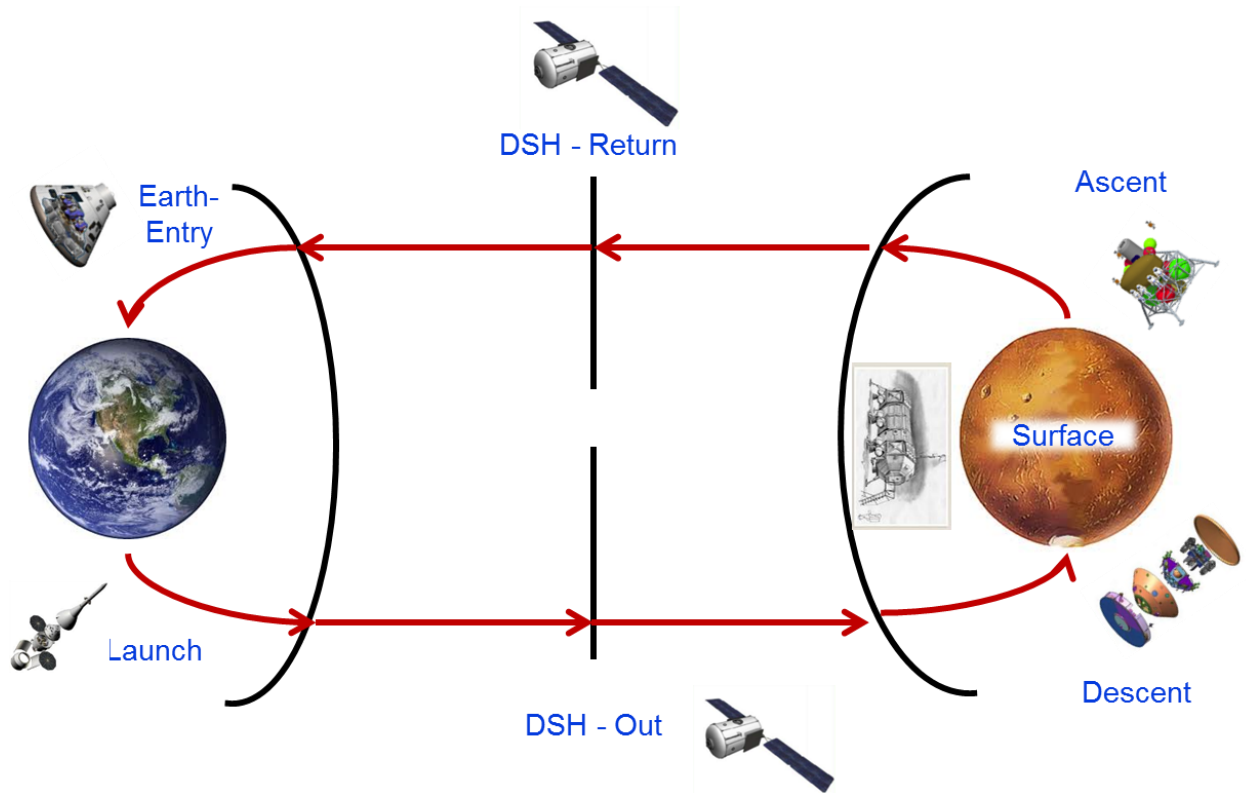


Figure 16: Habitation Sub-Functions in Mars Conjunction-Class Mission Context

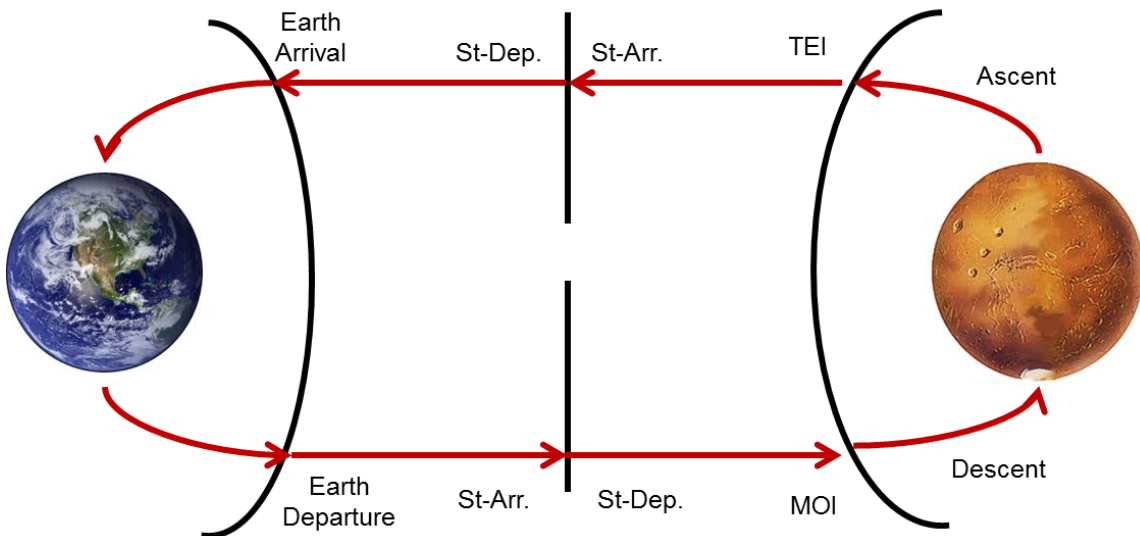


Figure 17: Transportation Sub-Functions in Mars Conjunction-Class Mission Context

2.2.4 Invariant Functions and Set Partitioning

This method of decomposition has advantageous features for the exploration of a rich architecture tradespace. The temporal nature of the decomposition indicates that these sub-

functions are invariant, meaning that they are both present and necessary in all architectures. For a few destinations, namely the NEAs, there are some exceptions. For the asteroids, there are also no traditional surface operations, and therefore the descent, surface, and ascent sub-functions in both domains are significantly different. They are instead replaced with exploration vehicle requirements, where a small capsule approaches and examines the asteroid from the primary habitat. In general, it is also not necessary to stop at one or more intermediate staging locations, and therefore the stage arrival and departure sub-functions in the transportation domain become irrelevant. However, the mission must always pass through these phases in the model. Therefore, by “zeroing out” the requirements for these phases, driving propulsion element masses to zero, these sub-functions are still present and satisfied, although irrelevant. Under these conditions, all of the sub-functions can be considered to be invariant, given that the mission must always pass through these phases, even when irrelevant.

Because of the invariance of these sub-functions, along with their non-repeatable nature (each sub-function must be accomplished once and only once), the function-to-form mapping, which assigns these sub-functions to elements of form, can be accomplished through a **set partitioning method**. For each of the primal functions, the corresponding set of sub-functions is partitioned such that each group corresponds to a formal element that integrates the requirements inherent in each of the sub-functions. An example for the habitation sub-functions is shown in Figure 18, using Apollo’s lunar orbit rendezvous. In this case, the command and service module groups four of the seven sub-functions and the lunar excursion module groups three.

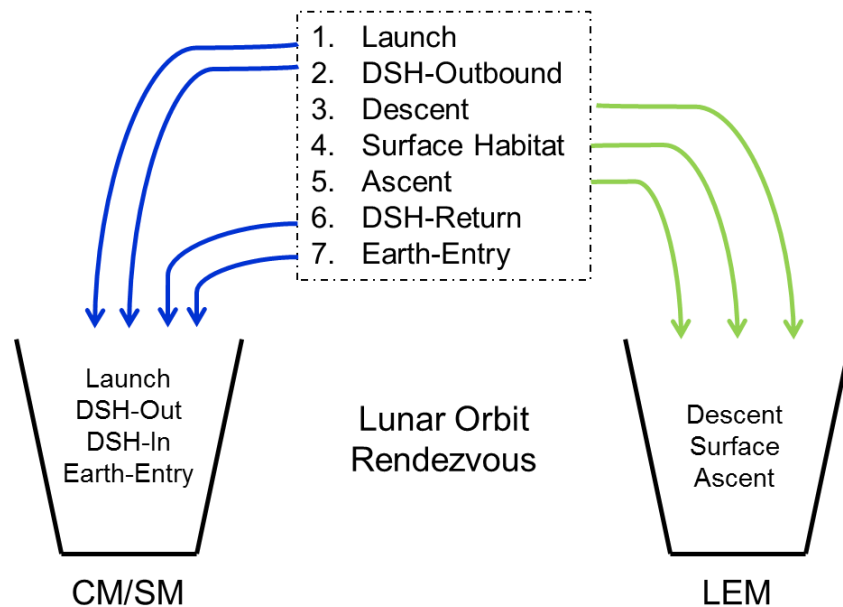


Figure 18: Lunar Orbit Rendezvous Set Partitioning Example

The use of set partitioning is advantageous given that it is a well-studied mathematical structure [41], and therefore there are many known efficient methods of analysis and enumeration [42][43]. It also creates a rich tradespace of interesting architectural elements. The extent of the set of possible combinations is beyond the capabilities of experts to trade using traditional methods without computational tools. Even with modern computational techniques, such an extensive tradespace is daunting to analyze. Because this analysis only takes place at the architectural level, the amount of computational power necessary for such an analysis is much decreased as compared to a high-fidelity analysis, and therefore this is within the grasp of current technology with the use of parallel computing. This also implies that **this tradespace analysis has the potential to explore portions of the habitat and propulsion element combinations that have never been considered by experts conducting point designs**. Due to the complex nature of the system, these portions of the tradespace may have emergent properties that lead to advantageous architectures that have never before been considered. Truly, this is the key contribution of this study, given that these areas are explored along with their coupling with architecture-level technologies.

After elimination of logical inconsistencies present in many of the set partitions, each of the problems corresponding to the primal functions has a selection group of 120 and 776 options, respectively. These are down-selected from the full set through pre-deployment assumptions. Specifically, in-space elements must travel on the fast trajectory and surface (descent, surface, and ascent) elements should be pre-deployed (or not) as a group. Unfortunately, the richness of this tradespace leads to difficulties with the intelligibility of the system for both the engineer and interested stakeholders. Presenting the set of partitioned sub-functions is more intelligible than the set of resulting groups, and this is again more intelligible than the worst-case scenario of $(2^{10}-1)(2^7-1)$ binary options associated with grouping sub-functions with each other. Despite this issue, the uniqueness and richness of the tradespace is more desirable than increased intelligibility gained from an alternative decomposition.

2.3 ARCHITECTURE-LEVEL TECHNOLOGIES

To complement the set of habitation and transportation features, which may be regarded as more traditional architectural features, a set of architecture-level technologies were also included in the tradespace. As previously stated, these technologies were chosen from among the set of near- and mid-term technologies that have the potential to heavily impact the mass of the resulting overall architecture. HEXANE includes four such technologies: *in-situ* resource utilization (ISRU) for those destinations with appropriate resources, orbital aerocapture at atmospheric planets, boil-off control for use with advanced cryogenic propellants, and a set of advanced propellants.

Propellant options for the major in-space maneuvers include liquid oxygen and liquid hydrogen (LOX/LH₂), liquid oxygen and liquid methane (LOX/LCH₄), and nuclear thermal rockets (NTR) with liquid hydrogen fuel. Propellant options for the descent and ascent maneuvers include LOX/LH₂, LOX/CH₄, and nitrogen tetroxide and monomethylhydrazine (NTO/MMH). The options between in-space maneuvers and descent and ascent maneuvers differ given that NTR is clearly not suited for descent and ascent stages, with the very large fixed mass and thrusting characteristics, and NTO/MMH is not sufficiently mass-efficient for in-space maneuvers. Technical details can be found in Appendix A.

In addition to these technologies, each architecture includes an option to pre-deploy cargo elements on a low-thrust trajectory using a separate launch stack. The model assumes the use of a solar-electric propulsion (SEP) element in all pre-deployment cases. An option to pre-deploy using a high-thrust propellant was not included, as this has no mass impact on the architecture under the level of fidelity analyzed. From a mass perspective, using two separate rockets with the same propulsion technology and staging does not provide any advantage. Therefore, since this separation does not influence any of the metrics employed in this model, the option to separate out a high-thrust pre-deployment stack is not included. The choice of SEP, as opposed to other low-thrust options, was directly related to HAT's decision to include this propulsion technology in their own analysis [44]. Their internal, high fidelity studies led to the conclusion that SEP was the most viable option, and this will not be further discussed in this thesis. Performance characteristics for the SEP elements were taken from recent NASA HAT studies [44][45]. The sizing method for SEP elements, along with energetic requirement estimation can be found in Appendix A.

2.4 FORMULATION AS AN ASSIGNMENT PROBLEM

Integration of analysis at an architecture level into decision-making processes often presents difficulties due to its abstracted nature and lack of detail typically associated with technical analysis. A useful tool that both aids in the development of architecture-level models and improves the translation between model results and decision-makers is the assignment formulation developed by Willard Simmons [14]. In this formulation, architecture options are expressed as decisions for the system architect. For each system element, a set of options exists from which to choose, among which the architect may choose one and only one. This can most easily be presented in the form of a morphological matrix [46]. Figure 19 presents the morphological matrix for this model.

In the case of the HEXANE model, the function-to-form mapping of the architecture elements is highly conducive to the use of the assignment formulation. The decision problems are divided into three sets. The first set includes the **fixed science parameters**, which are static for any given tradespace enumeration. These are options that affect both the architectural elements as well

as the science value of the mission. Since it is desired that the set of architectures has a fixed science value, these must be fixed for any given analysis. However, by including them as options, more flexibility is granted within the HEXANE model. Specifically, this allows for the manipulation of the science mission parameters as requirements change. These include features such as the number of crew, the duration of surface operations, and the intermediate staging location options, as well as the basic destination options.

The second set of decisions relates to the more traditional architectural features, namely the **habitation and transportation partition options** along with the pre-deployment option. These are exhaustively enumerated for each analysis and are primarily responsible for the expansion of the tradespace due to the number of options for the set partitions. The third set includes the **architecture-level technologies**. These are fundamentally different from the “architectural features” due to the binary nature of most options (either being present or not) and trinary nature of the propellant options. Furthermore, these correspond to significant R&D investments, rather than primarily development work that would be done for habitats and propulsion stages with well-developed techniques.

Fixed Science Parameters									
Destination	Mars	Moon	NEA (High Energy)	NEA (Low Energy)					
Number of Crew	3	4	5	6					(any user input)
Surface Mission Duration	7	14	21	30	90	180	360	500	(any user input)
Possible Outbound Staging Locations	EML1	EML2	SEL1	SEL2	Phobos	None			
Possible Inbound Staging Locations	EML1	EML2	SEL1	SEL2	Phobos	None			
Enumerated Features									
Architectural Features									
Habitation Distribution	α	β	γ	δ	...	120 Combinations			
Propulsion Element Distribution	α	β	γ	δ	...	776 Combinations			
Pre-Deployment (via SEP)	Yes	No							
Technologies									
Boil-off control for propellants	Yes	No							
ISRU	Yes	No							
Aerocapture	Yes	No							
TDI Propellant Type	LOX/LH2	LOX/LCH4	NTR						
Descent Propellant	LOX/LH2	LOX/LCH4	N2O4/MMH						
Ascent Propellant	LOX/LH2	LOX/LCH4	N2O4/MMH						
TEI Propellant	LOX/LH2	LOX/LCH4	NTR						
(Pre-Deployment Propellant)	SEP								

Figure 19: HEXANE Assignment Problem Morphological Matrix

In a given enumeration of architectures, the destination and other science parameters are set by the architect, while the remaining decision sets are exhaustively enumerated. This gives a combined tradespace of over 120 million architectures per fixed science parameter set.

2.5 PARAMETRICS

2.5.1 The Need for Parametrics

Given the unique functional decomposition of the in-space infrastructure and the richness of the resulting tradespace, the question of how to enable the analysis of such a breadth of architectures becomes prominent. The analytical engine must both allow for extreme flexibility in the definition of habitats and transportation elements as well as exceptionally fast computation. This drives toward the use of top-down analysis, where system-level properties are used to derive higher fidelity information from established correlations. Parametric relationships are a well-established method to estimate such values from limited system-level information [47]. Parametrics draw on established information from known system parameters to describe a relationship between those properties.

In this case, parametrics enable the computation of habitat masses and logistics masses. For point design studies, these elements are typically designed using a bottom-up method, where domain experts determine the complete design from the component level. This is highly resource intensive and therefore not appropriate for this analysis. The parametrics compromise both fidelity and a level of robustness for a considerable reduction in required resources. The lack of system heritage for elements such as surface habitats leads to the compromise of robustness, given that the parametric data must be drawn from point designs rather than real data. Because these parametrics are not based in real systems, their robustness to changes in available data is limited. The logistics parametrics are more reliable due to data from ISS elements, and therefore only the fidelity loss from the use of parametrics is apparent in the results. For the habitat elements, construction method assumptions allow for the generalization of the parametrics to the combinations of habitation sub-functions and therefore the flexibility desired by the decomposition of the model. More specifically, it is assumed that all habitats are constructed using rigid wall methods rather than inflatable technology. Although the latter may be a viable option for future missions and future models, the lack of data for inflatable habitats restricts their incorporation into the current model.

Under the assumption of rigid wall habitats, a parametric was drawn relating total habitat volume to total mass using data from ISS modules and Skylab [48][49], whose data is shown in Table 11, and the parametric is found in Figure 20. It should be noted that this parametric is only applicable for use in habitats experiencing minimal stress in zero-g environments, similar to the ISS

environment. Other relationships were determined for the remainder of the operating environments.

Table 11: Habitat Parametric Data

Historical Reference	Volume [m³]	Mass [kg]
ISS USOS US habitat	160	20230
Skylab OWS	270	35100
ISS Destiny	106	14520

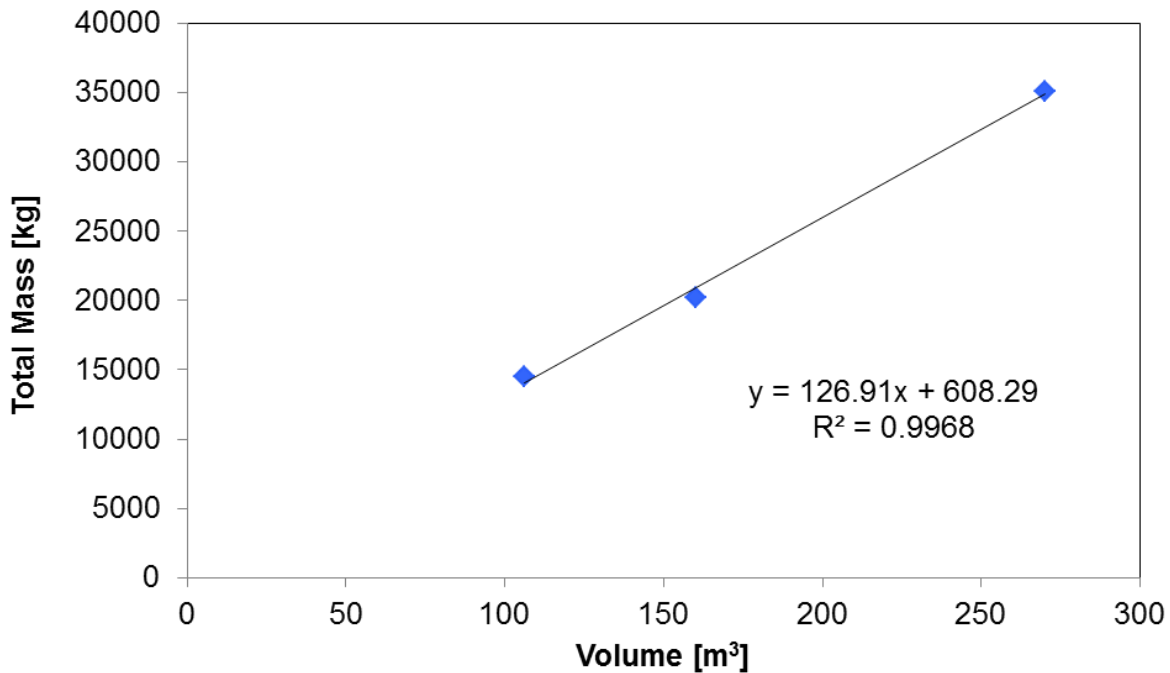


Figure 20: Habitat Parametric between Total Mass and Total Volume

With this establishment of this relationship, the known properties of the architecture must be used to determine the required volume for each habitat. For long-duration habitats, HEXANE’s parametric is based on recent work by NASA’s Habitable Volume Workshop [50]. Figure 21 shows their parametric relationship between specific volume and duration using both historical data and recent detailed ground-up point designs. For crewed segments in deep space habitats with flight times of over 10 days, this parametric is used in conjunction with that in Figure 20 to produce an overall habitat mass from the TOF and number of crew.

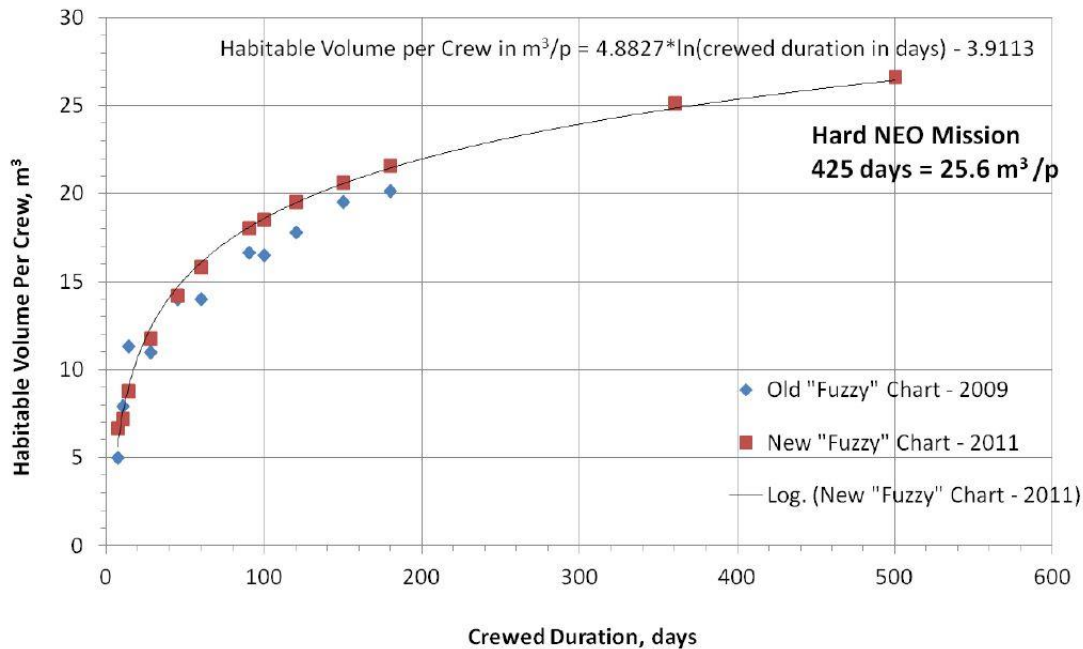


Figure 21: NASA Habitable Volume Workshop Parametric

This relationship is not applicable for habitats not operating in the same environment as the historical missions, and therefore other parametrics have been established for short duration habitats, re-entry vehicles, descent, ascent, and surface habitation. Short-duration and re-entry vehicle parametrics are drawn from historical data of capsules with similar requirements [51] and information available in the NASA Handbook on Human Integration Design (HIDH) [52]. Descent, ascent, and surface vehicle parametrics were designed using the most detailed and vetted point designs available [17], [19], [22]. Further information on these relationships can be found in Appendix A.

In short, the mass estimation for habitats and logistics in the in-space infrastructure model are dependent on the use of parametrics, which enables reliable, top-down, and quick calculation. These properties therefore enable the exploration of a broad and rich tradespace of habitat sub-function combinations under the constraints of limited resources.

2.5.2 Assumptions

The methodology for decomposing the overall system and the top-down development of major element properties has been presented. However, there are many assumptions involved in the development of this methodology that may impact the results generated from this methodology.

There are several technical assumptions that may influence the final feasibility of the presented architectures. Although all of these assumptions are recognized as possible shortcomings of the model, most assumptions should not impact the system metrics at this level of abstraction (*i.e.* the architectural level). The majority of these assumptions would need to be addressed for higher fidelity studies, but due to the nature of this work, such fidelity is not necessary. Not all of the assumptions present in the model will be stated here; rather, a set of assumptions that potentially impact the reliability of the resulting analysis will be presented.

Possibly the most impactful assumption arises from the allocation of multiple functions to elements of form. It is assumed that the complexity involved in the combination of multiple functions can be designed into any given element of form, even when all required functions are so allocated. Furthermore, it is assumed in the case of the habitation functions that the largest sub-function dominates the final form. For example, if both the descent and ascent functions are combined, the descent mass dominates due to the greater loading environment during descent, which drives structure mass. Therefore, the mass of the combined ascent/descent vehicle is assumed to be approximately the same as the descent vehicle alone. While it is recognized that the combination of functions would require additional complexity in design, likely resulting in increased mass, there is insufficient data to determine the increase in mass due to function-driven complexity. Ideally, each functional combination would be associated with a relationship between complexity and mass. However, no such data exists to extrapolate these relationships. Therefore, it is assumed that this simplification is sufficient at this level of abstraction.

For the propulsion functional allocation, the masses are driven by the ΔV requirements of the stages and therefore do not suffer from this limitation. There are other technical assumptions, although less impactful, that also influence the fidelity of the propulsion stage results. For example, the dry mass fraction is assumed to be constant, regardless of stage size, and this fraction incorporates thruster mass. Thrusters are therefore not sized by application, as there are, in many cases, no such thrusters in existence for reference data. Boil-off rate is also constant by propulsion type, regardless of tank size and prior boil-off.

One significant assumption impacts both habitation and propulsion elements: packing volume and assembly. Due to the decoupling from the launch infrastructure, no assumptions are made about limitations on tank volume or habitat diameter. However, the same result can be accomplished with current or mid-term future technology under the assumption that on-orbit assembly can be done with little additional structural mass requirements. This does impact final mass requirements. It is reasonable to assume that all architectures will be influenced similarly, thus retaining the relative ordering of the results.

Some additional assumptions pertaining to the technology options should also be mentioned. For aerocapture systems, it is assumed that an aerocapture shroud can be developed for any of the

proposed propulsion systems, up to very large sizes. Shielding of this magnitude has been researched primarily for future EDL systems and has been shown to be feasible, such as in Samareh and Komar’s work [53]. All propulsion technologies are assumed to be scalable to the mission requirements. ISRU is assumed to always be capable of producing the necessary ascent propellant, although this changes by destination resources. It is also assumed that this propellant can be produced in the mission timeline, either prior to astronaut landing or during the crewed phase.

A more complete list of model assumptions can be found in Appendix A. Those presented here are assumed to be the most impactful at the architectural level and therefore the most relevant to those interpreting the results presented in Chapter 3.

2.5.3 Metrics

Another key to properly interpreting the results of the model and the following analysis is understanding the metrics used to evaluate the architectures. The relationship between architectures heavily depends on exactly how the metrics are calculated, and therefore they are here presented in detail. In general, when establishing system-level metrics, all aspects of the iron triangle should be considered: performance, cost, schedule, and risk [54]. In the case of HEXANE, performance of the architecture is directly tied to the science value that is produced by the mission. As stated, for any given enumeration and evaluation, this science value is fixed, and therefore the analysis becomes iso-performance in science value. In all other relevant aspects, the in-space portion of a mission architecture remains constant in the value it delivers by simply transporting the astronauts and keeping them alive and safe as constrained by relevant regulations. Therefore, the performance aspect of the iron triangle is not addressed directly by any metrics. Schedule, in the purely temporal sense, is also fixed internally. The architect sets the surface mission duration, while the times of flight for all other transportation legs are fixed by the propellant and start and end points, given assumptions about energetic requirements. There are some schedule concerns related to development of the individual elements present in the architecture as well as alignment with favorable launch environments due to planetary movement. These are both assumed to be accounted for outside of the in-space architecture, and therefore they are not addressed by the model.

The remaining components of the iron triangle following the elimination of both performance and schedule are cost and risk. Unfortunately, risk is difficult to establish in general at the level of fidelity desired and with very limited system heritage. To assess failure risk, one possible method is to assign a likelihood of failure to each of the system components and therefore establish an overall estimate of failure risk. However, such information is not available for regimes of engineering design that have never been attempted. Furthermore, the information on manned space exploration missions available from Apollo and following development work is both limited and dated.

Therefore, any information gained from the establishment of risk values is questionable. Other very rough metrics of risk, such as number of launches required, are either directly tied to other metrics or do not adequately distinguish between most architectures in the tradespace to produce value. Thus, risk metrics were not included in this evaluation.

Given that the only remaining portion of the iron triangle is cost, it becomes necessary to establish multiple metrics with a natural tension in order to create a trade between architectures. Two such metrics were established: the initial mass in low-Earth orbit (IMLEO) and a lifecycle cost proxy (LCC). In order to reduce the mass of the components, more development of advanced technologies is required, therefore driving up the lifecycle cost. It is expected that an expert trading along these metrics would use his or her experience to establish a given architecture's value in terms of the resulting risk, schedule constraints, and performance parameters.

Mass drives cost. This has been well established in the aerospace community over the past decades [47]. Mass on the destination surface drives the mass of the EDL system, which drives the mass of the in-space system, which drives the launch cost from Earth's surface. Although mass clearly does not encompass all of the aspects of system operational cost, it is a primary component of it. An IMLEO metric perpetuates the concept of decoupling from the launch infrastructure while measuring an established cost driver. IMLEO is calculated using the basic formulation in Equation 1.

Equation 1: IMLEO Formulation

$$IMLEO = m_{pl} + m_{crew} + m_{log} + m_{prop} + m_{hab}$$

where m_{pl} is the payload mass

m_{crew} is the crew mass

m_{log} is the logistics mass

m_{prop} is the propulsion stages' mass

m_{hab} is the total mass of all habitat elements

Although IMLEO has been well-established as an indicator of launch costs, it does not capture all aspects of the cost of mission infrastructures. Introduced in Mr. Battat's master's thesis [55], the Lifecycle Cost (LCC) proxy attempts to account for the technology portfolio lifecycle cost that must be fulfilled for a given architecture. It accounts for both the development and operating costs and does not rely on Cost Estimating Relationships (CER). Fundamentally, this metric is driven by two cost factors: the readiness level of a technology, which influences the development cost, and the demand for that technology, which influences the procurement cost. While this metric does not

estimate absolute cost, it does create an ordinal ranking of the architectures considering the relative investment of resources for the development and operation of the technology package embedded. The metric output follows Equation 2.

Equation 2: Lifecycle Cost Proxy Formulation

$$LCC = \sum_i C_i T_i$$

where LCC is lifecycle cost proxy

C_i is the cost coefficient (see below)

T_i is the technology presence coefficient

i is the index of each possible technology

In this case, the technology coefficient is simply 1 if the technology is present in the architecture and 0 if it is not. The cost coefficient is based on the readiness level of the technology and the potential for other users of that technology, according to Table 12. Note that the readiness level is an extremely simplified version of the NASA TRL scale, having only three levels.

Table 12: Cost Coefficient Information

Technology has other users?		
	NO	YES
Low Readiness	1.000	0.500
Relevant Demonstration	0.667	0.333
Existing Capability	0.333	0.167

TRL
↓

2.6 MODEL STRUCTURE

Sections 2.1 through 2.5 presented the theoretical background for the development of HEXANE. This section will describe the implementation of this theory. HEXANE is designed as a MATLAB-based evaluator with a Microsoft Excel front end for setting both the fixed science parameters as well as a variety of internal model variables that may change as additional knowledge is gained. These include values related to propellants, consumables, and spare parts, along with the matrices that hold ΔV and TOF information and the parametric relationship data. This is separated from the hard-coded values internal to the MATLAB structure in order to facilitate these assumption changes with different expert opinions as well as adapting to technology changes over

time. Figure 22 describes the six primary steps for the enumeration and evaluation code, which are designed to minimize feedback loops requiring iteration during the process.

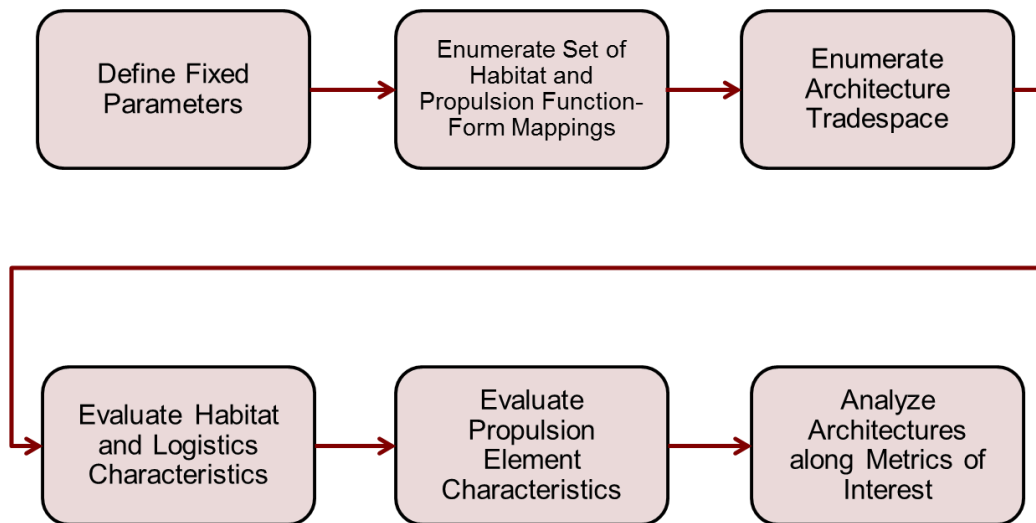


Figure 22: HEXANE Key Steps

As can be seen in Figure 23, the model is set up in such a way that major feedback loops are entirely eliminated. For reference, the parameters listed in Figure 23 (off-diagonal elements and feed-forward parameters) can be found in Appendix A. This is enabled by several properties. Firstly, propulsion (a.k.a. transportation) requirements are dependent purely on the mass of the payload and properties of the propellant and maneuver. This means that once the habitat and other payload masses are determined, the propulsion element sizing does not require iterative feedback with any other part of the architecture determination structure. In reality, this is not entirely true, as the structural requirements of the habitats, for example, would be dependent on the loading caused by acceleration from the propulsion system. However, the structure of the habitats is assumed to follow the parametrics previously described and therefore is independent in the model. The habitats, in turn, are only dependent on the fixed system parameters, such as the number of crew, time of flight, and spares mass (as a percentage of the total structure mass). Therefore, the information can be fed forward from the inputs to the habitation calculator to the transportation and propulsion sizing calculator without the need for feedback loops. This is secondly enabled by the fidelity of the model, which does not require the more detailed information that would be gained from feedback patterns. Lastly, the remaining feedback requirements are internalized to these primary blocks. This means that there are, in fact, some feedback requirements in the calculations for propulsion elements, but they are minor in comparison with otherwise significant feedback loops.

Model Inputs		I6 - I25, I32 - I38	I6,I7,I11,I2,I3,I23,I9 ,I18,I16,I4,I10,I21, I4,I31,I22,I20	I26,I27,I8,I17,I24,I28,I 29,I30	I23, I31 - I36
	Functional Grouping Enumerator		I23		
		Feasible Architecture Enumerator	O1, O3	O1	O1
			Habitation Calculator	O14, O13	
				Transportation and Propulsion Sizing Calculator	O45
					Metrics Calculator

Figure 23: HEXANE Functional Block Diagram

The primary steps from Figure 22 and reflected in Figure 23 are as follows. “Define Fixed Parameters” refers to the process of setting the fixed science values and setting any remaining assumptions through the Excel front end. Following this, the complete set of habitation and transportation function-to-form mappings is enumerated. This is typically done *a priori* in order to avoid redundant definition of this set, since the set is constant across destinations. This information, along with the fixed parameters, is then used to enumerate the full set of architectures for analysis, under the constraints previously described. Parametrics are then used to determine logistics and habitat element masses and other characteristics, which are then fed into the evaluator for propulsion elements. The propulsion calculations are fundamentally based on the physics of the Tsiolkovsky rocket equation [56]. This process also accounts for propellant boil-off, tank re-use during ISRU, sizing of thrusters, and reserve propellant. Because of the possibility of re-use of propulsion elements, this is the only place where feedback loops are necessary to iteratively determine propellant mass. Specifics of this process can be found in Appendix A. Figure 24 shows an example of a situation where this becomes necessary. In this example, the colors represent propulsion elements, while the numbers represent propulsive maneuvers. Maneuver 1 and maneuver 3 are therefore performed by the same element while maneuver 2 is performed by a separate propulsion stage. The necessary propellant for maneuver 3 is calculated first, along with

the associated dry mass for that propellant load. These properties are then calculated for maneuver 2, which has to push the propulsion element for maneuver 3 as a portion of its payload. This is then done for maneuver 1, which pushes both the propulsion element and additional propellant for maneuver 3 as well as the propulsion element for maneuver 2. However, this increases the overall dry mass for the propulsion element required for maneuvers 1 and 3 by increasing the tank size for the “yellow” propulsion element, and therefore the propellant needed for maneuver 3 must be recalculated in order to carry the additional dry mass. Therefore the remaining maneuvers must be recalculated as well, since they are dependent on the mass associated with maneuver 3 in the process described. This must therefore be iterated until a fixed solution is reached, since each iteration increases the necessary propellant for maneuver 3. Although such a situation, where propulsion elements’ functions are nested, does not occur in every architecture, it is necessary to allow for this occurrence under the set partitioning conditions.



Figure 24: Nested Propulsion Example

The final step is to calculate and evaluate the metrics of interest. This includes both the physical calculation of the metrics as described in Section 2.5.3, as well as the visualization of the tradespace. Some modules for processing of the data are included in HEXANE beyond the basic metric calculator. For reference, the entirety of the MATLAB code for HEXANE is included in the electronic attachment, and additional information, including much of the Excel front end, can be found in Appendix A.

2.7 VALIDATION

Both the theory behind the modeling methodology and implementation of the theory has been presented. In order to build confidence in the model results, a series of validation studies were performed. They are herein presented.

Given the lack of system heritage and relative dearth of accepted and validated information regarding manned exploration architectures, general validation of this model is restricted. Given this restriction, validation can be accomplished through two paths. Both methods require the use of the most widely accepted reference architectures and missions for each of the destinations. The first

method assumes that these reference missions are optimal along the analyzed metrics. In this case, the full tradespace is produced, and the location of the reference architectures is determined. If they are optimal in the model, it is assumed that the model produces reasonable results. This method has many limitations, stemming both from the assumption of optimality as well as the lack of insight into the model. Due to the complexity of the system, it is assumed that not all aspects of this tradespace have been previously explored, thus driving the analysis. Therefore, the assumption that a given point design, reference architecture, or previous mission is optimal is questionable. Furthermore, it is possible that the model would indicate that the mission architecture is optimal with incorrect analysis, since this method does not in any way analyze how the results are produced. Therefore, this method of validation was not pursued.

The alternate method, which was utilized in the following analysis, also relies on prior high-fidelity point designs and missions. In this case, the point design is encoded in the program and the analysis is performed upon that architecture. The results of that analysis are then compared side-by-side with similar analysis conducted in the original point design study. If these align, this implies that the analysis engine of the model is performing correctly without making assumptions regarding the optimality of the reference design in the greater tradespace. It will be shown that, for each of the destinations, following adjustments for significant underlying assumptions, the analysis engine of HEXANE produces results within tolerance for mass estimation of the mission elements. Therefore it can be assumed, given the lack of alternatives, that the remainder of the architectures are analyzed to an extent that allows for confidence in the ordinality of the results.

2.7.1 Mars Validation

As there is no flight history for manned Mars missions, the most detailed and vetted design study was taken to be the baseline for comparison in the validation of the Mars case. Design Reference Architecture 5.0 is NASA's latest Mars reference mission, published in 2009 [17]. Once the reference mission was encoded in the formulation required for the established model, it was found that there were fundamental assumption differences between DRA 5.0 and the model baseline.

When unaccounted for, these assumption differences caused a significant shift in the model results away from those established by the design study. However, when adjusted in the model to match that of DRA 5.0, it can be seen that the mass results from the model match well with those of the design reference architecture. The adjustments and their effects on the validation are shown in Table 13 as pure mass effects and in Table 14 as a percentage of the DRA 5.0 baseline. The graphical form of these changes is given in Figure 25. The assumption differences found to have the greatest impact include the ΔV requirements, propellant boil-off rate, consumable usage rate, and the size of the deep space habitat. Each will be addressed in sequence, comparing the DRA 5.0

assumptions to those of HEXANE.

In the detailed reference study, NASA assumed that the mission would launch on a highly favorable launch date in the early 2030s, requiring significantly less ΔV capability. The model, on the other hand, assumes a more average energetic requirement, although it still assumes that the mission will be launched within the favorable portion of the Mars launch windows [57]. DRA 5.0 also assumes that the propulsion stages will have zero boil-off capability, meaning that no propellant will be lost in the system during the long in-space segments. NASA’s more recent HAT studies [58] as well as outside group studies [59] have shown that this is unreasonable. The boil-off rates used by NASA and assumed in this model are given in Appendix A. Consumable rates were also significantly different between DRA 5.0 and the model. NASA JPL produces a consumable intake estimation tool, and this tool is integrated into the framework of the model calculations. However, DRA 5.0 makes the assumption that consumables will be used at a lower rate. As these consumables are present during the entirety of the mission, the ripple effect of even a small change in consumable mass creates a much bigger impact on the overall system IMLEO.

The final assumption difference relates to the sizing of the deep space habitat. Recent sizing estimates produced by the global space community were used in the model, as discussed in Section 2.5.1. DRA 5.0, on the other hand, used ground-up creation of custom habitats. These estimates were significantly different, with the model estimating a more conservative mass.

Table 13: Mars Validation Study Model Adjustment Effects on Mass

		Model Adjustments					
		DRA 5.0 Baseline Mass (kg)	Unadjusted Model Mass (kg)	Delta-V Adjustment	Zero Boil- Off Adjustment	Consumable Rate Adjustment	DSH Size Adjustment
Architecture Element	Deep Space Habitat	19,124	37,778	37,778	37,778	37,778	19,124
	Surface Habitat	28,007	25,690	25,690	25,690	25,690	25,690
	Earth Entry Capsule (Orion)	10,000	12,242	12,242	12,242	12,242	12,242
	NTR Propellant	202,700	677,280	291,820	265,390	255,660	225,300
	NTR Stage	303,300	916,450	442,340	409,830	397,870	360,520
	Ascent Stage	21,486	23,314	23,314	13,707	13,707	13,707
	IMLEO	846,700	1,370,800	896,630	823,220	778,360	720,490

Table 14: Mars Validation Study Model Adjustments on Mass as a Percent of the DRA 5.0 Baseline

		Model Adjustments					
		DRA 5.0 Baseline Mass (kg)	Unadjusted Model % Above Baseline	Delta-V Adjustment	Zero Boil-Off Adjustment	Consumable Rate Adjustment	DSH Size Adjustment
Architecture Element	Deep Space Habitat	19,124	97.5%	97.5%	97.5%	97.5%	0.0%
	Surface Habitat	28,007	-8.3%	-8.3%	-8.3%	-8.3%	-8.3%
	Earth Entry Capsule (Orion)	10,000	22.4%	22.4%	22.4%	22.4%	22.4%
	NTR Propellant	202,700	234.1%	44.0%	30.9%	26.1%	11.1%
	NTR Stage	303,300	202.2%	45.8%	35.1%	31.2%	18.9%
	Ascent Stage	21,486	8.5%	8.5%	-36.2%	-36.2%	-36.2%
	IMLEO	846,700	61.9%	5.9%	-2.8%	-8.1%	-14.9%

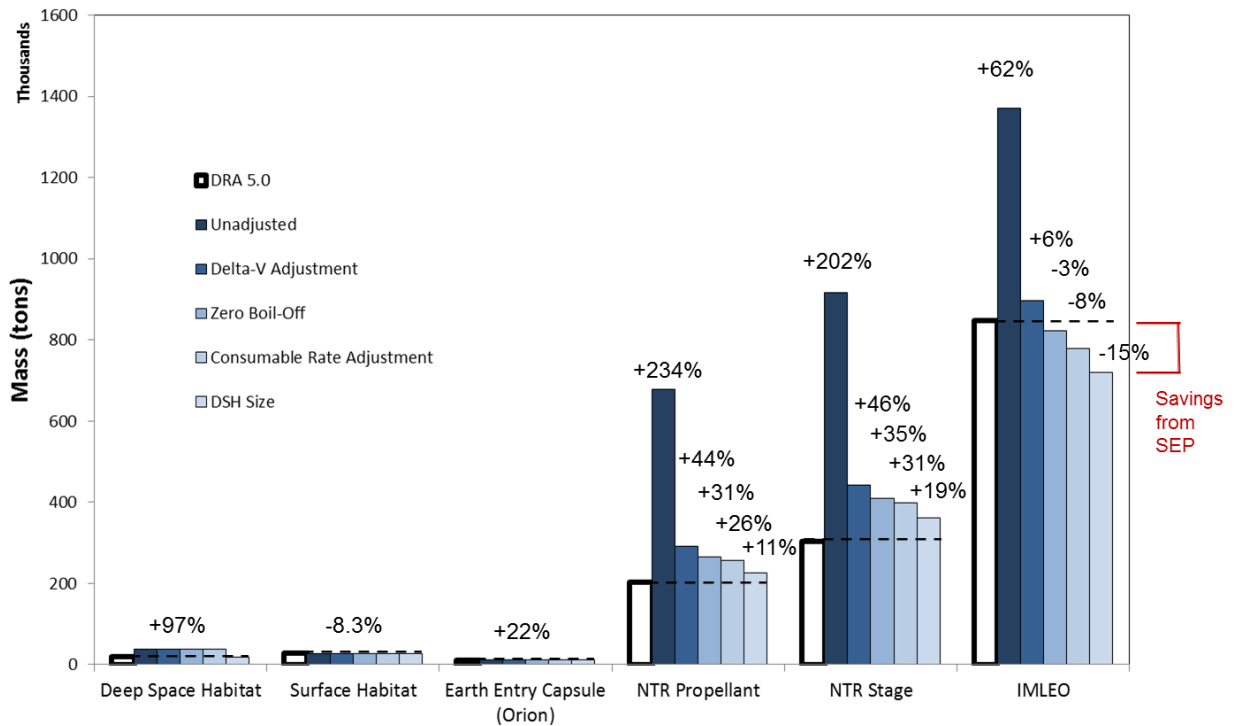


Figure 25: Validation with DRA 5.0

Figure 25 shows a series of bars for various system elements that drive IMLEO. The left-most white bar represents the reference mission. The blue bars represent the progression of assumption adjustments from no adjustment to the final validation case. The overall IMLEO difference of 15% between the model output and DRA 5.0's baseline IMLEO is believed to be associated with the savings from pre-deployment with SEP instead of NTR as present in DRA 5.0. This is within reasonable error bounds for both the study and DRA 5.0.

2.7.2 Lunar Validation

The validation for the Moon case was performed against the Apollo missions. Full results can be seen in Figure 26. Once encoded, the original validation without any adjustment came within 16% of the overall IMLEO. However, it was again found that there were fundamental assumption differences between the model and the actual Apollo missions. The principal difference was, once again, the energetic requirements. The model assumes that a Moon mission would require full lunar access, which innately requires a greater ΔV capability than the Apollo equatorial access requirements [60]. Once adjusted, the total IMLEO from the model estimate came down to +3.7%. However, a 20% difference in mass in the command module also affected the system, for similar reasons as the Mars deep space habitat. This resulted in a final IMLEO difference between the model and Apollo data of -3.4%.

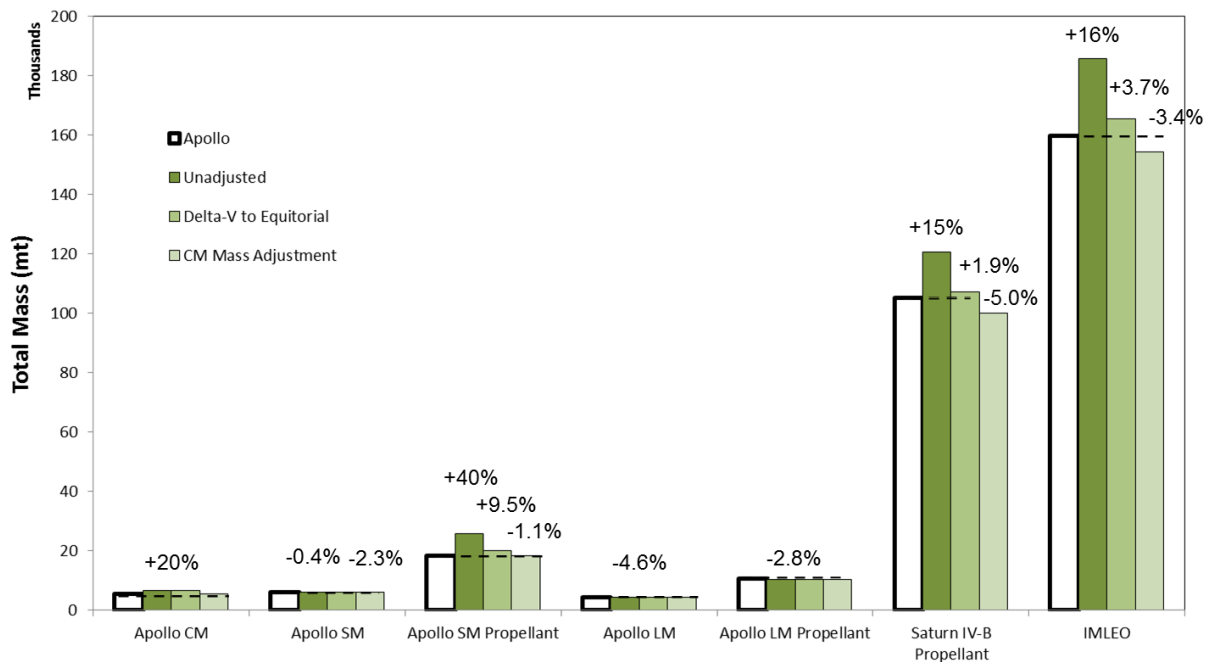


Figure 26: Apollo Validation

2.7.3 NEA Validation

Validation studies were also performed for the NEAs against preliminary data from NASA HAT [58]. This validation study showed adequate agreement (within 20%) with the point designs. This validation is not published in this thesis due to the internal nature of the NASA HAT studies at this time. The generality of the assumptions in the model is more pronounced in the NEA designs due to the variety of possible destinations in the two primary categories. It is re-emphasized that these are meant to be representative of the broader class of asteroids, and therefore the agreement with particular point designs is not as important as for the Lunar and Mars cases.

2.8 CHAPTER SUMMARY

This chapter has discussed the development and internal structure of the HEXANE model. The downscoping of the model from a general analysis of manned space exploration missions to an analysis of the in-space transportation infrastructure of missions to hard solar system bodies was discussed. It was then shown how the unique functional decomposition of this system was accomplished using a set-partitioning formulation and therefore how the model produces new value to the field. Additional architecture-level features also included in the model were discussed, including low-thrust pre-deployment, use of advanced near- and mid-term technologies, and propellant options. The overall formulation as an assignment problem, as derived from Simmons' work, and the resulting morphological matrix were shown. Parametrics, which allow for the analysis of the sub-function formulation, were discussed and specifically presented for deep space habitats. Additional model assumptions were addressed, and the metrics along which the analysis is described were presented. HEXANE's structure, as founded in MATLAB code with an Excel front end, was then described, focusing on the six primary steps. Finally, the validation study of the model was shown. This combination allows the model to describe architectures for Mars, Moon, low-energy NEA, and high-energy NEA missions. A large tradespace of architectures can be generated for each destination, and the model is adaptable to changes in the science mission over time. The tradespaces can be used to analyze the need for the various technologies as well as determine trends in architecture element arrangement in order to aid in the early decision-making process for technology investment and infrastructure design.

3. PRIMARY FINDINGS: MARS

Chapter 2 has given an introduction to the theory and methodology used in HEXANE. Chapter 3 presents a set of results generated by the model in order to both demonstrate its abilities and provide insight into manned spaceflight architectures. The analysis generated provides quantitative data to support managerial decisions for investment in future manned spaceflight systems. More specifically, the analysis identifies elements of Mars surface mission architectures that potentially influence cost proxy metrics to a greater extent than the remaining mission elements. These elements are identified by evaluating the influence of the architecture decisions, identified in Section 2.4, through a series of metrics designed to elucidate various properties of the influence over the cost proxy metrics described in Section 2.5.3. This information, combined with qualitative assessments of decision robustness, leads to a set of recommendations for the timing of architecture-level managerial decision making. These results will also be used to develop strategies for demonstrating technologies prior to final surface missions, described in Chapter 4.

For the sake of brevity, only the results from the analysis of Mars architectures using HEXANE will be discussed in detail in the bulk of the thesis. The Mars results were chosen for three reasons: 1) this follows the general trend focusing on long-term Mars exploration missions for reference architectures, 2) Mars exploration encompasses the range of architecture-level technologies and decisions captured by HEXANE and therefore produces the widest breadth of results, and 3) the most detailed analysis using HEXANE to date has been performed on the Mars architectures. A brief discussion of the results for lunar, low-energy NEA, and high-energy NEA architectures follows. The results from the set of analysis performed for the Mars architectures as applied to lunar and NEA architectures can be found in Appendix B.

3.1 ANALYSIS GOALS AND SUMMARY

The analysis of manned Mars exploration mission architectures has three general goals. The first is to assess the impact of the architecture-level decisions presented in Section 2.4, which are expected to influence Mars exploration capabilities on a significant scale. This means both an assessment of the effect generated by these decisions as well as the impact of their absence or alternatives. Much of the analysis presented will focus on these two effects. Further, this also implies an analysis of the influence these decisions have on architectures whose other properties are fixed, as has been traditionally done by NASA in DRMs and DRA 5.0. The influence of a set of decisions on otherwise fixed, individual architectures will be shown, although not to the detail of typical point design studies.

The second goal of the analysis is to identify and assess areas of the more general tradespace of architectures that have not been explicitly considered in previous point design studies, such as Design Reference Architecture 5.0, MarsOz, and Austere. These areas are anticipated to emerge as combinations of technologies and decisions create unexpected system-level behaviors. Recommendations to NASA based on advantageous system-level behavior are presented in Section 3.5. This differs from the first goal in that the emergent behavior, leading to favorable architectures not previously considered, is studied, rather than isolating specific decisions. Characteristics of regions of the general tradespace will be discussed, followed by the in-depth analysis of the decisions described above, culminating in an analysis of the coupling effects between decisions. The combination of general tradespace characteristics and the understanding of decision coupling will reveal further information about areas of interest to NASA for in-depth review.

The third goal is to identify complete in-space infrastructure architectures that lie on a Pareto frontier. Two cost-related metrics, described in Section 2.5.3, generate the frontier through a natural tension. A limited tradeoff analysis between the Pareto-optimal architectures will be discussed in conjunction with the above analysis.

To begin addressing goals one and two, Section 3.2 presents an evaluation of the IMLEO-LCC Proxy tradespace. A description of how the tradespace is constrained prior to analysis is first given. The characteristics identified in the constrained tradespace lead to a selection of decisions that clearly influence the regions of the tradespace, as well as a set of coupling relationships between decisions that similarly influence the tradespace. This begins to address goal one by identifying those decisions with the greatest impact on the metrics. It also begins to identify decisions and coupling relationships that create architecture-level properties in regions of the tradespace that have not previously been quantitatively studied, addressing goal two.

Section 3.3 presents the evaluation of the IMLEO-LCC Pareto frontier. This analysis furthers the identification of decisions and coupling relationships for in-depth analysis, aiding in the completion of goals one and two. This analysis also completes goal three by presenting and assessing the properties of the Pareto-optimal architectures for Mars conjunction-class surface missions with four crew members.

To complete goal one, the assessment of the impact of decisions on the metrics presented, the in-depth analysis of the set of decisions and coupling relationships identified by the previous analysis is presented in Section 3.4. Three measures allow for multiple perspectives on the influence of these decisions: IMLEO-Minimal Decision “Switches,” Fixed Architecture Decision Switches, and the Technology Influence Measure. Each measure shows limitations in its ability to capture the influence of these decisions, but the combined set leads to conclusions about the quantity of influence each decision has in comparison to the others in the set identified in prior analysis. Following the comparative analysis, an further in-depth analysis of the coverage of the tradespace

and Pareto frontier for each decision is given. The coverage provides a qualitative assessment of robustness properties for each decision. Coupling relationships are analyzed in the final portion of the section through the use of the Technology Interaction Coupling Effects (TICE) measure and the Technology Coupling Interaction Matrix (TCIM).

3.2 CONSTRAINED TRADESPACE ANALYSIS

To constrain both the resources required for the described analysis as well as create meaningful results, several constraints have been placed on the tradespace of architectures for the Mars conjunction-class missions. The constraints create meaningful results by limiting the architectures to those that are interesting and feasible. This also means that the comparative analysis, where one or a group of architectures is evaluated against another architecture or group of architectures, assesses the differences between interesting and feasible architectures or groups. The full tradespace would include extreme outlier values that would skew many effects seen in comparative analysis. Section 3.2 begins to address the goals described in Section 3.1 by first describing the limitations placed on the tradespace analyzed as well as providing an analysis of the resulting tradespace. Specifically, the constrained tradespace analysis works to identify those decisions and decision coupling relationships that are critical to the success of manned spaceflight architectures through their influence of the tradespace metrics.

3.2.1 Mass Feasibility Constraint

Constraint: IMLEO maximum of 900mt (9×10^5 kg, $\sim 2 \times$ ISS masses)

Impact: All analysis performed only addresses characteristics of the reduced “feasible” tradespace

Based on the decisions and choices represented in HEXANE, the full combinatorial space for a Mars mission with set science parameters is approximately 120 million architectures. Of that, 2.995 million remain after filtering for propellant conflicts (the attempted use of two propellants in a single tank) and the exponential behavior of the rocket equation resulting in infinite mass requirements [61]. Although this means that only 2.5% of the total possible architectures remain in the tradespace, it is still infeasible to analyze or visualize a tradespace with this magnitude of data. A constraint was placed to limit the IMLEO of architectures analyzed, based on the general feasibility of future operations. A constraint of 900mt, approximately two times the mass of the ISS [62], was placed for Mars architectures. This reflects the infeasibility of lifting very large masses to orbit, as well as the resulting schedule slippage from similar large projects [63][64][65]. As will be shown, the reduction in the tradespace area increases the clarity of interesting characteristics, as compared

with their compressed nature in the complete tradespace. For all further analysis, except where specified, this feasibility constraint limits the extent of the tradespace analyzed, therefore impacting both the data observed as well as the results of the analysis performed. A further discussion of the need for a more refined tradespace in such analysis can be found in [55].

3.2.2 Orion Multi-Purpose Crew Vehicle Constraint

Constraint: Capsule habitats assumed to be Orion MPCVs

Impact: Mass of most architectures increased due to increase in capsule mass

The previous constraint described how the “feasible” architectures are limited in total mass to reflect launch infrastructure limitations. A constraint on the sizing of capsules, on the other hand, retains the goal of limiting re-architecting of developed assets by forcing the inclusion of the Orion MPCV. Mass sizing of each habitat in HEXANE is accomplished by a set of parametric relationships (see Appendix A), including a separate parametric for the sizing of entry capsules. However, as mentioned in Section 2.1, HEXANE explicitly avoids the re-definition of NASA’s developed assets, specifically the SLS and MPCV. In accordance with this policy, all capsules whose requirements comply with the abilities of the proposed MPCV (minus the service module segment), including flight time, volume requirements, and energetic capabilities, have been sized to match the mass estimates of the Orion MPCV. Mass estimates are based on the information in Figure 27, taken from NASA’s MPCV Quick Facts Sheet [66]. Given a ΔV of 1500 m/s, combined with the total mass information provided for the crew module, the capsule is assumed to be 8.6mt with the heat shield. A derivate vehicle without the heat shield is assumed to be possible with a total mass of 6.4mt. No such vehicle has been explicitly developed, but this is assumed to be a trivial development task when derived from the baseline vehicle. This variant would be used for mission segments where entry or re-entry of an atmosphere is not required.

Three methods were used to assess the impact mass estimation technique for MPCV-like capsules. The original parametric sizing relationships, the mass estimates described above, and a fixed mass (with and without heat shield requirements) of 15mt produced the results shown in Table 15. The fixed mass of 15mt was chosen to reflect estimates of the final mass of the MPCV without the service module [44], which exceeds the current mass of the vehicle reflected in the estimate of 8.6mt.



Orion Summary

Number of crew 4
 Crewed mission duration 21-210 days
 Total change in velocity 4920 ft/s
 Gross liftoff weight 69,181 lbs
 Effective mass to orbit 50,231 lbs

Launch Abort System – Emergency Crew Escape System
 During Launch

Mass Properties

Dry mass/propellant 10,369 lbs
 Gross liftoff weight 16,125 lbs

Crew Module – Crew and Cargo Transport

Pressurized volume (total) 690.6 ft³
 Habitable volume (net) 316 ft³
 Reaction control system (RCS) engine thrust 160 lbf/engine
 Return payload 220 lbs

Mass Properties

Dry mass/propellant 21,350 lbs
 Oxygen/nitrogen/water 77 lbs
 Landing weight 19,463 lbs
 Gross liftoff weight 21,650 lbs

Service Module – Propulsion, Electrical Power, Fluids Storage

Mass Properties

Oxygen/nitrogen/water 694 lbs
 Propellant weight 17,433 lbs
 Gross liftoff weight 27,198 lbs

Figure 27: Orion MPCV Quick Fact Sheet

Table 15: Capsule Mass Sizing Parametric Sensitivity to Methods

		8.6mt MPCV IMLEO (mt)	8.6mt MPCV LCC	Parametric MPCV IMLEO (mt)	Parametric MPCV LCC	15mt MPCV IMLEO (mt)	15mt MPCV LCC
Non-Dominated Architectures	1	775	2.833	775	2.833	781	2.833
	2	744	3.333	744	3.333	751	3.333
	3	561	3.667	561	3.667	567	3.667
	4	549	4.167	549	4.167	555	4.167
	5	494	4.333	494	4.333	500	4.333
	6	454	4.667	454	4.667	460	4.667
	7	381	5.167	381	5.167	388	5.167
Tradespace	Mean:	772		771		775	

The study of the three fundamentally different options for sizing of the capsules reveals that the overall architecture masses and tradespace characteristics are not highly sensitive to the mass of the capsule. The minimum IMLEO architectures for all three scenarios vary in total mass by approximately 4mt, and the largest variance across non-dominated architectures is approximately 7mt. This is not a reflection of the change in just the capsule mass but also the propagated change in required propellant mass and associated propulsion dry mass. It should be noted that this change also does not affect the Pareto-optimal architecture set, as all properties of these architectures remain the same under all methods. In addition, the mean IMLEO value in the feasible tradespace varies by approximately 4mt between the parametric sizing tradespace and the set 15mt MPCV tradespace. This means that, on average, the architectures are affected by even less than the change in the capsule mass incurred by the change in sizing method, due to the fact that not all architectures employ an MPCV-like capsule. Although these results are not sufficient to show true sensitivity, they indicate that, in general, the final IMLEO value of the average and non-dominated architectures in the feasible tradespace are not heavily influenced or sensitive to the sizing method for the capsule.

The common use of capsules in the Mars tradespace likely influences this result. As described in Section 3.3 and 3.4.10, capsules are typically left in Earth orbit and not carried during the bulk of the Mars missions for these architectures. This implies that the increase in mass of the capsule has less influence on the mass of the propulsion system, as the mass of the capsule is not carried by the majority of the propulsive stages. If the model changes to reflect a need to carry the capsule through the architecture, the influence of the sizing parametric is likely to change.

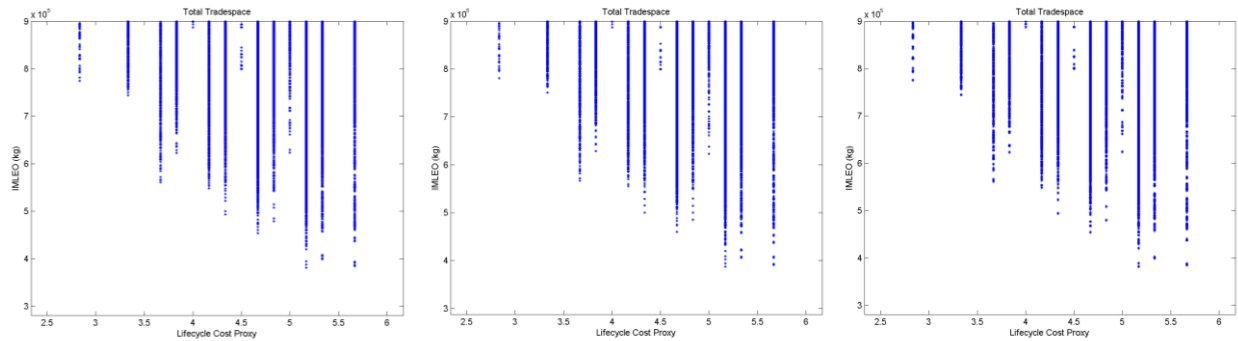


Figure 28: MPCV Parametric Tradespaces (8.6mt, Parametric, and 15mt, respectively)

Figure 28 also shows a side-by-side comparison of the feasible tradespaces for the three sizing methods. The consistency of shape in the tradespace indicates that the tradespace properties are also robust to changes in the capsule sizing parametric. Given the consistency shown in the non-dominated architectures, the average masses of the architectures in the feasible region, and the

properties of the tradespaces themselves, it is concluded that the 8.6mt sizing method is the most logical and is not likely to heavily influence the results.

3.2.3 General Tradespace Characteristics

HEXANE outputs two primary metrics, both related to cost. The resulting constrained tradespace is shown in Figure 29, with the LCC Proxy on the x-axis and IMLEO on the y-axis. Figure 30 presents the full tradespace, without the aforementioned constraints, for comparison. The architectures seen in the constrained tradespace are flattened in the full tradespace, given that the scale is three orders of magnitude greater, and only a few of the extreme outliers are easily visible. For all tradespace plots, as stated in Section 2.5.3, IMLEO acts as a proxy for operational costs, where LCC represents development and procurement costs.

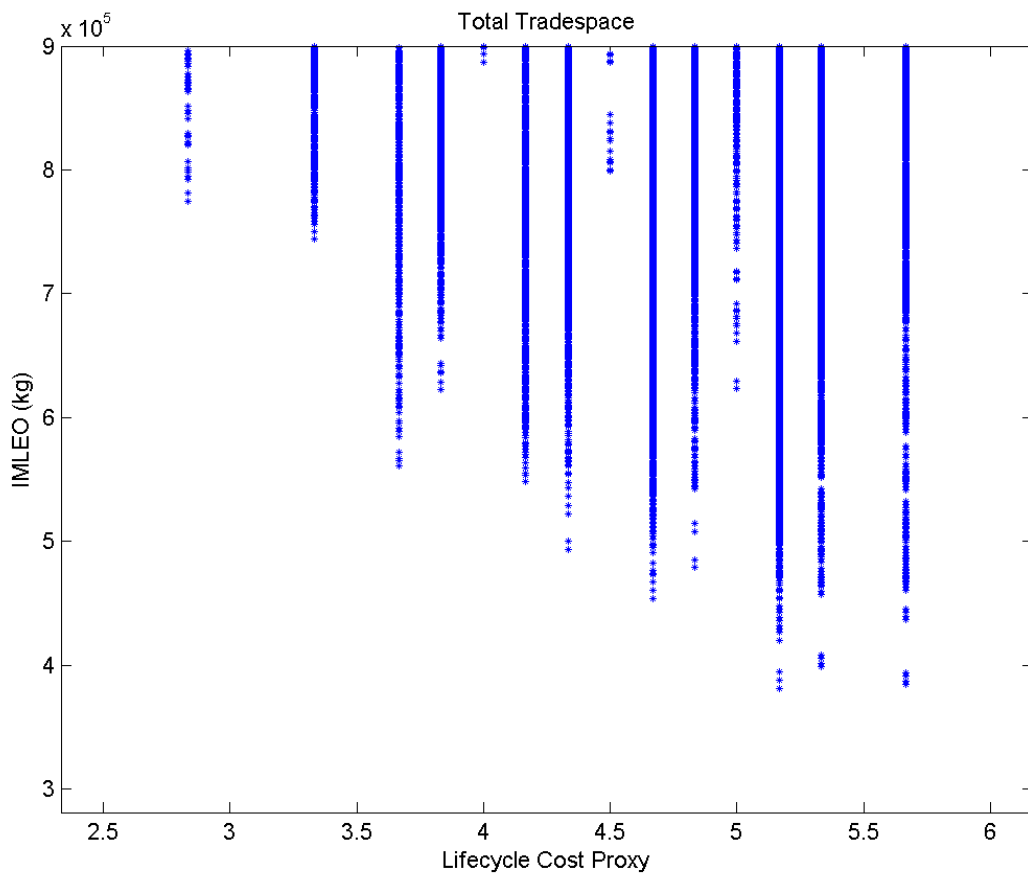


Figure 29: Constrained Mars Tradespace

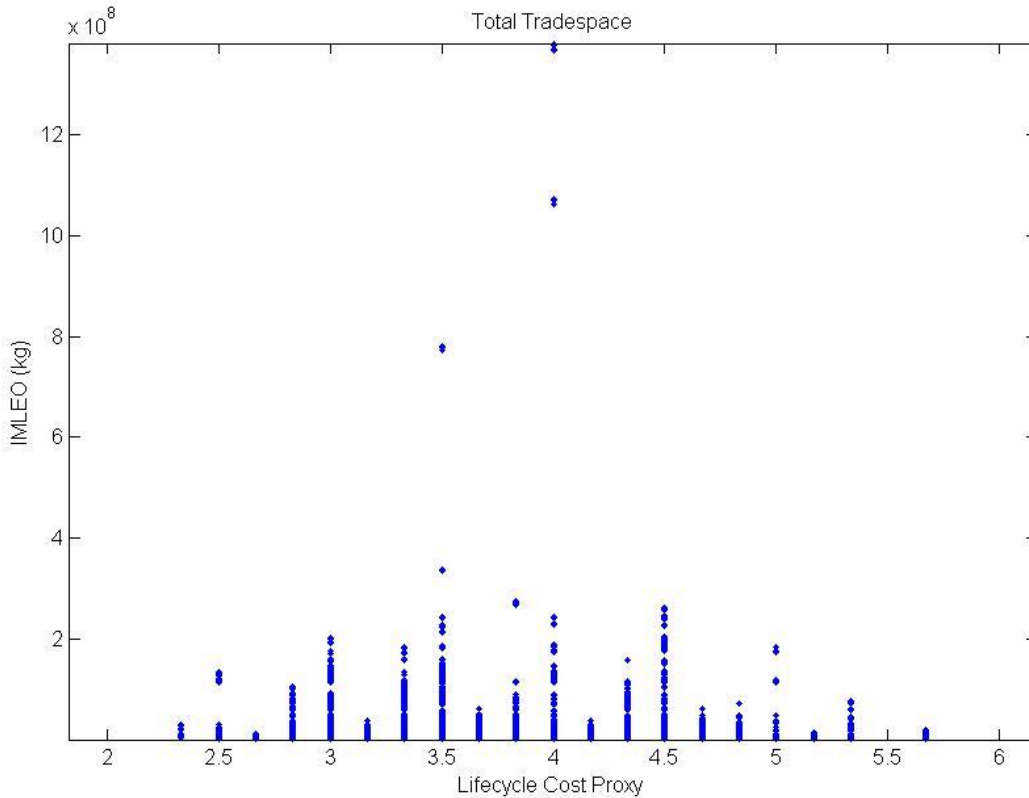


Figure 30: Mars Architecture Unconstrained Tradespace

The discrete nature of the LCC proxy metric is prevalent in the tradespace. Under the description presented in Section 2.5.3, there are 1296 possible combinations of technologies, with 26 unique values in the LCC proxy. Of the 26, 14 combinations can be found within the feasible region (*i.e.* only 14 values are associated with feasible architectures), with the proxy ranging from 2.833 to 5.667. This also means that 12 of the 26 values are either outside of the range of 2.833 to 5.667 or are “gaps” in the discrete values within that range. The minimum separation between LCC proxy values is 0.167, but several values in the range between 2.833 and 5.667 are not represented in the feasible region. Figure 30 reveals that most of the “gaps,” in particular the 3.167 and 3.500 gaps, are combinations of technologies that are solvable (*i.e.* they do not have infinite mass) but are not low enough mass to be present in the feasible region. However, the 5.500 gap represents a combination of technologies that are completely unsolvable. The tradespace also reveals that there are solvable architectures with an LCC of less than 2.667 but none greater than 5.667. These properties will be discussed as part of the tradespace properties analysis.

Figure 29 also shows that the IMLEO and LCC proxy metrics are in tension, meaning that an increase in one typically results in a decrease in the other. This creates a Pareto frontier, allowing for the analysis of the tradeoff between the types of cost imbedded in the metrics. This general

trend arises from the concept that an investment in advanced technologies can be used to reduce the overall mass of the system, although not all combinations of investment portfolios result in a mass reduction from a baseline, minimum LCC architecture. A more complete description of the Pareto frontier will be given in Section 3.3.

Figure 31 shows representative tradespace areas where the interplay of these metrics produces a tradespace property that may be of importance when designing future manned exploration missions. These include regions where the increase in development and procurement spending, represented by the LCC proxy, also increases the IMLEO, as well as the extreme cases where the trade between these metrics produces combinations of technologies not represented in the tradespace at all. The frontier behavior is also of great importance to future decisions.

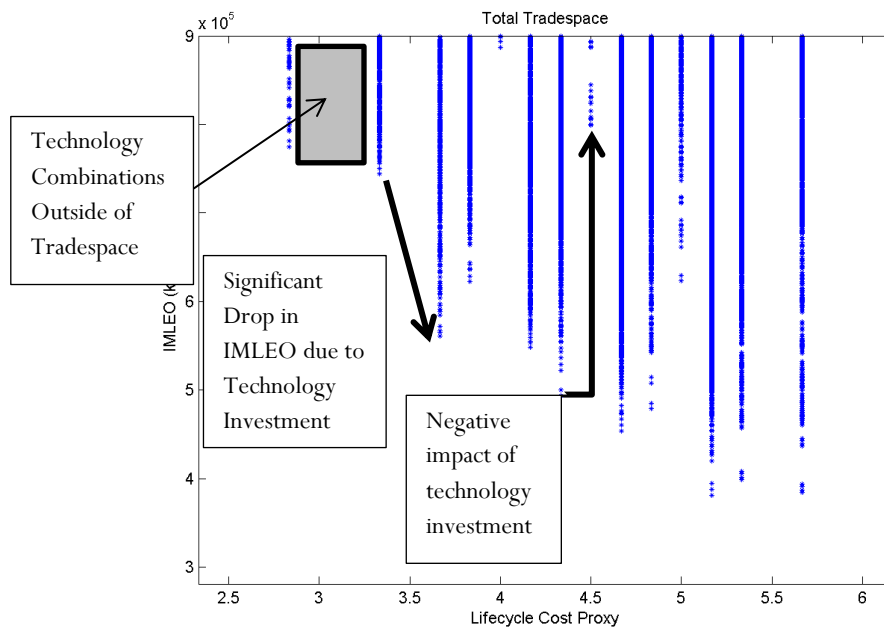


Figure 31: Example Mars Tradespace Features

The changes in architecture properties between discrete LCC values drive the tradespace features seen in Figure 31. As the combinations of technologies change, the properties of the resulting architectures also change, leading to the creation of these tradespace features. Because the LCC proxy is dependent on 13 separate technology inputs, multiple combinations of technologies may result in the same LCC value. Therefore, in order to understand the underlying drivers for the tradespace features, an analysis of the predominant technologies and architectural decisions for each LCC value is necessary. As shown in Figure 32, this analysis found that the overall impact of decisions on IMLEO is dominated by propellant choices due to the >1 gear ratio between habitat dry mass and propellant mass. As the habitat masses are increased due to inefficiencies associated with the choice of set partitioning, an even greater mass of propellant is also required to push said

habitat mass. Therefore, many of the IMLEO-LCC interactions, manifested as properties of the tradespace, are most heavily influenced by propellant options until the symbiotic coupling between certain technology decisions begin to dominate.

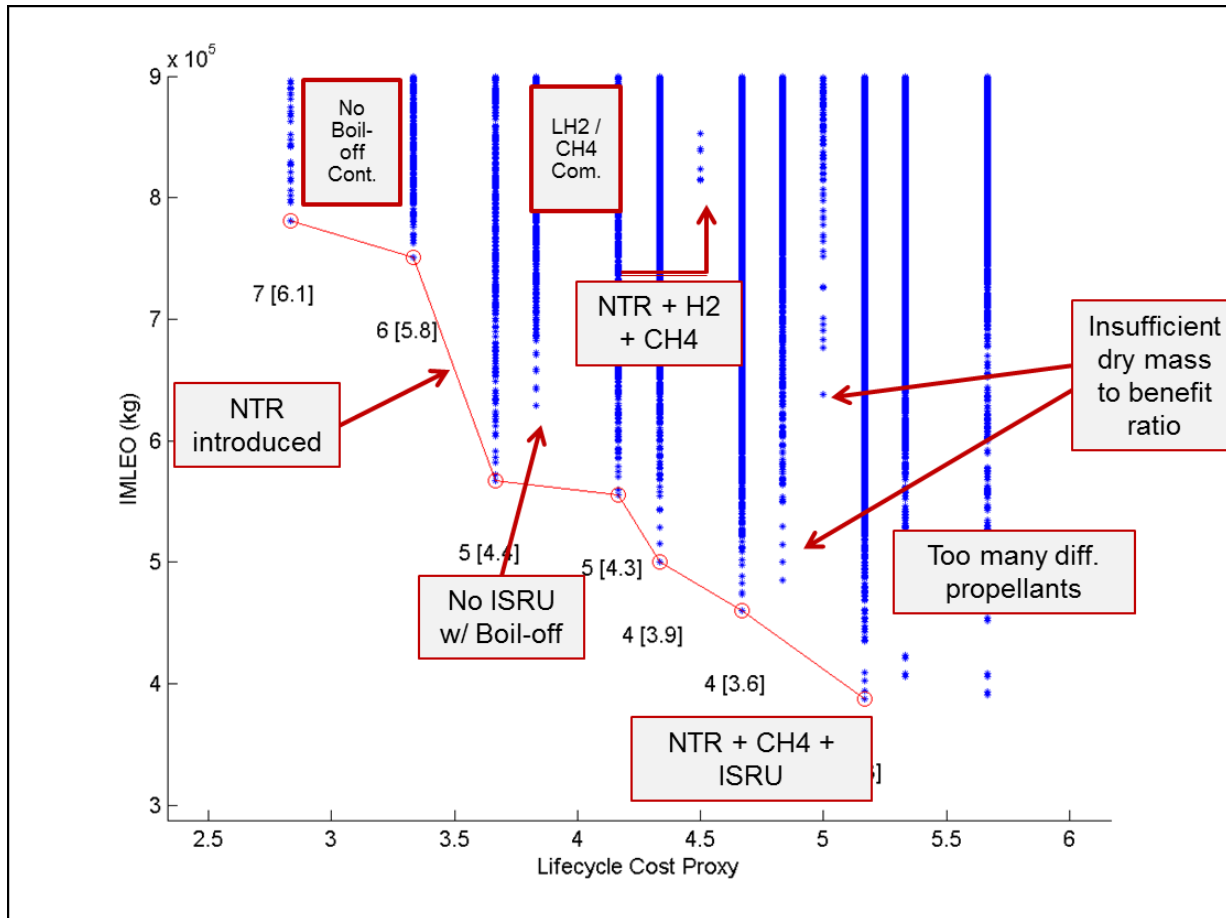


Figure 32: Constrained Tradespace Feature Drivers

The minimal LCC architectures, the left-most “line” of architectures in Figure 32, consist of purely hypergolic propellant stages, resulting in a low LCC considering the flight heritage of hypergolic propellants as well as a very high mass due to the poor properties of these propellants, in this case primarily a low I_{sp} of 324 s (full propellant properties can be found in Appendix A). The first set of architectures to be excluded from the feasible region due to high mass, evidenced by the gap in LCC values between 2.667 and 3.333, occurs due to the introduction of advanced cryogenic propellants without boil-off control. This indicates that there is a necessary synergism between the hypergolic propellants and boil-off control capabilities.

A significant drop in IMLEO occurs as NTR is introduced. The forced coupling between NTR and boil-off control (*i.e.* NTR must include cryogenic boil-off control due to its use of cryogenically

cooled hydrogen, which would otherwise boil-off at a high rate), explicitly enforced in HEXANE, excludes nuclear rockets in low LCC regimes. The coupling derives from the use of hydrogen as the sole propellant of NTR, which has a very high boil-off rate when unmitigated, therefore rapidly driving up architecture mass. Despite the increased dry mass due to the need for a radiation shield and additional power plant structure associated with NTR, the significant improvement in I_{sp} above both hypergolic and cryogenic propellants creates a significant drop in mass for many architectures employing this technology.

A negative return between technology investment and IMLEO occurs with the introduction of the combination of boil-off control with LOX/LH₂ but no ISRU. This indicates that despite having boil-off control, the long idling duration for LH₂ and associated boil-off outweighs the mass advantage from higher I_{sp} . The combination of no boil-off LOX/LH₂ and LOX/CH₄ has even worse mass properties, creating a gap of LCC values between 3.667 and 4.167 (*i.e.* there are no architectures with a value of 4.000 in the feasible region) due to the mass of these architectures falling outside of the feasible region. Similarly, the combination of NTR, LOX/LH₂, and LOX/LCH₄ performs poorly, although some architectures remain in the feasible region.

The best performance, in terms of IMLEO properties, occurs with the symbiotic relationship between NTR, LOX/LCH₄, and ISRU is exploited. The high performance of NTR for Mars injection, combined with the ability to manufacture most of the propellant for LOX/LCH₄ on the surface with ISRU makes this combination particularly favorable. Section 3.4.12 presents a further detailed analysis of this symbiotic relationship.

Beyond an LCC value of 5.167, architectures become less mass-favorable due to the unnecessary combination of many propellants (leading to many development projects and hence a higher LCC). This implies that more commonality of propellants between stages tends to be more favorable. This derives from the fact that the LCC proxy is a function of the number of large development projects necessary to produce the elements in the architectures. Therefore, an increase in the number of propellants in an architecture, when unnecessary, increases the LCC value without benefiting IMLEO.

Conclusion

From the general tradespace analysis, three specific decisions and three couplings have been identified as items of interest to further investigate. These include:

Decisions

1. Cryogenic Propellants
2. Boil-off Control
3. Nuclear Thermal Rockets

Couplings

1. LOX/LH₂ with Boil-off Control without ISRU as a negative effect
2. LOX/LH₂ and LOX/LCH₄ in combination as a negative effect
3. NTR, LOX/CH₄, and ISRU in combination as a positive effect

This differs from previous analysis in [55] in the inclusion of 3-way coupling, rather than just 2-way interactions, although similar techniques are employed.

3.3 OPTIMAL ARCHITECTURES

An analysis of the optimal architectures in this tradespace serves two purposes. It addresses the third goal of the overall analysis: to identify “good” architectures that should be considered for future point designs. Both “optimal” and “good” refer to non-dominated architectures that lie on the Pareto frontier created by IMLEO and the LCC proxy, as seen in Figure 33. Other methods of assessing “good” architectures exist, such as fuzzy Pareto frontiers, but these are not addressed in this thesis. These architectures represent the best trade-offs between IMLEO and the LCC Proxy. This analysis also serves to identify further decisions for more in-depth analysis by ascertaining patterns in the optimal architectures. These patterns emerge from decisions and the couplings of decisions that drive the architectures to the Pareto frontier. This is distinctly different from the patterns detected in the previous tradespace properties analysis. In the case of tradespace property analysis, specific combinations of technologies create the discrete values, resulting in general effects on both LCC and IMLEO. In the case of Pareto frontier analysis, the patterns that drive architectures toward the non-dominated front are instead detected, and patterns between combinations of technologies, such as habitat set partitions, may be discovered.

The full set of non-dominated architectures is shown pictorially in Figure 33, each architecture labeled sequentially from left to right. This designation holds for all further analysis. The two end points, Pareto-optimal architectures 1 and 7, will be first analyzed to understand the extremes for overall architecture methods. This information will then be used to further analyze the full set of seven non-dominated architectures and glean the important architectural decisions for further analysis.

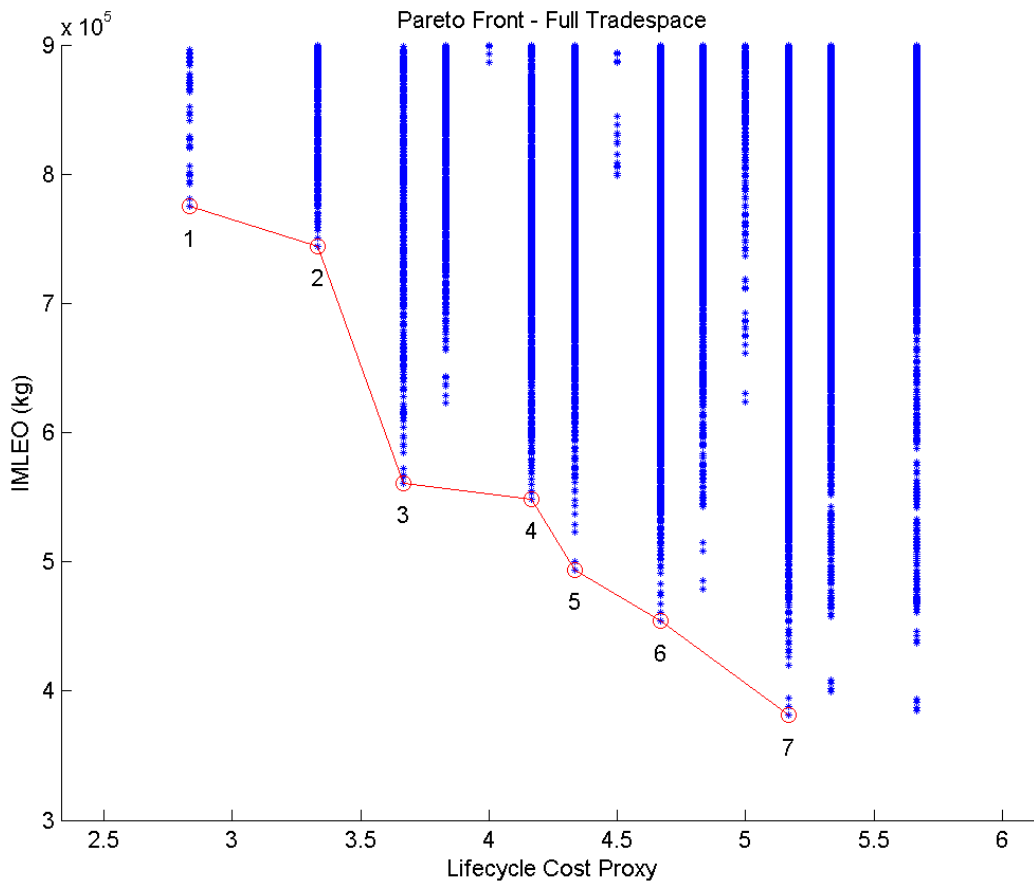


Figure 33: Mars Constrained Tradespace Pareto Frontier

3.3.1 Minimum IMLEO Architecture

Architecture 7 represents the minimum IMLEO for the Mars architectures under the fidelity of the HEXANE analysis. More importantly, it represents a mission needing long-term investment in advanced technologies in order to produce a highly mass-efficient mission architecture. This would be appropriate for a well-funded program with many intermediate missions for technology demonstration and the upkeep of the public interest. In order to understand how the mission architecture operates, the overall ConOps of this mission is presented in a traditional BAT chart in Figure 34.

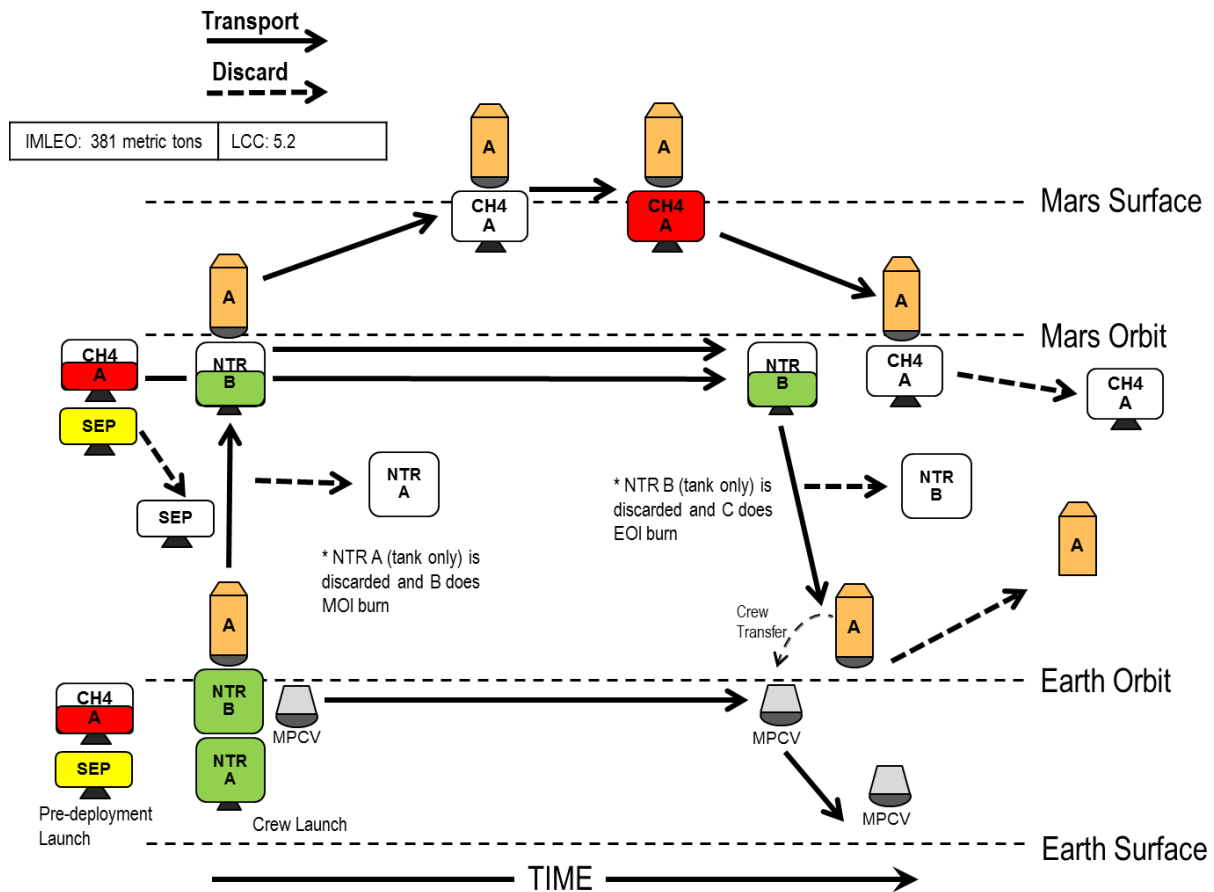


Figure 34: Mars Minimum IMLEO BAT Chart

In this architecture, two launch stacks are sent, one with the crew using NTR as a primary propellant, and another which pre-deploys a LOX/LCH₄ tank with boil-off control for descent and ascent after ISRU. An MPCV is also put into orbit but is not used by the crew for launch. One tank of the NTR is used for trans-Mars injection, while the other is used for orbit insertion and trans-Earth injection following surface operations. Mars orbit insertion is accomplished by a combination of aerocapture and a small burn by the NTR. The LOX/LCH₄ tank is then rendezvoused with for descent to the surface. That same tank is then refilled using ISRU for ascent. The second NTR tank is dropped following the Earth return burn, and aerocapture is used to rendezvous with the MPCV in Earth orbit for descent to Earth's surface. The crew travels in a semi-monolithic habitat, which serves the functions of a launch environment, deep space habitat, descent, ascent, and surface habitat. This is a large, highly complex habitat that also includes ablative aeroshielding.

This minimum IMLEO architecture has a total mass in orbit prior to Earth departure of 381mt. Figure 35 and Figure 36 visualize the mass breakdown as bar and pie charts, respectively. High energetic requirements for the trans-Mars injection and trans-Earth injection stages, combined with

boil-off of cryogenic propellants, drives the total propellant mass (excluding propellant produced with ISRU) to approximately 50% of the total IMLEO. At 15% of the total mass, SEP propellant, dry mass, and pre-deployed cargo is the next most significant component. However, this is still comparable to the logistics and cargo brought on the manned stack, the total habitat mass, and the additional dry mass for the NTR stage.

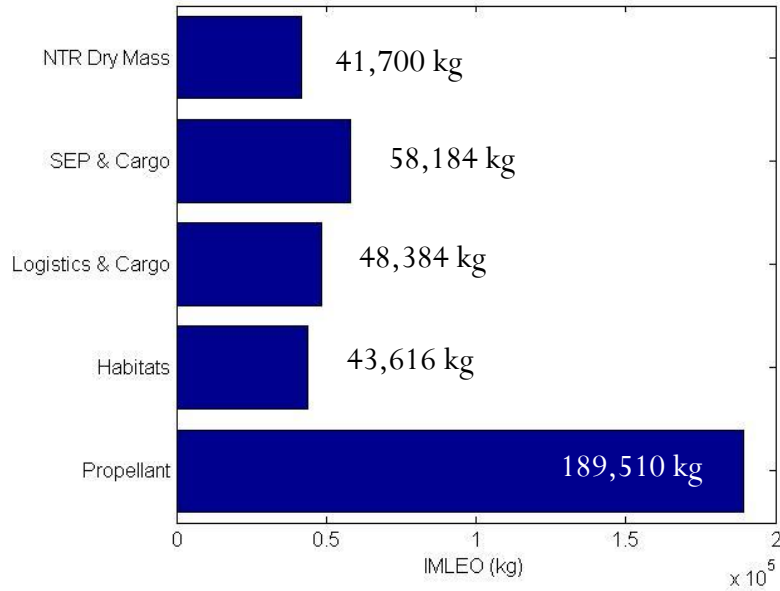


Figure 35: Mars Minimum IMLEO Architecture Mass Bar Chart

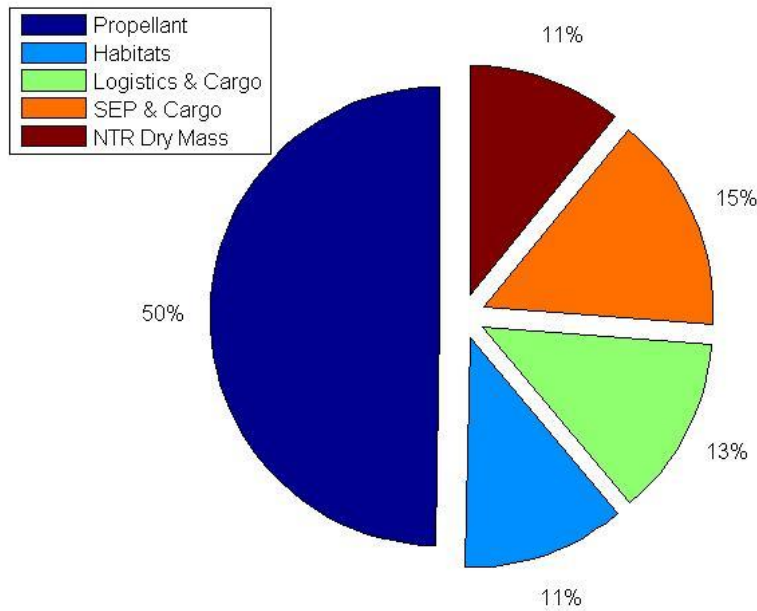


Figure 36: Mars Minimum IMLEO Architecture Mass Pie Chart

This architecture also corresponds to the highest LCC value of the Pareto frontier architectures, with a resulting value of 5.167. This links to the use of 7 of the 13 LCC-impacting technologies. For reference, the 13 LCC-impacting technologies (*i.e.* the technologies that require discrete development projects and therefore are captured by the LCC metric) are:

- NTR in-space stages
- LOX/LH₂ in-space stages
- LOX/LCH₄ in-space stages
- LOX/LH₂ descent stages
- LOX/LH₂ ascent stages
- LOX/LCH₄ descent stages
- LOX/LCH₄ ascent stages
- Hypergolic descent stages
- Hypergolic ascent stages
- ISRU
- SEP pre-deployment
- Cryogenic boil-off control
- Ablative aerocapture

The 7 included in the minimum IMLEO architecture are:

- NTR
- LOX/LCH₄ descent stage
- LOX/LCH₄ ascent stage
- ISRU
- SEP Pre-Deployment
- Boil-off control
- Aerocapture

This means that of the four primary technologies found in Figure 19 (aerocapture, ISRU, boil-off control, and SEP pre-deployment) all are utilized in this architecture.

3.3.2 Minimum LCC Architecture

In contrast, Architecture 1 represents the minimum LCC architecture and a fundamentally different approach to Mars exploration. This symbolizes the case where the program schedule has dominant importance and therefore drives the architecture to use the smallest number of elements

that require additional research and development. In comparison to established point designs, this most closely mimics that of the JPL Austere mission, which was produced as a follow-up to DRA 5.0 [17][18]. The Austere mission was designed to demonstrate the possibility of flying a manned Mars mission with minimal investment into additional capabilities and technologies. Figure 37 shows the BAT chart for Architecture 1.

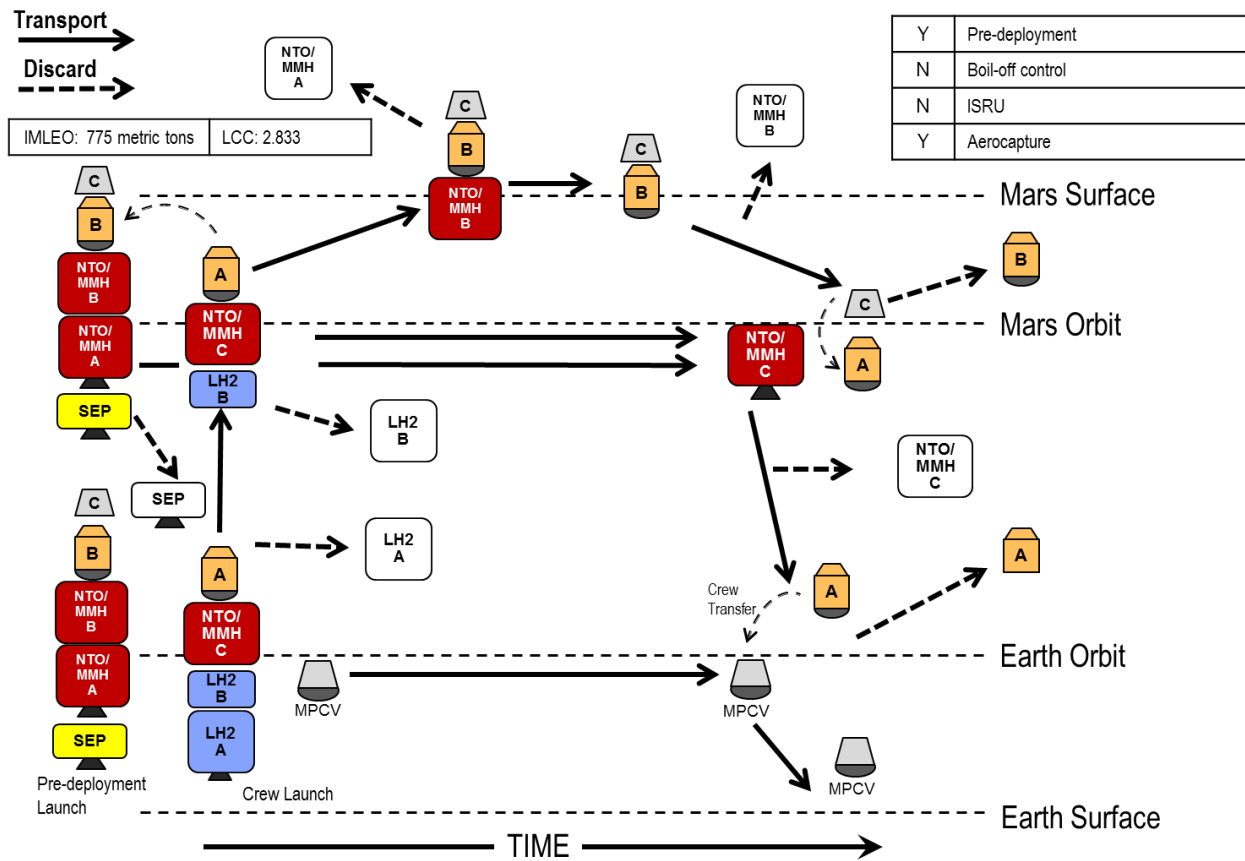


Figure 37: Mars Minimum LCC Architecture BAT Chart

This architecture is dependent on 5 propulsion stages and 4 habitats. A non-boil-off controlled LOX/LH₂ stage is used for trans-Mars injection, and a second LOX/LH₂ stage is used for Mars orbit insertion. Separate hypergolic propulsion stages (NTO/MMH) are pre-deployed for use as independent descent and ascent stages. A third hypergolic stage is carried by the crewed stack and used for trans-Earth injection. For the habitats, an MPCV is used for launch and stays in orbit for Earth re-entry after rendezvousing with the returning crew in LEO. A deep space habitat is used both inbound and outbound, which stays in orbit around Mars while the surface operations take place. The descent habitat is combined with the surface habitat, but a separate ascent vehicle is used. Overall, two of the four primary technologies are included, despite the “minimum LCC”

labeling, including both pre-deployment with SEP and ablative aerocapture. **This means that the case of zero primary technologies or even one primary technology lies outside of the feasible region. In order to achieve a manned Mars mission within these constraints, at least some R&D must be done.**

As with the minimum IMLEO architecture, a mass breakdown was performed as shown in Figure 38 and Figure 39. There are several key distinctions between the mass breakdown for Architecture 1 and Architecture 7. Sixty-two percent of the 775mt total mass is pre-deployed using SEP. This includes the bulk of the propulsion stages, which are labeled as pre-deployment cargo rather than as propellant. This demonstrates that, overall, the considerable increase in mass is manifested as propellant mass, both as an increase in the amount on the crewed stack as well as approximately 480mt of pre-deployment stack mass. The mass of 213mt for the LOX/LH₂ propulsion and one hypergolic stage, which amounts to 27% of the overall mass, shows that there is a large amount of propellant necessary for trans-Mars injection and orbit insertion when boil-off control is not developed. This is a 12.7% increase above the total propellant mass for the minimum IMLEO architecture, despite the amount of pre-deployed stages in Architecture 1.

There is a slight decrease in overall habitat masses to 34mt from 44mt. This demonstrates that an architecture with less overall habitat mass does not necessarily correspond to an optimal arrangement of those architectures for minimum overall mass. Logistics and cargo remain approximately the same, with a slight decrease due to the decrease in spares for the habitats. Because there is no NTR stage, there is no associated additional NTR dry mass for this architecture.

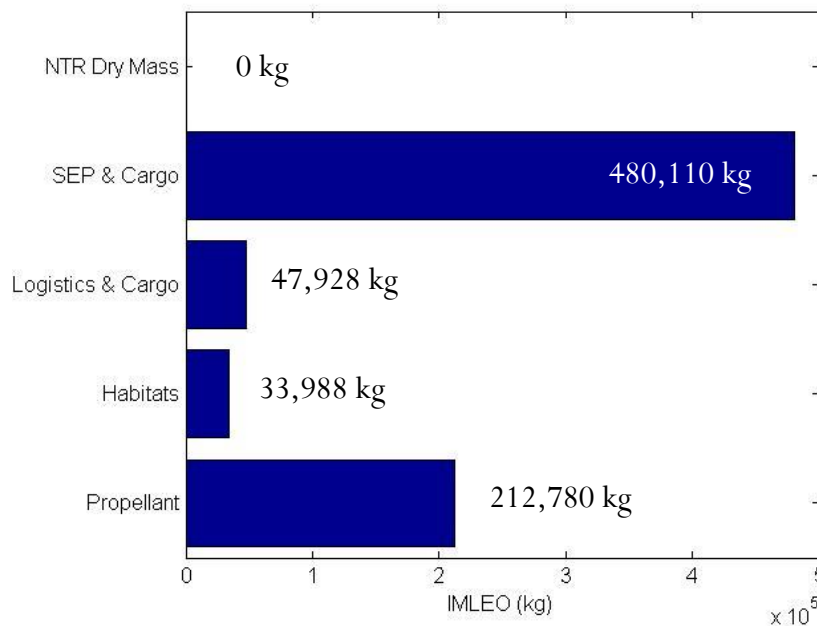


Figure 38: Mars Minimum LCC Architecture Mass Bar Chart

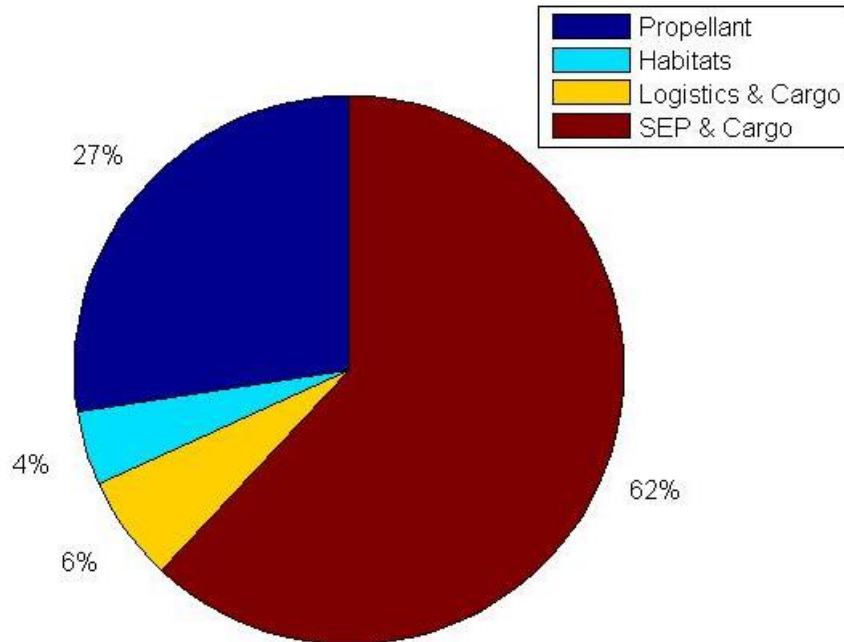


Figure 39: Mars Minimum LCC Architecture Mass Pie Chart

The total LCC value for this architecture is 2.833. This corresponds to a use of 5 of the 13 LCC-impacting technologies. These include:

- In-space LOX/LH₂ stage
- Hypergolic descent stage
- Hypergolic ascent stage
- SEP Pre-Deployment
- Aerocapture

As stated, of the four primary technologies seen in Figure 19, only two are present in this architecture (SEP pre-deployment and aerocapture).

Three trends emerge from the analysis of Architectures 1 and 7. The consistent use of two technologies across these architectures, SEP pre-deployment and ablative aerocapture, likely indicates their wider use. Additionally, an independent capsule for Earth re-entry is present in both architectures. To further understand these trends as well as identify others, an analysis of the set of all seven non-dominated architectures has been performed.

3.3.3 All Non-Dominated Architectures

The extreme cases for the non-dominated architectures (*i.e.* those that minimize one of the metrics) revealed the properties of fundamentally different approaches to architecting the Mars conjunction class mission. Combining the information from these architectures with an analysis of the complete set of non-dominated architectures aids in the identification of architecture-level decisions that heavily influence the metrics.

The metric properties and presence of the four primary technologies is shown for all seven non-dominated architectures in Table 16. It is clear from this table that both SEP pre-deployment and ablative aerocapture are present in all non-dominated architectures, and boil-off control is present in four of the seven architectures. This indicates that these are important and impactful decisions for well-designed manned Mars exploration architectures.

Table 16: Mars Non-Dominated Architecture Metrics and Primary Technology Presence

Architecture	IMLEO (mt)	LCC	SEP	Boil-off	ISRU	Aerocapture
1	775	2.833	Yes	No	No	Yes
2	744	3.333	Yes	Yes	No	Yes
3	561	3.667	Yes	Yes	No	Yes
4	549	4.167	Yes	Yes	No	Yes
5	494	4.333	Yes	Yes	Yes	Yes
6	454	4.667	Yes	No	Yes	Yes
7	381	5.167	Yes	Yes	Yes	Yes

Like the four primary technologies, the LCC-impacting technologies may also reveal trends in the non-dominated architectures. A stoplight chart is shown in Figure 40 for the remaining 9 of the 13 LCC-impacting technologies and their use in the seven non-dominated architectures.

From this chart no further clear trends emerge for the use of technology. Of interest, however, is the lack of use of LOX/LCH₄ for in-space propulsion in all architectures. This is surprising, given that liquid methane stages have significantly lower boil-off rates than the other cryogenic propellants and that most of the propellant can be extracted with ISRU. It appears that, at least in the non-dominated architectures, the combination of architectural elements is not conducive to the use of in-space methane stages.

Architecture	NTR	In-Space LOX/LH ₂	In-Space LOX/LCH ₄	LOX/LH ₂ Descent	LOX/LH ₂ Ascent	LOX/LCH ₄ Descent	LOX/LCH ₄ Ascent	Hypergolic Descent	Hypergolic Ascent
1	Red	Green	Red	Red	Red	Red	Red	Green	Green
2	Red	Green	Red	Green	Red	Red	Red	Red	Green
3	Green	Red	Red	Red	Red	Red	Red	Green	Green
4	Green	Red	Red	Green	Red	Red	Red	Red	Green
5	Red	Green	Red	Green	Green	Red	Red	Red	Red
6	Green	Red	Red	Red	Red	Green	Green	Red	Red
7	Green	Red	Red	Red	Red	Green	Green	Red	Red

Figure 40: Mars Non-Dominated Architecture Technology Stoplight Chart

Two of the three trends identified by the analysis of Architectures 1 and 7 have been described for the non-dominated architectures, excluding the use of MPCV capsules. One method for analysis for identifying trends within the non-dominated population is to overlay the architectures on the Pareto frontier with the remaining tradespace and indicate the presence of specific decisions in those non-dominated architectures. The use of the MPCV capsule in the non-dominated space can be found in Figure 41. Like SEP pre-deployment and aerocapture, capsules are used in all of the non-dominated architectures (100% coverage). This implies that the use of capsules should be analyzed as a decision of interest in the broader tradespace.

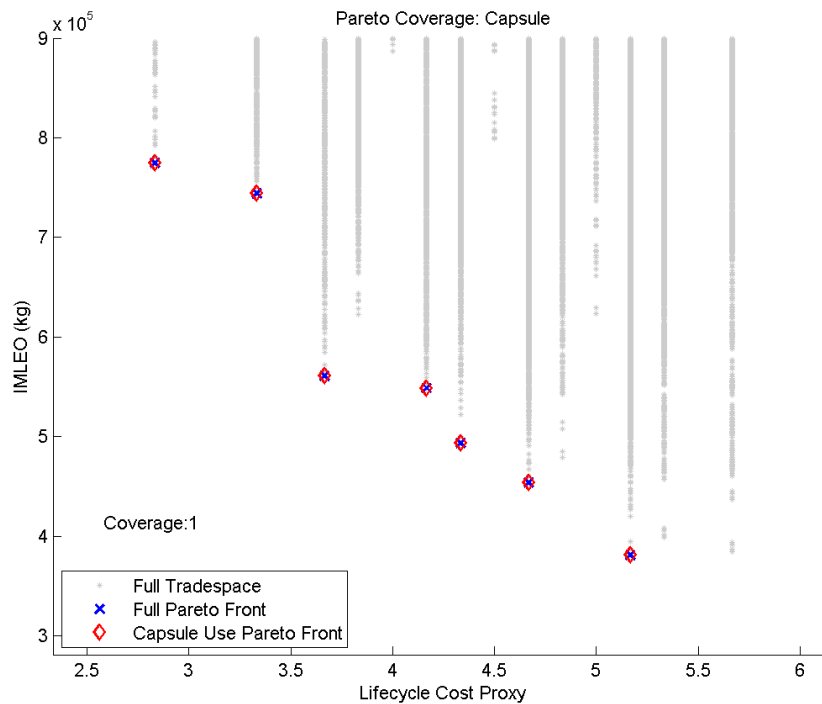


Figure 41: Mars Tradespace MPCV Capsule Pareto Frontier Coverage

In addition to the trends identified in the general tradespace as well as between Architectures 1 and 7, there is an unexpected habitat set partitioning decision that manifested in Architecture 7. This was the semi-monolithic habitat, which incorporated the functionality of six of the seven habitation sub-functions into a single habitat. Fully monolithic habitats are those that incorporate all seven sub-functions into a single habitat. Semi-monolithic habitats incorporate all of the five interior sub-functions (all except “launch” and “re-entry” sub-functions, as seen in Figure 16). Figure 42 shows that the use of monolithic or semi-monolithic habitats exists in the three lowest IMLEO architectures, for coverage of 43% of the non-dominated architectures. This coincides with the coverage of ISRU in these architectures, indicating that there may be a correlation between these decisions (although this does not imply causation). Although the evidence for the importance of this decision is not as strong as for other decisions, the incorporation in the lowest IMLEO architectures as well as the unusual nature of the decision itself indicates that it should be included in the further analysis on the whole tradespace, shown in Section 3.4.11.

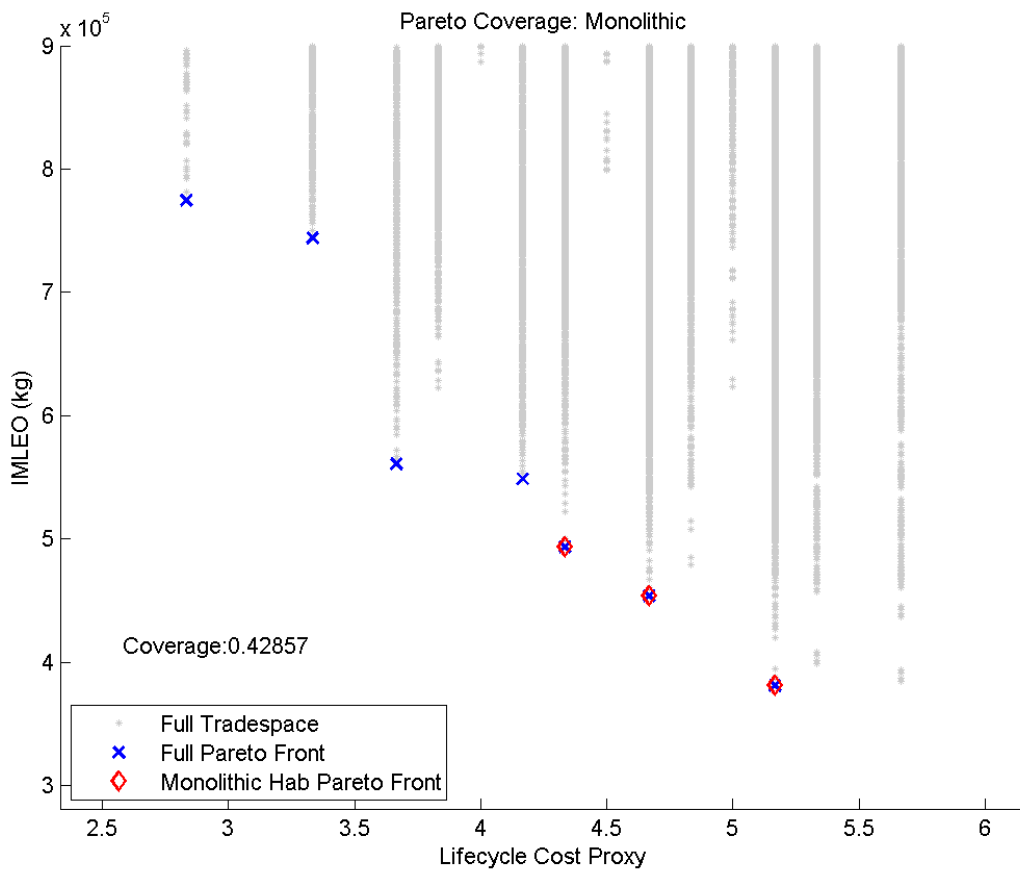


Figure 42: Mars Tradespace Monolithic and Semi-Monolithic Habitat Pareto Frontier Coverage

Conclusion

From the analysis of the non-dominated architectures, five specific architectural decisions and one coupling relationship have been identified for further analysis. These include:

Decisions

1. SEP Pre-Deployment
2. Ablative Aerocapture
3. In-Space LOX/LCH₄ stages
4. MPCV Capsules
5. Monolithic and semi-monolithic habitats

Coupling

1. Semi-monolithic habitats with ISRU as a positive effect

In this context, semi-monolithic habitats are those habitats which are monolithic with the exception of the use of an MPCV-like capsule. The combination of this list with the decisions and coupling relationships identified by the general tradespace analysis guides the deeper analysis.

3.4 ARCHITECTURAL DECISIONS AND COUPLING

From a combination of the general tradespace evaluation and non-dominated architectures analysis, a set of eight architectural decisions and four couplings have been identified for deeper analysis of their impact on the tradespace. The final list includes:

Decisions

1. Cryogenic propellants
2. Boil-off control
3. Nuclear Thermal Rockets
4. SEP pre-deployment
5. Ablative aerocapture
6. In-space LOX/LCH₄ stages
7. MPCV Capsules
8. Monolithic and semi-monolithic habitats

Coupling

1. LOX/LH₂ with Boil-off Control without ISRU as a negative effect

2. LOX/LH₂ and LOX/LCH₄ in combination as a negative effect
3. NTR, LOX/CH₄, and ISRU in combination as a positive effect
4. Semi-monolithic habitats with ISRU as a positive effect

All but ISRU of the four primary technologies are represented in the list. The set will be investigated as a whole, followed by more targeted analysis. Coupling relationships will be studied last.

The assessment of the influence of these decisions employs a set of three analysis methods. The first looks at the IMLEO-minimal decision “switches,” meaning that the decision under investigation is switched from the position (off or on) in the globally minimum IMLEO architecture and the new global minimum, under the constraint of the decision position, is located. This change in mass is assessed as a simple measure for the influence of a given decision on the mass of minimum IMLEO architectures. The second method also employs a decision “switch.” Referred to as the Fixed Architecture Decision Switch, this analysis looks at all architectures with the given decision in the “on” position. It looks at the change in mass for the complementary architectures, where the remainder of the architecture (*i.e.* everything except for the given decision) is held constant. The average change in mass, between the architectures with the decision in the “on” and those in the “off” positions, is reported. The third method uses the Technology Influence Measure (TIM) developed in [55]. This measure is based on Design of Experiment (DOE) methods and also analyzes the average effects caused by decision position changes.

Although all three of these methods provide important perspectives, the application of these methods shows that each has limitations that should be considered in all similar analysis. After completion of this analysis, an assessment of the magnitude of influence for each decision is presented.

3.4.1 IMLEO-Minimal Decision “Switches”

A rudimentary approach to understanding the impact of the architectural decisions is to analyze the feasible tradespace with and without the allowance of each decision (*i.e.* “switching” the decision ‘on’ and ‘off’). There are similarities with one-at-a-time analysis from DOE, but in this case the remainder of the architecture-level decisions is allowed to change. For this first pass analysis, the minimum IMLEO architecture in the tradespace is located for each decision in the switch position opposite that of the globally minimum IMLEO architecture (*i.e.* the minimum IMLEO architecture is identified for the case where the decision is disallowed from the tradespace). Table 17 and Figure 43 show the results.

Table 17: Mars Minimum IMLEO Decision Switch Results

Decision #	Decision Position	Resulting Minimum IMLEO (kg)	Resulting LCC Value	% Mass Increase from Global Minimum
1	LOX/LH ₂ Off	381,390	5.167	0%
	LOX/LH ₂ On	388,270	5.167	+1.8%
	LOX/CH ₄ Off	388,270	5.167	+1.8%
	LOX/CH ₄ On	381,390	5.167	0%
2	Boil-off Control Off	612,130	4.333	+60.5%
3	NTR Off	479,200	4.833	+25.7%
4	SEP Off	565,720	4.333	+48.3%
5	Aerocapture Off	602,790	5.333	+58.1%
6	In-space CH ₄ On	384,800	5.667	+0.9%
7	No MPCV	420,270	5.167	+10.2%
8	No Monolithic Hab.	461,040	5.667	+20.9%

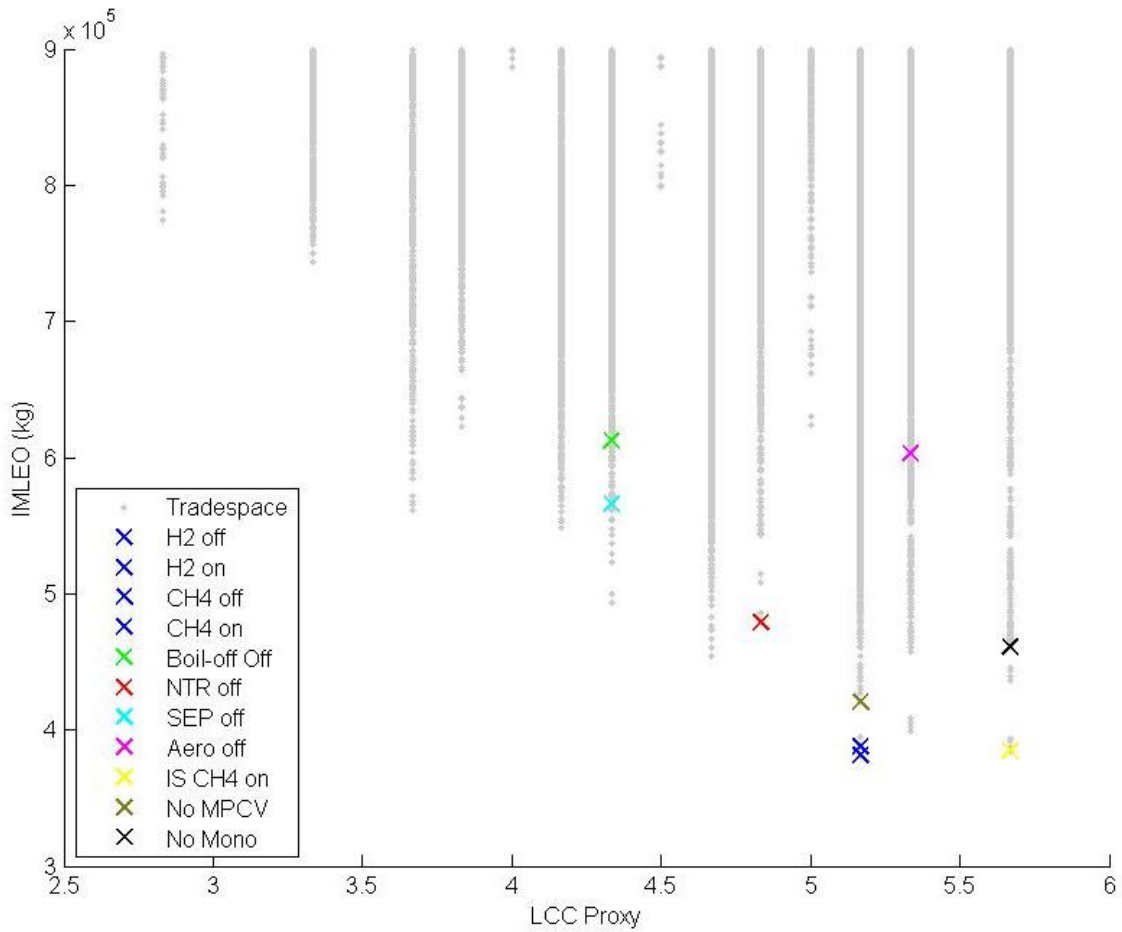


Figure 43: Mars Minimum IMLEO Decision Switch Architectures

For this and the remaining analysis, the first decision under question, the use of cryogenic propellants, is addressed using four decision states in an attempt to assess the spectrum of cryogenic propellant applications. Both hydrogen- and methane-based propulsion are set to both “off” and “on” for any stage in the architectures. For example, a state of hydrogen off disallows any hydrogen stages in the architecture, where a state of hydrogen on allows hydrogen to be in as few as one stage or as many as all stages in the architectures. For all analysis, this forces the position of the baseline to be opposite the setting shown (*i.e.* a setting of hydrogen off means that the baseline has hydrogen on). Although the effect on this analysis method is clear, the effect on the other methods may be convoluted. For the Fixed Architecture Decision Switches, the decision shown is the initial position (the method looks for the complement of the architectures with the shown setting). For TIM analysis, the shown position is the baseline for “on” under the formulation shown in Section 3.4.3. This creates some symmetry in the measure, revealed in the results shown in Section 3.4.3.

These results are distinct from the typical analysis performed on point designs, due to the fact that the remaining architectural elements are not fixed when the switch is implemented. Point design studies instead hold the architecture constant and analyze the impact of adding and removing technologies. Instead, the entire tradespace of architectural element combinations is searched to find the IMLEO-optimal solution. This is representative of when a decision maker knows that a particular technology will not be in the investment portfolio and wishes to find the best overall architecture given that information. Such a decision would occur prior to any further restrictions on the architecture.

Figure 43 shows the graphical version of the data presented in Table 17. Most importantly, it shows where the minimum IMLEO architectures exist under each of the given conditions relative to both the tradespace and the overall minimum IMLEO architecture. For example, the minimum IMLEO architecture without aerocapture, represented by the fuchsia marker, is clearly more massive and requires a small increase in LCC proxy to obtain. Furthermore, its placement reveals that it is well within the tradespace of architectures, meaning that there are many other architectures employing aerocapture that are more IMLEO-optimal.

This analysis employs the same decision-switching method present in [55]. However, this analysis was performed on an updated model which has both more accurate results and allows for the mixture of boil-off-controlled and non-boil-off controlled propulsion elements. By allowing this mixture, the model produces significantly different results for boil-off control and alters the set of architectures analyzed for the remainder of the decisions.

Boil-off control marginally has the greatest impact on IMLEO, necessitating a 60.5% increase in mass when disallowed in the architecture for a total of 612mt. A lack of ablative aerocapture requires an increase of 58.1% to 603mt. However, the lack of aerocapture also requires an LCC value much greater than the non-boil-off control architecture at 5.333 vs. 4.333. The marginal

difference of 9mt is likely outweighed by the 25% increase in LCC, meaning that the architecture with no boil-off control is likely to be favored above the one without ablative aerocapture.

SEP pre-deployment also has a significant impact, increasing total mass by 48.3% while retaining an LCC of 4.333. Of significance in many other ways is the fact that the loss of NTR only impacts the architecture with a 25.7% increase in mass. Although the increase of almost 100mt is large, this indicates that a non-NTR architecture is not as infeasible as many experts believe [17][67][68]. The non-NTR architecture also has a lower LCC than the overall minimum IMLEO architecture with a value of 4.833. This is, however, a fundamentally different architecture than the minimum IMLEO architecture, and therefore the decision to move forward with a non-NTR design would need to be made early in the decision-making process.

The most surprising architectural decision of the non-dominated architectures, the use of a semi-monolithic habitat, has nearly the same impact as NTR, resulting in a mass increase of 20.9% for the minimum IMLEO architecture without the monolithic or semi-monolithic design. This architecture, however, requires an LCC of 5.667, which is even greater than the minimum IMLEO architecture by 0.5. The disallowance of an MPCV capsule has approximately half of the impact of monolithic habitats with an increase of 10.2% in mass.

The remaining decisions focus on the use of the two primary cryogenic propellants. For the first decision, a set of four circumstances were analyzed to understand the breadth of the impact in the tradespace. It is clear from this analysis that two architectures switch propellant decision states with each other. The overall minimum IMLEO architecture has methane and not hydrogen propulsion, while an architecture with a 1.8% increase in mass has hydrogen and not methane propulsion. And despite the fact that no non-dominated architectures include the use of methane in-space stages, an architecture with less than a 1% increase in mass utilizes this configuration, although it comes at the cost of LCC value in comparison to the global minimum IMLEO architecture.

3.4.2 Fixed Architecture Decision Switches

Another method for understanding the impact of decisions is to analyze how they influence fixed architectures. In fixed architecture decision switch analysis, every architecture in the feasible tradespace with the switch in the “on” position is located. For each of these architectures, the complementary architecture is also located (if it exists in the feasible tradespace), which has all other properties fixed (*i.e.* the architecture has all the same properties except for the properties associated with the decision) with the exception of the decision in the “off” position. For each pair, the difference in IMLEO between the “on” and “off” positions is tabulated, and a box-and-whisker plot is generated for the complete set of architecture pairs. These plots have the advantage of showing the range of impacts, as well as the 25th and 75th quartiles and mean. These plots are shown in Figure 44, and the mean values are tabulated in Table 18.

Table 18: Mars Fixed Architecture Decision Switch Impact Mean Values

Decision #	Decision	Mean Impact (kg)
1	H ₂ Off	-17,243
	H ₂ On	23,515
	CH ₄ Off	-23,701
	CH ₄ On	25,735
2	Boil-off Control	-71,495
3	NTR	-97,364
4	SEP Pre-Deployment	N/A
5	Aerocapture	N/A
6	In-Space CH ₄	117,450
7	MPCV	-31,022
8	Monolithic Hab.	-63,782

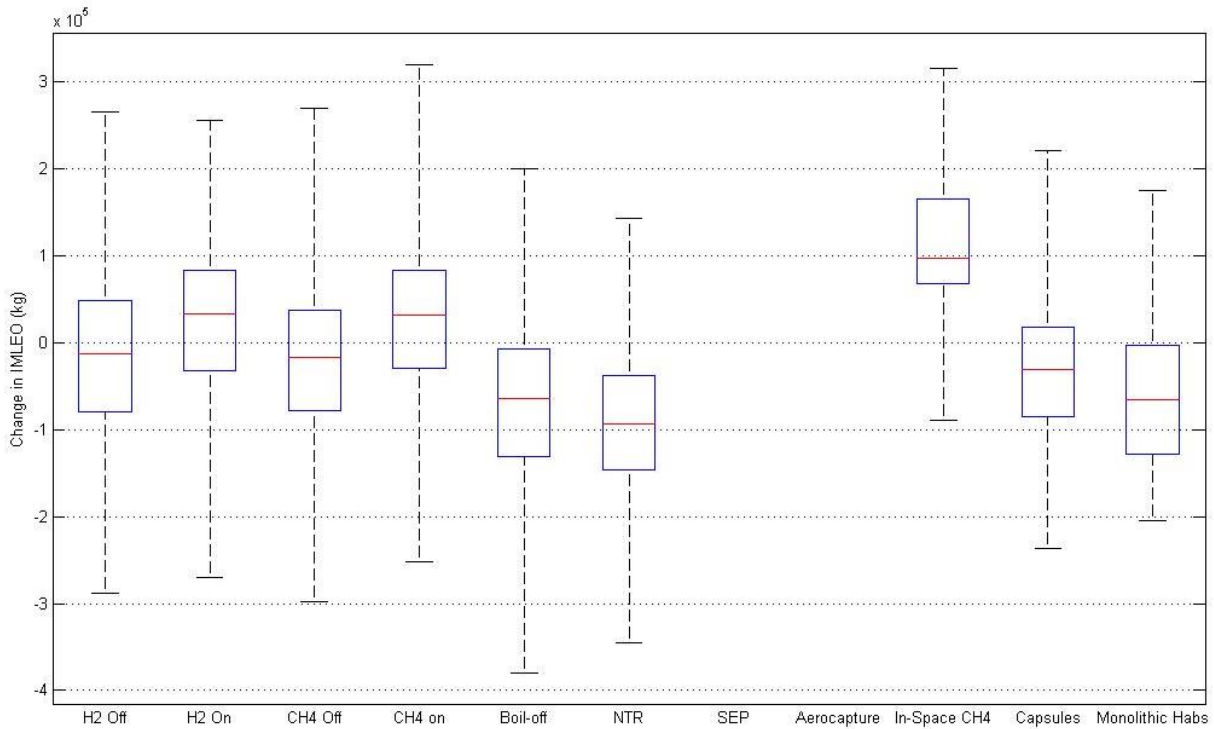


Figure 44: Mars Fixed Architecture Decision Switch Box Plots

This analysis differs from the previous analysis in two ways. Firstly, it keeps the architectures fixed in all respects with the exception of the decision of interest. Secondly, it looks at the full tradespace of affected architectures, rather than just the corresponding mass-optimal complementary architecture. It is superior in the fact that the full range of impacts can be

understood, rather than just one case. The single case can be deceiving, as it may rely on a very particular circumstance to create the mass-optimal complementary architecture.

For the vast majority of the decisions analyzed, the mean impact stays between +100mt and -100mt. However, for SEP pre-deployment and aerocapture, for every architecture with the switch “on” there appears to be no complementary architecture within the feasible region. This indicates that, on the average, both decisions have a very significant impact when constrained to the same architectural elements outside of these decisions. The employment of these technologies in the non-dominated architectures indicates that only architectures having these technologies are in the feasible region, meaning that those without the technologies are either infeasible or completely impossible under the constraints of the rocket equation. Therefore, the resulting effect is highly favorable.

Many of these results mirror those obtained from the minimum IMLEO architecture switches. Boil-off control still has a significant impact, as does the use of NTR and monolithic/semi-monolithic habitats. However, NTR shows about a 50% larger influence than the monolithic/semi-monolithic habitats in this analysis, indicating that fixed architectures have a better tendency to benefit from NTR than from monolithic/semi-monolithic habitats. MPCV capsules continue to have around half of the impact of the monolithic/semi-monolithic habitats, having a net impact of -31mt on average. This means that for an architecture with everything but the habitat arrangement fixed, the inclusion of a capsule in the set tends to decrease the mass by an average of 31mt. The cryogenic propellants once again trade on positive and negative impacts at a relatively low level compared with the other decisions, although the magnitude of the impact has grown from the minimum IMLEO architecture analysis to being almost comparable with the use of the MPCV.

The most surprising result difference is the impact of in-space CH_4 stages, which have the largest magnitude impact at approximately 117mt. This impact changed from the smallest non-zero impact in the previous analysis to the largest measurable impact. As expected, this is an average negative impact on the architecture (an increase in mass), although the magnitude is very high. This implies that the minimum IMLEO architecture identified in the earlier analysis is unusual in its ability to remain at a low mass with an in-space CH_4 stage.

Because of the manner in which this analysis is performed, it may be expected that the cryogenic propellant states would be mirrored across the “zero influence” point for the “off” and “on” states. However, as shown in Figure 44, the states are non-symmetric. The exponential nature of the rocket equation makes some architectural combinations impossible, requiring infinite mass [61]. This means that not all architecture decision combinations are present in the analysis. This also means that for each starting decision state, there is a slightly different set of other fixed architectural decisions, due to the fact that not all architectures are represented in the tradespace. Since the analysis relies on the beginning state of the decision, the results differ across the “off” and

“on” states.

3.4.3 Technology Influence Measure

In addition to the previous methods, a more robust method for the evaluation of decision influence stemming from established literature is desired. The Technology Influence Measure (TIM) was first introduced in [55]. It builds on the concept of main effects analysis from design of experiments (DOE) literature, and it fundamentally measures the sensitivity of a metric to the inclusion of a technology element or architectural decision. It was originally designed to describe only pure technologies in HEXANE but has here been adapted to measure the sensitivity of IMLEO to the eight decisions described. TIM is simply the difference between the mean IMLEO when the decision is switched “on” and the mean IMLEO when the decision is switched “off.” Effectively, this is the “non-fixed” version of the previous analysis. However, this theoretically gives the best understanding of the sensitivity of IMLEO to these decisions by employing a well-validated method from the field of DOE. Figure 45 and Table 19 show the results of the TIM analysis.

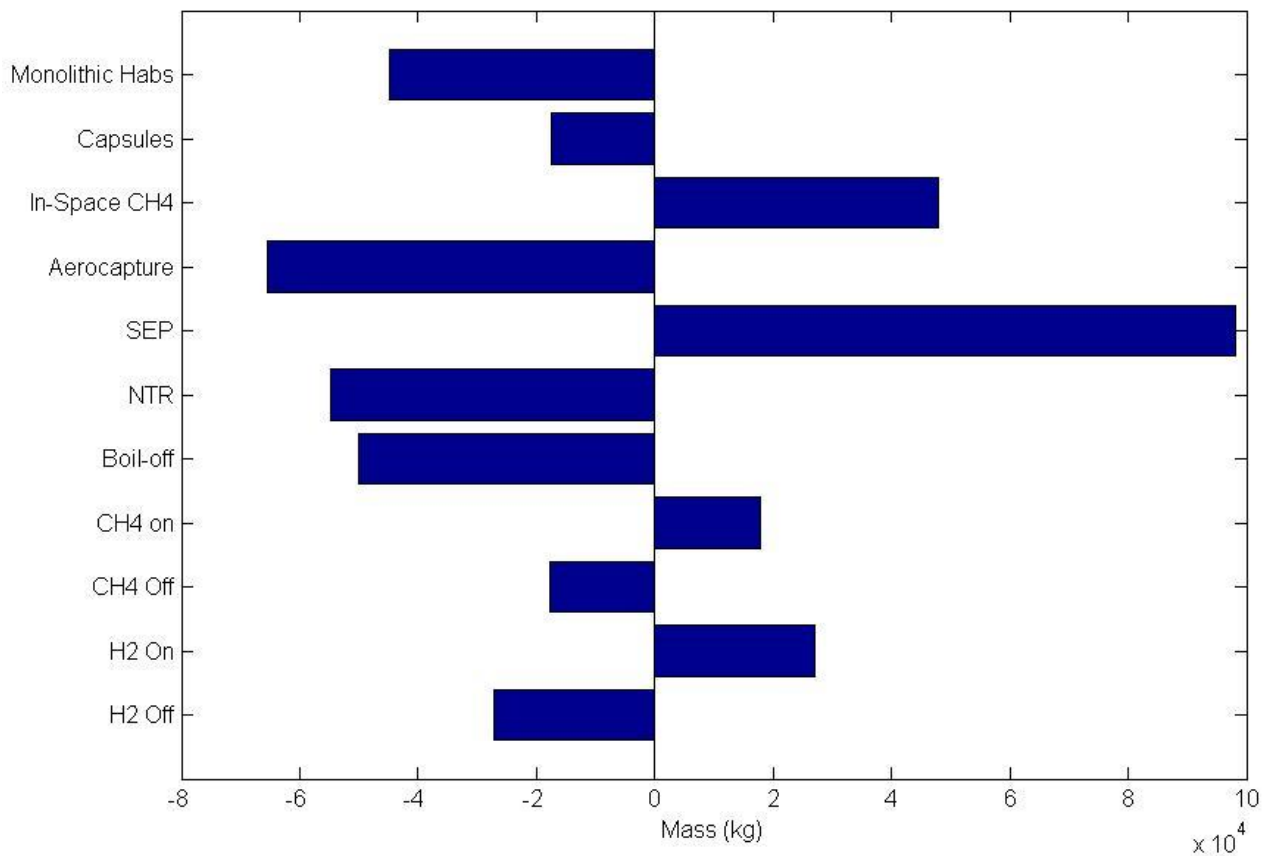


Figure 45: Mars Decision TIM Bar Chart

Table 19: Decision TIM Values

Decision #	Decision	TIM (kg)
1	H ₂ Off	-27,051
	H ₂ On	27,051
	CH ₄ Off	-17,785
	CH ₄ On	17,785
2	Boil-off Control	-50,049
3	NTR	-54,642
4	SEP Pre-Deployment	98,162
5	Aerocapture	-65,354
6	In-Space CH ₄	47,872
7	MPCV	-17,549
8	Monolithic Hab.	-44,717

While most of the decisions follow the same trend as previous analyses, there is one striking difference in the TIM measurements. This analysis superficially shows that SEP pre-deployment heavily negatively impacts architectures (increases mass) on the average. An unbalance between the number of architectures with and without SEP pre-deployment causes this misconception, further described in Section 3.4.7. This large increase in mass was shown as a definitive result in [55] using the same analysis methods. However, Section 3.4.7 describes why this is an erroneous result.

Aerocapture, NTR, and boil-off control have the greatest influence on IMLEO, respectively, following the SEP anomaly. Monolithic habitats also have comparable influence to boil-off control and NTR, with MPCV capsules having approximately half the influence of the monolithic habitats. The cryogenic propellants have gained in influence to the level of the MPCV, and, as expected, they are symmetric for “on” and “off” states using TIM. In-space CH₄ has reduced its influence under this analysis to a level comparable with NTR, boil-off control, and monolithic habitats, although this is still a much greater impact than seen in the minimum IMLEO architecture analysis. This metric continues to indicate that the use of in-space CH₄ has a primarily negative effect, although some well-designed architectures can implement use of these stages with good results.

Conclusions

The quantitative analyses of the decisions of interest have shown mostly consistent results, indicating that a few of these identified decisions can have a significant impact on the mass of Mars in-space architectures. A summary of these results is given in Table 20, with the most influential decisions highlighted.

Table 20: Mars Decisions - General Analysis Summary

Decision #	Property	Min. IMLEO % Mass Increase	Mean Impact (kg)	TIM (kg)
1	LOX/LH ₂ Off	0%	-17,243	-27,051
	LOX/LH ₂ On	+1.8%	23,515	27,051
	LOX/CH ₄ Off	+1.8%	-23,701	-17,785
	LOX/CH ₄ On	0%	25,735	17,785
2	Boil-off Control	+60.5% (off)	-71,495 (on)	-50,049 (on)
3	NTR	+25.7% (off)	-97,364 (on)	-54,642 (on)
4	SEP	+48.3% (off)	N/A (on)	98,162 (on)
5	Aerocapture	+58.1% (off)	N/A (on)	-65,354 (on)
6	In-space CH ₄	+0.9% (on)	117,450 (off)	47,872 (off)
7	MPCV	+10.2% (off)	-31,022 (on)	-17,549 (on)
8	Monolithic Hab.	+20.9% (off)	-63,782 (on)	-44,717 (on)

Each of these decisions will be discussed in further detail. Analysis of their tradespace coverage will provide insight into their robustness to changes in the architecture elements and changes in the technology portfolio, and a qualitative understanding of how this influences the decision process will also be given. In-depth analysis of each of the eight identified decisions, in the order listed, follows.

3.4.4 Cryogenic Propellant Usage

With the analysis of the decisions identified as they affect the tradespace in general completed, a more in-depth analysis focusing on tradespace coverage and decision robustness can be performed. For each decision, this detailed analysis follows a brief discussion of the technology's or element's application in the tradespace.

“Cryogenic propellants” refers to liquid oxygen / liquid hydrogen and liquid oxygen / liquid methane bi-propellant systems which require cryogenic cooling. These propellant options offer superior performance in terms of specific impulse and mass energy density in exchange for larger volumes and the need for active cooling. Recent improvements in capabilities have driven these propellants for further consideration in manned exploration architectures, as energetic requirements tend to drive mass by increasing large propellant loads. However, the general inquiry into the use of cryogenic propellants in the system is vague and ambiguous. The prior analysis has focused on the use of hydrogen and methane in the general architecture (*i.e.* the allowance or disallowance in the architecture in general). In order to further this analysis, a closer look at the propellants used in the system in each of the three primary propulsion environments (in-space, descent, and ascent) is necessary. The fixed architecture switch analysis and TIM for these

propulsion environments are shown in Figure 46 and Figure 47, respectively.

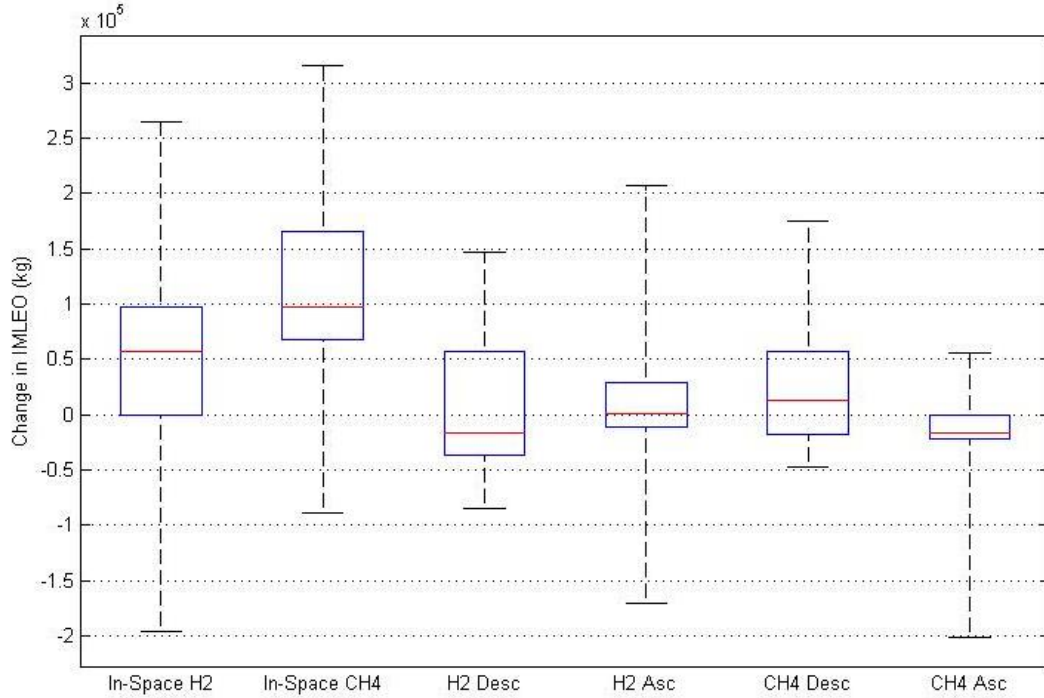


Figure 46: Mars Cryogenic Propellant IMLEO Influence Box Plot

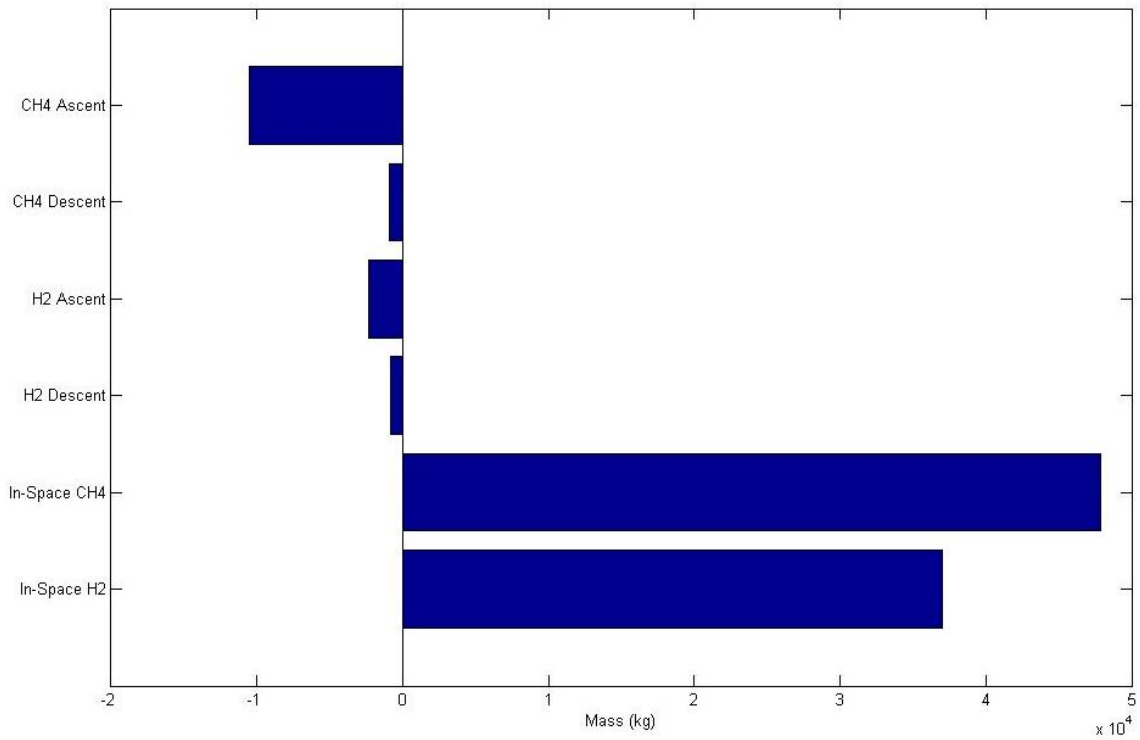


Figure 47: Mars Cryogenic Propellant TIM Bar Chart

The fixed architecture switch analysis and TIM agree on the sign and magnitude of the impact for each of these options. In general, the in-space propulsion elements tend to suffer from the use of cryogenic propellants, primarily due to the dominance of NTR in the tradespace and its superior performance. Descent favors hydrogen, if only slightly, whereas ascent favors methane. Methane and hydrogen ascent, however, are very close in their mean, quartiles, and range, with hydrogen having a longer upper tail as the only major departure from this trend. The longer upper tail for hydrogen and longer lower tail for methane indicate that, given uncertainty in the architecture, methane is more likely to have a benefit to the architecture for the ascent stage.

Combined with the previous analysis, it is clear that the use of cryogenic propellants is not as impactful as the majority of other decisions. This is summarized in Table 21. With impacts ranging from 17mt to 27mt, these decisions have a relatively minor influence compared to those impacting at the 50-100mt level. It should be noted, however, that this typically relies on switching between the propellant options, rather than abandoning cryogenic propellants all together.

Table 21: Mars Cryogenic Propellant Analysis Summary

	Min. IMLEO Switch Arch.	Mean Switch Impact (kg)	TIM (kg)
H ₂ off	0%	-17,243	-27,051
H ₂ on	+1.8%	23,515	27,051
CH ₄ off	+1.8%	-23,701	-17,785
CH ₄ on	0%	25,735	17,785

3.4.5 Boil-Off Control

Boil-off control has been estimated to have one of the greatest impacts on long-duration manned exploration missions of the set of possible technologies [69]. It is therefore also expected to lead in the influence and impact measures previously described. However, unlike the analysis performed in [55], architectures in the tradespace analyzed in this thesis allow for the mix of boil-off controlled and non-boil-off controlled propulsion stages. This departure from previous analysis stems from the large propellant mass used for the EDS. This short burn from LEO suffers much less from propellant boil-off but also constitutes a large portion of required propellant mass. The significant increase in dry mass from boil-off control technology is therefore not justified for the maneuver. Later stages, however, suffer greatly from the lack of boil-off control, and therefore it was deemed likely that a combination of control states would be beneficial to many architectures. This likely has a significant impact on the results, given that most mixed use cases likely have poorer performance than the pure cases. Despite this change, boil-off control has been shown to be

one of the most influential architectural decisions, although not *the* most influential in most analysis performed, contradictory to the results reflected in [55]. A tradespace coverage plot is shown in Figure 48, which demonstrates that 94.6% of the feasible architectures employ boil-off control in at least one propulsion stage. The architectures to the left, with low LCC value, are those that specifically only utilize hypergolic propellants throughout the architectures. It should be noted that boil-off control can be on or off for hydrogen and methane stages and it is forced on for NTR propulsion stages as an explicit rule due to the use of pure hydrogen in NTR stages.

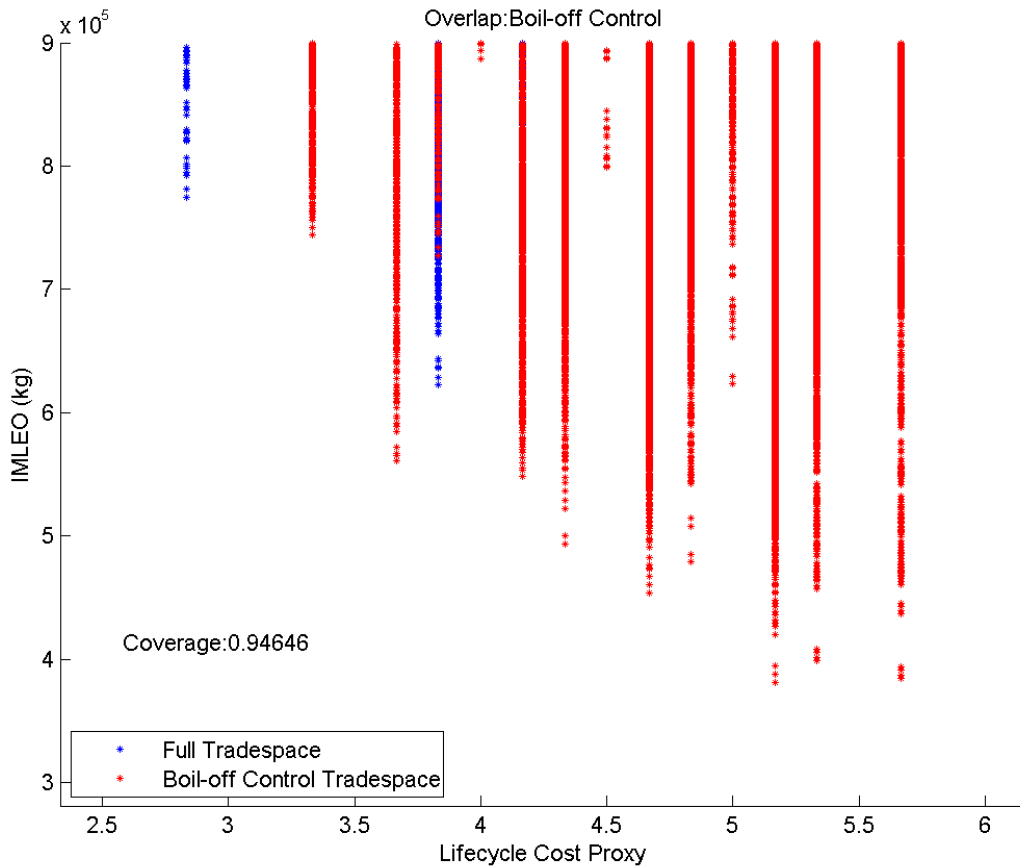


Figure 48: Mars Boil-off Control Tradespace Coverage

Table 22: Mars Boil-off Control Analysis Summary

Pareto Coverage	Min. IMLEO Switch Arch.	Mean Switch Impact	TIM	Constrained Tradespace Coverage
85.7%	+60.5%	-71,495 kg	-50,049 kg	94.6%

Table 22 summarizes the set of analysis that has been performed for boil-off control. Combined with the tradespace coverage plot, the data implies that, unless a minimum technology portfolio approach is desired, boil-off control should be considered for use, given its benefit to the architecture, likely saving between 50 and 75mt on orbit. This also implies that boil-off control is robust to changes in the other architectural elements, given its prevalence in the tradespace and relatively minor impacts on the engineering of the remaining components. It is not, however, very robust to a change in its own status for the same reason.

3.4.6 Nuclear Thermal Rockets

The viability of nuclear technology in terms of both its technological capabilities as well as political survivability has been hotly debated in the space community since the NERVA tests in the 1950s and 1960s [70][71][72]. A complete understanding of its impacts on the tradespace of architectures may be critical for future investment decisions. Combined with the information gained from the general tradespace analysis, it is clear that NTR is critical for a complete evaluation of the architecture tradespace.

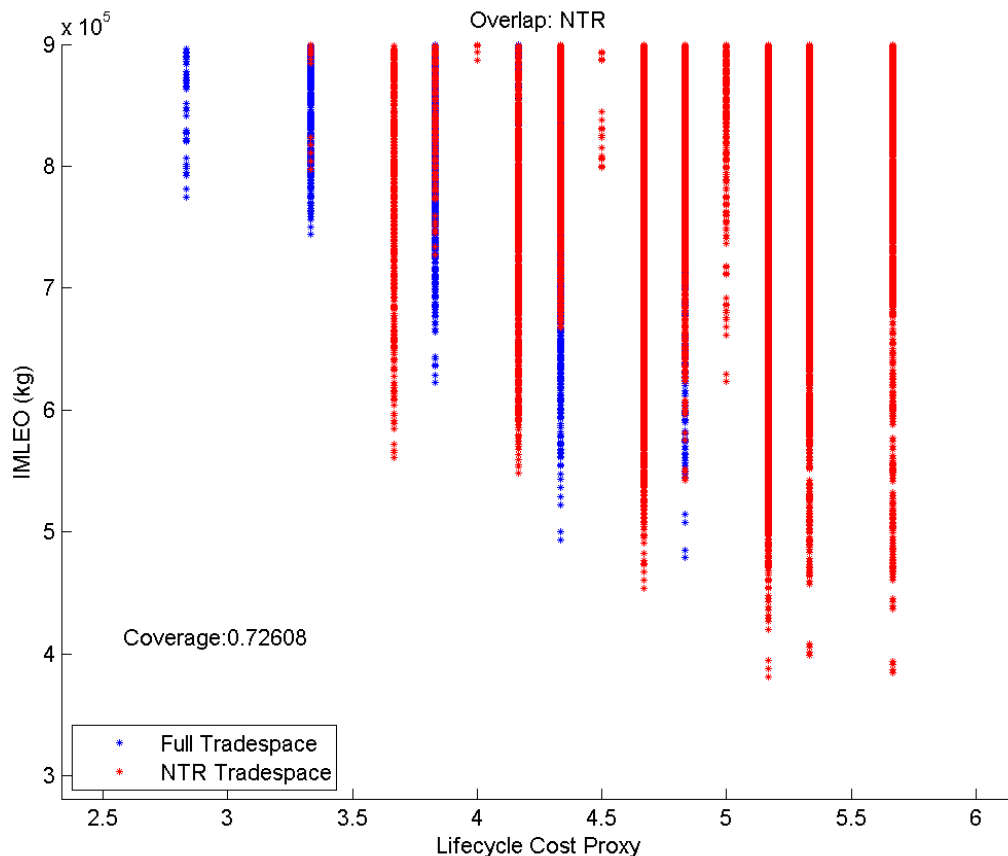


Figure 49: Mars NTR Overlap with Full Tradespace

NTR tradespace coverage is shown in Figure 49. Approximately 72.6% of the total feasible architectures contain at least one NTR segment, beginning at an LCC of 3.333 and upward. However, as described with the general characteristics, NTR begins to dominate in architectures at an LCC of 3.667. There are several LCC values where the NTR-utilizing architectures are no longer mass-optimal, including the 4.333 and 4.833 values. Non-dominated Architecture 5, which is the IMLEO-optimal architecture at LCC 4.333, represents a fully hydrogen propulsion architecture, combining non-boil-off controlled and boil-off controlled stages. The particular combination of technologies that allows NTR to also have a presence on this LCC value also restricts it from being mass-optimal compared to the fully hydrogen-based architectures.

Table 23: Mars NTR Analysis Summary

Pareto Coverage	Min. IMLEO Switch Arch.	Mean Switch Impact	TIM	Constrained Tradespace Coverage
57.1%	+25.7%	-97,364 kg	-54,642 kg	72.6%

From the summarized data in Table 23, it is clear that NTR has a significant impact on the architectures, but it is highly dependent on the way in which the impact is measured. For example, there are some architectures that have relatively low IMLEO without NTR, allowing for a minimum IMLEO switch with an increase of 25.7% above the absolute minimum IMLEO architecture. Yet, at the same time, for an architecture whose elements are otherwise fixed, the change of NTR from “off” to “on” has a mean impact of almost 100mt improvement. Combined with the fact that the vast majority of the constrained tradespace is covered by NTR-utilizing architectures, it is implied that the use of NTR is robust to changes in other parts of the architecture, with some exceptions. Overall, it is therefore recommended that NTR be implemented, given its robustness, unless an architecture is set in the regime where NTR is not mass-favorable, such as when low LCC is desired.

3.4.7 Pre-Deployment using Solar-Electric Propulsion

HEXANE has been initially set to only allow pre-deployment with a low-thrust system, namely solar-electric propulsion. Although there are a variety of alternative low-thrust options [73], SEP has been chosen by NASA HAT as the option of interest due to a combination of its established abilities and the rate of development for the technology. NASA has already invested in the development of Xenon-fueled thrusters, but it has yet to put significant effort into developing the class of thrusters needed for manned exploration mission requirement satisfaction. Therefore it is still very much key to understand how SEP influences in-space architectures for these missions.

Table 24 shows that prior analysis has given mixed results, leading to some confusion about the benefits of SEP in these architectures. However, given the coverage revealed by Figure 50, only 0.03% of the feasible architectures do not include pre-deployment, meaning that the “averaging” effect seen in the analysis may be misleading. To help show the portion of the tradespace not employing pre-deployment, the complementary graph is shown in Figure 51. Those few architectures revealed in this figure have relatively good mass properties in comparison to the mass feasibility boundary, allowing for the minimum IMLEO switch influence to amount to 48.3%. On the other hand, TIM analysis considers only the mean values of the architectures. For the set of 24 architectures that do not employ SEP pre-deployment, their mean IMLEO is low. For the remainder of the architectures, the mean is weighted by the existence of many architectures near the feasible boundary of 900mt, meaning that their mean is much higher than the many optimal architectures. This results in the surprising TIM value of +98mt on average.

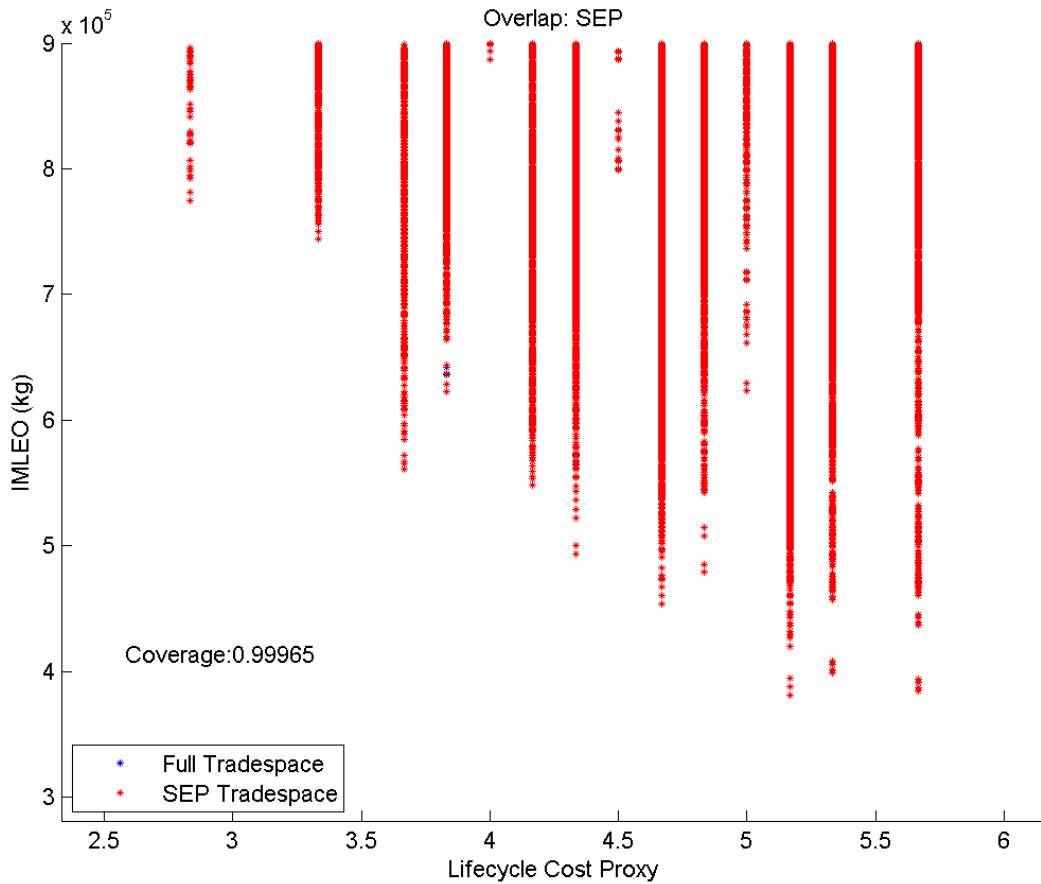


Figure 50: Mars SEP Pre-Deployment Tradespace Coverage

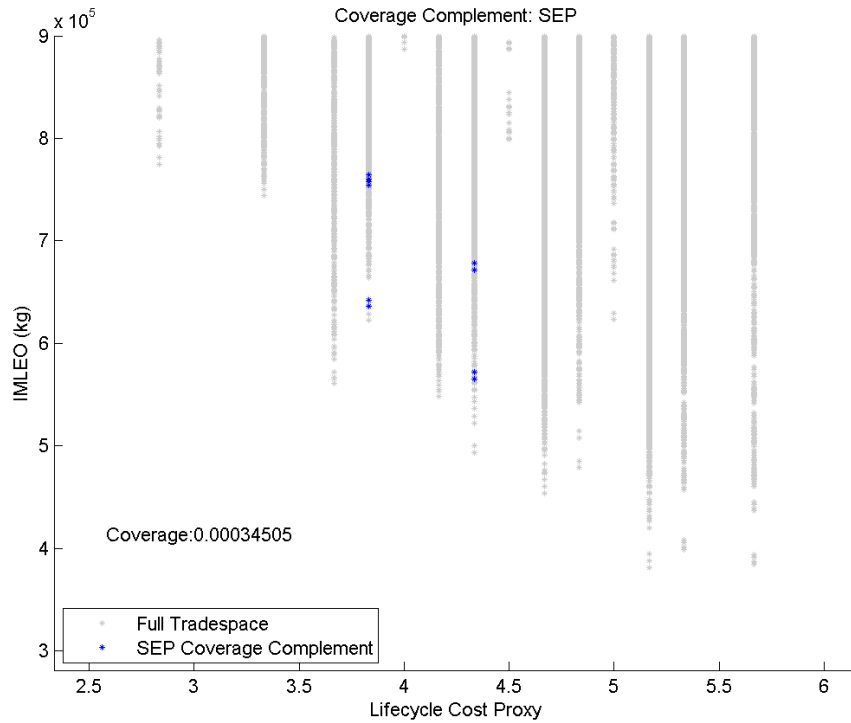


Figure 51: Mars SEP Pre-Deployment Tradespace Complement

Table 24: Mars SEP Pre-Deployment Analysis Summary

Pareto Coverage	Min. IMLEO Switch Arch.	Mean Switch Impact	TIM	Constrained Tradespace Coverage
100%	+48.3%	N/A	98,162 kg	99.97%

It is therefore the conclusion that the inclusion of SEP in the architecture is both beneficial and robust in almost 100% of feasible architecture arrangements, although it is possible to create moderate-mass feasible architectures without SEP pre-deployment in very rare circumstances.

3.4.8 Ablative Aerocapture

During the Design Reference Architecture 5.0 study, the inclusion of aerocapture capabilities at Mars became a significant difficulty for large-mass, manned elements. Ablative aerocapture significantly reduces the energetic requirements in exchange for the increased mass and complexity associated with aeroshielding [74]. Following the publication of the DRA 5.0 report, several studies were conducted to analyze the feasibility of creating sufficient aeroshielding structures for this purpose, which showed that it would, in fact, be possible [53][75]. Aerocapture for manned vehicles has never been attempted under such circumstances, and so it is vitally important to

understand how the inclusion of such an element would impact in-space architectures in order to trade with associated risks.

The analysis conducted has shown that aerocapture has one of the largest impacts on the architectures and appears on all of the Pareto frontier architectures. This is reinforced by Figure 52, which illustrates that 95.9% of the feasible architectures employ aerocapture either at Mars or on return to Earth for braking in LEO to rendezvous with a re-entry capsule. Table 25 summarizes the results of the analysis conducted for aerocapture. This decision consistently has the second greatest impact of the decisions, trailing boil-off control for the minimum IMLEO switch and pre-deployment for TIM analysis. In addition, the lack of fixed architectures for analysis in the fixed architecture switch analysis indicates that aerocapture is necessary under most conditions. Furthermore, this indicates that the use of aerocapture in a given architecture is not robust to change and must be firmly kept in the technology portfolio once designed for in order to produce a feasible mission architecture. It is, however, robust to changes in the remainder of the architecture in the fact that it is likely to be a necessary element despite almost any given change.

Table 25: Mars Aerocapture Analysis Summary

Pareto Coverage	Min. IMLEO Switch Arch.	Mean Switch Impact	TIM	Constrained Tradespace Coverage
100%	+58.1%	N/A	65,354 kg	95.9%

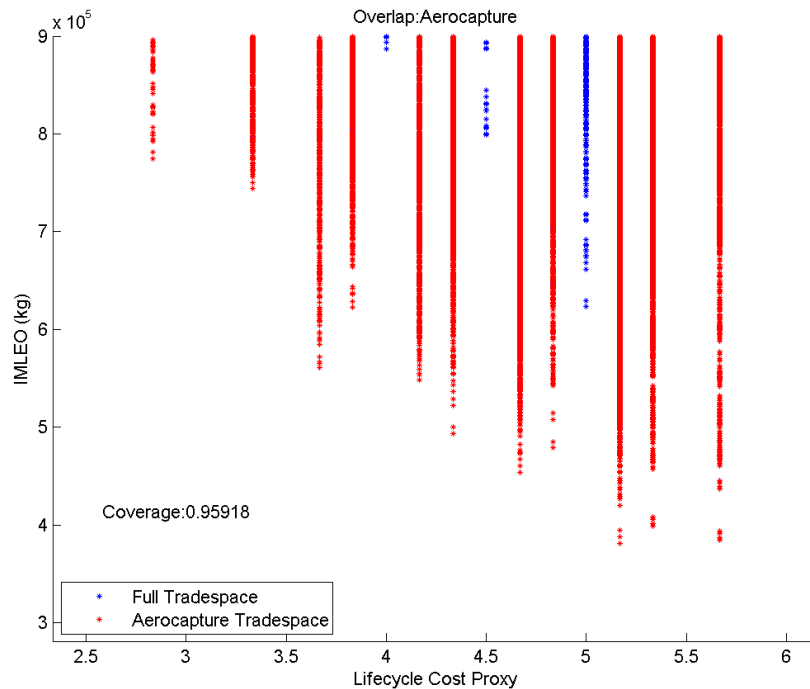


Figure 52: Mars Aerocapture Tradespace Coverage

3.4.9 In-Space LOX/LCH₄ Stages

The inclusion of methane in-space propulsion elements is not entirely independent of the analysis performed for the general class of cryogenic propellants, but the focus allows for additional analysis not easily performed for the entire set of cryogenic propulsion stages. The analysis, as summarized in Table 26, has been highly inconsistent and is heavily dependent on the particular properties of the tradespace. As Figure 53 shows, the small set of feasible, low-mass architectures that employ this element allows for a minimum IMLEO architecture with a less than 1% increase in mass from the IMLEO-optimal solution. At the same time, the majority of architectures with in-space methane stages tend to lie nearer to the feasibility cap, influencing TIM and the fixed arch. switch analysis. For most architecture arrangements, the use of methane is detrimental, which means that the fixed switch analysis should indicate a large increase in mass, as it does. There are a sufficient number of low-mass solutions to counter the high-mass solutions, given that there are few in the tradespace at only 18.8% coverage, which reduces the impact as seen by TIM.

This indicates that, overall, use of in-space methane propulsion is likely to be unwise unless there is a significant technology investment and the globally mass-optimal solution becomes unattainable.

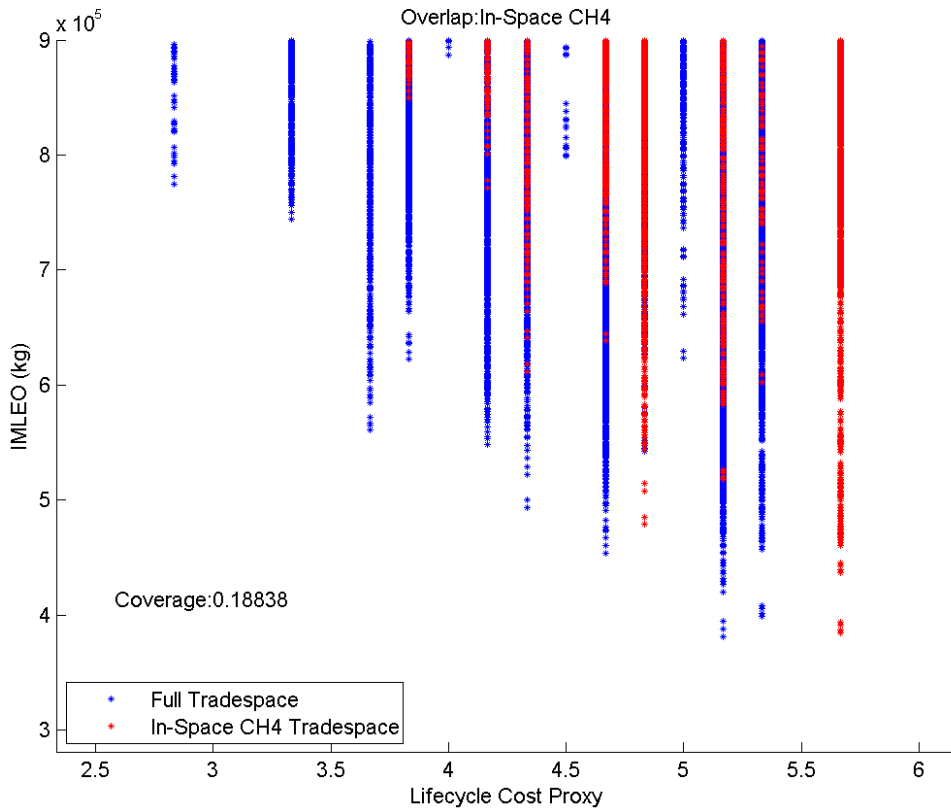


Figure 53: Mars In-Space CH₄ Stage Tradespace Coverage

Table 26: Mars In-Space CH₄ Analysis Summary

Pareto Coverage	Min. IMLEO Switch Arch.	Mean Switch Impact	TIM	Constrained Tradespace Coverage
0%	+0.9%	117,450 kg	47,872 kg	18.8%

3.4.10 Capsules and the MPCV

The Orion capsule was originally designed for use in the Constellation Program [2]. Following the collapse of the program, NASA and the U.S. government continued to fund the development of the Orion, which was later renamed the MPCV or Multi-Purpose Crew Vehicle [5]. Because of the amount of development work that has already been done on the MPCV, it is unlikely that NASA would consider architectures that do not include the capsule. The analysis engine in HEXANE already constrains the size of “capsule-like” habitats to the mass of the MPCV, therefore approximating its use in the architectures. Prior analysis has shown that all non-dominated architectures on the IMLEO-LCC Pareto frontier utilize a capsule and therefore include the MPCV. It has also been shown, however, that the exclusion of the MPCV from an architecture only has an impact of approximately 10% of the mass. The general trend shows that the average impact for including an MPCV in the architecture is net positive, indicating that NASA has made a sound investment in developing a small crew capsule.

A summary of the analysis results is shown in Table 27. In addition to this analysis, the total coverage of the tradespace is shown in Figure 54. A particularly important result is that 83% of the feasible architectures employ an MPCV-like vehicle. This means that a restriction forcing the use of an MPCV in a future architecture would only eliminate 17% of all possible feasible architectures. Furthermore, all non-dominated architectures use an MPCV-like vehicle, meaning that none of the likely architectures to be used in a mission are eliminated by such a constraint.

Table 27: Mars MPCV Analysis Summary

Pareto Coverage	Min. IMLEO Switch Arch.	Mean Switch Impact	TIM	Constrained Tradespace Coverage
100%	+10.2%	-31,022	-17,049	83.4%

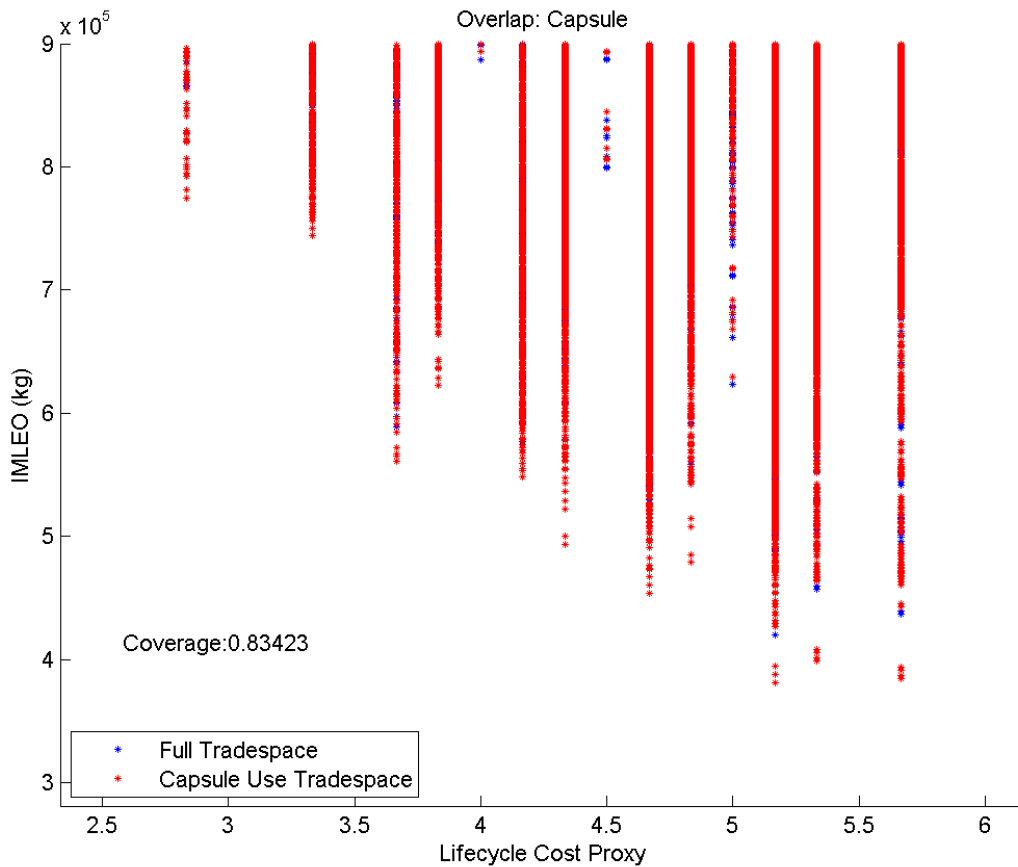


Figure 54: Mars Capsule Overlap with Full Tradespace

3.4.11 Monolithic and Semi-Monolithic Habitats

One of the most surprising results from the analysis of the non-dominated architectures was the existence of monolithic and semi-monolithic habitats amongst many of the best configurations. The use of semi-monolithic habitats is very rare in point design studies, indicating that many experts dismiss the concept entirely. However, this analysis has shown that, under the right conditions, such habitat configurations can be highly advantageous, given that certain caveats are addressed. These caveats include several important assumptions in HEXANE that influence the nature of these habitats as well as use requirements that are not addressed in the model. The most important assumption to impact the “correctness” of the analysis is the combination of habitat functions into their largest mass component. In other words, the combination of between 5 and 7 of these functions, as is present in the semi- and fully-monolithic habitats, assumes that the final habitat takes on the mass of the largest component, adjusted for aeroshield mass and extended ECLSS lifetime. The logic behind this is addressed in Section 2.5.2. This is clearly not the case in the

combination of so many sub-functions into a single habitat, although there is no known way to correct for this at the level of abstraction in which HEXANE operates.

Additionally, the complexity of the combination of so many sub-functions is quite significant, meaning that the habitat must also survive a variety of environments. This includes the operational complexity in switching between zero- or micro-gravity and $\sim 1/3g$ environments. This is not included in the sizing parametric for such habitats, and therefore it must be carefully considered in any detailed analysis. The risk associated with operating in these environments is also not considered, along with the lack of redundancy in the habitation space. The redundancy of habitable volume has been desired by the space community both for reduced-use cases as well as for failure backup. A monolithic habitat inherently creates a single-point failure, and the inclusion of a second habitable volume reduces the associated risks. The amount of habitat fractionation should therefore be carefully considered for its impact on complexity and risk.

Under these assumptions, it has been shown that the use of semi-monolithic habitats can have approximately the same impact as the use of NTR. This indicates that it would be advantageous for NASA to consider the use of these habitats despite the aforementioned downsides. The tradespace coverage plot is shown in Figure 55, and the summary of prior analysis is shown in Table 28. The coverage analysis shows that despite the coverage of almost half of the non-dominated architectures, only 5.3% of the overall feasible tradespace employs monolithic or semi-monolithic habitats. This indicates that, despite its value, architectures including this architectural decision may not be very robust to changes throughout the lifecycle of the mission or missions. In other words, such architectures are not likely to be adaptable to changes in the investment portfolio of NASA during the development of the architecture, and therefore the decision must be set firmly in order to successfully implement this architectural element.

Table 28: Mars Monolithic and Semi-Monolithic Habitat Analysis Summary

Pareto Coverage	Min. IMLEO Switch Arch.	Mean Switch Impact	TIM	Constrained Tradespace Coverage
43%	+20.7%	-63,782	-44,717	5.3%

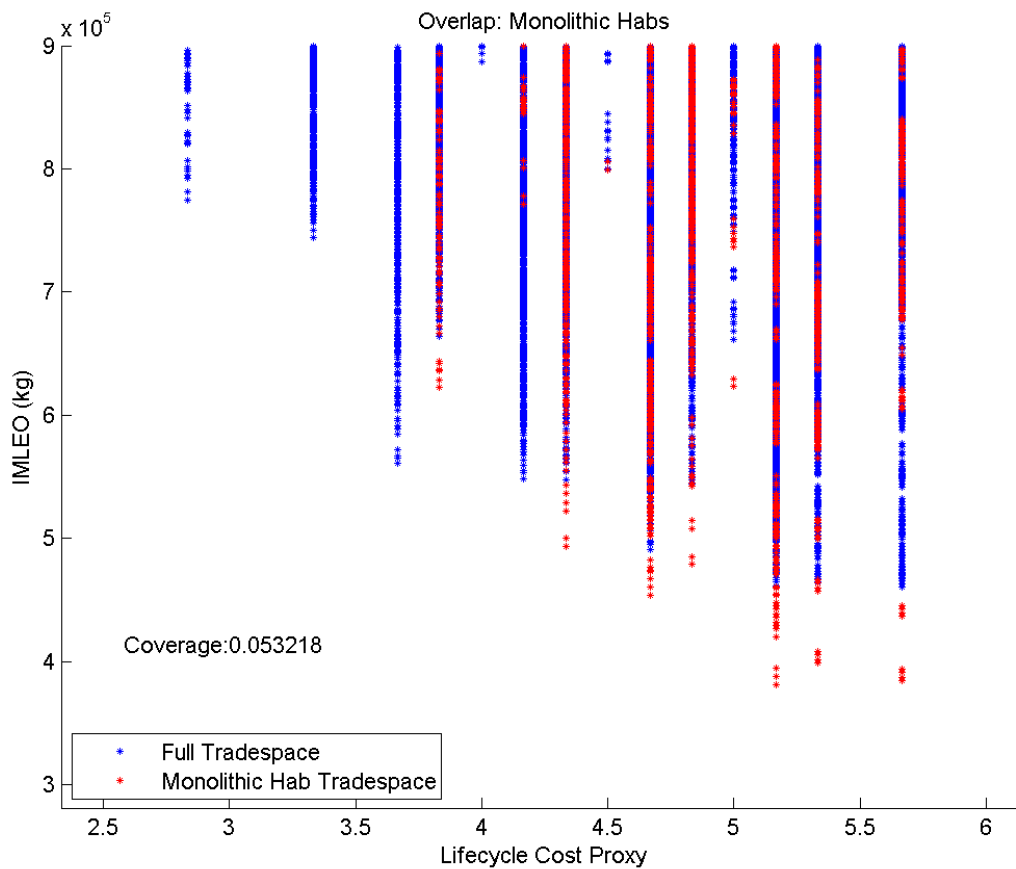


Figure 55: Mars Monolithic and Semi-Monolithic Habitat Overlap with the Full Tradespace

3.4.12 Decision Coupling

Beyond the measure of how each decision influences the architectures and architectural tradespace, it is also important to understand how architectural decisions and technologies interact with each other. In addition to the eight decisions, four coupling relationships were identified as possibly impactful to a broad range of architectures. These include:

1. LOX/LH₂ with Boil-off Control without ISRU as a negative effect
2. LOX/LH₂ and LOX/LCH₄ in combination as a negative effect
3. NTR, LOX/CH₄, and ISRU in combination as a positive effect
4. Semi-monolithic habitats with ISRU as a positive effect

A methodology for analyzing coupling relationships was developed in [55], once again drawing from DOE literature and the concept of interaction effects [76]. This measure, known as

Technology Interaction Coupling Effects (TICE), is a measure of the influence of one technology or decision on another technology or decision's influence. Like the previous measures, including TIM, the values should be read relative to each other rather than as absolute measures. Equation 3 defines the exact nature of the TICE values, with defined variables in Table 29.

Equation 3: TICE Definition

$$TICE_{M,T^1,T^2} = [\bar{M}\{T_{on}^1 \cap T_{on}^2\} - \bar{M}\{T_{on}^1 \cap T_{off}^2\}] - [\bar{M}\{T_{off}^1 \cap T_{on}^2\} - \bar{M}\{T_{off}^1 \cap T_{off}^2\}]$$

$$T^1 \neq T^2$$

$$T_{on}^1 \cup T_{off}^1 = P$$

$$T_{on}^2 \cup T_{off}^2 = P$$

Table 29: TCIE Variables

Variable	Description
<i>TICE</i>	Technology Interaction Coupling Effect
<i>M</i>	A specific metric
<i>Tⁿ</i>	A specific technology or architectural decision (<i>n</i> is an arbitrary index)
\bar{M}	Average metric value for relevant subset of architectures
<i>T_{state}ⁿ</i>	The set of architectures with the <i>n</i> th technology or decision either on or off (represented by <i>state</i>)
$\{T_{on}^1 \cap T_{on}^2\}$	The set of architectures that have both technology 1 on and technology 2 on (provided as an example)
<i>P</i>	The full set of evaluated architectures across the tradespace

To analyze a large set of TICE values simultaneously, a Technology Coupling Interaction Matrix (TCIM) is used. This places the TICE values in an N^2 matrix to easily identify strong interactions. In Figure 56, the four identified coupling relationships are analyzed alongside the remainder of the primary technologies in order to identify additional strong coupling relationships. Because two of the four coupling relationships previously identified exist between three decisions or technologies, they are simplified by combining the first two decisions into a single property. Although this does not fully represent the complexity of these relationships, it is adequate for the analysis of the combination of all three decisions in the architectures.

	Hydrogen & Boil-off	Hydrogen	NTR & Methane	Semi-Monolithic Hab	Methane	ISRU	Aerocapture	NTR	SEP	Boil-off
Hydrogen & Boil-off	X	Undef.	54	-6	53	-7	2	28	114	Undef.
Hydrogen		X	28	-7	26	0	20	38	Undef.	69
NTR & Methane			X	-12	Undef.	-16	-14	Undef.	Undef.	Undef.
Semi-Mono. Hab				X	11	Undef.	-35	-7	Undef.	1
Methane					X	2	21	-6	Undef.	7
ISRU						X	-11	6	Undef.	7
Aerocapture							X	Undef.	Undef.	Undef.
NTR								X	Undef.	Undef.
SEP									X	52
Boil-off										X

Figure 56: Mars Decision TCIM

Figure 56 shows the TCIM, labeled with the influence of decisions on each other in metric tons of IMLEO. “Undef” boxes indicate that there are insufficient data points to extrapolate a relationship. Many of the relationships presented are as expected from both prior analysis and experience, while a few are unexpected and often deceiving.

The first coupling relationship identified in prior analysis exists between the combination of hydrogen stages with boil-off control and ISRU, which is expected to have a negative effect. This expectation is counter-intuitive, given that much of the propellant can be extracted from the surface and therefore would be of benefit to the overall architecture. However, as seen from the general tradespace analysis, the use of boil-off control negates the need to extract propellant from the surface, combined with the knowledge that ISRU requires a significant additional dry mass for powering the system. As seen in Figure 56, the combination has, on average, a non-effect, or zero influence. There are relatively few architectures with this combination of decisions, and they counter each other with both positive and negative effects. The balance is not exactly zero, but it is smaller than 10mt of influence. The small value of this influence indicates that this is not as

important of a coupling relationship as others that have been identified.

The second relationship of interest exists between hydrogen and methane stages combined in an architecture. This is expected to have an overall negative effect. The TCIM shows that this is, in fact, the case, with a weak negative relationship. Many architectures have an overall design that is conducive to the use of one propellant type or the other, typically in descent or ascent stages as NTR dominates in-space stages. The combination, therefore, on average, is not beneficial. However, methane is more advantageous for ascent with ISRU, given the proportion of the mass that may be extracted on site, despite the decrease in specific impulse. Thus, there are some architectures where the combination is, in fact, advantageous, countering the negative impacts and thus producing a lower impact on average.

The third relationship exists between NTR, methane, and ISRU as a combination. As alluded to in the previous paragraph, methane is more advantageous with ISRU due to the proportion extracted on the surface. As expected, the TCIM shows that there is a weak positive effect produced by this combination. This leads to the fourth relationship between semi-monolithic habitats and ISRU. The TCIM shows that there are insufficient data points to extrapolate a relationship. From prior analysis, it is known that the combination of semi-monolithic habitats and ISRU exists in non-dominated architectures. Since no architectures exist in the feasible region that do not have this combination, it is likely that the coupling is highly symbiotic.

Other strong coupling relationships are revealed in the TCIM. A highly symbiotic relationship exists between semi-monolithic habitats and aerocapture. This is intuitive, as aerocapture tends to be more mass-optimal than propulsive orbit insertion, and this effect is exaggerated with large masses to brake. Another point of interest is the mutually negative relationship between NTR and hydrogen. In effect, NTR is the higher performance version of hydrogen with a large dry mass to counter the increase in specific impulse. For these highly energetic missions, the need for large masses of propellant outweighs the increase in dry mass by reducing the propellant needed with high specific impulse. Therefore there are few architectures where the combination of these propulsion options are beneficial.

SEP pre-deployment once again produces misleading results. With only 25 architectures of the approximately 3 million in the tradespace not employing pre-deployment, the averaging effect is highly deceptive. This is the same effect seen in the TIM results, shown specifically, in this case, between hydrogen with boil-off control and SEP pre-deployment, as well as between boil-off control in general and SEP. Boil-off control covers 95% of the tradespace but produces similarly deceptive results when analyzing coupling with hydrogen stages. There is a set of architectures utilizing non-boil-off controlled hydrogen stages that are relatively low mass, thus skewing the averaging effect in a similar fashion to SEP pre-deployment.

In summary, the four coupling effects identified prior to this analysis were evaluated, and two

additional strong relationships were identified. The combination of hydrogen stages with boil-off and ISRU was found to have a non-effect. The coupling between hydrogen and methane stages was found to have a weak negative (mass increasing) effect. The triple combination of NTR, methane, and ISRU was found to have a weak positive (mass decreasing) effect. Semi-monolithic habitats were found to have a interactive coupling relationship with aerocapture, and NTR was found to have a negative relationship with hydrogen stages. In addition, SEP pre-deployment and boil-off control were shown to have misleading results from this analysis due to the lack of architectures with appropriate properties in the tradespace.

3.5 CONCLUSIONS AND RECOMMENDATIONS

For each of the decisions identified by the feasible tradespace analysis and the non-dominated architecture analysis, the influence of each decision was assessed using three methods for general impact on the tradespace. An evaluation of feasible tradespace coverage for each decision allowed qualitative assessment of the decision’s robustness to change, although these conclusions were not explicitly stated for each decision. A summary of the general influence as well as the robustness characteristics is given in Table 30, along with a recommendation for the decision period in which the use of the decision should be chosen. While much of the analysis has been quantitative, the conclusions regarding robustness and recommendations for the decision period are purely qualitative in nature and should therefore be considered only guidelines for more detailed analysis.

Table 30: Decision Summary and Recommendations

	Influence	Robustness to Decision Switch	Robustness to Architecture Changes	Decision Period
Cryogenic Propellant Use	Low	Moderate	Moderate	Mid-term
Boil-off Control	Medium	Low	Moderate	Mid-term
NTR	High	Low	High	Early
SEP Pre-Deployment	High	Low	High	Early
Ablative Aerocapture	High	Low	High	Early
In-Space Methane	Low	Moderate	Low	Early to Mid-term
MPCV Employment	Low	Low	High	Mid- to Late-term
Semi-Monolithic Habitats	Medium	Moderate	Low	Early

The most influential decisions were found to be aerocapture, SEP pre-deployment, and NTR, followed closely by boil-off control. These decisions were also found to be present in the vast majority of architectures in the feasible region, making their robustness to changes in the decisions very low. However, this also means that, because there are many architectures that employ the elements, they are also very robust to changes in the remainder of the architectural elements. It is

recommended that these decisions be made early because they require significant investment, the architectures depend upon them, and they allow for changes in the rest of the architectural elements.

The use of semi-monolithic habitats should also be decided early due to its relatively large influence and low robustness, meaning that, unless the decision is made early, it should not be included in the architecture. Mid-term decisions include those decisions that have a low or moderate influence with some level of robustness, including cryogenic propellants, boil-off control, in-space methane, and the use of the MPCV.

In addition, several strong coupling relationships were identified using the TICE and TCIM methodologies. The most important of these include the interactive coupling between semi-monolithic habitats and aerocapture, semi-monolithic habitats and ISRU, and NTR with methane and ISRU. Strong exclusive couplings identified include hydrogen with boil-off control and methane and NTR with hydrogen. The strength of these relationships indicates that the decisions regarding these architectural features should be made in parallel.

3.6 A BRIEF DISCUSSION OF LUNAR AND NEA RESULTS

The complete set of analysis shown for Mars missions was also conducted for Lunar, low-energy NEA, and high-energy NEA missions. Appendix B contains those results without any of the associated discussion. However, several important implications emerge from the combination of the Mars, Lunar, and NEA results. This section gives a brief summary of results from each destination, along with a short discussion of the emergent results from the combination of destination results.

3.6.1 Lunar Architecture Results

The baseline science values for the lunar results are representative of a four crew, 30 day (long stay), full access mission, without the use of any intermediate staging locations. Methane and oxygen are assumed to be recoverable on the surface from lunar regolith, although this requires a larger energy source than for Mars surface missions (see Appendix A for more details). Missions are assumed to stop in LLO before descent to the surface.

As expected, the IMLEOs for the seven non-dominated architectures are much less than those of the Mars surface missions, ranging from 159mt to 262mt. The feasible region for lunar missions is capped at 450mt (approximately one ISS mass). The LCC values of the non-dominated set range from 2.333 for the 262mt mission to 4.333 for the 159mt mission. SEP pre-deployment is present in all non-dominated architectures, boil-off control is present on the four minimal IMLEO architectures, aerocapture on three architectures, and ISRU on the two minimal IMLEO

architectures. The global minimum IMLEO architecture uses purely hydrogen stages, the return stages with boil-off control and the EDS without boil-off control. The habitat allocation is nearly LOR, with the exception that there is also a LEO rendezvous with an MPCV capsule.

The largest influence technologies, in terms of TIM, are aerocapture (decrease in mass), semi-monolithic habitats (decrease in mass), and the use of hydrogen stages (decrease in mass). SEP pre-deployment is shown to have a large influence, but this is once again attributed to the lack of architectures without SEP in the tradespace. NTR is shown to have a small, mass-increasing influence.

Like the Mars architectures, the lunar missions also have a majority of architectures that employ MPCV capsules, at a coverage of 77%. However, most non-dominated architectures do not use capsules. This indicates that a policy to force the use of the MPCV on a lunar mission would likely cause an increase in mass above the set of non-dominated architectures, although it is a robust architectural decision given the coverage of the feasible tradespace. Semi-monolithic and monolithic habitats have a coverage of 4.6% of the tradespace, but the non-dominated architectures are not included in this set. In the lunar case, however, these architectures are far more dispersed in the tradespace in comparison to the Mars mission architectures, therefore increasing the robustness of the decision to include a semi-monolithic or monolithic habitat.

Lastly, the strongest coupling relationship identified for lunar missions is a positive (mass decreasing) relationship between aerocapture and capsule use. This is logical, given that the use of a capsule typically coincides with Earth orbit rendezvous on return, meaning that there would be a significant savings in propellant need with ablative aerocapture during this maneuver.

3.6.2 Low-Energy NEA Results

The science value baseline for low-energy NEA missions include a four crew, 30 day mission without intermediate staging locations. No ISRU is allowed for NEA architectures. There are no descent, ascent, or surface stages for these architectures. Interaction is assumed to be through either EVA or the use of an SEV.

Three architectures create the Pareto frontier for the low-energy NEA tradespace. These architectures are limited to approximately one half of the ISS mass, or 225mt. The non-dominated architectures range in mass from 151mt to 183mt. Because there are no surface stages, the LCC values range from 0.500 to 1.333. SEP pre-deployment is once again seen in all non-dominated architectures, with aerocapture on the two lowest IMLEO cases and boil-off control on the minimum IMLEO architecture. Similar to the lunar architecture, the low-energy minimum IMLEO architecture consists of purely hydrogen-based propulsion stages. However, the habitat allocation is that of the semi-monolithic habitat, with a capsule for launch and Earth re-entry.

Semi-monolithic habitats have, by far, the largest TIM influence (mass reducing), followed by

capsules, aerocapture, and NTR. SEP pre-deployment once again shows signs of the same easily misinterpreted results due to the coverage in the tradespace. Capsules also show 77% coverage of the feasible region, with 2/3 of the non-dominated architectures employing the allocation of a capsule. Semi-monolithic habitats have a coverage of 14.3%, covering many of the lower IMLEO architectures in the tradespace. The strongest coupling relationships are shown to be in-space methane with SEP pre-deployment as a mass-reducing coupling and NTR with SEP as a mass-increasing coupling relationship.

3.6.3 High-Energy NEA Results

The science value baseline for high-energy NEA missions includes four crew members, a 30 day stay, and no intermediate staging locations. No ISRU is included in the architectures, and no descent, surface, or ascent stages are allowed. Interaction with the asteroid is once again assumed to be through EVA or the use of an SEV, which is sized with the architecture.

Due to the high energetic requirements, the high-energy NEAs are expected to have a higher mass than lunar and low-energy NEA architectures. The mass limit on the feasible region is set to be approximately one ISS mass (450mt). Three architectures lie on the IMLEO-LCC Pareto frontier, ranging in IMLEO from 218mt to 378mt. The corresponding LCC values range from 0.833 to 1.667. SEP pre-deployment is present on the two lowest IMLEO architectures, aerocapture is present on two of the three architectures, and boil-off control is seen on the two lowest IMLEO architectures. Similar to the Mars minimum IMLEO mission, the minimum IMLEO architecture for the high-energy NEA mission uses NTR with a drop tank along with an NTO/MMH stage and a semi-monolithic habitat allocation.

NTR, boil-off control, SEP pre-deployment, and semi-monolithic habitats have the greatest architecture influence by the TIM analysis, respectively. Capsules cover 75% of the feasible tradespace, with 2/3 coverage of the non-dominated architectures. Semi-monolithic habitats cover 4.9% of the tradespace and all of the non-dominated architectures. NTR and SEP both cover 95% of the feasible region. However, NTR covers all but the lowest LCC architectures in the tradespace, while SEP pre-deployment covers all but the lowest IMLEO architectures (*i.e.* the interior of the tradespace).

In terms of coupling relationships, in-space hydrogen with SEP has a net positive (mass-decreasing) relationship, followed by aerocapture with SEP and aerocapture with capsules as positive relationships. In-space hydrogen with in-space methane creates a exclusive coupling.

3.6.4 Combined Results Analysis

The majority of the important results for all destinations analyzed by HEXANE have now been

presented. Several overall results emerge from this set of information, including a reinforcement of the grouping of these destinations and general results about technology investment.

The first, and perhaps most important, result is that the destinations can be classified into two categories which match the energetic requirements. High energy missions, including Mars surface missions and high-energy NEAs, not only have similar energetic requirements, but the overall architectures have similar properties. When comparing the globally minimum IMLEO architectures, both employ NTR with a drop tank setup and use a semi-monolithic habitat allocation. They also both employ a separate SEP pre-deployment stack to deliver the Earth return stage to the destination orbit. Low energy destinations, including the Moon and low-energy NEAs, also have both similar energetic requirements as well as architectural similarities. Comparing their globally minimum IMLEO architectures, both destinations' architectures have approximately the same mass (159mt vs. 151mt), both use purely hydrogen stages with boil-off control, and they both have aerocapture and SEP pre-deployment. Although they are not directly related in the habitat allocation, both destinations' feasible tradespaces show that the semi-monolithic habitat allocation is less favorable in general than for the high energy destinations. For lunar missions, many have modified LOR or EOR allocations, while for low-energy NEAs, the semi-monolithic habitat coverage does not include many of the best mass architectures.

Therefore, it can be concluded that these four destinations can be grouped by their overall energetic requirements to reflect both fundamental requirements as well as "best" architecture tendencies. This may have long-term implications for mission campaigns. Technology build-up for similarly grouped destinations can occur regardless of the choice within the group, meaning that the decision for the choice of destination, given that the choice remains within the energy class, can be deferred. Furthermore, this grouping may have implications for the technology buildup and demonstration phases. Similar energy destinations can be used as demonstration locations for technologies employed on any mission in the class of destinations, given that such demonstrations remain mass-optimal even at a different destination. Although this has in no way been shown definitively in this analysis, the implications of this grouping should be carefully considered.

The other significant results from the combined analysis from all destinations are related to coverage of feasible tradespaces for the various architecture-level decisions. For example, capsules were shown to have very good coverage in all destinations, but their presence on the non-dominated architecture set is less strong for destinations other than Mars. This implies that NASA's investment in the MPCV program is robust to the choice of destination but may lead to an overall mass increase from the optimal architectures. Semi-monolithic habitats are shown to have a small coverage of all tradespaces, ranging from approximately 4% to 14%. This indicates that their robustness is low across all destinations. Combined with the many caveats related to the use of semi-monolithic habitats, it is unlikely that their use in exploration architectures would be

advisable. Lastly, SEP pre-deployment is shown to be prevalent in all tradespaces and likely has a very positive (mass-reducing) influence on most architectures. Therefore, NASA's continued investment into Xenon-based SEP thrusters is highly encouraged.

3.7 SUMMARY

This chapter has analyzed the primary results for Mars in-space architectures. A combination of constrained feasible tradespace analysis and a deeper look at the non-dominated architectures in the IMLEO-LCC tradespace identified eight decisions and four coupling relationships for further analysis. These included most of the primary technologies identified in the decomposition process along with several additional decisions. Most unusual amongst these was the existence of semi-monolithic habitats among many of the non-dominated architectures. Although they were shown to exist in only 5% of the feasible architectures, these habitats have a unique synergistic relationship with the remaining decisions and technologies that allow them to create the most IMLEO-optimal architectures. The semi-monolithic habitat and other seven decisions were shown to have a variety of influences on the architectures as well as a variety of levels of robustness to future changes in architecture design. Based on the properties of these decisions, a qualitative assessment was made to recommend a time period for the decision process associated with each decision.

This chapter also gave a brief analysis of the remaining destinations analyzed by HEXANE. The combination of these sets of analysis revealed that destinations can be classified into two categories: high energy and low energy. This classification incorporates both energetic requirements and typical architecture traits. High energy missions typically include NTR stages with drop tanks and semi-monolithic habitats with SEP pre-deployment stacks, while low energy missions typically include all hydrogen propulsion architectures with SEP pre-deployment, aerocapture, and boil-off control. This classification implies that the grouping may be advantageous for deferring destination decisions while investing in architecture-level technologies. The analysis further showed that the investment in the MPCV program is robust to the selection of destinations and that the investment in solar-electric propulsion should be continued.

4. STEPPING STONES: PROGRESSION TOWARD LOW-ENERGY DESTINATIONS

Chapter 1 has given an introduction to the topic of systems architecture as a method for the analysis of manned exploration architectures, while Chapter 2 gave an overview of a modeling tool for analyzing the tradespace of in-space exploration architectures. Chapter 3 reviewed the results from the model for Mars conjunction-class surface missions as described in Chapter 2, focusing on trends identified in the tradespace tied to particular architectural decisions in the context of these Mars surface missions. Chapter 3 also analyzed the set of non-dominated architectures for the Mars case as a final destination. However, the issue of demonstrating the necessary technologies to achieve final mission goals remains outstanding. Chapter 4 introduces an additional modeling tool for capturing sets of demonstration missions that may be used to build to final mission capabilities. For each individual surface mission identified by HEXANE, a set of demonstration missions, referred to herein as “sub-missions” in order to differentiate from the primary surface mission, can be used to build confidence in the use of new elements and buy down risk. The sequencing of these sub-missions, both in total number and aggregation of elements for each sub-mission, is analyzed within this chapter. Lunar and low-energy NEA end missions create the baseline for this analysis. Trends in the sub-mission sequences emerge to inform decisions about acceptable risks, the use of non-surface destinations, and launch vehicle needs.

4.1 MOTIVATION AND PROBLEM STATEMENT

Although Mars has been the unofficial long-term destination of interest to the space community for many years [20][21][22][77][78][79][80], destinations with lower overall energy requirements have reduced propellant mass and mission cost. These missions provide more immediate value return and retain the interest of the public through more frequent missions [81]. Of the locations analyzed by HEXANE, both lunar missions and low-energy NEA missions are low energy destinations. U.S. space policy explicitly lists NEAs as NASA’s destination goal over the next 15 years, while many international space agencies are working toward lunar missions [82][83]. It is therefore of value to determine not only the most optimal “surface mission” architectures (*e.g.* Lunar surface missions) but also the pathway for building the technology and capabilities to perform these missions, which may include “demonstration sub-missions” to intermediate points like Earth-Moon Lagrange points. For the purposes of this analysis, “technologies” refer to the primary technologies identified in Chapter 2, namely aerocapture, ISRU, SEP pre-deployment, cryogenic boil-off control, and advanced propellants. “Capabilities” refer to habitat and propulsion element

functional combinations that have not been previously developed. This may include elements such as combined descent and ascent vehicles or combined MOI and TEI propulsion elements. The Orion MPCV is considered, for the purposes of this model, to be fully demonstrated, while functional combinations previously built for Apollo missions are considered to be at a higher development level than new combinations but lower than the MPCV.

Demonstration sub-missions, which have a more limited scope and reduced overall risk in comparison with the final surface mission taken from HEXANE, provide such a pathway. These missions are similar in concept to the stepping stones and flexible path described in Chapter 2 in the fact that they build capabilities through incremental missions. This builds into the overall structure of building a long-term mission strategy, shown in Figure 57. At the highest level, the end-goal of a long-term strategy is to design a multi-mission campaign. The campaign is composed of multiple sortie-like science missions to different surface destinations. This is the level of mission strategy and architecture addressed by HEXANE. In order to build up the technologies and capabilities necessary to perform these final surface missions, a set of demonstration sub-missions is necessary. For the purposes of this analysis, the final surface mission is always the final sub-mission in the sequence of sub-missions. The demonstration sub-missions build up the technologies and capabilities prior to the implementation of the final surface mission.

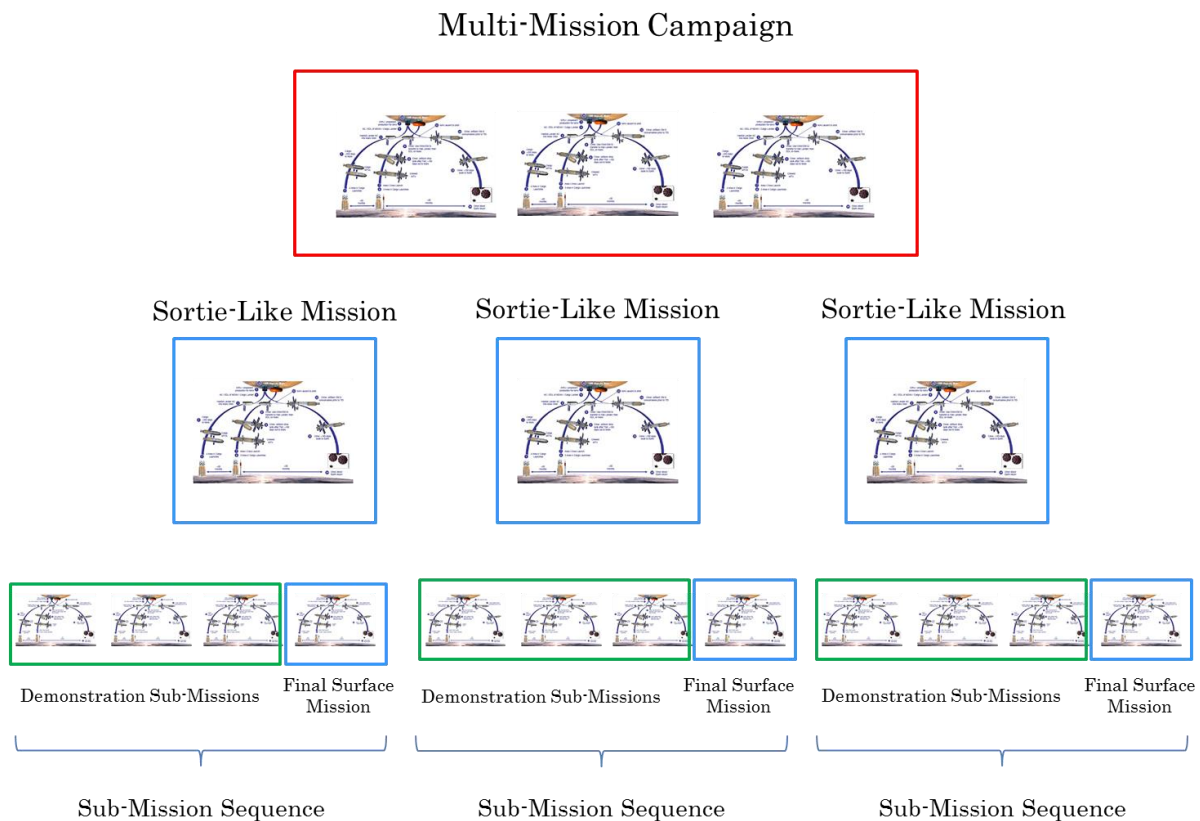


Figure 57: Long-term Mission Strategy Breakdown

The value of each sub-mission lies in the successful demonstration of one or more technology and/or capability. Therefore, the scope of the mission is typically much less than the final surface mission for which the technologies and capabilities are demonstrated. Reduced risk is achieved by primarily using well developed elements and implementing only one or a few new technologies and/or capabilities. Determination of the sequence of demonstration sub-missions leverages the results from HEXANE by integrating the non-dominated architectures as final surface mission goals and utilizing the element sizing capabilities of the model. One or many missions analyzed by HEXANE are chosen for analysis, each representing a final mission for the set of demonstration sub-missions. The model then determines the set of technologies and capabilities to demonstrate along with a set of possible destinations for the sub-missions. The possible aggregations of the demonstrable technologies and capabilities are computed and the resulting tradespace of possibilities is generated for analysis. “Aggregation” refers to the grouping of multiple technologies and/or capabilities into a demonstration sub-mission. For example, a single sub-mission may demonstrate technology 1, technology 2, and capability 1. The alternative may be three sub-missions, each demonstrating one technology or capability.

A sequence of demonstration sub-missions requires three pieces of information: the destination pathway, *i.e.* the sequence of locations for the demonstration sub-missions prior to the final surface mission; the technology and capability pathway, *i.e.* the aggregation of demonstrable technologies and capabilities on each of the sub-missions; and information about the risks, costs, and value of both the overall campaign of missions and the individual demonstration sub-missions. Different aggregations of demonstrable technologies and capabilities will result in different mission risks and costs. For example, grouping many technologies and/or capabilities into the first sub-mission will increase the risk to that sub-mission while decreasing mass (and therefore a portion of operational cost) through the use of more advanced elements. Demonstrating a single technology, on the other hand, would require more mass but pose less risk through the use of well-established mission elements. Sequence-level metrics are expected to be in tension with some sub-mission-level metrics for much the same reason. By aggregating many demonstrable technologies and/or capabilities upfront, the total risk may be reduced at the sequence level due to the reduction in total sub-mission count, as each new mission includes additional crew transfers and assembly operations. To acquire this information, Low-E, a model to generate the set of sub-missions and evaluate their properties, acts as an additional module to HEXANE by leveraging its outputs.

Each point on the resulting tradespace represents the complete set of demonstration sub-missions, including the final surface mission. Table 31 gives an example of what this information looks like. The Sequence # refers to the point in the tradespace, which represents a full set of demonstration sub-missions. This set will have associated metric values. Each sub-mission in the sequence will have a different set of technologies and/or capabilities aggregated for demonstration.

Once one of these technologies and/or capabilities is demonstrated, it is not repeated for demonstration in following sub-missions. However, it may be employed within the following sub-missions as a fully demonstrated technology or capability. The number of sub-missions may be as few as one, representing an all-up demonstration during the actual surface mission, or as many as the total number of demonstrable technologies and capabilities. In this example, four technologies and five capabilities are demonstrated on a set of four sub-missions. Each sub-mission will also have an associated destination. The sequencing of these destinations is given in the final column.

Table 31: Demonstration Mission Set Example

Sequence #	Metric 1	Metric 2	Sub-mission 1	Sub-mission 2	Sub-mission 3	Sub-mission 4	Destination Sequence
#	Value	Value	Tech. 1, Tech. 2, Cap. 1	Tech. 3, Cap. 2	Cap. 3	Tech. 4, Cap. 5	Dest. 1, Dest. 2, Dest. 3, Dest. 4

4.2 LOW-E AS A BACKEND TO HEXANE

Low-E is designed to complement the capabilities of HEXANE by leveraging output information to determine the set of demonstrable technologies and capabilities for the sequence of sub-missions. Low-E, like HEXANE, is MATLAB-based and explores a fully enumerated tradespace of sub-mission architecture sequences. The process collects end-mission (*i.e.* final surface mission) data from the model, determines the necessary technologies and capabilities to demonstrate, enumerates the full set of possible sub-mission destinations and aggregations of technologies and/or capabilities to demonstrate on each sub-mission, and analyzes the tradespace of these sequences on a set of risk and cost metrics.

4.2.1 Demonstrable Technologies & Capabilities

In order to assess the sequencing of demonstrations, the list of demonstrable technologies and capabilities must be established. Because Low-E is reliant on HEXANE data, the level of abstraction is retained between the models, meaning that Low-E can only capture the level of detail present in the results from HEXANE in terms of the breakdown of demonstrable technologies and capabilities. Therefore only the architecture-level elements, both technologies and capabilities, are demonstrable during the sub-missions. Although the technologies are tightly linked with those discussed in Section 2.3, the remainder of the capabilities, specifically habitat and propulsion capabilities, are highly coupled with the set partition decisions for the habitation and transportation sub-functions discussed in Section 2.2. Of the possible habitat types and propulsion elements

created by these set partitions, those that require demonstration missions as major capabilities must be defined. Table 32 shows a hierarchy of habitat and propulsion elements which allows for the complete development of any set of elements while constraining the set of demonstrable capabilities. This hierarchy is necessary given the explosion of the number of possible demonstrable capabilities, *i.e.* types of habitats and propulsion elements, created through the set partitions. If each were handled separately, this would require the analysis of 83 separate possible demonstrable capabilities to account for both habitats and propulsion elements. By creating a hierarchy, the dominant set of requirements for any given habitat element is captured, as related to both mass and functionality, while reducing the number of possible demonstrable capabilities. The hierarchy also enables the use of the full range of HEXANE-level set partitions by grouping the resulting habitat combinations into tiered hierarchies.

This hierarchy is intended to determine the dominance of habitat and propulsion element properties as multiple sub-functions are combined. For the habitat elements, the tiers are primarily based on mass, environmental restrictions, and common coupling with other sub-functions. For propulsion elements, the tiers are based on similar properties, most heavily influenced by mass and common coupling properties. For example, if the functionality of a deep space habitat is combined with an ascent habitat, the necessary demonstration capability is assessed as only a deep space habitat. Similarly, when an in-space propulsion element is combined with a descent element, it is assessed as only a deep-space propulsion element for the purposes of demonstration. Launch and entry capsules are not included, as it is assumed that an Orion MPCV will be used for these purposes when not combined with other functionality, and therefore no additional demonstration mission is necessary. Sufficient development of the MPCV reduces the necessity for an independent demonstration [5].

Table 32: Habitat and Propulsion Element Hierarchy

Hierarchy Level	Habitats	Propulsion Elements
1	Monolithic Habitat	In-Space Propulsion
2	Semi-Monolithic Habitat	Descent Propulsion
3	Deep Space Habitat A	Ascent Propulsion
4	Deep Space Habitat B	Exploration Vehicle Propulsion
5	Exploration Vehicle	
6	Descent Vehicle	
7	Ascent Vehicle	
8	Surface Habitat	

A monolithic habitat refers to a habitat that combines all seven sub-functions of habitation. Semi-monolithic habitats combine five or six of these sub-functions, specifically in the case of the exclusion of the launch or re-entry vehicles. This is included as a separate category, given the complexity of re-entering large vehicles as well as the fact that this is the most common case for HEXANE-IMLEO-optimal architectures. Deep Space Habitat B refers to the case where a second deep space habitat is included in the architecture, *i.e.* a different in-bound deep space habitat from the outbound deep space habitat, which has different functionality from the Deep Space Habitat A. DSH B combines with additional habitat requirements, necessitating a different structure. In the case where two DSHs exist physically but with the same functionality, there is not a DSH B, given that the development of one implies the development of the other. The exploration vehicle combines the descent, surface, and ascent vehicle functionality into a single entity under the conditions of a zero- or micro-g environment, such as an asteroid. This, in effect, is the habitat portion of a Space Exploration Vehicle (SEV). The SEV is a concept being developed by NASA for both in-space interactions with asteroids as well as pressurized surface operations at Mars and the Moon. In this case, the SEV refers to the pressurized cabin used for asteroid interaction, as shown in Figure 58 [84]. The remaining habitats are self-evident. Similarly, the only non-evident propulsion element is the exploration vehicle propulsion, which refers to the propulsion portion of the SEV under the same conditions as the habitat.

The Space Exploration Vehicle Characteristics (In-Space Concept)



Figure 58: SEV Characteristics from NASA Facts Sheet

This hierarchy for habitats is founded primarily on mass, environmental restrictions, and

common coupling with other sub-functions. Mass separation is evident with Level 1 and Level 2, the monolithic and semi-monolithic habitats. Deep space elements follow due to their large size, unique zero- or micro-g environment, and likelihood of separation from other sub-functions in many architectures to form Level 3 and Level 4. Level 5, the exploration vehicle, is a special exception in low-energy architectures, and given that it combines the remaining sub-functions, it is allocated to the next level of the hierarchy. Descent vehicles have a more strenuous environment than the ascent vehicles due to entry stresses, and therefore they often dominate in mass and complexity to create Level 6 and 7. Surface habitats are the lowest hierarchy at Level 8, despite their typically harsh environment and large mass, given that they are either integral parts of a combination with descent and/or ascent vehicles or are completely separate entities. This means that they are typically not combined with elements other than descent and/or ascent, with the exception of the monolithic and semi-monolithic cases. Surface habitats are also not requisite for technology demonstration any more so than descent or ascent vehicles, indicating that an assessment of the existence in an architecture is not as important as that of other elements. The hierarchy for propulsion elements follows similar logic. The exploration vehicle portion is lower than the descent and ascent propulsion elements due to its minimal energetic requirements and therefore small mass.

This element hierarchy, combined with the architecture-level technologies explored by HEXANE, produces a set of 20 possible demonstrable technologies and capabilities for a given end-mission. They are as follows:

- Atmospheric Aerocapture
- ISRU
- Cryogenic Boil-off Control
- SEP
- Monolithic Habitat
- Semi-Monolithic Habitat
- Deep Space Habitat A
- Deep Space Habitat B
- Space Exploration Vehicle
- Descent Habitat
- Ascent Habitat
- Surface Habitat
- LOX/LH₂ In-Space Propulsion
- LOX/LH₂ Descent Propulsion
- LOX/LH₂ Ascent Propulsion

- LOX/CH₄ In-Space Propulsion
- LOX/CH₄ Descent Propulsion
- LOX/CH₄ Ascent Propulsion
- Nuclear Thermal Rockets
- Space Exploration Vehicle Propulsion

Unlike the hierarchy, this list is not intended to indicate any order, dominance, precedence, or process. It is simply a listing of the possible technologies that may be present in end-mission architectures and require independent demonstration missions within the context of the habitat and propulsion hierarchies described. Given the nature of overlap between propellant technologies and habitat elements, the maximum number of possible technologies to be demonstrated for a given end mission is 13. This also implies that the maximum number of sub-missions is also 13, given that one or more new technologies or capabilities are demonstrated on any given sub-mission. There is also a set of sequencing constraints, meaning that some technologies or capabilities cannot be demonstrated before others or the mission properties must be conducive to the demonstration. These include:

Constraint 1: Boil-off Control without Propellant

This refers to the fact that boil-off control cannot be implemented prior to the use of a cryogenic propellant. Hydrogen, methane, and NTR, or any combination thereof, must first be demonstrated either on a prior sub-mission or on the same sub-mission.

Constraint 2: Descent Vehicle without Ascent Vehicle

This refers to the condition that a descent vehicle cannot be demonstrated without an ascent vehicle, and visa-versa.

Constraint 3: Surface Habitat without Descent and Ascent Vehicles

Similar to Constraint 2, this indicates that a surface vehicle cannot be demonstrated without demonstration of both a descent and ascent vehicle. These may either be demonstrated prior to the sub-mission or during the sub-mission.

Constraint 4: ISRU without a Surface Destination

Since Low-E includes non-surface destination options, ISRU must be constrained to only be allowed when the destination is a surface, *i.e.* Mars or the Moon.

4.2.2 Demonstration Destinations

Section 4.2.1 has described the set of demonstrable technologies and capabilities for the sequence of sub-missions. The second piece of information required is the set of destinations. Complementing the set of demonstrable technologies is the set of destinations for demonstration sub-missions. Unlike the destinations in HEXANE, this set theoretically includes non-surface destinations, such as libration points and planetary orbits, which can be used for testing of mission technologies and capabilities not requiring surface operations. In the case of the demonstration sub-missions, the value of the mission is dominated by the successful testing of the technology or capability in its operating environment rather than science return. Therefore these low energy points and orbits are more likely to be used for demonstration purposes. For missions testing descent, ascent, or surface capabilities, including ISRU, these non-surface destinations are not used, as they do not provide the necessary environment for realistic testing.

In order to keep computational requirements within feasible limits, the set of possible low-energy points, such as Lagrange points and orbits, are not explicitly differentiated for the purposes of Low-E. Instead, a generic low energy, non-surface destination that has properties similar to the average of the set of low-energy points is used as the “alternate” destination in combination with the final surface mission destination. EM-L1 was chosen to be representative of this class, with an arrival braking ΔV of 750m/s from LEO [85] and a departure ΔV dependent on the final destination. For the set of sub-missions, the non-surface destination is used for demonstration until a surface becomes necessary to demonstrate capabilities. The capabilities requiring a surface include ISRU and all descent, surface, and ascent elements. Aerocapture does not explicitly require a surface destination with an atmosphere, given that it may be demonstrated with Earth braking on return.

4.2.3 Assumptions

In order to understand which combinations of destinations and demonstrable technologies and capabilities are infeasible due to modeling assumptions, this section presents the set of assumptions associated with the modeling of the low-energy space. Low-E relies directly on HEXANE, and therefore the same assumptions that are present in the analysis engine of HEXANE are also present in Low-E analysis. A list of these assumptions can be found in Appendix A. An additional set of assumptions is necessary for simplifying the system to a level for feasible computation. The most important assumption of this analysis is the integration of additional technologies and capabilities into the LCC proxy. The original LCC proxy assumed that the set of technologies were similar, given the fact that they would each require significant investment in both time and money. However, with the introduction of habitats and propulsion elements, this may no longer hold,

given that similar elements have been previously developed. In addition, each of the capabilities on the list of twenty is assumed to be independent, with the exception of those expressly stated in Section 4.2.1 to be coupled. This also relates directly to the hierarchy approach, which assumes that the hierarchy applies to the development and operation environments equally. The simplification of the set of possible non-surface destinations assumes that these are equal in all relevant properties on the order of the fidelity of the analysis engine, including energetic requirements, environmental requirements, and station-keeping propulsion, along with an additional generic mass for science equipment. Finally, there are general assumptions made regarding the stability and success of demonstrated capabilities and technologies. The demonstration missions are assumed to be successful in all cases, and the state of the technology is assumed to be stable enough to retain high TRL between missions. In reality, this may fail with very long-term mission campaigns and/or rapidly developing technologies or “game changing capabilities” [86].

4.2.4 Metrics

Low-E investigates a tradespace with both striking similarities to and distinct differences from HEXANE. Both models analyze architectures at the same level of fidelity with nearly identical descriptions of the mission properties. Both programs also operate under the same basic scoping assumptions, with the exception of destination characteristics and commonality constraints with adjacent sub-missions. However, Low-E’s missions and sub-missions have significantly different value delivery goals, and therefore the metrics of interest to the decision makers must address this alternative value mechanism. In particular, risk plays a larger role in demonstration missions.

In order to account for these differences as well as recognize the similarities with HEXANE’s analysis, a set of six metrics are used to evaluate each of the sets of sub-missions enumerated by Low-E. These reflect both total sequence-level characteristics, with cumulative metrics, as well as individual sub-mission characteristics, with peak metrics. They are as follows:

1. Cumulative Modified LCC
2. Peak Modified LCC
3. Cumulative IMLEO
4. Peak IMLEO
5. Cumulative Operational Risk
6. Final surface mission metrics

The lifecycle cost proxy (LCC), a representation of development and procurement costs, has been modified, in this case, to include the development costs associated with complex habitats. As

described in Chapter 2, the portion of the LCC assessing development costs is based on a simplified TRL scale. Low TRL indicates that a technology or capability has no prior testing. Medium TRL indicates that a relevant demonstration has been conducted on Earth. High TRL indicates that the technology or capability has been flight tested. In HEXANE’s LCC, habitats are not included in the metric. Two modifications have been made to enable the inclusion of the habitats. Firstly, all habitats beside MPCV-derived vehicles are considered to be at medium TRL, meaning that a relevant demonstration has been given prior to the demonstration missions. This is true for all basic, hard-walled habitats, given the flight history on Skylab and ISS. They are not, however, considered “flight tested,” *i.e.* high TRL, due to the additional requirements associated with usage in the end-missions. Secondly, any habitat that has three or more habitation sub-function requirements integrated into it is considered to be of low TRL, given the additional complexity associated with the combination of requirements. Monolithic and semi-monolithic habitats clearly fall into this category. Another example would be a combined descent, surface, and ascent habitat. This is a generalization to take into account the unprecedented nature of the additional complexity stemming from the grouping of many functions into a single form, as compared with prior habitat elements, although it is not flexible enough to capture grouping differences.

Operational risk has been added to reflect the emphasis on risk reduction during demonstration missions. During demonstration missions, the goal is primarily the successful testing of technologies and/or capabilities, and therefore risk is less acceptable than with many long-duration science missions. There are two types of risk involved. There are technical risks, associated with the use of new technologies or capabilities. This is captured partially by the LCC proxy metric. Human risks arise from maneuvers that pose a danger to the astronauts, such as on-orbit assemblies and crew transfers. There are additional risk factors, but the level of fidelity necessary to assess the parameters is beyond the capabilities of this model. Operational Risk measures the total number of crew transfers and assembly operations, therefore producing a rough metric capturing the risk to crew during significant mission operations.

Final surface mission metrics are provided as part of the evaluation package in order to differentiate classes of missions and associated sub-mission sets. These are fed directly from HEXANE and therefore come at no additional computational cost. They include the mission IMLEO and original LCC values.

4.3 RESULTS AND FINDINGS

The results will be presented in two sections: Lunar results and Low-Energy NEA results. These results include comparative graphs of the metrics described in Section 4.2.4, along with a brief analysis of the chart features. For each destination, the minimum IMLEO architecture from

HEXANE produces the baseline for sub-mission sequencing. The choice of this base mission architecture reflects the completeness of the mission architecture, given the tension between IMLEO and LCC for the HEXANE tradespace. The minimum IMLEO architecture corresponds to the highest LCC proxy and therefore the most development projects of the non-dominated architectures for these destinations. For each destination, charts of the Cumulative LCC vs. Cumulative IMLEO, Peak LCC vs. Peak IMLEO, Peak LCC vs. Cumulative IMLEO, and Cumulative LCC vs. Peak IMLEO will be explored.

For both lunar and NEA missions, the goal of this analysis is to provide quantitative data to aid in the decision-making process for the determination of the set of demonstration sub-missions to achieve respective minimum-IMLEO surface missions. When each sub-mission is considered individually, optimization of the sub-mission does not necessarily lead to an optimal overall sequence of demonstration sub-missions. The full set of tradespaces is presented in order to present all trades between sub-mission-level metrics (peak) and sequence-level metrics (cumulative).

4.3.1 Lunar Results

The final surface mission for the lunar sub-mission sequences, *i.e.* the mission to which the demonstration sub-missions are building, is the minimum IMLEO architecture described in Figure 59. Its primary properties are described in Table 33, including the relevant technologies that must be demonstrated during a set of sub-missions. This list does not include an MPCV capsule, as it is assumed to be sufficiently developed and therefore does not require a separate demonstration mission.

Table 33: Lunar Final Surface Mission Properties

IMLEO (mt)	LCC Proxy	Operational Risk	Demonstrable Technologies
159	4.333	4	Aerocapture, ISRU, Boil-off Control, SEP Pre-Deployment, Semi-Monolithic Habitat, In-Space Hydrogen Propulsion

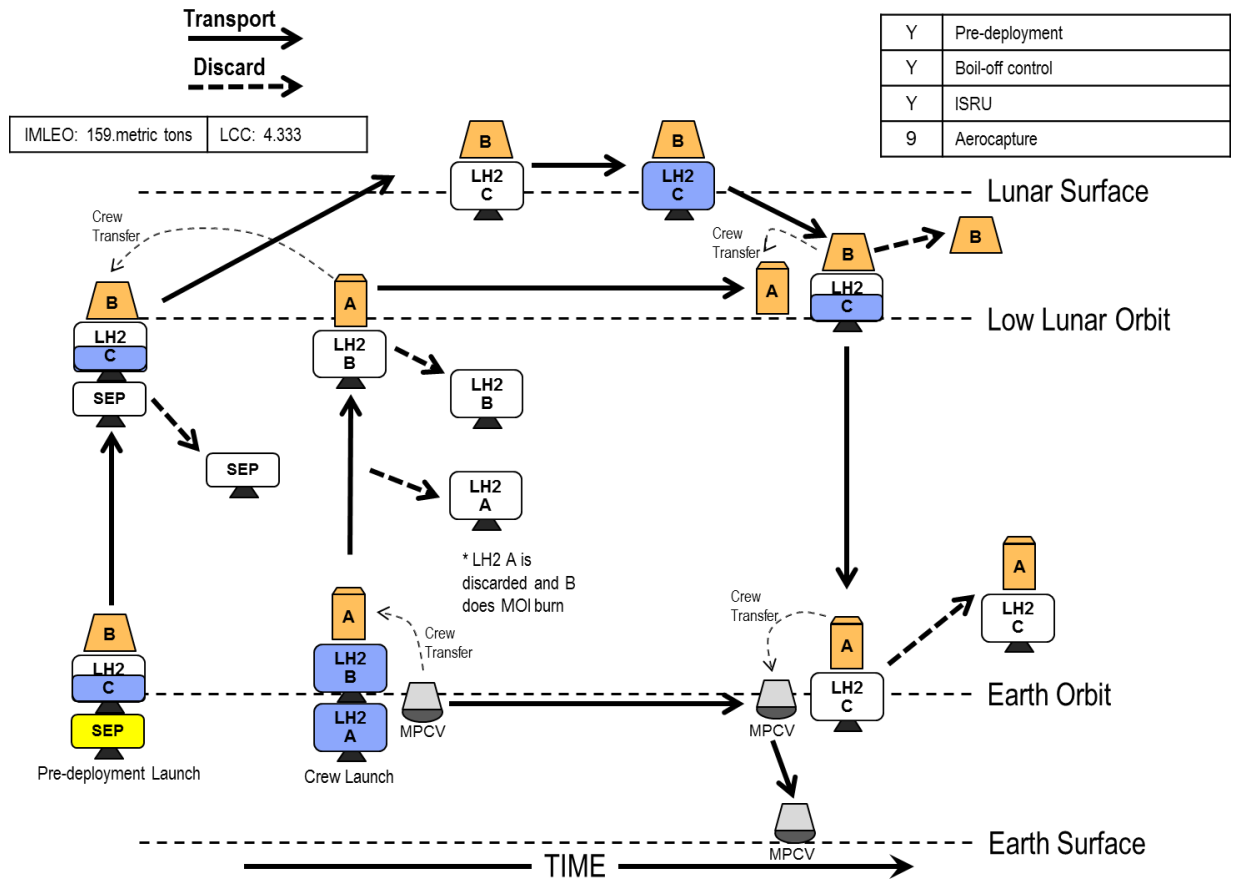


Figure 59: Lunar Minimum IMLEO Mission BAT Chart

Of the 203 possible aggregations (Bell number of 6) [87] of these technologies and capabilities with destinations, 50 are possible. Down-selection from 203 to 50 occurs by two mechanisms: falling outside of the possible energetic requirements due to the exponential nature of the rocket equation and improper sequencing of technologies that require prior developments (such as ISRU before a descent habitat) as described by the sequencing constraints. Figure 60 plots the Cumulative LCC vs. Cumulative IMLEO of the 50 possible variants, with additional color coding corresponding to the Cumulative Operational Risk for the set of sub-missions.

Each point in the tradespace represents a sub-mission sequence building to the set final surface mission. The final sub-mission in each sequence is therefore that surface mission, as shown in Figure 59. Table 34 gives the information for three example points on the tradespace, which are circled in red in Figure 60. The first example point is the extreme case where the first sub-mission is also the final surface mission. This is the case where no prior demonstration sub-missions are conducted prior to the final surface mission and all of the technologies and capabilities employed in that mission are at their lowest development level. This naturally has both low Cumulative IMLEO as well as Cumulative LCC, given that only one sub-mission is performed. The second example

sequence is taken from the middle of the tradespace. This is a sequence of three sub-missions, the first having only aerocapture, the second aggregating ISRU, boil-off control, in-space hydrogen stages, and a semi-monolithic habitat as demonstration technologies and capabilities, and the third sub-mission demonstrates SEP pre-deployment. The first sub-mission goes to EM-L1 and the remaining sub-missions go to the lunar surface. This sequence has both moderate Cumulative IMLEO at 507mt and moderate Cumulative LCC of 5.000 in comparison to the remainder of the tradespace. It also has a Cumulative Operational Risk of 7. Point C represents a disaggregated mission, resulting in a high cumulative IMLEO of 770mt and high cumulative LCC with 6.333. This is due to the spreading of demonstrations between four sub-missions.

Table 34: Lunar Cumulative IMLEO vs. Cumulative LCC Proxy Tradespace Examples

#	Cumulative IMLEO (mt)	Cumulative LCC	Peak IMLEO (mt)	Peak LCC	Sub-Mission 1	Sub-Mission 2	Sub-Mission 3	Sub-Mission 4	Destination Sequence
A	159	3.500	159	3.500	Aero., ISRU, Boil-off Ctrl, SEP, Semi-Mono., In-Space H2				Moon
B	507	5.000	216	3.000	Aero.	ISRU, Boil-off, Semi-Mono., In-Space H2	SEP		EM-L1, Moon, Moon
C	770	6.333	280	1.667	Aero., Semi-Mono.	ISRU	Boil-off, In-Space H2	SEP	EM-L1, Moon, Moon, Moon

In general, with each additional sub-mission for each of these sequences, there is a marginal increase in the LCC for each sub-mission. Each previously demonstrated technology or element has a reduced contribution to the sub-mission's individual LCC, but there tends to be an increase in the overall LCC of each sequential sub-mission with the addition of new technologies and elements. As such, it is expected that an increase in the number of total sub-missions coincides with an increase in the Cumulative LCC. Furthermore, it is also expected that this correlates with an increase in Cumulative IMLEO as well as Cumulative Operational Risk. This expectation holds for the architectures shown in Figure 60, with the overall set of architectures trending up and to the right. However, there are also several flat tradespace features. This indicates that there are sub-mission sequences that trade an increase in LCC for little IMLEO gain. For example, the flat feature at ~500mt of Cumulative IMLEO is a set of sequences using three sub-missions. These trade the set of technologies mostly in the second sub-mission. The different technology combinations tend to

have only small influence on IMLEO while changing the LCC values by moving around the demonstration of boil-off control. This has a small influence on mass in the low-energy space while changing LCC values. In this case, it is most beneficial to use those sub-mission sequences with the lowest LCC and Cumulative Operational Risk, which coincide to be the left-most in the trend.

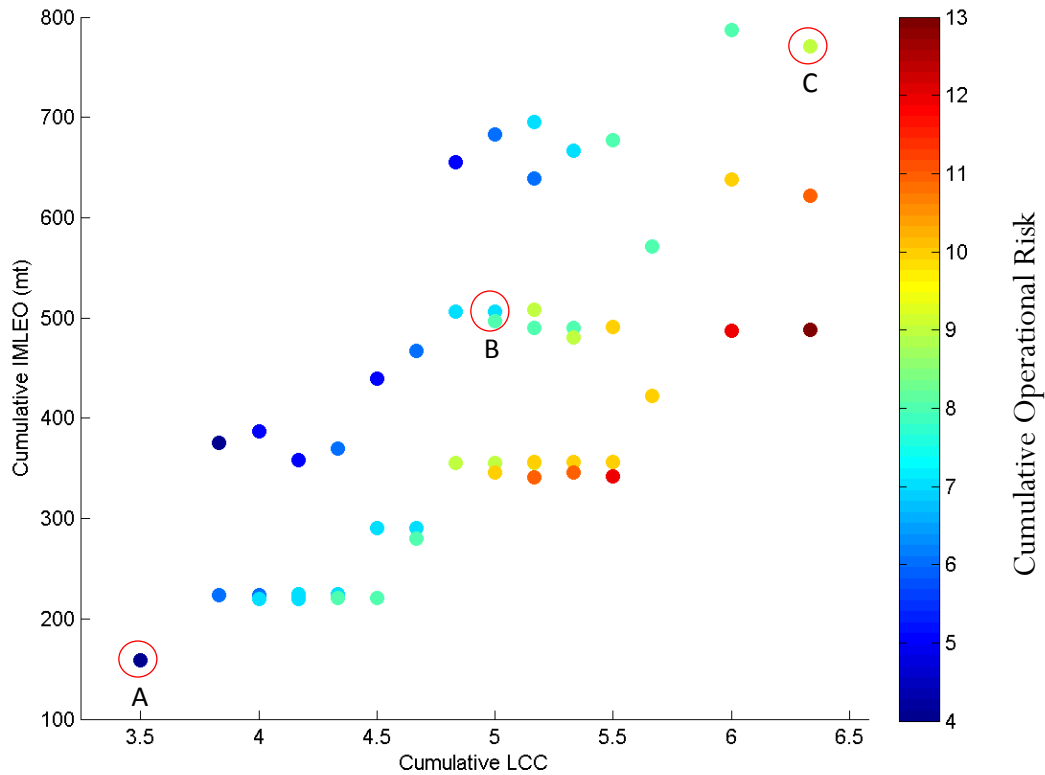


Figure 60: Lunar Cumulative IMLEO vs. Cumulative LCC

This analysis alone can be misleading without considering sub-mission-level metrics. The utopia point between these three metrics in Figure 60 is achievable by choosing the sub-mission sequence in the lower left corner. However, this also represents the sequence where all technologies and elements are demonstrated simultaneously, corresponding to a high peak in IMLEO and LCC. In contrast, Figure 61 shows Peak LCC vs. Peak IMLEO, which has much different tradespace features, as expected. These metrics are purely sub-mission-level, with the exception of the operational risk, whereas the previous were purely sequence-level. In this case, a reduction in Cumulative Operational Risk can be achieved through an increase in Peak LCC and/or an increase in Peak IMLEO. There are flat trends also within this tradespace due to the fact that the maximum IMLEO missions tend to be the same across many architectures, most often being the final surface mission mass. This means that the Peak IMLEO, representing the highest mass sub-

mission, tends to be similar across several sequences due to a similar aggregation of demonstrable technologies and/or capabilities leading to the same highest-mass sub-mission in the sequence. In many cases this is the final surface mission since it is the most demanding architecture, requiring surface access and usually a longer surface duration.

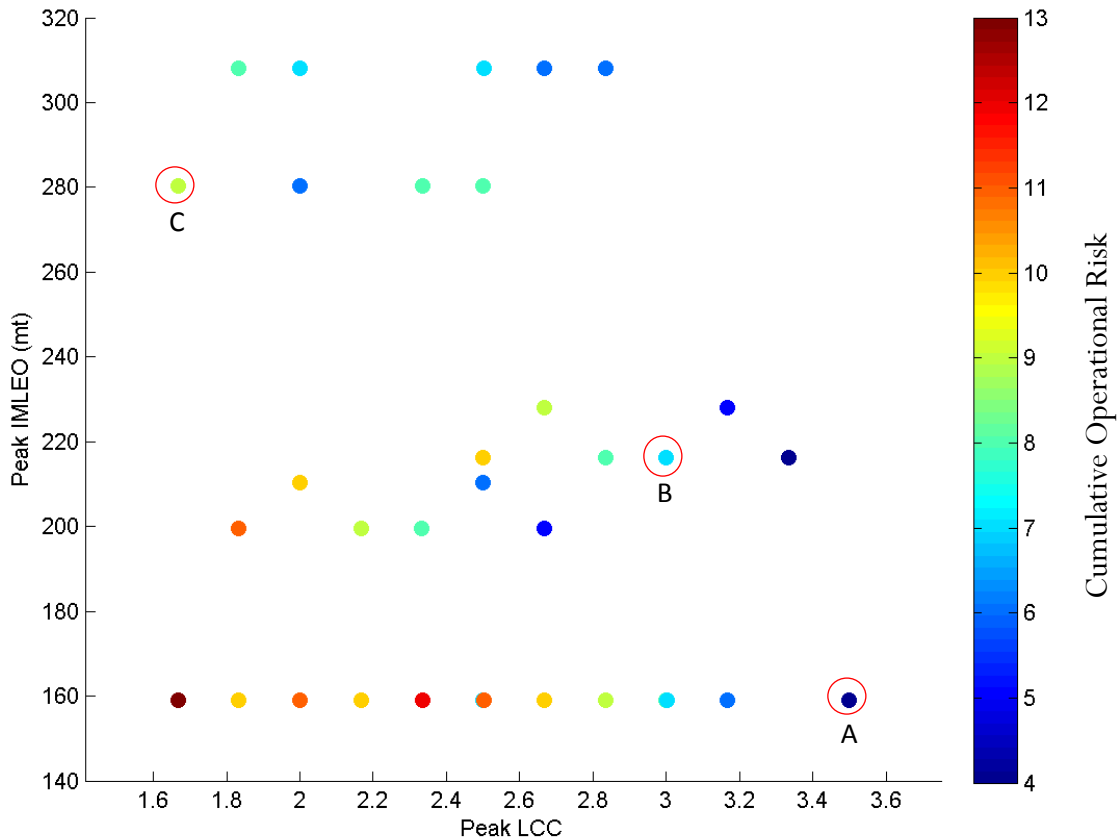


Figure 61: Lunar Peak IMLEO vs. Peak LCC

The features of Figure 60 and Figure 61 are as expected, which both partially validates the methodology as well as confirms the intuition. More interesting relationships are revealed from the plotting of peak vs. cumulative metrics, which mix the sub-mission-level and sequence-level of assessment. Figure 62 shows the Peak IMLEO vs. the Cumulative LCC. This represents a trade between the mass and therefore operating cost of the most massive sub-mission and the total sequence development and procurement cost. The primary difference between the trends in Figure 61 and the trends in Figure 62 is the progression of Cumulative Operational Risk. For the Peak LCC, this metric decreases from left to right. For the Cumulative LCC, the metric increases from left to right. This again is intuitive, given that increasing the fractionation of the sub-missions increases the cumulative metrics. As with Figure 61, three general regimes of Peak IMLEO can be

seen. The first is the set of sub-missions where the final surface mission also represents the most massive of the sub-missions. This is the group at a Peak IMLEO of 159mt, with an example as sequence A in Table 35. The second group is a spread in the center, where a relatively large number of sub-mission combinations create a moderate increase in mass. These are the missions where descent, ascent, and surface technologies and elements are demonstrated in the middle of the sub-mission set, necessitating at least one lunar sub-mission. An example is given as sequence B in Table 35. The surface missions typically are larger mass due to the need for larger quantities of propellant for entering and exiting a gravity well. The third regime is a set of two Peak IMLEO values around 280mt and 310mt. These are the sub-mission sets where descent, ascent, and surface technologies and elements are demonstrated early but in a fractionated manner. This means that these missions are also lunar missions but are inefficient in comparison to the final surface mission, due to a lack of other advanced technologies and elements that have not yet been demonstrated. An example is given as sequence C in Table 35.

Table 35: Lunar Peak IMLEO vs. Cumulative LCC Tradespace Examples

Seq.	Peak IMLEO (mt)	Cumulative LCC	Sub-Mission 1	Sub-Mission 2	Sub-Mission 3	Sub-Mission 4	Destination Sequence
A	159	3.500	Aero., ISRU, Boil-off Ctrl, SEP, Semi-Mono., In-Space H2				Moon
B	216	5.000	Aero.	ISRU, Boil-off, Semi-Mono., In-Space H2	SEP		EM-L1, Moon, Moon
C	280	6.333	Aero., Semi-Mono.	ISRU	Boil-off, In-Space H2	SEP	EM-L1, Moon, Moon, Moon

These regimes potentially coincide with launch vehicle needs for mission campaigns. If the base mission is the most massive, the launch vehicle should be sized to accommodate the IMLEO of that mission. However, if the demonstration missions require a greater launch capability, the base launch system should instead match those needs. A caveat to this statement is the assumption of on-orbit assembly, meaning that these missions do not necessarily imply the need for larger and larger launch vehicles, so long as the elements are sufficiently fractionated to allow for assembly in LEO. Therefore despite the fact that the upper regime rests at 280-310mt, multiple 130mt or smaller SLS launches may still be appropriate. In order to fully assess the matching of launch vehicles with the sub-mission sequence needs, an understanding of the relation between launch vehicle packing and element fractionation must be gained. Such analysis is outside of the scope of this thesis.

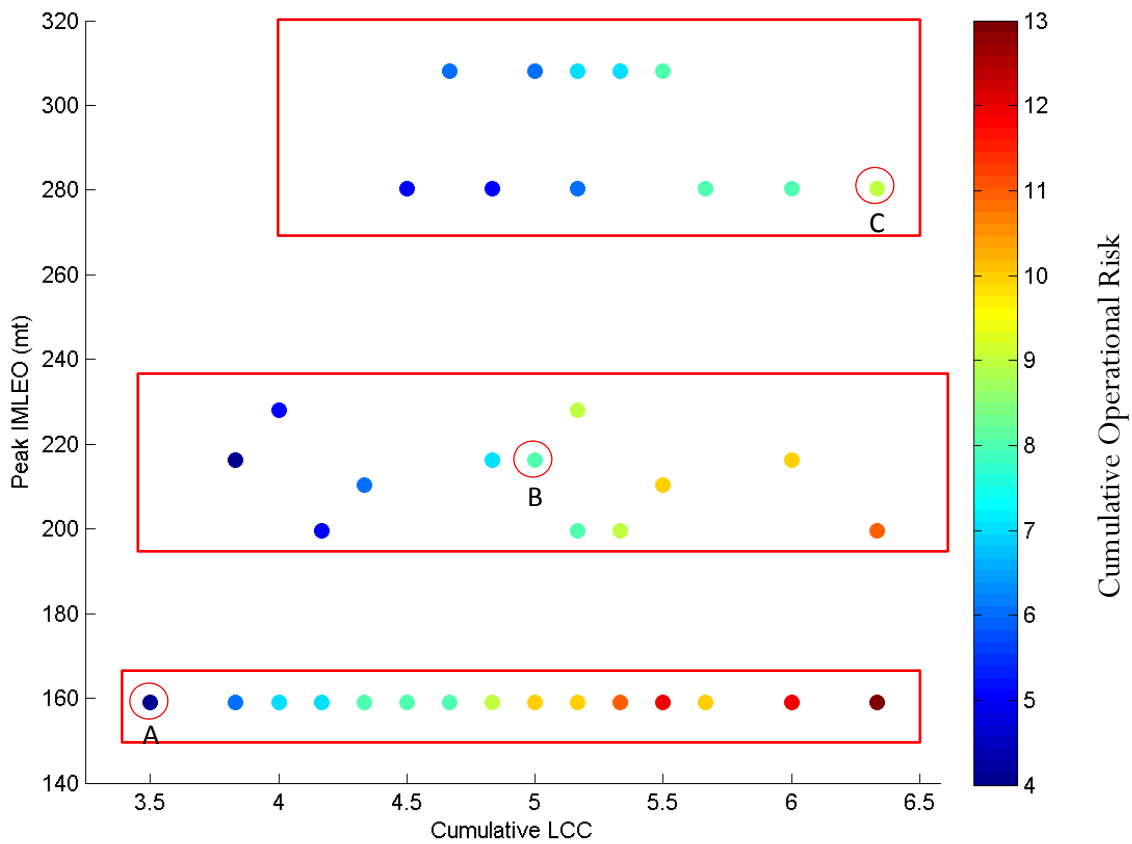


Figure 62: Lunar Peak IMLEO vs. Cumulative LCC

The sub-mission sequences are most dispersed when Cumulative IMLEO is plotted against Peak LCC, as shown in Figure 63. In effect, this graph shows the total campaign operational cost, embodied in the Cumulative IMLEO, versus the sub-mission-level demonstration risk, embedded in the Peak LCC metric. The individual LCC values of the sub-missions indicate the number of technologies and their respective development states. The higher the individual LCC, the greater the inherent demonstration risk due to the combination of less developed technologies and elements. Figure 63 reveals that these two properties are in tension. The Peak LCC may be reduced, but only at the cost of Cumulative IMLEO. The dispersal also means that this trade is where the differences between the architectures are most prevalent. In the previous tradespaces, the sequences grouped together, indicating that sets of these sequences have similar properties. Without these clear groups, the more subtle differences can be understood.

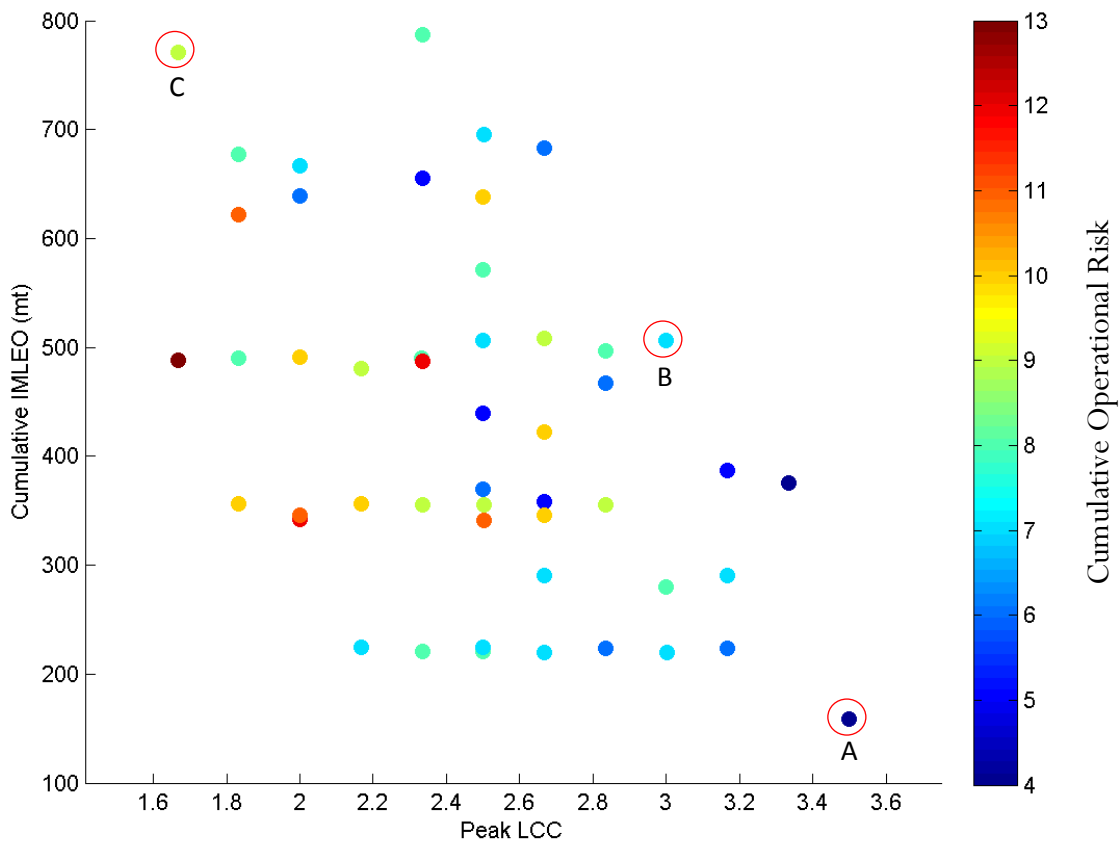


Figure 63: Lunar Cumulative IMLEO vs. Peak LCC

Because these properties are in tension, a Pareto frontier can be calculated for this set. The Pareto frontier is juxtaposed on the Cumulative IMLEO versus Peak LCC plot in Figure 64. Scrutiny of the non-dominated sub-mission architecture sequences reveals that there is also a tension between the Cumulative Operational Risk and Peak LCC. The left-most non-dominated sub-mission sequence, which is also the highest Cumulative IMLEO value of the non-dominated set, coincides with the maximum Cumulative Operational Risk shown in this tradespace. Progressing along the Pareto frontier to the highest Peak LCC value also reduces the Cumulative Operational Risk. The final non-dominated point is the single mission set, where all technologies and elements are demonstrated on the final surface mission. Because this has the lowest fractionation, this sub-mission sequence also has the lowest Cumulative IMLEO along with the highest Peak LCC and lowest Cumulative Operational Risk. This tension and resulting Pareto frontier implies that 1) it costs ~50mt in Cumulative IMLEO and therefore proportional operational cost to buy down individual sub-mission risk from an LCC value of 3.5 to an LCC value of 2.167, 2) buying down sub-mission risk has a steep trade with cumulative operational costs to

achieve an individual sub-mission LCC for all sub-missions of less than 2.167. It therefore seems likely that the non-dominated sequence at an LCC value of 2.167 would be chosen in the context of these metrics, due to the relatively small increase in Cumulative IMLEO (~50mt from a 159mt mission) and Cumulative Operational Risk of 7.

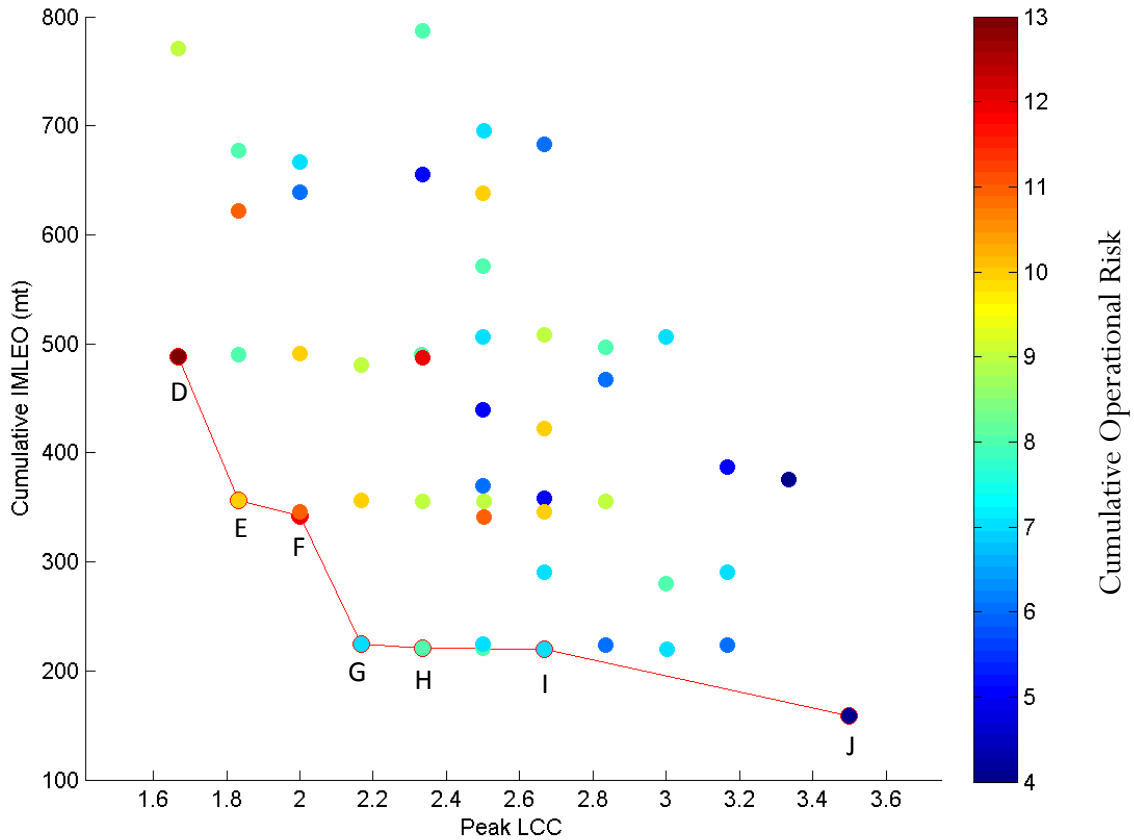


Figure 64: Lunar Cumulative IMLEO vs. Peak LCC with Pareto Frontier

Properties of the set of non-dominated sub-mission sequences are given in Table 36. This table includes both the metric values and information about the sequencing of the technologies and capabilities. For all non-dominated sequences, the demonstration missions are front-loaded, such that the first sub-mission demonstrates the majority of the technologies and capabilities. For the lunar case, this initial set always includes aerocapture and in-space hydrogen propulsion stages, even when the initial destination is not the lunar surface. The second sub-mission sequence, when one is integrated, consistently includes ISRU. This is likely due to the fact that the demonstration of ISRU requires the use of the lunar surface. However, it is not sequenced after the second sub-mission even when more than two sub-missions are used for demonstration purposes. This may indicate that ISRU is necessary to reduce the IMLEO of following sub-missions. Boil-off control

and SEP tend to trend similarly, although this pattern is not as consistent as that of ISRU. This implies that, for a similar lunar final surface mission, ISRU should be sequenced second, the remainder of the demonstrable capabilities for a non-surface sub-mission should be demonstrated upfront, and, if more sub-missions are used to spread risk, boil-off control should be demonstrated later rather than sooner.

Table 36: Non-Dominated Lunar Sub-Mission Sequence Properties for the Peak IMLEO vs. Cumulative LCC Tradespace

Sequence	Peak LCC	Cumulative IMLEO (mt)	Sub-Mission 1	Sub-Mission 2	Sub-Mission 3	Sub-Mission 4	Destination Sequence
D	1.667	488	Aero., Semi-Mono., In-Space H2	ISRU	Boil-off Ctrl	SEP	EM-L1, Moon, Moon, Moon
E	1.833	356	Aero., Semi-Mono., In-Space H2	ISRU	Boil-off Ctrl, SEP		EM-L1, Moon, Moon
F	2.000	342	Aero., SEP, Semi-Mono., In-Space H2	ISRU	Boil-off Ctrl		EM-L1, Moon, Moon
G	2.167	225	Aero., Boil-off Ctrl, Semi-Mono., In-Space H2	ISRU, SEP			EM-L1, Moon
H	2.333	221	Aero., SEP, Semi-Mono., In-Space H2	ISRU, Boil-off Control			EM-L1, Moon
I	2.667	220	Aero., Boil-off Ctrl, SEP, In-Space H2	ISRU, Semi-Mono.			EM-L1, Moon
J	3.500	159	Aero., ISRU, Boil-off Ctrl, SEP, Semi-Mono., In-Space H2				Moon

Conclusions

- *As technology and element demonstration becomes more fractionated, all cumulative metrics increase.*
- *Three regimes for Peak IMLEO exist, indicating the possible need for launch vehicle capability regimes.*
- *Tension exists between Cumulative IMLEO and Peak LCC, indicating a trade between total operations costs and peak demonstration risks.*

- When a second mission is sequenced, ISRU is delegated to the second mission for non-dominated architectures on the Cumulative IMLEO and Peak LCC Pareto frontier.

4.3.2 Low-Energy NEAs

Complementing the lunar architectures in the low-energy space are the low-energy NEAs. Official U.S. space policy states that NASA will conduct NEA missions by the year 2025 [4], indicating the importance of these destinations for NASA. The same set of analysis as the lunar architectures shows that there are similarities between the sequencing of demonstration missions for NEA architectures and lunar architectures.

For the purposes of this analysis, the final mission for the low-energy NEA architectures has the properties listed in Table 37. This reflects the minimum IMLEO mission for low-energy NEAs given in Figure 65. The total IMLEO for the base mission is approximately 8mt less than the lunar architecture, the operational risk is the same value, and, with the exception of ISRU, all of the same technologies are included in the architecture. Given that the demonstration mission campaign has the same starting architecture as the “zero technology” case and that the final mission has comparable properties, similar trends should be expected between the lunar sub-mission sequencing and respective low-energy NEA sub-mission sequencing. If the similarities are strong, this may imply that, if the elements themselves are also similar, lunar and NEA sub-missions may be used to demonstrate technologies and/or capabilities for each other. That is to say that a lunar demonstration sub-mission could be used to demonstrate low-energy NEA technologies or capabilities and visa-versa. This could be especially beneficial in a long-term campaign strategy.

Table 37: Low-Energy NEA Base Mission Properties

IMLEO (mt)	LCC Proxy	Operational Risk	Demonstrable Technologies
151	1.333	4	Aerocapture, Boil-off Control, SEP Pre-Deployment, Semi-Monolithic Habitat, In-Space Hydrogen Propulsion

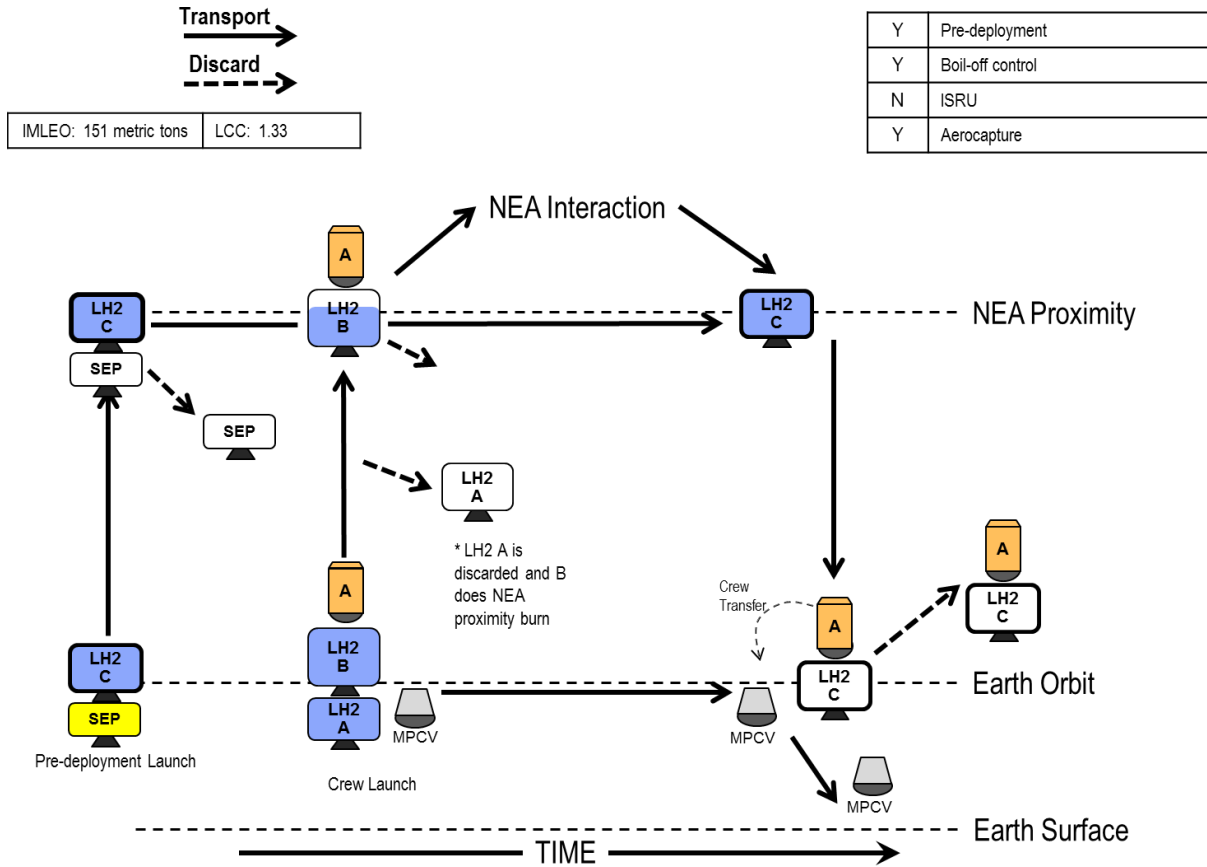


Figure 65: Low-Energy NEA Minimum IMLEO Mission BAT Chart

The intuitive increase in Cumulative IMLEO with Cumulative LCC and corresponding Cumulative Operational Risk is again manifested in the low-energy NEA sub-mission sequences. As such, this tradespace is not shown. Similarly, the reversal in Operational Risk increase is the only prominent difference between the Peak IMLEO vs. Peak LCC and Peak IMLEO vs. Cumulative LCC tradespaces, and so only the latter is shown in Figure 66. As with the lunar case, three Peak IMLEO regimes are revealed, with examples given in Table 38. The low Peak IMLEO regime represents the case where the final mission has the highest mass in all sequences. The middle and upper regimes represent the case where one or more sub-missions of mass greater than the final mission are required for the demonstration of the technologies and capabilities. Since the masses of these regimes are similar, this further supports the concept of tiered launch vehicle sizing, building to the desired sub-mission sequencing regime. In the case of the low-energy NEAs, the early use of semi-monolithic habitats seems to be unfavorable, pushing up IMLEO properties.

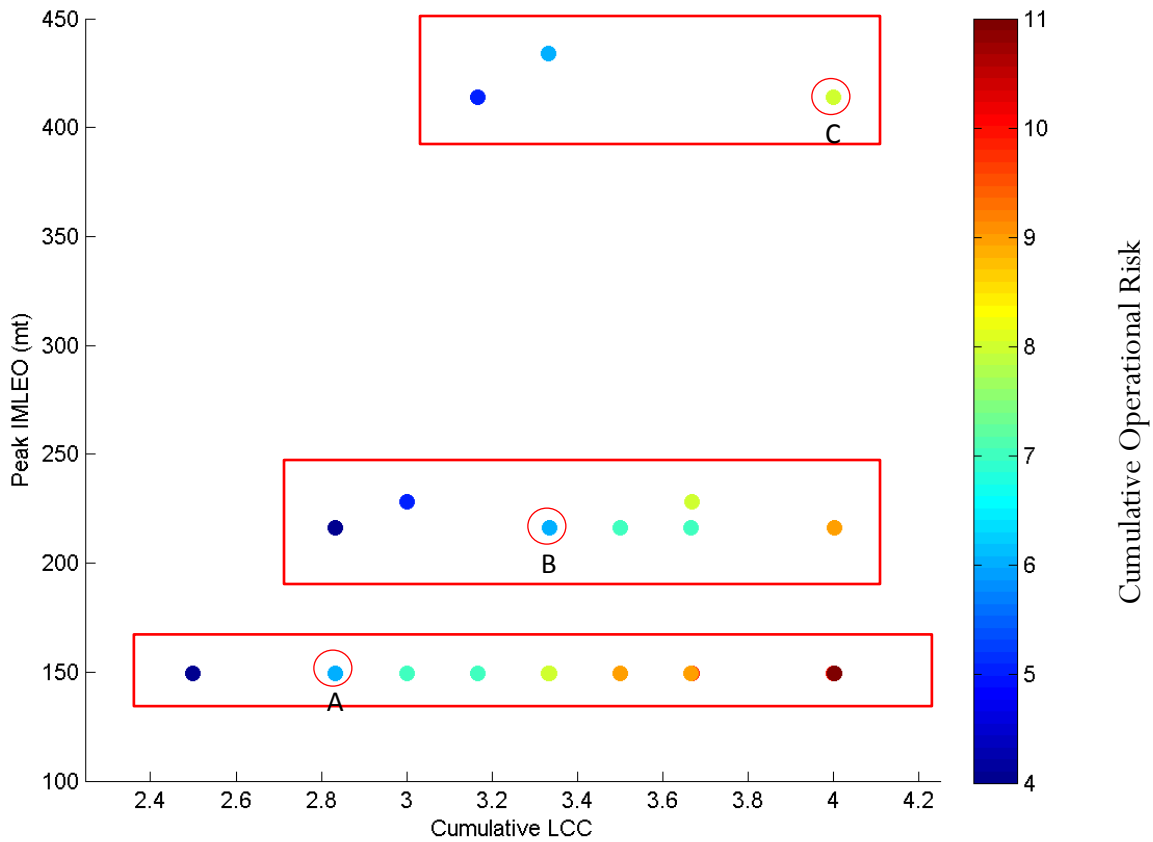


Figure 66: Low-Energy NEA Peak IMLEO vs. Cumulative LCC

Table 38: Low-Energy NEA Peak IMLEO vs. Cumulative LCC Tradespace Examples

Seq.	Peak IMLEO (mt)	Cumulative LCC	Sub-Mission 1	Sub-Mission 2	Sub-Mission 3	Destination Sequence
A	150	2.833	Aero., In-Space H2	Boil-off, SEP, Semi-Mono.		EM-L1, NEA
B	216	3.333	Aero.	Boil-off, In-Space H2	SEP, Semi-Mono.	EM-L1, EM-L1, NEA
C	414	4.000	Aero., Semi-Mono.	Boil-off, In-Space H2	SEP	EM-L1, EM-L1, NEA

The Cumulative IMLEO versus Peak LCC plots, with and without the Pareto frontier, can be seen in Figure 67 and Figure 68. The spread of architectures in this tradespace is much more restricted in comparison to the lunar results. Tension between the Cumulative IMLEO and Peak LCC metrics still manifests in the tradespace. The set of sub-mission sequences shown in the red box in Figure 67 indicate that under many different fractionation schemes, a common Peak LCC still occurs, even over a wide range of Cumulative Operational Risk values. In the tradespace of

these two metrics, most of these sub-mission sequences are dominated by the second sub-mission in the set shown in Figure 68. A sharp drop also occurs between the left-most non-dominated sequence and the following non-dominated sequence in terms of Cumulative IMLEO. It should be noted that there is only a single sequence to the left of the bulk of the architectures, *i.e.* the first non-dominated point. This is the same sequence as sequence C in Table 38. This property indicates that this sequence represents a unique set of sub-missions creating a synergism not utilized by the majority of sub-mission sequences. In reality, this is due to the early use of the semi-monolithic habitat. Having multiple fractionated habitats reduces the IMLEO properties but increases the total LCC properties. Therefore, when designing the sequence of demonstration sub-missions, the decision to demonstrate semi-monolithic habitats in the first sub-mission would need to be made early in the process.

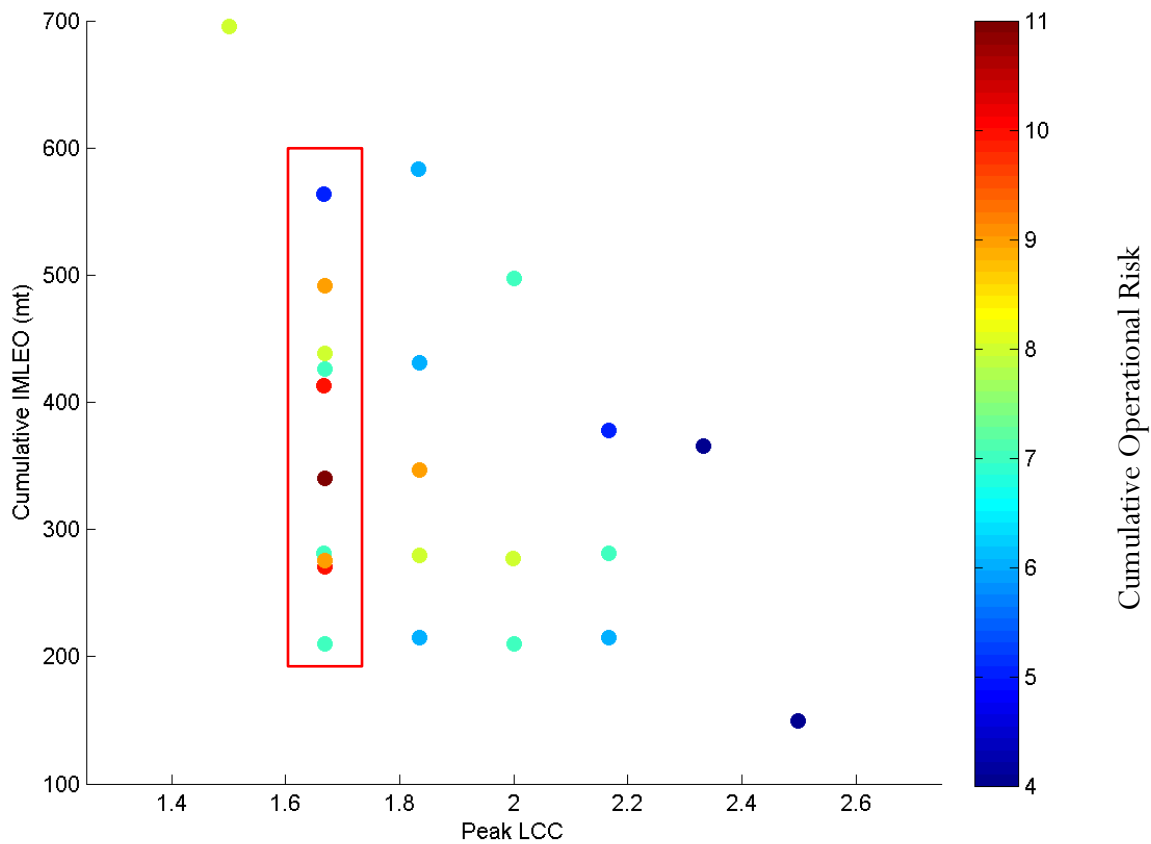


Figure 67: Low-Energy NEA Cumulative IMLEO vs. Peak LCC

The properties of the three non-dominated architectures shown in Figure 68 are given in Table 39. The reduced set of points on the Pareto frontier prevents further trends from appearing. However, unlike the lunar analysis, the multi-sub-mission sequences for the low-energy NEAs

include multiple demonstrations at EM-L1 before proceeding to the final destination. This is likely correlated with the lack of surface operation requirements for NEA missions, thus not requiring earlier use of the final destination.

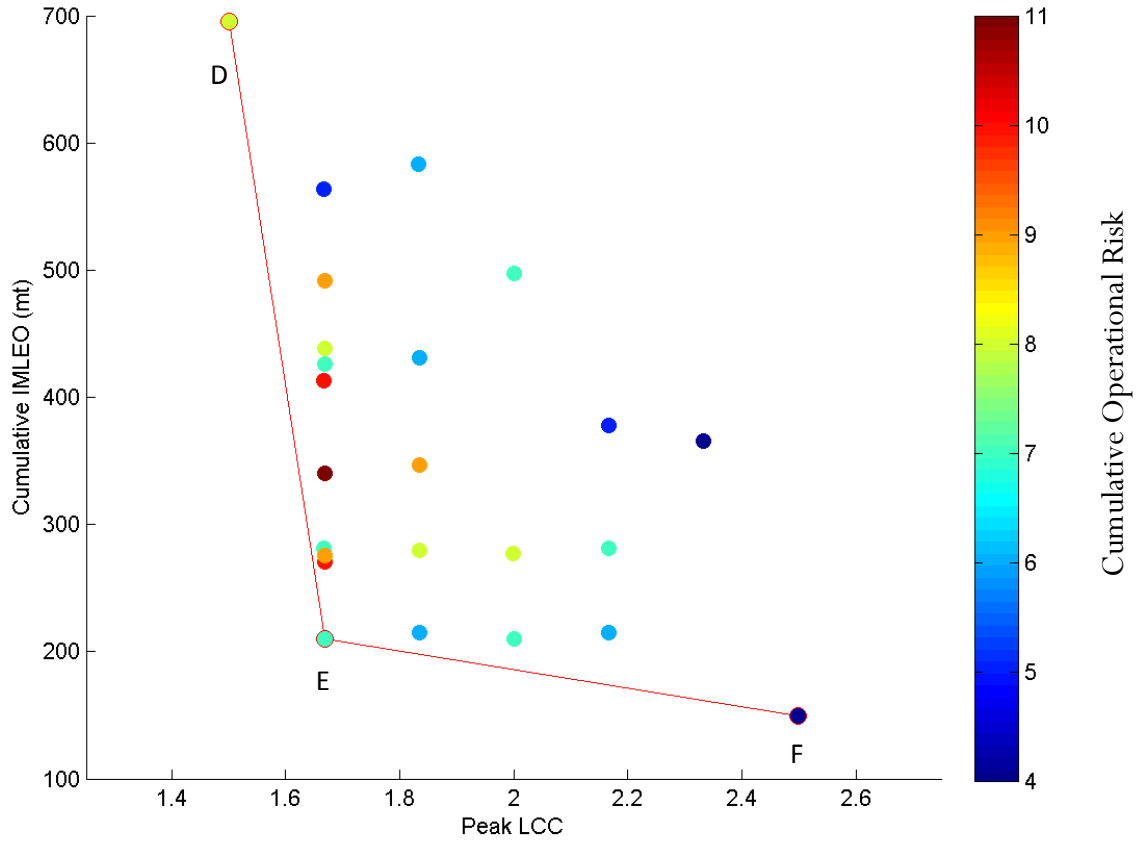


Figure 68: Low-Energy NEA Cumulative IMLEO vs. Peak LCC with Pareto Frontier

Table 39: Non-Dominated Low-Energy NEA Sub-Mission Architecture Sequence Properties

Sequence	Peak LCC	Cumulative IMLEO (mt)	Sub-mission 1	Sub-mission 2	Sub-mission 3	Destination Sequence
D	1.500	695	Aero., Semi-Mono.	Boil-off Ctrl, In-Space H2	SEP	EM-L1, EM-L1, NEA
E	1.167	210	Aero., Boil-off Ctrl, SEP, In-Space H2	Semi-Mono.		EM-L1, NEA
F	2.500	151	Aero., Boil-off Ctrl, SEP, Semi-Mono., In-Space H2			NEA

Conclusions

- *The base mission properties, including demonstrable technologies and elements, between the lunar and low-energy NEA sub-mission architecture sequences are similar, leading to comparable features in the various tradespaces.*
- *The three launch vehicle regimes are also supported by the low-energy NEA analysis. The mass of the architectures also matches with the lunar analysis, indicating commonality in the launch and assembly requirements between these sub-mission campaigns.*
- *Low-energy NEA sub-missions are not reliant on surface operations and therefore favor repeated use of low-energy Lagrange points rather than early surface missions.*
- *Early demonstration of the semi-monolithic habitat element reduces Peak LCC properties while increasing Cumulative IMLEO. Choice of timing for demonstration of this capability appears to be critical for developing the sequence of demonstration sub-missions when designing for the minimum IMLEO final mission architecture.*

4.4 CONCLUSIONS AND RECOMMENDATIONS

Trends in the tradespace of sub-mission sequences indicate that increased fractionation of demonstration missions increases total sequence costs and risks while reducing the risks and costs associated with individual sub-missions. Emergent tradespace features for both lunar and low-energy NEA sequences indicate the possible need for matching between launch capabilities and demonstration sub-mission decisions. For non-dominated sequences in the Cumulative IMLEO and Peak LCC tradespace, technology and capability demonstration tends to be front-loaded, allowing for the use of more advanced technologies and capabilities in later sub-missions at the cost of increased risk on the initial demonstration flight.

For the final missions analyzed, lunar sub-mission sequences favor the use of early surface missions in order to demonstrate surface technologies (ISRU) and capabilities (landers, habitats, *etc.*). This increases the mass of the missions due to the need for these surface elements. However, if they are deemed necessary to demonstrate prior to the final mission, surface missions are the only method for sufficient demonstration to reach a high TRL. For low-energy NEAs, Lagrange points are used for the majority of sub-missions in the sequence, since NEAs typically do not require many “surface” components. This is exaggerated in this case, since a semi-monolithic habitat is in the

architecture. For other final mission architectures employing SEV's, NEA missions would be required earlier in the sequence in order to allow for demonstration.

There are strong similarities between the results found for lunar architectures and low-energy NEA architectures, indicating commonality in the sub-mission sequences. Such commonality could be used to delay destination decisions while investing in the development of technologies and capabilities common to both low-energy final missions. Furthermore, the matching of launch capabilities and mission needs indicates that a tiered launch vehicle capability may be beneficial to complete campaigns.

4.5 CHAPTER SUMMARY

A motivation for the analysis of low-energy destinations was presented, focusing on the need for low-cost, near-term returns for NASA and international space organizations. The motivation for the exploration of demonstration missions prior to final missions described by HEXANE was also discussed. A methodology was examined for the exploration of the tradespace of demonstration sub-mission sequences. The methodology is reliant on a breakdown of demonstrable technologies and elements in the final mission architectures, as well as the existence of a set of mission elements that are already sufficiently developed for use in manned space exploration. A set of analysis was shown for the lunar and low-energy NEA minimum IMLEO final mission states. For both cases, a set of three regimes was located for the Peak IMLEO metric, indicating a possible matching between launch vehicles and desired sub-mission sequencing decisions. A tension was found between the Cumulative IMLEO and Peak LCC metrics. The Pareto frontier for this tension revealed consistencies in the lunar sub-mission sequences favoring the use of ISRU in the second sub-mission. No such trend was found for the low-energy NEA sub-mission sequences, attributed to the lack of surface operations associated with NEA missions.

5. A FRAMEWORK FOR THE MODELING OF COMPLEX SYSTEMS

“Any intelligent fool can make things bigger, more complex, and more violent. It takes a touch of genius – and a lot of courage – to move in the opposite direction.”

-E.F. Shumacher [88]

Chapters 1-4 discussed the specific application of systems architecting tools in the evaluation of an important tradespace. However, the process of creating the tools necessary for the evaluation revealed a more general problem in the field of system architecture: the lack of guidance in the use of methods and tools when faced with building models of complex systems. For example, the structuring of HEXANE was greatly improved through the use of an assignment problem formulation with nested set-partitioning sub-problems. However, this may never have been achieved without knowledge of their existence through academic study of previous work employing these methods. Guidance toward these methods would have been extremely helpful if this problem had been approached by someone outside of the academic community who was unfamiliar with these techniques. Chapter 5 introduces a framework that makes a first attempt to guide complex system model builders in the use of tools and methods by building a generic structure to address the most prominent fundamental issues in the creation of such models.

5.1 INTRODUCTION

5.1.1 Motivation: Modeling of Complex Systems as a General Challenge

Complex systems are defined as systems which are composed of interconnected parts that, as a whole, exhibit properties or behaviors not obvious from the properties or behaviors of the individual parts [89][90][91]. Sometimes short-handed as the “whole being more than the sum of its parts,” this property is known as emergence or emergent behavior [92]. For engineers wishing to model these systems, it is the non-obvious property of this emergence that hinders the modeling process, often due to a lack of insight into the system’s internal workings. To aid in this process, a set of formal methods and tools has been developed over the last 20 years to decipher the origins of emergence and abstract it to its fundamental underpinnings. However, few pathways between these methods and tools and their applicability to specific systems have been formalized, leaving the

difficulty of matching between a system model and the set of tools to the system architect.

5.1.2 Lessons Learned from HEXANE

The process of building HEXANE revealed many difficulties associated with the modeling of complex systems. Most importantly, it revealed the lack of guidance for the creation of efficient and effective models. This is, in part, due to the number of complex system configurations and the immaturity of the field. The field of system architecture does not have a well-defined beginning, but the term “system architecture” was coined by Rechtin in the late 1980s [12]. Many of the methods and tools are produced by the academic community and professional societies, and it has taken many years for them to begin to permeate industry. For example, SysML is a systems modeling tool developed by a working group of INCOSE in 2001, which is only now being implemented by portions of the industry. The following industrial entities are listed as SysML Partners: American Systems, Astrium Space, BAE Systems, Boeing, Deere & Company, Eurostep, Israel Aircraft Industries, Lockheed Martin, Motorola, Northrop Grumman, Oose.de, Raytheon, and THALES [93]. In industry applications, not all of the users are experts in systems architecture and there are typically many such users. But in academia, these tools and methods are not necessarily refined for use by untrained people prior to the release to industry. Furthermore, not all tools and methods are described in relation to other tools and methods. Therefore, very little information exists with regards to guidance on the path of model building. This is compounded by the sheer number of complex systems. The methods and tools produced are often applicable to only one or a few classes of complex systems, and therefore they remain outside of the integration in more generalized frameworks. Combined, these effects have created a field that is only accessible by experts with training in the multitude of system architecting methods and tools, and even those experts are often ill-equipped to use methods and tools outside of their immediate specialty.

Another major issue encountered during the creation of HEXANE was the number of iterations required to produce a refined model. Each iteration necessitated the rework of many aspects of the model and required significant resources. Even when the general framing of the model was well-developed, the details that were critical to the proper creation were in flux. A reduction in the number of iterations therefore would have significant impacts on the resources allocated to the modeling process and on the quality of the results.

Therefore, it is the desire to correct two difficulties with the building of HEXANE:

- Providing a way of **organizing the methods and tools in systems architecting** in order to guide model builders in their appropriate use without prior expert knowledge of each specific method and tool

- **Reducing the number of iterations** required to produce efficient, effective models in order to reduce the resources necessary for model creation

5.1.3 Gratuitous & Modeling-Induced Complexity vs. Essential Complexity

In order to reduce the number of iterations necessary for model creation, the system properties necessary for accurate and appropriate modeling must be understood. Since the framework is directly applied to complex systems, it is the complexity itself that must be addressed. There are three forms of complexity that are important to the complex system modeling process. The first two deal with the excess complexity, being the complexity that is not necessary to model in order to simulate the emergent aspects of the system. The third is attributed to that complexity which is absolutely necessary, or essential, to the appropriate simulation of the system within the model. A system modeler should aim to minimize the first two types of complexity while retaining the third.

Gratuitous Complexity

Gratuitous complexity generally refers to any complexity in a system that is not necessary to produce the value delivery mechanism [37]. In the case of system models, this more specifically refers to any complexity that is not necessary for the production of the emergent properties of interest. Given the multitude of internal interactions inherent in many large complex systems, it is often difficult to determine where any gratuitous complexity exists in these systems, but it is an important system property to understand in order to efficiently model these complex systems.

Modeling-Induced Complexity

Models often become more complex than necessary to model the interesting behavior, properties, or functions of a system. Modeling-induced complexity often manifests as the application of unnecessary constraints applied to the defined system model. If the system model had been defined more prudently, many such constraints would not be necessary to produce appropriate results. For example, if HEXANE had been formulated as a series of down-selection problems, this would require a problem formulation for every equivalent decision, along with a set of constraints for what options are allowed during the down-selection and how these would affect sequential down-selection problems. Although this formulation accurately reflects the system architecture and does not necessarily include any gratuitous complexity inherent in the natural system, it does make the model of the system far more complex by requiring the application of many constraints on a large set of problems. This contrasts the use of the assignment problem formulation, which only requires a single overall formulation and does not necessitate a series of

constraints to accurately model the system. Because this increase in complexity originates purely from the modeling process, this is referred to as *modeling-induced* complexity. This type of complexity is the primary concern of the framework presented, as it is the most avoidable when appropriate methods are followed in the creation of complex system models. The primary difference between *gratuitous complexity* and *modeling-induced complexity* is that gratuitous complexity is already present in the system (*i.e.* the natural system has unnecessary complexity) which may or may not be modeled, while modeling-induced complexity is not inherent in the system and is only produced by the modeling process.

Essential Complexity

The internal relationships that define the complex behavior, properties, and functions of interest in a system are related to the components of essential complexity. So long as sufficient complex interactions remain to produce the emergent behaviors, properties, and functions at a detectable level, given appropriate consistency and completeness throughout the range of interest, the essential complexity is retained. Under this definition, *essential complexity* can be perceived differently at different levels of abstraction. More importantly, the identification of essential complexity depends on what the observer considers to be the essential emergent behavior, properties, and/or functions. Elements of a system aggregate into different drivers of system-level emergence when considered at various levels of abstraction, and it is vital for the modeler to understand what should be considered essential for the purposes of the modeling effort. There are thus two areas of non-essential (*i.e.* gratuitous) complexity inherent in a system (as opposed to the model, which also contains modeling-induced complexity), as defined by their relation to essential complexity. All complex relationships that are not coupled with the relationships that produce the behaviors, properties, and functions of interest are non-essential for complex system models. The underlying relationships that do not have a significant effect on the behaviors, properties, and/or functions of interest over the range of interest are also therefore non-essential, given that their contribution to emergence is insignificant.

5.1.4 Objectives

The framework here proposed addresses these issues in order to create efficient, appropriate, and useful complex system models. The general objective statement is as follows:

To create a framework that enables the creation of complex systems models with minimal gratuitous and model-induced complexity while retaining system essential complexity information.

To accomplish this objective, the framework proposed is structured to guide model-building

system architects in the creation of such appropriate models both for understanding from the modeler and associated stakeholders' standpoints as well as for effective, efficient computation when analysis is required.

More specifically, this chapter works to accomplish the following:

To introduce a simple framework for creating humanly understandable models of complex systems.

Humanly understandable system models are key for relating the system concepts to the architect as well as to the interested stakeholders. In this case, the framework for the creation of humanly understandable models puts a greater emphasis on the cognitive psychology aspects of modeling rather than computational efficiency. The simple framework consists of the basic steps necessary to build these models.

To introduce a simple framework for creating computationally efficient models of complex systems.

In contrast to the humanly understandable models, some modeling efforts require the creation of system representations that are computationally efficient. This framework focuses on reducing complexity and creating computationally efficient model structures. Again, the simple model is a series of basic steps necessary for the creation of such models.

To introduce a simple framework for the combination of both humanly understandable and computationally efficient complex system models.

The combination of both of the above models into an overall framework describes how information flows between these models as well as how they may become a single model under particular circumstances.

To introduce a classification for coupling relationships within complex systems and discuss related properties.

There are many different kinds of coupling relationships, and many classification schemes have been proposed to organize them. The scheme here presented seeks to create a classification that is both easy to identify in real systems as well as aids in filtering which aspects of a system to consider during the model creation process.

To discuss and classify sub-problems within complex system models.

Like the set-partitioning problems in HEXANE, many systems contain portions that are more appropriately modeled using additional techniques within a larger formulation. This classification scheme seeks to identify these relationships and how they interact with the modeling and evaluation processes.

To introduce extended frameworks for the creation of humanly understandable complex system models, computationally efficient complex system models, and the integration of both.

Extended frameworks include steps that direct the use of the various coupling relationships and sub-problems as well as addressing interactions using specific system information between the models.

To compare the extended framework for humanly understandable complex system models with previous work.

This refers to a validation study that seeks to compare the presented frameworks with prior work by Herbert Simon and Willard Simmons. This demonstrates coverage of the concepts presented in previous work by the newly presented frameworks.

To present a case study comparing the use of the extended framework with unguided complex system model creation.

Using Hofstetter's manned spaceflight model as a baseline, a study is presented that shows how the use of the concepts presented and the framework for the modeling process may help to reduce the amount of complexity in the final model without the need for as much rework as is typically required by the process without the frameworks presented.

5.2 IDEOLOGICAL VS. PHYSICAL MODELS AND THE FUNNEL FRAMEWORK

When decomposing a physical or theoretical system to model, often two separate models are created. The first is occasionally referred to as the Mental Model [94][95], which is created by the architect as a way of easily visualizing or understanding the system from a human perspective. This either exists purely mentally, as implied by the term Mental Model, or is a basic computer or paper model for use by the architect and/or his or her team. This model is henceforth referred to as the "ideological model," in order to encompass those models that are not purely mental. The second model is the physical model of the system, typically a computer model, which is encoded for efficient evaluation (and sometimes enumeration, depending on the type of model) of the system. In some instances, this may take the same form as the mental model, although this is only efficient in particular circumstances. There are also some circumstances where the physical model is not necessary at all, typically when the motive of decomposing the complex system is purely to gain an appropriate human-level understanding of the system. The same is true for the physical model, where only an efficient computational model is necessary for analysis. Both of these concepts are addressed individually in the proceeding sections, followed by a discussion of their interaction and

the resulting integrated modeling process.

5.2.1 Ideological Model

The ideological model building process consists of five fundamental steps. These take the most generalized version of the system down to the portion of interest with an appropriate structure for simulating internal interactions. Figure 69 shows these steps and the short name for each.

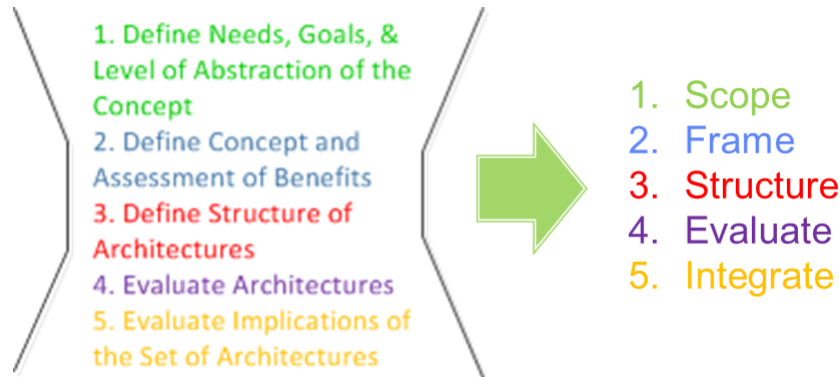


Figure 69: Ideological Model Fundamental Steps

The first of these steps is to scope the system. This answers the question “What is the system?” It also defines the boundaries, interfaces, and simplifications imbedded in the model. All systems exist within larger systems and contain smaller systems [37]. It is therefore necessary to scope the model to address the portion of the complex system of interest. For example, HEXANE was scoped from the entire manned exploration mission architecture to the in-space transportation portion under the constraints of final surface destinations and sortie-like missions only. This scoping step is heavily dependent on the level of abstraction that is desired, and it is during this process that the appropriate level of abstraction should be determined. For many systems, this is also heavily reliant on stakeholder inputs [37][96]. The needs and goals of the analysis should drive the appropriate construction of the model. For HEXANE, the goal of the modeling process is to determine the architecture-level elements that should be invested in for a long-term exploration strategy in order to enable optimal mission design. This has many associated needs, driving the system abstraction to that of metric ton plus and billion dollar plus development investment elements. If the goal were to determine the most effective life support strategy for long-duration missions, the level of abstraction would have been more granular and scoped to the habitats.

The second step is to frame the system, as driven by the level of abstraction determined during the scoping step. This step answers the question “What type of system is it?” For this step, the architect may analyze the differences between dynamic and static systems, centralized vs. de-

centralized systems, and monolithic vs. fractionated systems. At this point, the architect chooses from amongst the set of possible overall System Architecture Problem (SAP) formulations, outlined by [97]. The list of SAPs described by this work include:

- Assignment problems
- Connecting problems
- Down-selection problems
- Set-partitioning problems
- Covering problems
- Permuting problems

This provides a general pattern or mold to be filled in by the particular characteristics of the system. HEXANE is formulated as an assignment problem, whose literature is extensive [98][99], allowing for more well-organized formulation of the remainder of the details associated with the in-space transportation infrastructure. Framing of the system should be driven by the value delivery mechanism, since this defines what system-level behavior and properties are of interest. If the value delivery mechanism is not easily discernible in the context of the chosen SAP, it is likely that the framing is not appropriate.

This third step, structuring, involves the next level of granularity from the framing step. The question answered here is “How does the system work?” This is where the bulk of the complexity is modeled, and it is therefore the least strictly formulated of the steps. It is also often the most time-consuming, requiring many iterations before a final structure is chosen. By formalizing many of the issues inherent in this step, it is hoped that the number of iterations required will be reduced and the final formulation superior to a non-structured approach. Because this is the step where most of the complexity in the system is modeled, it is also the step where the modeling-induced complexity is minimized through appropriate formulation. Most of the additional gratuitous complexity is eliminated during the scoping step as well as the structure step. Section 5.3.3 addresses methods for the reduction of complexity in models.

The fourth step is more self-evident in its purpose, being the evaluation step. Once the model is developed to a point where the essential complexity is retained while the gratuitous and modeling-induced complexity is minimized, the analysis may take place. This step is included in both the ideological model as well as the physical model, although the evaluation step is often a result of the combination of the two. Although the overall methodology of this step may seem simple, given that it is the process of executing the evaluation mechanisms in the model, there are some properties of certain complex systems that complicate the process. There are also properties that may be

exploited for improved evaluation efficiency. These will both be discussed in Section 5.3.

The fifth and final step, integration, is the feedback of knowledge gained by the analysis into the formulation of the model. Unlike the preceding four steps, the fifth step is not always necessary and is highly dependent on the available resources. This concept follows the famous saying that “hindsight is 20/20” [100], meaning, in this context, that the intricacies of the system, and therefore how to model them, are more evident following the evaluation step. In the larger context, this step is tied back to step one, but in reality it is tied to all preceding formulation steps (1-3). Assuming that appropriate documentation practices have been followed and therefore traceability remains throughout the steps, the information gained from the final steps can be integrated into the model at any level.

The steps in Figure 69 are also surrounded by a contracting and expanding shape to symbolize the nature of the information needed and created during the steps. The model begins as a broad system and is scoped and refined to its essential elements. Once evaluation begins, the amount of information expands, leading to a re-assessment of the model itself. This is taken from a similar concept from the process of systems architecting, shown in Figure 70. The stakeholder needs are used to determine value delivery and system goals, which are refined into a concept, for which an architecture is created and used to define a complete design for operation [37].

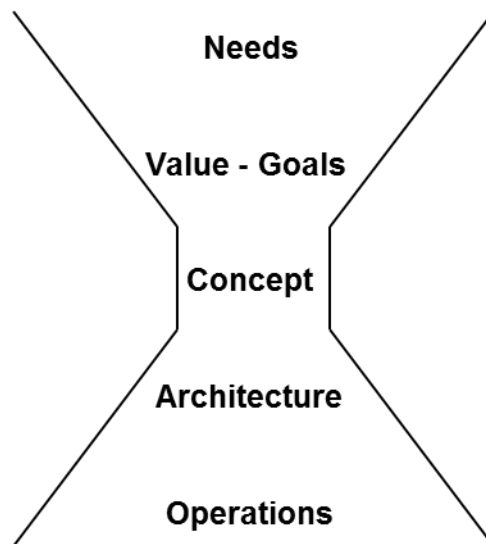


Figure 70: Systems Architecting Flow

5.2.2 Physical Model

The five fundamental steps of building the physical model are similar to those of the ideological model, with the first three gaining information from the initial steps of the ideological model creation. In this sense, the physical model building process flows down from the ideological model building process. These steps are outlined in Figure 71.

1. Generate FOMs
2. Develop Proxy Metrics
3. Construct Code
4. Evaluation
5. Re-assessment

Figure 71: Physical Model Fundamental Steps

“Generate FOMs” refers to the generation of Figures of Merit. These are the quantities used to characterize the system, typically in terms of its performance relative to alternatives [101]. These are higher order characterizations in comparison to metrics or TPMs, therefore addressing what general characteristics of the system are important to the architect and other stakeholders. These are also formulated following the scoping step of the ideological model, after stakeholder input limits the model to the portion of interest. FOMs may be as broad as components of the iron triangle [54], identifying performance, schedule, cost, or risk as primary characteristics to model in the system. They may also take a form in the next level of abstraction, such as types of risk. In Low-E, operational risk was identified as a characteristic of interest for the evaluated architectures, and this would be considered a FOM.

Once the FOMs are determined, proxy metrics must be developed. Metrics, in this case, are the more specific definition of how to assess the FOMs. This often includes a mathematical formulation either of the physical laws governing the system or a simplified method for determining the property from the complex interactions of the system. Like abstraction in the scoping portion of the ideological model, it is during this step that the necessary level of realism is assessed and the modeling environment, in terms of programming language and/or software, is chosen.

Once the interactions of interest are chosen and their mathematical formulation determined, the model itself must be constructed by encoding it in the physical model. The title “construct code” implies the use of computer programming to create the physical model. However, this is not always necessary or beneficial, as some complex systems can better be simulated using literally physical models. This statement implies that a literally physical model would be a simplified or scaled version of the real system. Scaling is often an effective method in this domain, such as with

railroad systems. If the properties of interest are related to the interaction of trains on intersecting rail lines, a physical model, like a model train set, can easily represent the system without including the intricate complexities of train mechanisms. When the system is encoded using more typical programming languages or software, this step interacts with the field of computer science and computer engineering, and therefore concepts such as utilization of the Spiral Model [102] become important. This step also ends with the validation of the model.

The evaluation and re-assessment steps follow the properties of steps four and five of the ideological model building process, with the exception of the modeling environment. Like the evaluation step in the ideological model, there are specific properties of the system and model that may be advantageous to exploit. These properties will be discussed along with the related properties of the ideological model. Re-assessment is the analogous term for integration in the ideological model and therefore refers to the integration of gained knowledge from the previous portions of the model building and evaluation back into the model.

5.2.3 Funnel Framework

The ideological and physical models are inherently intertwined, and therefore it is vital to understand the connection between the models, when they must be separated, and when they can be combined. The Funnel Framework is simply a tool for visualizing these interactions, shown in Figure 72.

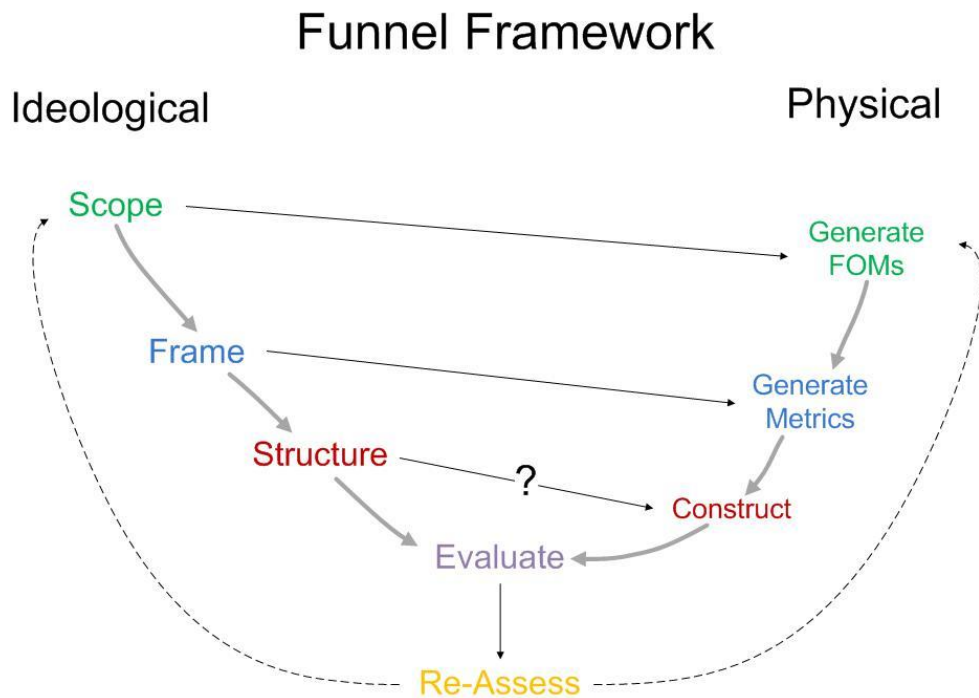


Figure 72: Funnel Framework

On the left is the ideological model building process, flowing down from scoping to evaluating, ending in the re-assessment (i.e. integration) step. On the right is the physical model building process, flowing down from the generation of FOMs and meeting the ideological model at the evaluation and re-assessment steps. Information also flows across and slightly downward from the ideological model to the physical model prior to the meeting at evaluation. The flow downward and across, along with the convergence at the evaluation step, leads to a bowl shape to the two model building processes. The re-assessment step, which is downward from the evaluation step, gives the overall framework the last piece of the funnel shape, with all information flowing downward toward re-assessment.

Cross-flow in the framework exists between steps 1-3 in the ideological model process to the corresponding steps in the physical model process. The one-to-one flow (Scope to Generate FOMs) has already been discussed. The two-to-two flow (Frame to Generate Metrics), which is between the framing step in the ideological model and the metrics generation step in the physical model, is slightly more convoluted. The mathematical structure of a metric should make sense within the SAP chosen, *i.e.* the mathematics should be easily formulated within the context of the SAP, and therefore the structure of the SAP will influence the development of the proxy metrics. Heritage system models also play a key role, providing information about what approaches do and do not work in the context of certain SAPs.

Three-to-three flow (Structure to Construct) occurs when the models become integrated. Simmons showed that this is possible and desirable in models using assignment formulations under certain conditions [14]. If the construction of the physical model duplicates the structure of the ideological model, there is no reason to separate the actual models from each other. The human comprehensibility is the same between the models, given the determination of the model complexity from this process, and therefore the physical model serves the purposes of both models. When the models are separated, sometimes a translation mechanism for transferring the information from one model to the other becomes necessary. On occasion, the systems are simple enough that the model builder may simply be able to translate the information without an additional device. However, the method for translating the information should be considered when constructing the models.

5.3 THE EXPANDED FRAMEWORK

For the modeling of simple systems or for experts familiar with the modeling process and system architecting methods and tools, the simple frameworks may suffice for building minimum complexity models. For most circumstances, a more directed framework aids in the application of system information and specific methods and tools in order to reduce the overall complexity of the

model as well as reduce the number of iterations necessary to create the model. Therefore, an extended framework building to this capability is presented. In order to introduce the full, expanded framework and the individual steps within the fundamental groups, several concepts must first be introduced. These concepts are essential for understanding how the framework reduces model-induced complexity by exploiting key system properties.

5.3.1 Classification of Coupling Relationships

A coupling, in the most general sense, is simply defined as a connection between two parts [103]. In the context of complex systems, this concept more specifically refers to the underlying influence between two components, functions, or properties of the system. This can either be in the physical or functional domain, but it always implies that a change in the state of one part or property of the system influences another state or property to which it is coupled. Complex systems often get their complexity from the number and types of coupling in the system. Because models seek to simplify a system to the necessary parts to exhibit desired behavior, understanding the types of coupling present in a system and how to exploit them is vital to system model development.

Exclusive Coupling

This general category refers to parts, properties, or functions that inherently exclude each other. For example, in assignment problems, this is often manifested as options for decisions. Only one option at a time is allowed because each excludes all others. This coupling is effectively outside of each possible system, since the parts, properties, or functions do not co-exist in any given system. Instead, the coupling often manifests itself in gaps in the objective tradespace. There are two types:

Absolute Exclusive Coupling: When two parts, properties, or functions cannot co-exist in a system, either because they directly conflict or because their combination would disobey a law of physics, this is referred to as absolute coupling. These parts, properties, or functions are coupled, in effect, externally to the system, since it is an absolute law of governance that causes the interaction. For example, in HEXANE LOX/LCH₄ in-space propellant and LOX/LH₂ in-space propellant are coupled absolutely, given that they cannot both be used in the same propulsion stage.

Intuitive Exclusive Coupling: In many cases, parts, properties, or functions in a system should not be combined, although they do not break any laws of physics or are in any other way impossible to combine. This coupling is referred to as intuitive because it is typically the intuition of the expert system architect that indicates the existence of these couplings.

Interactive Coupling

Interactive coupling refers to parts, properties, or functions that are inherently intertwined and therefore exist together in systems. The existence of one implies the existence of the other in the given system. Unlike exclusive coupling, this is manifested internally. There are three types of interactive coupling:

Absolute Interactive Coupling: This again refers to relationships that are dependent on absolute rules, such as laws of physics. The existence of a part, property, or function absolutely must accompany that of the coupled part, property, or function.

Intuitive Interactive Coupling: Experts may deem it illogical not to include one part, property, or function when another is present. This is therefore deemed intuitive interactive coupling. Again, these are not coupled by laws of physics or any other mechanism that inextricably combines them. Rather, they are combinations that are logical only when together. For example, multiple NTR propulsion stages in an architecture in HEXANE use a drop tank system rather than multiple complete stages, since it is well understood that the dry mass structure and radiation shield associated with complete stages should not be duplicated. This is not driven by physics but by expertise.

Value Function Coupling: In addition to the relationships of absolute and intuitive coupling, some parts, properties, or functions may be intertwined by the value function relationships defined by the architect. For example, although the solar arrays and logistics storage system of a spacecraft are decoupled in the physical and functional domains, they are coupled in any total mass metric. Both are necessary to assess the total mass of the system, although they are not strongly coupled beyond the value function associated with the mass metric.

5.3.2 Separability

Value function coupling has further properties of importance in reducing modeling-induced complexity. This ties directly with the internal complexity of the value function itself. In some cases, value functions are calculated with simple mathematical relationships, such as sums, differences, or a combination of simple functions. When the elements involved in the value function are not otherwise coupled and the value function itself follows a simple mathematical relationship, then the coupling relationship between the elements involved is weak and can be divided by the structure of the model. These are referred to as separable value functions. This manifests itself in HEXANE with the division of the modules into habitat and propulsion calculators. The high level definition of IMLEO is a weak value function coupling between these elements, and therefore the model is constructed to take advantage of this property. That is to say that IMLEO, at a high level, is simply the summation of all mass properties of all elements, and therefore the major contributors to mass can be separated in the model and simply summed for the

calculation of the metric.

Value functions become non-separable when the mathematical relationship between elements is complex (*i.e.* when the calculation of the metric involves non-linear relationships or complicated products). Any complexity in the mathematical formulation of a value function-associated metric influences the resulting complexity of the structuring when this property is used to formulate the model. The perceived complexity in the model therefore increases at the same rate as the complexity of the value function. Simple metrics, in the case of the separable value function coupling, are not perceived as complexity due to the simplicity of the formulation.

Abstraction levels for value functions also play a role in understanding separability. There are many metrics whose separability heavily depends on the abstraction level viewed. IMLEO, for example, is separable at the level of total architecture-level elements. However, to generate the element-level mass information, the metric requires far more complex underlying calculations, in this case based on parametric relationships and physical relationships in the rocket equation [56]. Therefore, at the lower level of abstraction, the IMLEO metric becomes non-separable. A general rule of thumb to understanding the usefulness of this information is to abstract the value function to the level at which it becomes separable. If the modularity relationships (*i.e.* the separation between elements of the calculation and how this translates to modules for evaluation purposes) between the separable components are still useful, then treat the value function as separable. If the value function must be abstracted to a point of non-usefulness, then it should be treated as non-separable. The modularity relationships (*i.e.* how the model itself is modularized for calculation purposes) of IMLEO were still of interest at the level of separability, showing that a clean division between major architectural elements for mass calculations would create few interfaces for the proper calculation of total mass, and therefore IMLEO is treated as a separable value function.

5.3.3 Reducible vs. Irreducible Coupling

The overall goal of the framework is to produce models that have minimum gratuitous and modeling-induced complexity. One method of eliminating modeling-induced complexity is to reduce the modeling complexity caused by coupling relationships. This is accomplished by model structuring methods, to be discussed in the following sections. To apply these complexity-reducing model structuring methods, the architect must identify the coupling relationships that are either reducible or irreducible. This reducibility refers to the ability to manipulate the model to be structured in such a way that the model itself does not create additional complexity (*i.e.* does not produce modeling-induced complexity).

Reducible Coupling: This is a class of coupling relationships that are generally reducible in the fashion above described. This reduction of complexity can be perceived in two ways. The first is that the model itself reduces the complexity that would otherwise be apparent to the architect by

changing the structure of the model. The second is to understand that the model has a minimum complexity state, and that the architect is trying to achieve this state through appropriate structuring. Reducible coupling is typically associated with absolute, intuitive, and separable value function coupling relationships. However, when implementing a reduced-complexity structure by utilizing this concept, there is often an intelligibility cost. Figure 73 demonstrates both the concept of reducibility and the impact on intelligibility.

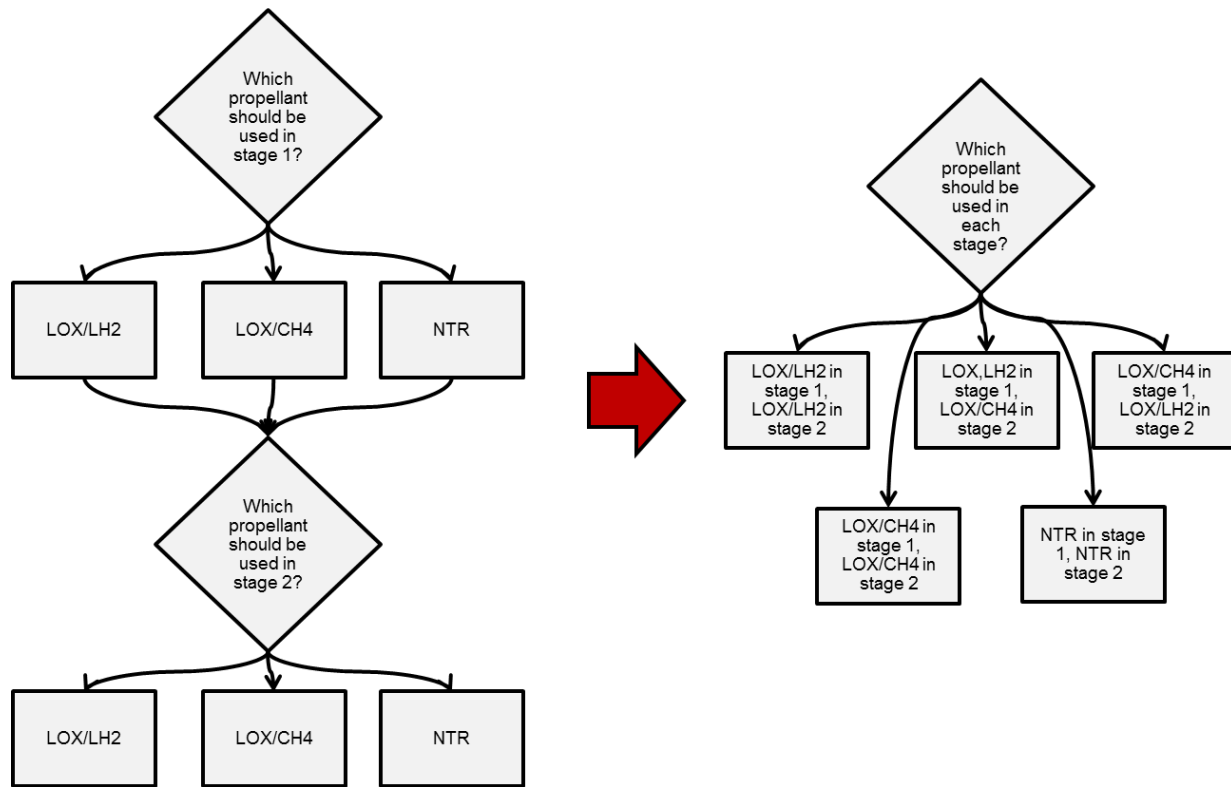


Figure 73: Reducible Coupling Example

In this example, the assignment of propellants to two stages is posed. On the left is an easily understood method of assigning one of the propellant options to stage 1 and one to stage 2. However, this method involves additional constraints caused by intuitive coupling with NTR. As an engineer, it is obvious that if NTR is developed for stage 1 it should be used for stage 2 as well, given the development cost associated with the technology as well as the additional dry mass associated with individual NTR stages. Therefore this additional constraint would have to be applied externally to the structure of the model. On the right is the reduced complexity version, where the constraint is built into the model as a down-selection of the option space. This also

comes at the cost of intelligibility, as this option space is more difficult to understand, in general, than the first. This is rooted in two properties. The first is the number of options. On the left, there are three options for each question, and each question is perceived individually. On the right there are five options perceived simultaneously. This information is harder to quickly understand. In addition, each option contains much more information. It includes not only the propellant, but the propellant for both stages and the respective assignment to those stages. Further discussion of the cognitive psychology aspects of modeling will be discussed in Section 5.3.5.

Irreducible Coupling: This term applies to the coupling relationships that are too complex to reflect in the structuring of the model and therefore are not used to reduce the perceived modeling-induced complexity. The primary source of this irreducible complexity is non-separable value functions. As the architect designs the system model, these couplings should be recognized as portions of the complexity that should not be analyzed for designing the structure of the model. In other words, these relationships represent aspects of the system that are highly complex interactions, and the effort required to model around these complex relationships is high in comparison to other complexity reduction methods. These relationships are the couplings that contain much of the essential complexity of the system.

5.3.4 Parallel vs. Serial Sub-problems

Another method for the reduction of modeling-induced complexity is to take advantage of sub-problems nested within the larger system. Figure 74 gives the classification scheme described in this section. Within the structure of the chosen SAP, these sub-problems emerge as patterns within sections of the model structure. HEXANE contains two obvious sub-problems: the habitation and transportation sub-function set partitions. These are recognized sub-problems because their patterns are conducive to the use of known analytical techniques, in this case set partitioning. In general, sub-problems are classified into two categories relating to the methods of grouping: parallel and serial.

Parallel: Much like the concepts in electrical engineering [104], parallel sub-problems occur when system information about two separate aspects can be gathered simultaneously. There are two forms of parallel sub-problems. The first is referred to as *structural* parallel sub-problems. This is the more intuitive concept associated with parallel computing, where groups of properties may be analyzed simultaneously. In HEXANE, architectures are analyzed in parallel. The matrix containing the set of architectures is broken down by row (*i.e.* architecture), and each row is analyzed in the module in parallel. This capability occurs when there is no entanglement between architectures, meaning that any given architecture does not influence the neighboring architectures.

Conceptual parallel sub-problems are similar to structural parallel sub-problems in the respect

that they can be decomposed and analyzed simultaneously. These are situations where the analysis itself can be decomposed and parallelized, rather than the structure of the system. For example, the consumables mass for the in-space portion of an architecture in HEXANE can be computed simultaneously with the size of the habitat, since this information is not intertwined. This is a parallel computation of the properties of the architecture, rather than parallelization of the overall computations for the architecture itself. The primary differentiating factor between these concepts is the application to the system versus the application to the analysis of that system. Like the structural parallel sub-problems, these can also be implemented in parallel computing clusters when properly encoded, given the assumption of zero entanglement.

Serial sub-problems are dependent on feedback loop structures. Similar to the parallel sub-problems, serial sub-problems are analogous to their electrical engineering counterparts [104]. A section of analysis may be done as a set prior to the next section of analysis, usually feeding reduced information forward. Internally, this grouping is dependent on the existence, or more importantly non-existence, of feedback loops. Serial sub-problems should be grouped such that the data reduction takes place prior to any feedback structures, therefore reducing the complexity of information flow during iterations. For example, the habitation calculator for HEXANE is in serial with the propulsion calculations, such that, if a feedback loop were necessary, it would occur after the propulsion calculation to feed back into the structural requirements for the habitats. These calculations are serial in the fact that the information is fed forward while it is organized to avoid feedback loops. If a system model is fully serial, for example, it would look much like a token system [105].

Additional concepts are necessary to fully understand parallel and serial sub-problems and their associated properties. The first is the concept of full vs. partial parallelization blocks. In some instances, only sections of either analysis or system structure can be parallelized, necessitating a fluctuation between serial and parallel processing. This often results in bottlenecks in the serial sub-portions, although this is dependent on the computation power necessary for each section. Full parallelization is always preferred but is not always possible or feasible.

The second important additional concept is the use of optimization within the sub-problems. One method of data reduction between sub-problems is to optimize the architectures or the properties of the architectures prior to data transfer. In systems architecture, this often takes the form of pruning, where regimes of architectures are eliminated from the tradespace due to poor properties determined early in the analysis [106]. This may significantly reduce the amount of data passed by reducing the number of architectures and associated information. These methods include everything from simple pruning to full MSDO methods [107]. However, optimization within the

sub-problems is not always good or necessary, and therefore there is also a class of non-optimized sub-problems.

Lastly, there is also the concept of grouping, which may occur as a nested part of parallel or serial sub-problems. These are the sub-problems most heavily associated with pattern matching. Here, the architect recognizes the applicability of mathematical techniques, such as set partitioning within a larger SAP. Set covering problems also fall within this category, although they, along with set partitioning problems, are also among the overall set of SAPs. When applied within the larger SAP, they are mathematically convenient groupings to take advantage of well-understood relationships and analytical techniques.

The overall classification scheme of sub-problems is presented in Figure 74. The applicability to the types of model, either ideological or physical, is also marked. The full conceptual parallel sub-problems are excluded from the classification scheme because this situation would imply the complete separation of the analysis and therefore the complete separation of the model into two models. Grouping is marked as a third classification alongside serial and parallel sub-problems, with partial applicability to the physical models, due to the nature of the methods associated.

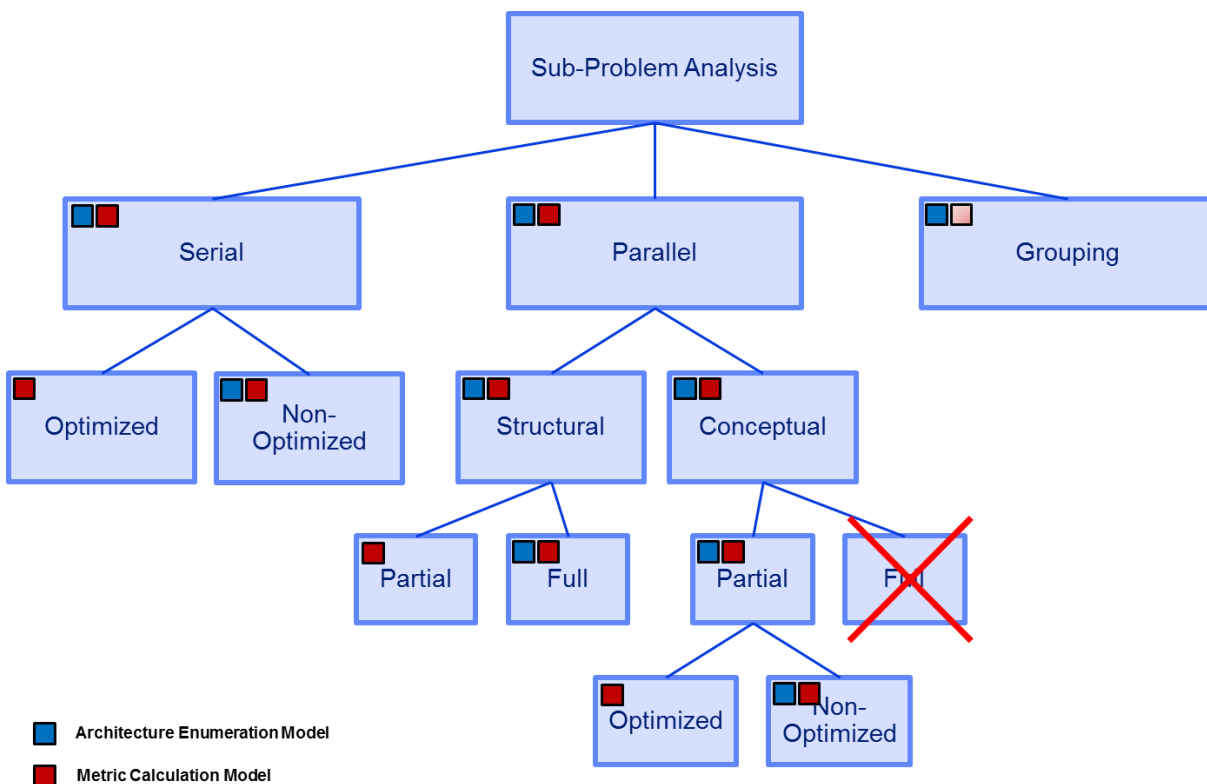


Figure 74: Sub-Problem Classification

5.3.5 The Role of Cognitive Psychology

Although understanding the technical aspects of model creation is vital for the creation of complex system models, understanding the human aspect may be just as important. Cognitive psychology, the study of mental processes [108], is therefore a relevant field to consider. “The Magical Number 7, Plus or Minus 2” is one of the most cited works in the field of cognitive psychology [109], written by Dr. George Miller in 1956 [110]. In this work, Dr. Miller describes the average capacity of humans to hold discrete pieces of information simultaneously. He came to the conclusion that people could hold approximately seven pieces of discrete information in short-term memory, with a range of plus or minus two. This concept plays a critical role in the intelligibility of complex system models and decomposition methods. Although a deeper reading of his works reveals that the cognition and retention of discrete information is not so simple, the general concept of limited human capacity is influential in the creation of understandable models. Each abstraction layer in a model decomposition should be composed of an appropriate, intelligible set of information that follows the aforementioned rule. This is further complicated by the complexity of the discrete pieces of information. In Figure 73, reduced modeling complexity was shown to have a negative effect on the intelligibility of the resulting decomposition. This was not just because there were more options at a single layer but also because those options involved more complex information.

The role of cognitive psychology in model building is not yet well characterized, but systems architects intuitively understand that it is important to make models intelligible as well as efficient. The general approach in the framework described is to create better overall intelligibility by eliminating unnecessary complexity in the model, but this sometimes comes at the cost of intelligibility at lower levels of abstraction. This concept is especially important in the ideological model, given that its explicit purpose is to create a decomposition that is understandable to both the architect and the interested stakeholders. Therefore it is critical for architects to recognize this limitation while formulating a model.

5.3.6 Expanded Ideological Model

Herein presented is the complete, expanded version of the ideological model building process, with directed steps in the use of the aforementioned properties of complex systems. The complete process will be shown, followed by an explanation of each step in further detail.

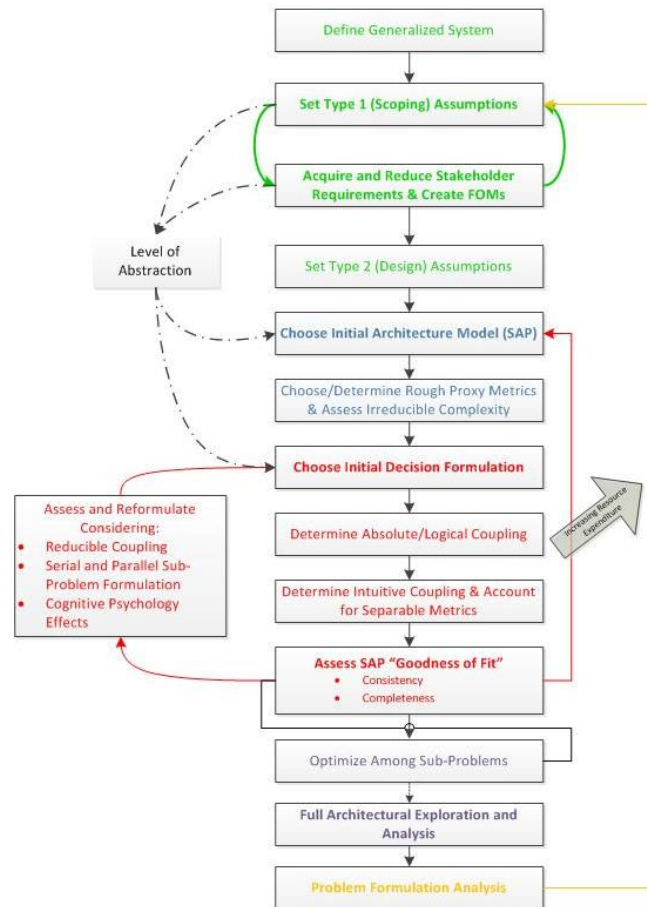


Figure 75: Expanded Ideological Model Building Process

The five fundamental steps are outlined by their respective color, with bolded steps indicating key points. Information feedback loops are shown in the color of the origin step. Dashed lines indicate an external feed-forward consideration, in this case the level of abstraction. The large box in the red feedback loop is the primary iteration step and will be discussed in the respective section. Additionally, the arrow indicating “Increasing Resource Expenditure” identifies the larger and larger feedback loops as being increasingly resource-intensive, given the amount of rework required.

The first fundamental step, identified as the *scoping* step, is composed of four sub-steps. First, the architect defines the generalized problem. Mapping this to HEXANE, this would be to architect manned space exploration missions. This leads to the first round of setting scoping assumptions. Assumptions are placed into type 1 and type 2 categories, indicating the differences in abstraction layers and applicability. Type 1 assumptions are the overall scoping or constraining assumptions. In HEXANE, these include the limitation of destinations and the down-scoping to the in-space infrastructure. This step then leads to the first iteration of acquiring stakeholder input in the form

of requirements and the creation of FOMs. This iterates directly with the preceding step, as it is likely that the architect and stakeholders will negotiate the overall scoping of the system and model. This is also the point at which the level of abstraction is chosen as appropriate to the scoping of the problem and the level of detail required for the FOMs. Once this is achieved, the architect then sets the more detailed assumptions, referred to as type 2 assumptions. These include the technical restrictions and domain limitation in terms of the design of the system. For HEXANE, this includes the assumptions that limit types of possible propellants, the types of other technologies, and the limitation of low-thrust trajectories to unmanned cargo stacks.

The second fundamental step has been identified as the *framing* step, shown in blue. This step's primary purpose is to determine the appropriate SAP to apply to the system model. A more complete discussion of SAPs and their origin can be found in [97]. Following the understanding of the overall framework for the model, being the SAP, the set of proxy metrics should be determined in order to understand the necessary complexity in the model. For those metrics that are non-separable value functions, the associated irreducible complexity should be assessed and noted.

The third step, structuring, is the most important and most difficult. In Figure 75, an example of the set of sub-steps is presented. For each SAP, a different set of sub-steps would be necessary as they apply to the SAP of choice. For the purposes of this discussion, only the steps associated with assignment problems will be described. Overall, this step is where the bulk of model construction iterations occur. More specifically, these are the steps where the final abstraction layers are determined and model decomposition details are set. For assignment problems, the first sub-step is to formulate the initial decision structure. For HEXANE, this began with the breakdown into three general decision categories and progressed until Figure 19 was set. To exploit the properties of the system that allow for complexity reduction, the absolute coupling is assessed, followed by the intuitive coupling and separable value functions. These can typically be used to structure the model in such a way that additional constraints do not need to be externally applied, therefore reducing the modeling-induced complexity, as discussed in Section 5.3.3. The overall step ends with an assessment of the “goodness of fit” between the real system and the chosen SAP. Assessment of this fit should include properties of both consistency and completeness. The model should produce consistent results when different aspects are analyzed, and the model should completely cover the desired system elements and properties. At this point, if the SAP is not appropriate, this information is fed back to the framing step and used in choosing an alternate SAP.

This step also involves the internal iteration required to properly formulate the details of the model. Reformulation should consider a variety of factors. Key factors include the reducible coupling characteristics, sub-problem existence and formulation, and cognitive psychology impacts. Without formal structuring methods, this is where many architects spend additional time reformulating the model. With formal methods and guidelines about what to be aware of and

account for in the model, it is hoped that the number of necessary iterations will be reduced and the final models more efficient.

The fourth step, evaluation, is fairly self-evident. When optimize-able sub-problems exist within the model, these are first assessed, followed by the overall evaluation and exploration of the resulting tradespace. However, sub-problem optimization may lead to a lack of global optimization. The use of local, sub-problem optimization should be selectively applied. Not all models will be tradespace exploration models, and so this step more generally refers to the analysis portion of the modeling process.

The final step re-assesses the formulation given knowledge gained from the analysis. Although the feedback loop shows only an arrow to the scoping step, knowledge gained in the process may be applied to any prior point, with increasing resource expenditure as the loop applies to prior steps. More detail is given in Section 5.2.1.

5.3.7 Expanded Physical Model

Accompanying the expanded version of the ideological model building process is the expanded version of the physical model building process, shown in Figure 76. Like the previous process, the fundamental steps are color-coded to match with the description in Section 5.2.2. Also like the previous process, there are a few overall features of note. Once again, feedback loops are shown using their respective colors of origin. The primary loops are shown on the left rather than the right, and although they are not marked to show the increase of resource expenditure with outer loops, the same rule applies to the physical model building process. Like the level of abstraction in the prior process, the decision regarding the programming language and/or software employed exists as an additional consideration outside of the explicit steps. This consideration falls before the code construction and is most heavily informed by the process of generating metric formulations.

The first step, generating FOMs, is directly informed by the equivalent process in the ideological model. This process may be seen as redundant with the separate model process, and it in fact may be in many circumstances. However, it is of vital importance to correctly identify the stakeholder needs and the FOMs associated with them prior to the design of the physical model. This process is once again iterative between the stakeholder input and FOMs generation.

The metric generation step may appear to be the most complicated step in terms of the sub-steps presented, but it is not the most time intensive step. Rough metrics are first generated, followed by the more detailed mathematical formulation. The realism inherent in the mathematical formulation is assessed against the desires of the stakeholders, and the process is iterated given the needs. This also informs the programming language and software choice. This choice should also be reflected in the regime of mathematics chosen. Many problems will not require advanced mathematics, but it is worthwhile for the architect to consider alternative formulations

implementing higher-level mathematics. The assessment of separability is also contained within the generation of metrics step, which informs the possible creation and separation of sub-problems. The decomposition of the separable metrics may enable enough modularity for the use of sub-problems, but this is also weakly tied back with the mathematical formulation of metrics. Depending on the modeled relationships, it may be worth the trade between metric accuracy and sub-problem formulation, given the computational benefits of parallelization or sub-grouping optimization.

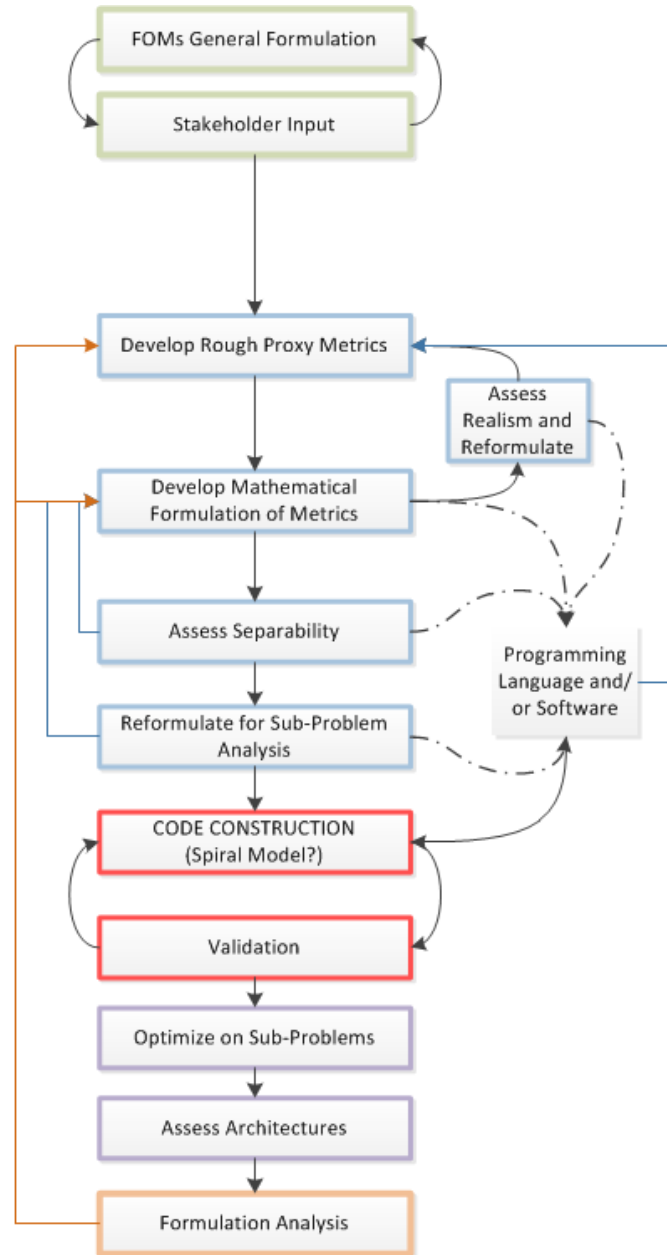


Figure 76: Expanded Physical Model Building Process

Once again, the most time-consuming and difficult portion of the model building process is the third step. The construction step, in this case referring to code construction, is heavily informed by the previous steps, and, given that it is fundamentally computer science, follows many of the iterative patterns of code construction, such as Spiral Models [102]. At the end of this process the code is validated against known quantities. The iteration loop runs back from validation due to the likelihood of imperfect coding during the process resulting in validation failure.

Once the physical model is properly encoded, having been successfully validated, the evaluation step takes place. This, like the ideological model (and often intertwined with the ideological model), takes place in two steps. First, the optimize-able sub-problems are optimized, followed by the full assessment of architectures. The re-assessment step follows this process, similar to that of the ideological model.

5.3.8 Integrated Expanded Models

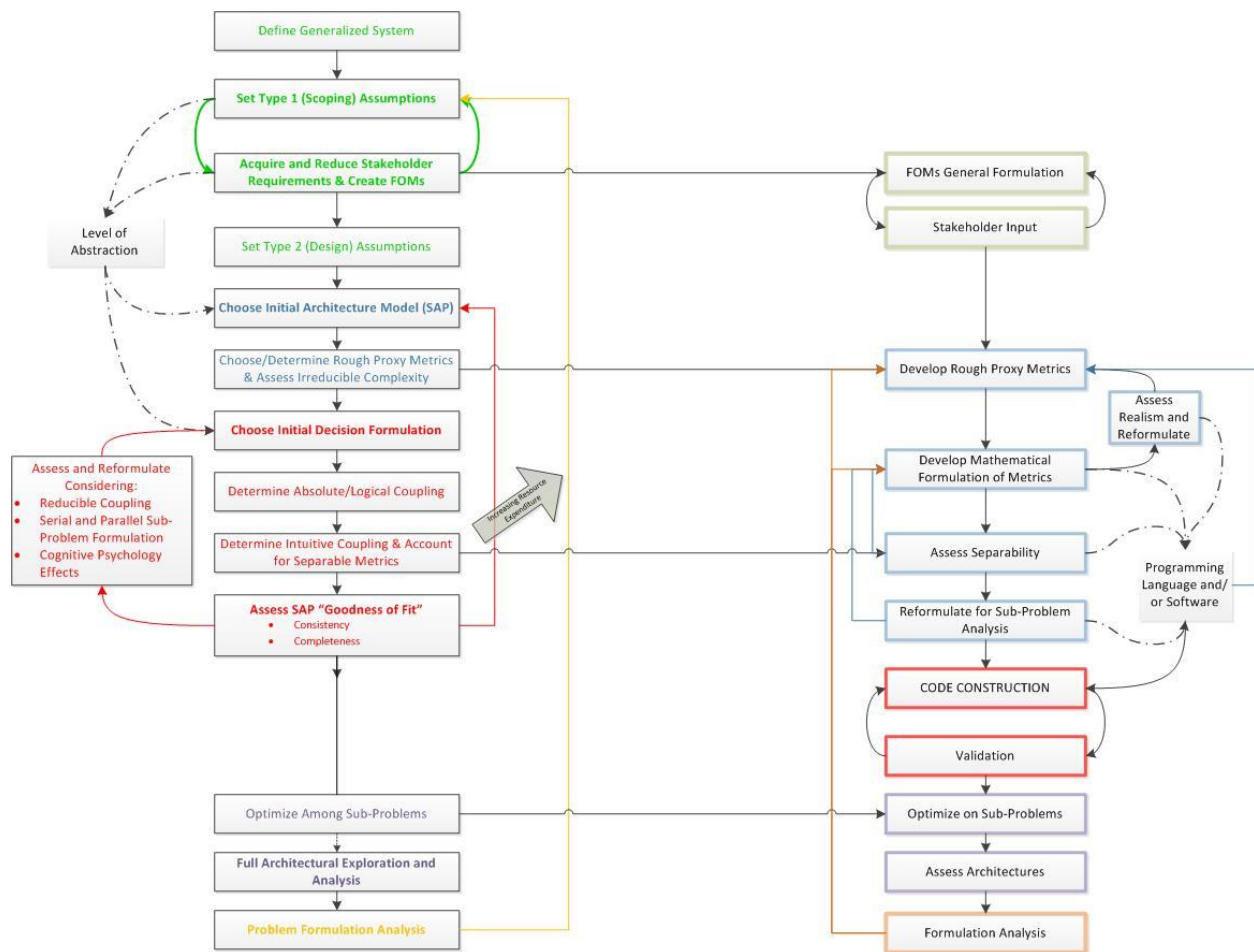


Figure 77: Integrated Expanded Ideological and Physical Models

Figure 77 shows the integration of the two model-building processes and the cross-feeds between them. This is the more expanded version of the Funnel Framework, showing the sub-steps where the cross-feeding occurs between the models. Although the combination of the models at the evaluation step is not explicitly shown, it should be understood that, in many cases, these models work together in order to produce understandable and appropriate analysis.

5.3.9 Topics for Further Consideration

There are many additional considerations for the architect when going about building the ideological and physical models. Those mentioned here are intended to be future work and therefore not discussed in detail.

Some topics of consideration for the ideological model building process include the classification of SAPs, a further consideration of patterns as they impact the structuring step, the difference between heuristic optimization and other algorithmic optimization techniques and their impact on the process, flow patterns in the structure outside of coupling relationships, and the entire structuring step for SAPs other than assignment problems. There is additionally a very significant consideration for the level of abstraction necessary in all complex system models. In most cases, the architect and stakeholders are interested in the emergent behavior of the system, which is often tied to the culminating effects of low-level coupling. Effectively, this mirrors the Butterfly Effect [111] in the fact that small coupling relationships may combine to create sizeable effects. Therefore, it is possible that the architect should always model at an additional level of fidelity beyond that which is well-characterized for the properties of interest in order to capture the low-level coupling relationships that may cause the interesting emergent behaviors or properties. However, this has not been well-discussed and therefore may not be relevant to these systems.

For the physical system model, there are also a variety of additional topics to consider. In general, the applicability of the model-building process beyond the usefulness for architecture-level analysis should be considered in order to further generalize the system. The handling of uncertainty, especially in the coupling relationships, should also be further considered. The overall integration of the process and framework into broader frameworks, such as Spiral Models, Waterfall Models, and other business practices such as 6-Sigma should be analyzed. Perhaps more importantly, the applicability of combining the processes between the physical and ideological models, as accomplished in [14], should be further considered.

5.4 COMPARISON WITH PREVIOUS CONCEPTS

The concept of creating a framework for a decision analysis tool is not unique to the framework herein described, nor are any of the issues inherent in the framework unique. A comparison with

two previous frameworks for decision analysis and model construction is presented in order to describe the unique characteristics of the framework described as well as validate the overall concept by comparison with well-established models.

5.4.1 Simon's Four Steps to Decision Making

In 1987, Herbert Simon, founder of the concepts of “satisficing” and “bounded rationality” [112], published the work “Decision Making and Problem Solving,” which described a three step process to decision making [113]. He and his colleagues proposed that the decision-making process was composed of an *intelligence* phase, where the information is collected; a *design* phase, where alternatives are developed; and a *choice* phase, where the evaluation takes place. This model of decision making was later extended to four and five steps to include *implementation* and *review*. One can argue that building a model of a complex system is a subset of decision-making, being that the ultimate purpose is to make a decision based on the model output. It is also clear that the steps proposed by Simon map well with the ideological model building process, and that mapping is shown in Figure 78. This mapping includes a fourth step beyond the original three steps, *review*, as proposed in [114].

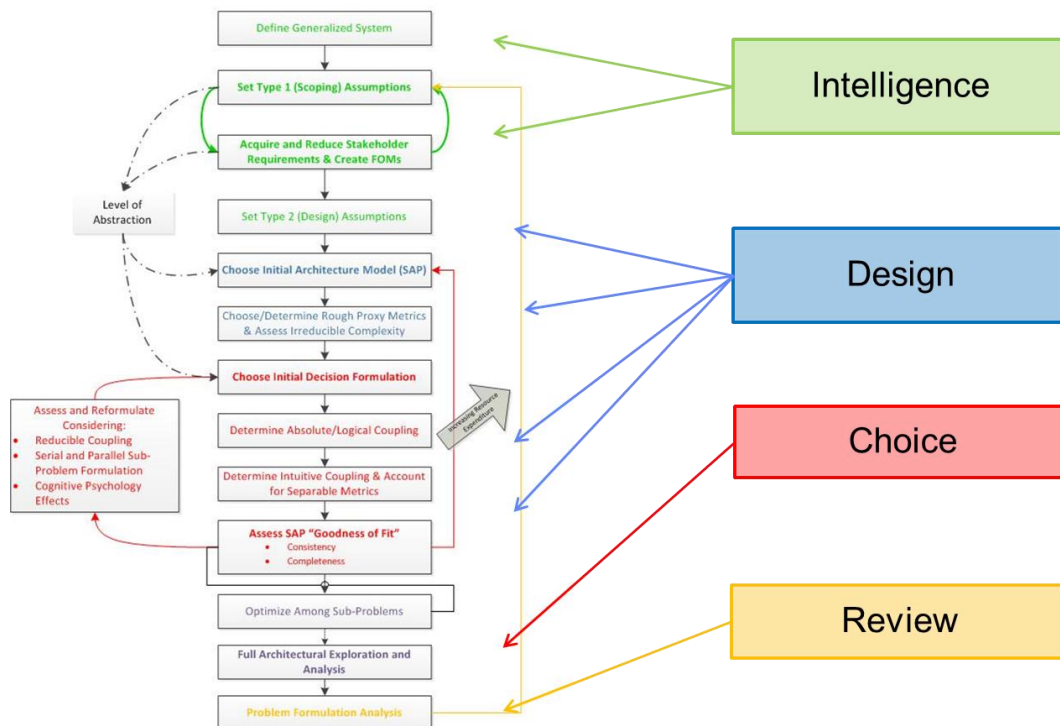


Figure 78: Comparison Between Ideological Model Building Process and Simon's Four Stages to Decision-Making

Intelligence and Design Phases

During the process of developing the ideological model, the first step is to define the system and gather the necessary information for designing the model, in this case mostly dealing with stakeholder requirements. This is much like what Simon called the *intelligence* phase, where the necessary information for the decision-making process is gathered. However, the scoping phase of the ideological model building process encompasses both the gathering and use of said information in order to down-scope the system to a manageable selection. This therefore overlaps with a part of Simon's *design* phase, where the alternative concepts are considered based on the information gathered. The ideological model building process is more directed in the use of the gathered information, and, as this is the main purpose of the ideological model building process, the majority of the steps described fall under Simon's *design* phase, including the last step of the model building process' scoping step.

Choice and Review Phases

In Simon's view, the *choice* phase is where the evaluation of the alternatives occurs. This clearly maps to the evaluation step of the model building process, and therefore is one-to-one with the phases of decision making. Similarly, the *review* phase, although not originally proposed by Simon, introduces the concept of post-processing the decision to assess the appropriateness in the context of the solution. In Simon's model, the choice has already been implemented, and so the review process is used purely for future decisions. By contrast, the ideological model building process allows for a re-assessment of the entire model, being much easier to change than most large-scale decisions to which Simon refers. Most importantly, this occurs *before* the effective implementation of the information, rather than after.

In conclusion, it has been shown that the framework proposed for the ideological model building process appropriately encompasses the phases of decision making as described by Herbert Simon, and can therefore be considered "complete" by coverage of the major phases of decision making. This holds true only under the assumption that the model building process is part of a subclass of decision-making.

5.4.2 Simmons' Four Steps

In his PhD thesis, Willard Simmons took the ideas described by Simon and developed a set of four steps to model building [14]. This process was explicitly created for framing architecture-level model construction, and therefore it is the closest match to the expanded framework herein presented. Simmons' steps are less ordered steps for designing the model itself but rather steps for consideration of tools and methods as they are applied to model building. He included the steps of

representing, structuring, simulating, and viewing, mapped to the ideological model building process in Figure 79.

Representing

Simmons did not include a step for gathering the information and scoping the problem, but he did define the *representing* step as the “methods and tools for representing the problem in a humanly understandable and computationally efficient fashion.” In effect, the ambiguity of this phrasing allows this step to be mapped to the entire model building process. However, the concept of creating a “humanly understandable” problem is reflected in the need for down-scoping to an achievable level of complexity and therefore can be mapped to sub-steps in the scoping step of the ideological model building process. Computational efficiency, as mentioned by Simmons, is more appropriately applied to the physical model building process, and therefore is not directly mapped in this case.

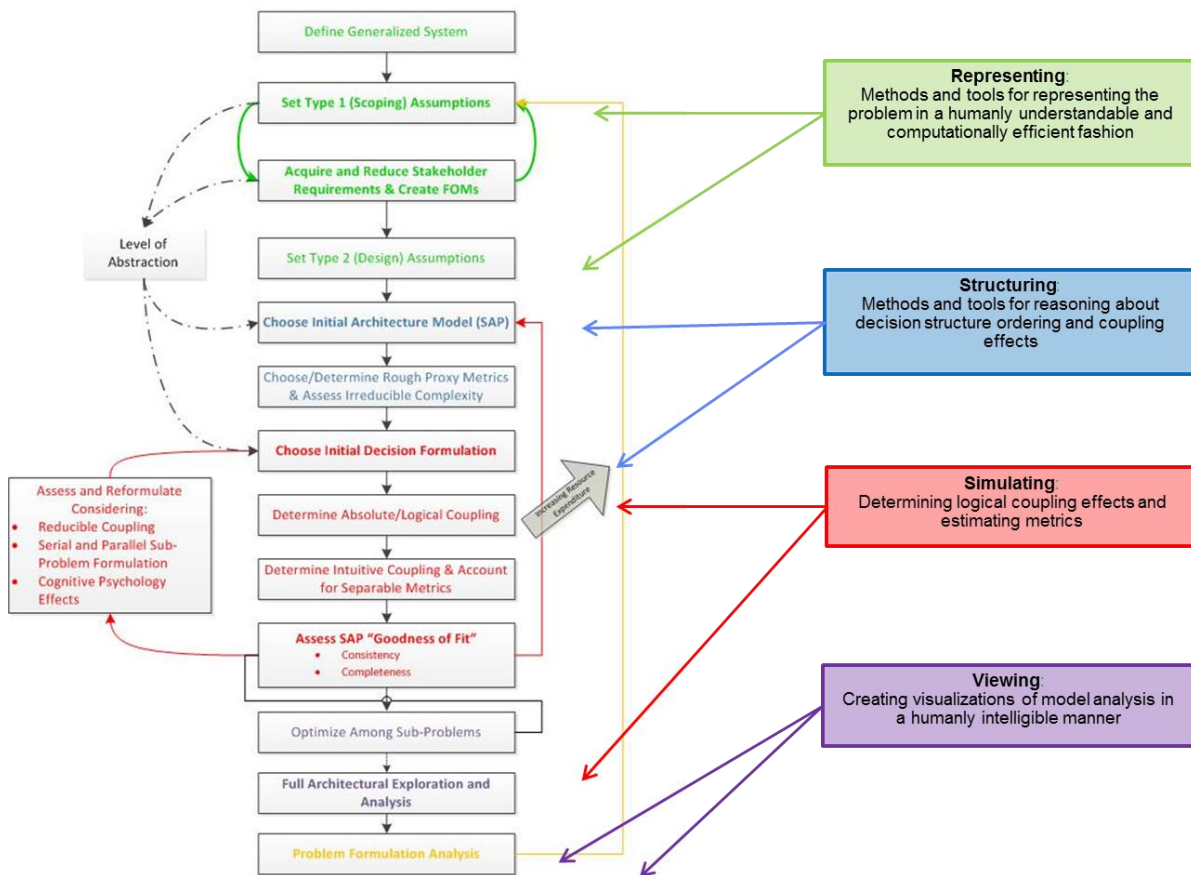


Figure 79: Comparison Between the Ideological Model Building Process and Simmons’ Four Steps to Model Building

Structuring

As defined by Simmons, the *structuring* step includes the “methods and tools for reasoning about decision structure ordering and coupling effects.” Simmons dealt exclusively with assignment problems, given their ability to combine both the ideological and physical models, and therefore directly refers to decision structures. The decision structure is directly tied with the choice of SAP, and therefore this is where the first mapping occurs. Coupling effects are considered throughout the structuring portion of the ideological model building process, and it is therefore logical to map this step to at least a portion of the structuring step of the process to Simmons’ structuring step.

Simulating

This is where Simmons described the architect as “determining the logical coupling effects and estimating metrics.” Simmons’ definition of logical coupling directly maps to the framework’s definition of absolute exclusive coupling, as they follow absolute rules of logic. Simmons identifies these coupling effects separately from the remainder of the coupling effects because they are both easily identifiable and can be used to prune the model. The *simulating* step also includes the evaluation and estimation of metrics, mapping to the step just prior to re-assessment in the ideological model building process.

Viewing

Simmons considered the way that the recipients of the results view the data as a critical part of the modeling process. This step was described as “creating visualizations of model analysis in a humanly intelligible manner.” The manipulation of the results and presentation to the users, while an important part of the job of a model architect, does not explicitly affect the way that a model is constructed. This should be a consideration during the creation of the FOMs and associated metrics, but it does not further influence the model building. Therefore, this is not considered to be mapped directly to the framework, lying beyond the scope of the evaluation and re-assessment steps.

Simmons is an influential figure in the creation of assignment problem-based models, and it is therefore important to map well with his understanding of the important aspects for architecture-level system modeling. It was shown that the three major steps dealing with the creating of the model can be mapped to portions of the ideological model building process, although Simmons also includes a further step of viewing the results in an appropriate manner that is humanly intelligible. It was also shown that there are some portions of the ideological model building process that Simmons does not, in fact, cover that have been shown to be important in the creation of new system models. Therefore, the framework, from the ideological model perspective, has adequate

coverage of the Simmons modeling method and has additional steps to benefit the architect.

5.5 ASSUMPTIONS AND LIMITATIONS

As this framework has now been shown to match well with previous frameworks, implying a level of coverage and completeness, the limitations and assumptions that reduce the applicability of the framework should be addressed. Because of the context under which this framework was derived, there are a great many assumptions and limitations in terms of the usefulness of the framework and specific model building processes presented. In general, the most appropriate application of this process is for architecture-level complex systems models with the intent of performing tradespace exploration by enumerating a set of architectures for metric-based evaluation. Despite the rather specific nature of this restriction, this framework is still applicable to a wide variety of complex systems and associated problems. The largest set of general cases for which this is applicable is for future complex system designs, where the general concept is not yet fully defined (hence the architectural level analysis) but there are well-known metrics for trading properties of the system. Areas where this is applicable include:

- Spaceflight and space systems
- Alternative energy infrastructures
- Advanced vehicle concepts
- Medical machinery
- *Etc.*

Another key assumption present in the framework is the ability to determine complex coupling relationships from known information. This is critical for the proper formulation of complex systems models in general. George Box once said that “all models are wrong, but some are useful” [115]. This certainly continues to apply to the models produced by this framework. Without having an exact replica of the system, which inherently is too complex, thus driving the use of a model, some fidelity in the underpinning relationships will be lost, as no exact analytical relationships will ever be absolutely true in real applications. This framework therefore assumes that enough information can be gathered to produce relationships that replicate the real system sufficiently for the level of analysis required.

There is also an assumption that tools and methods exist that allow for formulation in the manner directed by the model building processes. For example, some discussion was given regarding the appropriate use of mathematical regimes in the formulation of metrics. It is possible that the mathematics do not, in fact, exist that allow for the formulation desired. Prior to Newton

and Leibniz, there was no adequate mathematical language for describing curvature in graphs [116]. Likewise, there are likely to be areas of research where the desired emergent behavior cannot be analyzed with any known mathematics.

The limitations of the framework are very much tied to the assumptions described as well as the nature of complex systems. A great many complex systems exist and will exist in the future, both known and unknown, and therefore it is not the claim of the author that this framework will be appropriate for all complex systems. The known list of SAPs is likely incomplete, and the associated structuring steps are likewise limited. Furthermore, because this framework was developed in the context of architecture tradespace enumeration, it is not well-suited for use in simply describing known complex systems, beyond the use of appropriate SAP and structuring practices.

In short, this framework is most appropriate for use in architecture-level computational modeling for tradespace enumeration and evaluation of future complex systems with sufficient known internal coupling relationships. Although this is the best application of the framework, it has been shown that it covers the concepts also presented by Simon *et al* and Simmons, and therefore has at least limited applicability beyond the scope described.

5.6 CASE STUDY IN BRIEF: HOFSTETTER MANNED SPACEFLIGHT MODEL

Given the limitations on the appropriate application of the framework to architecture-level computational modeling for tradespace enumeration and evaluation of future systems, a case study within this limited scope will most appropriately demonstrate the uses of the framework. Wilfried Hofstetter's model for manned spaceflight architectures was introduced in Section 1.5.1 of Chapter 1. The existence of many external constraints implied the inefficiency of the modeling process. The simplicity of the model indicates that rework is not required for computation, thus the model remains as it is. This also implies that it is a simple enough model to use as a brief case study to show how the complexity manifested as many external constraints may be reduced through the use of the presented framework.

This case study will step through each of the extended ideological framework's sub-steps and demonstrate how the Hofstetter model is captured by the framework. The decision formulation of Hofstetter's model implies the integration of the ideological and physical models, and thus only the ideological framework is referenced, as shown in Figure 75. As the model inefficiencies arise from the original formulation, the mapping to the extended ideological model framework will show how these inefficiencies would be revealed and corrected by the framework. As a reminder of the formulation of Hofstetter's model, his morphological matrix is given in Figure 80 [16].

Number of crew transfers between vehicles	0	1	2	3	4
Number of vehicles	1	2	3		
Event 1	O	L	T		
Event 2	S	O	L	T	N
Event 3	S	O	L	T	N
Event 4	S	O	L	T	N
Event 5	S	O	L	T	N

Figure 80: Hofstetter Manned Spaceflight Model Morphological Matrix

The first step of the ideological model framework is to define the generalized system. In this case, Hofstetter was attempting to create a model for understanding manned landing systems for Moon and Mars exploration architectures. In general, however, he chose to approach it from the broader view of general Moon and Mars architectures. Step 2 of the framework is to set the scoping assumptions. To scope the architectures in order to address the underlying modeling of manned landing systems, he chose to apply the following scoping rules:

- A landing system is only the vehicle that makes contact with the destination surface while containing humans
- The launch vehicle for the architecture from Earth's surface is set
- Only habitats and human transportation elements are included in the architecture (therefore additional architecture-level elements, such as those seen in HEXANE, are not addressed)

The third step of the framework is to gather stakeholder needs and create FOMs. Hofstetter was the primary stakeholder for the model, and he was interested mainly in the cost of these systems, eventually as the cost relates to modularity and commonality of elements. In his thesis he also considers risk and performance to be key but does not address them directly.

This leads to the fourth step, setting design assumptions. This is where Hofstetter limits the options for habitat architectures and primary mission modes. Specifically, he designs his model to replicate Earth Orbit Rendezvous (EOR), Lunar Orbit Rendezvous (LOR), and Lunar Surface Rendezvous (LSR). With these limitations, the SAP selected was an assignment problem in the specific formulation of a decision problem. Although Hofstetter did not explicitly make this choice from the set of possible SAPs, he did choose to select a decision formulation from all possible problem formulations, as implied by the morphological matrix. For step six, he chose to use

IMLEO in a similar manner to the implementation in HEXANE in order to assess a basic cost measure. Also like the implementation in HEXANE, this metric is high-level separable, thus making the calculation simple at the architectural level.

Up until this point, Hofstetter's work falls well within the realm of reasonable model construction and is acceptable under the modeling framework. Step seven is the choice of decision formulation, and in this case the decisions were based on the number of crew, number of vehicles, and "events" occurring throughout the mission. Hofstetter's logic flowed approximately like this: he is interested in the habitats. The driver of mass for habitats is functionality. Functionality depends on crew activity, and crew activity relates to crew transfers. Therefore, by capturing the crew transfers in the architecture, the habitats and their mass can be assessed. This case study does not assert any conclusions about the correctness of this logic. In order to assert this, he moved on to step eight, determining absolute coupling. Here, constraints were placed on the total number of crew transfers between vehicles were allowed, along with the total number of vehicles. This is an absolute coupling, since the number of vehicles must be less than $n+1$ for n crew transfers, given that every vehicle must be used at least once.

Step nine, determining intuitive coupling, leads to the restriction of the model to include only five possible "events." In order to assess how the results of step eight and nine create model-induced complexity, the twelve rules, or constraints, that Hofstetter placed on the model are revisited below.

Rule 1: Only manned vehicles are modeled (*i.e.* vehicles with both crew and propulsion stages)

Rule 2: Every manned vehicle must be used at least once

Rule 3: For n crew transfers, the number of vehicles must be below $n+1$

Rule 4: A vehicle that the crew has used and then abandoned rests at the location where the crew last used it

Rule 5: Crew transfers on the surface can only occur after landing

Rule 6: The crew goes to the surface only once per mission and does not return

Rule 7: The vehicles are numbered in sequence of crew occupancy

Rule 8: The entire crew always stays together

Rule 9: No dedicated destination orbital space stations exist

Rule 10: No dedicated space stations in transit exist

Rule 11: Only one dedicated surface habitat is provided in every mission

Rule 12: Crew transfers in transit can only be the first and/or last crew transfer in an architecture

Not all of these rules relate to coupling relationships. Scoping assumptions lead to rules 1, 6, and 12. Design assumptions lead to rules 2, 4, 5, 8, 9, 10, and 11. Absolute coupling leads to rule

3. Rule 7 only relates to the method for numbering vehicles, and therefore it does not fit in any of these categories. Intuitive coupling leads to the limits on the total number of events in the mission.

Not all of these rules are necessary, indicating a level of modeling-induced complexity. For example, rules 2 and 8 imply rule 3. It is not necessary to apply this constraint when it is forced by other constraints separately. The assumption constraints should not be stated as constraints or rules, but rather they are implied by the model design. The implied constraints, such as the limits on total number of crew transfers, total number of vehicles, and total number of events, which derive from the decision and choice formulation, also lead to model-induced complexity. Hofstetter's analysis showed that five events were not necessary to capture all desired mission modes. Therefore there are unnecessary decisions which hold unused values. The number of vehicles and number of crew transfers should inherently reflect the constraints that couple these values. Choices of "2 vehicles with 1 crew transfer," "3 vehicles with 2 crew transfers," and "3 vehicles with 1 crew transfer" would, for instance, capture this coupling. It should be noted that this increases cognitive load while reducing complexity. Once again, the simplicity of the model means that these unnecessary design vectors caused by the constraint existing outside of the decision structure can be pruned easily. However, in a more complex model, the reduced complexity version should be considered carefully.

In short, Hofstetter's model has redundant constraints, an improper integration of constraints in the decision structure to reduce complexity, and unnecessary decisions. The model is simple enough that these factors do not have a large impact on the analysis of the resulting architectures, but larger, more complex models would suffer from these effects.

The remainder of the steps for the extended ideological model building framework are for evaluation and re-assessment. Evaluation does not reflect upon the complexity of the model beyond what has already been stated, and re-assessment cannot be addressed in hindsight. That is to say that the model presented is Hofstetter's final work, and therefore no iterations of the work can be evaluated.

5.7 FUTURE WORK

SAP Refinement

Following Selva's work [97], it is important to further refine the understanding of these System Architecting Problems and their implications on the models of complex systems. Some thought has been given to creating a hierarchy of these problems, with assignment and connecting problems likely to be of the highest level. These two types of problems can be used to model any of the other SAPs, and therefore they are of a "mother" class of SAPs. It can be mathematically shown that a set of assignment problems can be used to represent both covering and set partitioning problems,

although less efficiently and less intelligibly than their counterparts, given that it is an NP-Complete formulation [117]. The NP-completeness argument does not naturally imply a hierarchy, however, as all of the SAPs have been proven to be NP-complete. However, a simpler argument can be made. As an expert familiar with formulations with the various SAPs, it is clear how the assignment problem may be used to formulate problems that are conducive to set-partitioning, connecting, down-selecting, and permuting problems. Similarly, a formulation is easily made for a connecting formulation for each of these problems, although they typically require more constraints than assignment problem formulations. However, the same cannot be said for the remaining problem types. That is to say that it is not immediately understandable how an assignment problem would be reformulated as a series of set-partitioning problems. Although this is technically a mathematically possible transformation, it is not clear how this would occur from a non-mathematical perspective. Therefore, the “ease” of transformation implies a hierarchy to the SAPs. This would give further insight into the usefulness of the SAPs both as framing methods for models as well as their appropriate implementation in identified sub-problems.

Choosing the Correct SAP

There is no guidance given in the appropriate choice of SAP. This is partially due to the lack of complete understanding of the SAPs and their properties. However, as part of the sub-step dealing with this choice, guidance should be provided to the architect.

“Construction” Step for Alternative SAPs

Presented in this chapter was the framework for developing the ideological and physical models for assignment problem formulations. However, the steps in the construction step of the ideological model have not been defined or further considered for the remainder of the SAP classes. It is therefore left as future work.

Tying to Methods and Tools

The original goal of the framework was to both provide a framework for the creation of efficient and effective models as well as to provide a guide to the use of associated methods and tools. The latter remains to be done. These tools and methods should be tied to the specific expanded framework steps and described with additional detail on the appropriate application. These tools and methods have additional assumptions and limitations associated with them, and therefore there should have sufficient documentation to inform the model building system architects.

Validation

It has been shown how previous decision-making processes and model-building steps are mapped to the framework described. However, this is not sufficient to validate the framework as an appropriate tool. Considerable testing of the framework should be conducted to determine its usefulness and effectiveness in the creation of more efficient, effective models. One possible validation approach would be to provide two groups of systems engineers with no additional training with a complex system to model. One group would be given the framework to follow while another would design a model without the framework. However, this is highly dependent on the ability to “grade” the resulting models. A metric for resulting gratuitous and modeling-induced complexity would be necessary to effectively use this approach for validation. This case study would also have to be repeated a sufficient number of times to have statistical confidence in the validation results.

5.8 CHAPTER SUMMARY

This chapter has shown that the modeling of complex systems is, in general, a significant challenge for system architects, especially those untrained in the field. The concepts of gratuitous, modeling-induced, and essential complexity were introduced in order to assert that models are improved through the reduction of gratuitous and modeling-induced complexity while retaining essential complexity. Both the simple and expanded versions of the ideological, physical, and integrated models were presented. A classification of coupling relationships was introduced in order to show how they may be used to help formulate models. The concepts of separability and reducibility were also introduced for this purpose. A brief look at a classification of sub-problems within larger system contexts was also presented. These concepts lead to a further understanding of the expanded frameworks for ideological and physical model building.

Topics for further consideration were given, as the current frameworks are incomplete and limited. In order to assert the quality of coverage and completeness in comparison to previous frameworks, comparisons between the ideological model building framework and Simon’s four steps and Simmons’ four steps were presented. These showed that the framework captures the majority of what these prior frameworks captured, in some cases with additional capabilities and considerations beyond the previous frameworks. Further assumptions and limitations were discussed. It was asserted that the frameworks are most appropriate for architecture-level computational models for tradespace enumeration and evaluation of future complex systems with sufficient known internal coupling relationships.

A brief case study was given to show how Wilfried Hofstetter’s manned spaceflight model is captured by the model building framework and how it may have been improved by the use of the

framework. Several constraints and methods of formulations were shown to have created modeling-induced complexity, which may have been avoided with the use of the model building framework.

Finally, some areas of future work for the improvement of the frameworks were given. These included improvements to the scope of the framework as well as the integration of suggestions for methods and tools as they relate to the model. Validation of the framework through comparative modeling of systems is also suggested.

6. CONCLUSION

6.1 THESIS SUMMARY

This thesis has introduced a tool for the enumeration and analysis of the tradespace for in-space transportation infrastructures for manned space exploration missions to surface destinations. This model, referred to as HEXANE, is intended to aid in the decision process for the future of the U.S. and international manned spaceflight infrastructures by providing a method for comparing mission architecture options on a tradespace of cost-based metrics. The unique capabilities of this model to capture the primary architecture-level elements of the manned mission in-space infrastructures allow for the comparison of effects generated by the set of fundamental decisions associated with each architecture.

Detailed results for Mars conjunction-class missions are presented in Chapter 3, along with a compressed set of results for lunar, low-energy NEA, and high-energy NEA missions using HEXANE in Appendix B. A strong tension is seen between IMLEO and LCC Proxy metrics. Unique usage of architecture-level technologies and capabilities exists for each of the destinations, although a grouping of destinations based on energetic requirements emerges. Some recommendations for timing of major investment decisions are presented based on tradespace influence characteristics and qualitative assessment of robustness properties for the most highly influential architecture-level decisions.

An additional tool for the enumeration and analysis of precursor demonstration sub-missions, drawing from the results of HEXANE, was proposed in Chapter 4. The grouping of demonstrable technologies and capabilities for the sequence of sub-missions was considered, along with the use of low-energy Lagrange points in conjunction with final destinations for precursor sub-missions. A set of cumulative and peak metrics were provided to assess both campaign-level properties as well as individual sub-mission properties. A tension between Peak IMLEO, a proxy for operating costs, and Cumulative LCC, a proxy for total development and procurement costs, was revealed, indicating a trade between total mass-based operating costs and individual mission demonstration risk. Lunar and low-energy NEA missions were shown to have similar general tradespace properties for all metrics.

A framework for the guided modeling of complex systems was presented. The framework was shown to be design explicitly to aid in the reduction of gratuitous and modeling-induced complexity. A generalized framework named the Funnel Model was proposed. The model combines the process of creating the ideological model, used for understanding the complex system in question on a human level, along with the physical model, used for computing the properties of

the complex system. Expanded frameworks are given for creation of both the ideological model and the physical model. A case study was presented to qualitatively assert the advantages of following the guidelines of the framework in comparison to unguided modeling processes.

6.2 PRIMARY CONTRIBUTIONS

6.2.1 Methodology and Tool Contributions

This thesis has presented a set of three tools to aid in decision analysis for manned exploration missions to surface destinations beyond Earth orbit. Specifically:

- It **introduced a model for the enumeration and analysis of the in-space transportation infrastructure portion of manned exploration missions beyond LEO**, based on a unique functional decomposition leading to the use of multiple set partitioning problems in an overarching assignment problem formulation. The model describes the architecture-level design of individual exploration missions, including a set of high-level technologies and a description of habitat and propulsion element functional allocation.
- It **proposed a model for the enumeration and analysis of precursor demonstration sub-mission sequences**, which develop technologies and capabilities needed for high science value surface missions. The grouping of technologies and capabilities into the precursor sub-mission sequences is assessed, along with the use of low-energy Lagrange points as precursor sub-mission destinations.
- It **formulated a framework for the development of architecture-level complex system models**, specifically with the goal of reducing gratuitous and modeling-induced complexity in these complex system models. The generalized Funnel Framework was introduced, along with the full frameworks for the creation of ideological models and physical models.

These tools were each demonstrated for specific use cases. Mars results were analyzed in depth from the HEXANE tool, along with a brief overview of missions to the Moon and NEAs. Low-E results were given for lunar and low-energy NEA missions. A case study was performed using the Funnel Framework to demonstrate the gains from using the model development framework in comparison to unstructured model creation.

6.2.2 Analysis Findings

The analysis performed for both HEXANE and Low-E is summarized below:

HEXANE

- For Mars mission architectures, eight decisions were identified as being potentially highly impactful in comparison to the full set of ten decisions. These included:
 - The general use of cryogenic propellants
 - The development and use of cryogenic boil-off control
 - The use of Nuclear Thermal Rockets
 - The use of Solar-Electric Propulsion-based low-thrust pre-deployment
 - The use of ablative aerocapture at Mars and Earth
 - The use of in-space oxygen and methane propellant
 - The use of MPCV-like capsules
 - The use of monolithic and semi-monolithic habitats
- Of the eight decisions identified, ablative aerocapture, SEP pre-deployment, and the use of NTR were found to have the greatest influence on architecture mass across the set of analysis methods. Semi-monolithic habitats and cryogenic boil-off control were also found to have moderately high influence levels, with mixed results depending on the analysis method used to assess decision influence.
- NTR was found to heavily influence the mass for Mars missions but not absolutely necessary to design missions with a total mass of less than 900mt.
- The use of MPCV-like capsules were found in 84% of all mass constrained architectures, indicating that the forced use of an MPCV in Mars architectures does not eliminate a large portion of the available tradespace.
- Four decision couplings were identified as having potentially significant influences on architecture mass for Mars surface missions. These included:
 - LOX/LH₂ with Boil-off Control without ISRU as a mass-increasing effect
 - LOX/LH₂ and LOX/LCH₄ in combination as a mass-increasing effect
 - NTR, LOX/CH₄, and ISRU in combination as a mass-decreasing effect
 - Semi-monolithic habitats with ISRU as a mass-decreasing effect
- Use of Technology Influence Coupling Effects analysis identified several strong coupling relationships for decisions for Mars architectures, both among the expected set and outside of the expected set. These included:
 - Semi-monolithic habitats and ablative aerocapture as a strong mass-decreasing effect

- Semi-monolithic habitats and ISRU as a strong mass-decreasing effect
- NTR with LOX/CH₄ and ISRU as a strong mass-decreasing effect
- LOX/LH₂ and boil-off control as a mass-increasing effect
- LOX/CH₄, NTR, and LOX/LH₂ in combination as a strong mass-increasing effect
- The set of non-dominated architectures in the IMLEO-LCC Proxy space were identified for Mars, Moon, and NEA missions, including the minimum IMLEO and minimum LCC mission architectures.
- Two general classes of missions were identified from the set of Mars, Moon, and both NEA analysis. Low-energy architectures, for lunar and low-energy NEA missions, tend to employ multi-stage hydrogen propulsion elements with semi-monolithic habitat arrangements. High-energy architectures, for Mars and high-energy NEA missions, tend to include the use of NTR stages and semi-monolithic habitat arrangements.

Low-E

- Striations in the Peak IMLEO metric for both lunar and low-energy NEA results indicate that multiple size classes of launch vehicles may be beneficial for use in precursor sub-mission sequences.
- Tension between Cumulative IMLEO and Peak LCC for both lunar and low-energy NEA results indicates a trade between total operational cost and individual sub-mission demonstration risk for the sequence of sub-missions.
- Non-dominated architectures in the Cumulative IMLEO – Peak LCC tradespace favor front loading of technologies and capabilities for demonstration in both lunar and low-energy NEA cases. This occurs despite the impact on mission demonstration risk as manifested in the Peak LCC metric. Flat funding allocation and the need for consistent mission return may drive the demonstration sub-mission sequence away from this formulation, however.
- Lunar demonstration sub-mission sequences favor repeated use of the lunar surface as a demonstration destination after an initial low-energy Lagrange point sub-mission in the Cumulative IMLEO – Peak LCC tradespace.
- Low-energy NEA demonstration sub-mission sequences favor repeated use of low-energy Lagrange point demonstrations prior to the final NEA mission in the Cumulative IMLEO – Peak LCC tradespace.

6.3 FUTURE WORK

The future work for expanding and improving the tools and concepts presented in this thesis

can be divided by the tools for which they are relevant. The future work is therefore divided into sections for HEXANE, Low-E, and the Funnel Model.

6.3.1 HEXANE Refinement

Habitat Sizing Parametrics

HEXANE is heavily dependent on the information on which the internal calculations are based. Although the functional decomposition and method for the creation of in-space architectures is well established, the data and sizing methods for the build-up of the architectures may be improved with refined information. Of the sizing methods implemented in the model, the most debated is the habitat sizing parametric for hard shell habitats. Although the most current sizing methods are present in the model, there are many factors that contribute the overall sizing of habitats, and it remains unclear whether or not a generic sizing parametric is applicable to the entire set of situations. For example, the atmosphere (*i.e.* pressure, gas mix, etc.) selection for the habitat has a significant effect on the necessary structural requirements, but different use cases drive variations of the atmosphere selection. One may optimize the atmosphere for application in a surface habitat, but that would radically change if that habitat also had to rendezvous and dock with other habitable volumes or pressurized environments. This is only one consideration amongst many for the proper design of space habitats, and it may become necessary to use higher fidelity information to size the habitats in general. More importantly, it is imperative to understand how these relationships change with changes in the allocated sub-functions to each habitat. A deeper study into the details of habitat design and the elements that affect mass at the architecture level should be conducted. The changes in these elements as functions are combined in habitats should also be studied in order to appropriately integrate these relationships into the habitat sizing methodology.

Inflatable Habitats

One emerging technology with potential to greatly impact the mass requirements of manned spaceflight missions is inflatable habitats. These were not included in the work presented in this thesis due to the lack of current information for the sizing and use of these habitats. However, as they become more developed and the sizing of these habitats becomes understood, they should be included as alternative structures for many of the habitat options.

Logistics Sizing Parametric

The rate of consumables intake is currently based on a JPL estimation tool. This can be assumed to be correct at this level of fidelity. However, the sizing methodology for the containment of the logistics mass is currently very crude. Further work should be done to characterize the mass requirements for containment, both in terms of packaging material as well as the hard-shell or

inflatable containment units as attached or integrated into habitat elements.

Aerocapture and EDL Shielding

Both ablative aerocapture and EDL shielding estimates are based on paper studies that estimate the mass of said shielding based on significant assumptions. Although these are currently the best estimates available, there are many concerns about the applicability of the sizing methods and the extrapolation into the regimes being considered in this thesis (*i.e.* 150+ mt, manned-rated vehicles). Further, more detailed analysis should be conducted to verify the applicability in HEXANE.

SEP Sizing

Currently, the solar electric propulsion elements are sized based on early studies by NASA. These estimates are also based on recent research into Xenon-based SEP engines. As the technology progresses, the sizing methods for these elements should be updated to reflect new information. Furthermore, the estimation method for deriving the energetic requirements for the low-thrust trajectories is crude by comparison to other tools and methods employed by NASA. The methodology employed in this model, which can be seen in further detail in Appendix A, assumes a planar circular restricted low-thrust spiral, while more robust methods require numerical integration of low-thrust pathways. This method should be refined in conjunction with updating the methods for the sizing of pre-deployment elements.

Power Systems Sizing

Currently, HEXANE incorporates the mass of power systems into the habitat elements. However, power systems are typically integrated into the whole system of habitats in order to eliminate redundant mass. Furthermore, a range of technologies can be employed to reduce the mass of these power systems or buy down risk associated with nuclear sources. This is true both for in-space power systems as well as surface power systems. Particularly, assumptions are made regarding the use of nuclear fission plants for ISRU on Mars and the Moon. These generic assumptions may not hold for all architectural arrangements described by the model.

Sensitivity Analysis

Although the model has been validated against several vetted paper models and an historical case, the validation process raised some concerns regarding the sensitivity of the results to certain parameters, such as energetic requirements and parametric coefficients. Part of the issue in this regard is the running time of the model in order to assemble sufficient data for sensitivity analysis. In the long run, however, such analysis should be used to inform decision makers about the

influence of parameters in the model on the results. Specific values for which sensitivity analysis would be most helpful include: ΔV values, TOF values, number of crew, mass of additional payloads, propellant properties, and spares percentages.

Additional Metrics

The addition of risk and complexity metrics for assessing the quality of architectures as they relate to cost would be highly beneficial. Results indicating the benefit of semi-monolithic habitats, for instance, would likely be heavily influenced by measures of risk and complexity. However, these metrics typically rely on high fidelity information and are therefore difficult to integrate into a low granularity model. An understanding of the scheduling and phasing of the missions produced by the model, either in relation to the timing of the infrastructure or launch schedule, would also add a dimension currently not captured. Furthermore, an understanding of how the elements of the architectures would be integrated into a launch system, both in terms of mass and volume requirements, would be greatly beneficial to decisions concerning the future manned spaceflight infrastructure.

Refinement of Influence Measures

Chapter 3 described several measures of influence for individual decisions related to the design of mission architectures. However, each was shown to have flaws and limitations that could lead to misinterpretation of results. Measures of influence should be established that avoid this misinterpretations in order to effectively translate the technical outputs of the manned spaceflight model to the decision analysis domain.

Multi-Mission Campaigns

A serious limitation of the HEXANE model is the inability to create a sequence of missions. In reality, it is likely that multiple missions would be performed in sequence, making up a total campaign. This is partially reliant on the commonality of mission elements to enable multiple missions without the redevelopment of mission assets. HEXANE assumes that each mission will be individually optimized, but a campaign of missions would likely trade individual mission performance for campaign-level attributes. Furthermore, some technologies that positively influence missions at the campaign level should be integrated into such an analysis. These technologies could include dedicated on-orbit assembly platforms, fuel depots, and permanent propellant production plants. In general, these technologies and resources are too costly to implement for a single mission, but their benefits can be seen when a sequence of missions is implemented. This analysis could also include the temporal dimension for the scheduling of missions. In addition, the campaign-level study should leverage the results from both HEXANE and

Low-E in order to take advantage of previously derived multi-level data.

6.3.2 Low-E Refinement

Low-E draws from the capabilities of HEXANE, and so most of the refinements described in Section 6.3.1 also apply to Low-E. However, the results presented in Chapter 4 do not provide the same level of detail as results presented in Chapter 3. As such, two primary areas of refinement for Low-E also emerge.

Understanding Trends

Several trends were identified during the Low-E analysis, particularly in the Cumulative IMLEO versus Cumulative LCC plots. Some description of these trends was given, but the underlying cause of the groupings of sub-mission sequences were not analyzed in depth. Further analysis should be performed to understand the driving parameters behind the groupings seen.

Integration of Science Return

As part of the precursor sub-mission sequence, some importance is placed on returning science value for each mission in addition to demonstrating technologies and capabilities. The Low-E model makes the assumption that several low-energy non-surface destinations can be estimated to be equivalent to missions to EM-L1. However, repeated mission to this Lagrange point do not necessarily return the best science value while carrying out technology demonstrations. The integration of science return as part of the metrics package would increase the usefulness of the Low-E outputs.

6.3.3 Funnel Framework Development

Integration of Systems Architecting Methods and Tools

The framework described in Chapter 5 is still in an infantile state. Although many of the primary concepts are described, much work should be done to further develop the concept into a useable tool. Particularly, the methods and tools associated with systems architecting should be described in relation to the steps described in both parts of the framework. The framework was originally conceived to include all such tools and methods and act as a guide for architects to build complex system models without many of the pitfalls normally encountered. By integrating these methods and tools, much of the additional work associated with understanding the intricacies of systems architecting can be eliminated for the on-and-off system architect.

Case Study Validation

Furthermore, case studies should be performed to understand how the framework compares with other techniques, particularly in quantifying the advantages of the framework over unguided complex system model creation. Such a case study could involve the architecting of a previously-established model, where two groups of untrained engineers are given the system to model. One group may be given the framework and limited training on its use, while the other attempts to create a system model without the use of the framework. Unfortunately, this also requires the establishment of “goodness” metrics that measure the quality of a complex system model. It is likely that the two groups would create substantially different models, and a way to quantify their differences would have to be established. Rough metrics about the number of outside constraints may reveal the amount of modeling-induced complexity. However, these metrics would also need to be established and vetted prior to any comparative studies.

Integration into the Larger Context

The Funnel Framework should also be understood in how it integrates into the larger context of systems design and development. For different types of systems, this integration will be substantially changed by the context. For example, complex software systems may be incorporated into a software development spiral model, while vehicle design may integrate better into a waterfall design model. In order to be accepted and integrated into industry applications, the framework requires a clear and easy integration into larger industry system design and development contexts.

BIBLIOGRAPHY

- [1] NASA, "Space Shuttle," 2013. [Online]. Available: http://www.nasa.gov/mission_pages/shuttle/main/index.html.
- [2] NASA, "Constellation Program," 2011. [Online]. Available: http://www.nasa.gov/mission_pages/constellation/main/index2.html.
- [3] P. Committee, "Seeking a human spaceflight program worthy of a great nation," 2009.
- [4] B. Obama, "National Space Policy of the United States of America." 2010.
- [5] NASA, "Orion: America's New Spacecraft for Human Exploration," 2013. [Online]. Available: <http://www.nasa.gov/exploration/systems/mpcv/index.html>.
- [6] NASA, "NASA Fiscal Year 2011 Budget Estimates," 2011.
- [7] NASA, "Beyond Earth: Expanding Human Presence into the Solar System," 2013. [Online]. Available: <http://www.nasa.gov/exploration/systems/sls/>.
- [8] NASA, "Commercial Crew & Cargo," 2013. [Online]. Available: http://www.nasa.gov/offices/c3po/partners/ccdev_info.html.
- [9] NASA, "International Space Station: Commercial Resupply Launch," 2013. [Online]. Available: http://www.nasa.gov/mission_pages/station/structure/launch/index.html.
- [10] T. Al-Khatib, "Keeping Space Enthusiasm Going Strong," *news.discovery.com*, 2012. [Online]. Available: <http://news.discovery.com/space/space-exploration-mars-enthusiasm-120904.htm>.
- [11] M. W. Maier and E. Reichtin, *The Art of Systems Architecting*. CRC Press, 2000, p. 313 p.
- [12] E. Reichtin, *Systems Architecting: Creating and Building Complex Systems*. Prentice Hall, 1991, p. 352.
- [13] E. Crawley, O. De Weck, S. Eppinger, C. Magee, J. Moses, W. Seering, J. Schindall, D. Wallace, and D. Whitney, "ENGINEERING SYSTEMS MONOGRAPH: THE Influence of Architecture in Engineering Systems," 2004.
- [14] W. L. Simmons, "A Framework for Decision Support in Systems Architecting," Massachusetts Institute of Technology, 2008.
- [15] "Combinatorial Explosion," *Principia Cybernetica Web*, 2011. [Online]. Available: http://pespmc1.vub.ac.be/ASC/COMBIN_EXPLO.html.

- [16] W. Hofstetter, “Extensible Modular Landing Systems for Human Moon and Mars Exploration,” Technische Universitat Munchen, 2004.
- [17] B. G. Drake, “Design Reference Architecture 5.0,” 2009.
- [18] H. Price, A. Hawkins, and T. Radcliffe, “Austere Human Missions to Mars,” *AIAA SPACE 2009 Conference & Exposition*, pp. 1–20, Sep. 2009.
- [19] D. Willson and J. D. A. Clarke, “A Practical Architecture for Exploration-Focused Manned Mars Missions Using Chemical Propulsion , Solar Power Generation and In-Situ Resource Utilisation .,” no. 1, 2006.
- [20] R. M. Zubrin and D. B. Weaver, “Practical methods for near-term piloted Mars missions,” *Journal of the British Interplanetary Society*, pp. 1–20, 1993.
- [21] NASA, *Human Exploration of Mars : The Reference Mission of the NASA Mars Exploration Study Team*, no. July. Houston, TX: , 1997.
- [22] B. G. Drake, “Reference Mission Version 3 . 0 Addendum to the Human Exploration of Mars : The Reference Mission of the NASA Mars Exploration Study Team,” no. June, 1998.
- [23] NASA, “NASA’s Exploration Systems Architecture Study: Final Report,” 2005.
- [24] ESA, “European Mars Missions Architecture Study: Executive Summary,” 2002.
- [25] ESA, “CDF Study Report: Human Missions to Mars - Overall Architecture Assessment,” 2004.
- [26] Boeing and NASA, “CE&R CA-1 Final Review,” 2005.
- [27] NASA, “The Vision for Space Exploration,” no. February. 2004.
- [28] ISECG, “The Global Exploration Roadmap,” 2011.
- [29] C. Culbert, “Human Space Flight Architecture Team (HAT) Overview,” no. November. 2011.
- [30] ESA, “NEODyS-2: 2000SG344,” 2011. [Online]. Available: <http://newton.dm.unipi.it/neody2/index.php?pc=1.1.0&n=2000SG344>.
- [31] ESA, “NEODyS-2: (341843) 2008EV5,” 2012. [Online]. Available: <http://newton.dm.unipi.it/neody2/index.php?pc=1.1.0&n=341843>.

- [32] NASA, “WMAP: The Lagrange Points,” 2012. [Online]. Available: http://map.gsfc.nasa.gov/mission/observatory_12.html.
- [33] M. Buck and B. Lawson, “Development of a Building Elevator System,” 2003. [Online]. Available: <http://www.isr.umd.edu/~austin/ense621.d/projects04.d/project-elevator.html>.
- [34] I. Sommerville, “Software engineering (7th edition),” *Engineering*, p. 784, 2004.
- [35] R. Helmer, A. Yassine, and C. Meier, “Systematic module and interface definition using component design structure matrix,” *Journal of Engineering Design*, vol. 21, no. 6, pp. 647–675, Dec. 2010.
- [36] T. R. Browning, “Applying the design structure matrix to system decomposition and integration problems: a review and new directions,” *IEEE Transactions on Engineering Management*, vol. 48, no. 3, pp. 292–306, 2001.
- [37] E. Crawley, “ESD.34 - System Architecture Lecture Series.” Cambridge, MA, 2012.
- [38] NASA, “NASA SPACE FLIGHT HUMAN SYSTEM STANDARD VOLUME 1 : CREW HEALTH,” vol. 1. pp. 1–68, 2007.
- [39] NASA, “NASA SPACE FLIGHT HUMAN-SYSTEM STANDARD VOLUME 2 : HUMAN FACTORS , HABITABILITY , AND ENVIRONMENTAL HEALTH,” vol. 2. pp. 1–194, 2011.
- [40] NASA, “International Space Station: Environmental Control and Life Support System.” 2008.
- [41] R. A. Brualdi, *Introductory Combinatorics*, 4th ed. Pearson Education, 2004.
- [42] M. Wachs and D. White, “p, q-Stirling numbers and set partition statistics,” *Journal of Combinatorial Theory, Series A*, vol. 46, pp. 27–46, 1991.
- [43] P. Erdős, A. Máté, A. Hajnal, and P. Rado, *Combinatorial Set Theory: Partition Relations for Cardinals: Partition Relations for Cardinals*. Elsevier, 2011, p. 347.
- [44] NASA HAT, “Technology Development Assessment Team (aka TechDev Team): Cycle 2011-C Summary Brief.” Cambridge, MA, 2011.
- [45] NASA HAT, “Technology ‘TechDev One-Pagers’, Rev. G.” Cambridge, MA, 2011.
- [46] Center for Creative Thinking, “Morphological Matrix.” 2005.

- [47] W. J. Larson and J. R. Wertz, *Space Mission Analysis and Design*. Kluwer Academic Publishers, 1999, p. 791.
- [48] “Skylab,” *Encyclopedia Astronautica*. [Online]. Available: <http://www.astronautix.com/craft/skylab.htm>.
- [49] NASA, “International Space Station: Space Station Assembly - Destiny Laboratory,” 2012. [Online]. Available: http://www.nasa.gov/mission_pages/station/structure/elements/destiny.html.
- [50] NASA, “Factors Impacting Habitable Volume Requirements : Results from the 2011 Habitable Volume Workshop,” 2011.
- [51] B. A. and Electronics, “Space Transfer Concepts and Analysis for Exploration Missions: Second Quarterly Review,” 1990.
- [52] NASA, “National Aeronautics and Space Administration HUMAN INTEGRATION DESIGN HANDBOOK.” 2010.
- [53] J. A. Samareh and D. R. Komar, “Parametric Mass Modeling for Mars Entry, Descent and Landing System Analysis Study,” vol. 0, 2010.
- [54] D. Hulett, *Integrated Cost-Schedule Risk Analysis (Ebk - Epub) (Google eBook)*. Gower Publishing, Ltd., 2012, p. 240.
- [55] J. A. Battat, “Technology and Architecture : Informing Investment Decisions for the Future of Human Space Exploration by,” 2012.
- [56] NASA, “Ideal Rocket Equation.” [Online]. Available: <http://exploration.grc.nasa.gov/education/rocket/rktpow.html>.
- [57] P. R. Smith, “Athena Mars Exploration Rovers: Mars Facts - Launch Window: The Perfect Space in Time,” 2005. [Online]. Available: http://athena.cornell.edu/mars_facts/sb_launch_window.html.
- [58] NASA HAT, “HAT Cycle-C Draft Briefing for MIT.” Cambridge, MA, 2011.
- [59] M. Schaffer, “A Study of CPS Stages for Missions beyond LEO,” no. May. pp. 1–62, 2012.
- [60] NASA, “ESAS Report Chapter 4: Lunar Architecture.”
- [61] D. Pettit, “The Tyranny of the Rocket Equation,” 2012. [Online]. Available: http://www.nasa.gov/mission_pages/station/expeditions/expedition30/tyranny.html.

- [62] NASA, “International Space Station: Facts and Figures,” 2012. [Online]. Available: http://www.nasa.gov/mission_pages/station/main/onthestation/facts_and_figures.html.
- [63] G. F. Dubos, J. H. Saleh, and R. Braun, “Technology Readiness Level, Schedule Risk, and Slippage in Spacecraft Design,” *Journal of Spacecraft and Rockets*, vol. 45, no. 4, pp. 836–842, Jul. 2008.
- [64] H. E. McCurdy, *The Space Station Decision: Incremental Politics and Technological Choice*, vol. 2. JHU Press, 2007, p. 290.
- [65] R. N. Charette, “Large-Scale Project Management is Risk Management,” *IEEE*, no. July 1996, 1994.
- [66] NASA, “Orion Quick Facts.” .
- [67] F. Diep, “Nuclear-Powered Rocket Could Reach Mars for Less,” *TechNewsDaily*, 2013. [Online]. Available: <http://www.technewsdaily.com/16587-nuclear-thermal-rocket-petition.html>.
- [68] R. Allen, M. B., C. T., K. Shipley, and S. Howe, “Nuclear and Emerging Technologies for Space (2012).” 2012.
- [69] R. Braun, “Office of the Chief Technologist Town Hall Meeting Themes of the President's FY11 NASA Budget Request,” pp. 1–33, 2010.
- [70] W. H. Robbins and H. B. Finger, “An historical perspective of the NERVA nuclear rocket engine technology program,” *Test*, 1991.
- [71] “NERVA (Nuclear Engine for Rocket Vehicle Application),” *The Encyclopedia of Science*. .
- [72] B. Fishbine, Ro. Hanrahan, S. Howe, R. Malenfant, C. Scherer, H. Sheinberg, and O. Ramos Jr., “Nuclear Rockets: To Mars and Beyond,” 2011. [Online]. Available: http://www.lanl.gov/science/NSS/issue1_2011/story4full.shtml.
- [73] J. Dankanich, *Low-thrust Propulsion Technologies, Mission Design, and Application*, no. January. 2010.
- [74] S. Roy, “For Fuel Conservation in Space, NASA Engineers Prescribe Aerocapture,” 2006. [Online]. Available: <http://www.nasa.gov/vision/universe/features/aerocapture.html>.
- [75] A. M. D. Cianciolo, J. L. Davis, D. R. Komar, M. M. Munk, J. A. Samareh, J. A. Williamsbyrd, T. A. Zang, R. W. Powell, J. D. Shidner, D. O. Stanley, A. W. Wilhite, J. O. Arnold, A. R. Howard, and E. G. Llama, “Entry , Descent and Landing Systems Analysis Study : Phase 1 Report,” no. July, 2010.

- [76] R. Mead, *The Design of Experiments: Statistical Principles for Practical Applications*. Cambridge University Press, 1990, p. 620.
- [77] “EMPIRE Aeronutronic,” *Encyclopedia Astronautica*. 2001.
- [78] “Von Braun Mars Expedition,” *Encyclopedia Astronautica*. .
- [79] R. Zubrin and D. Baker, “Mars direct: humans to the red planet by 1999,” *Acta Astronautica*, vol. 26, no. 12, pp. 899–912, 1992.
- [80] P. J. Boston, *AAS Science and Technology Series Volume 57, Proceedings of The Case for Mars I*. 1984.
- [81] J. Hoffman, J. Logsdon, and L. Mcglynn, “The Future of Human Spaceflight.” 2008.
- [82] ESA, “Lunar Lander: Human Spaceflight and Exploration,” 2013. [Online]. Available: http://www.esa.int/Our_Activities/Human_Spaceflight/Lunar_Lander.
- [83] JAXA, “SELenological and ENgineering Explorer ‘KAGUYA’ (SELENE),” 2010. [Online]. Available: http://www.jaxa.jp/projects/sat/selene/index_e.html.
- [84] NASA, “Space Exploration Vehicle Concept.” 2012.
- [85] R. W. Farquhar, D. W. Dunham, Y. Guo, and J. V McAdams, “Utilization of libration points for human exploration in the Sun–Earth–Moon system and beyond,” *Acta Astronautica*, vol. 55, no. 3–9, pp. 687–700, Aug. 2004.
- [86] NASA, “Office of the Chief Technologist: Game Changing Technology,” 2012. [Online]. Available: http://www.nasa.gov/offices/oct/stp/game_changing_development/game_changing_technology.html.
- [87] J. Katriel, “Bell numbers and coherent states,” *Physics Letters A*, no. August, pp. 159–161, 2000.
- [88] E. F. Shumacher, *Small is Beautiful - Economics as if People Really Mattered*. London: Harper & Row, 1973, p. 352.
- [89] Complex Systems Society, “About Complex Systems,” 2013. [Online]. Available: <http://www.complexssociety.eu/aboutComplexSystems.html>.
- [90] C. Ormand, “What Constitutes a Complex System,” 2010. [Online]. Available: <http://serc.carleton.edu/NAGTWorkshops/complexsystems/introduction.html>.

- [91] J. Sterman, "Learning in and about complex systems," *System Dynamics Review*, vol. 10, no. February, pp. 291–330, 1994.
- [92] Aristotle, *Metaphysics*. Cambridge, MA: Harvard University Press, 1933.
- [93] R. M. Soley, "SysML & Industry: Improving Systems Engineering." 2011.
- [94] J. E. ALBRECHT and E. J. O'BRIEN, "Updating a mental model: maintaining both local and global coherence," *Journal of experimental psychology. Learning, memory, and cognition*, vol. 19, no. 5, pp. 1061–1070.
- [95] P. W. Cheng and K. J. Holyoak, "Pragmatic reasoning schemas.," *Cognitive psychology*, vol. 17, no. 4, pp. 391–416, Oct. 1985.
- [96] Z. Varvasovszky, "Review article Stakeholder analysis : a review," vol. 15, no. 3, pp. 239–246, 2000.
- [97] D. S. Valero, "Rule-Based System Architecting of Earth Observation Satellite Systems," Massachusetts Institute of Technology, 2012.
- [98] R. Burkard, M. Dell'Amico, and S. Martello, *Assignment Problems*, vol. 6, no. 3–4. Society for Industrial and Applied Mathematics, 2009, p. 382.
- [99] T. Biggerstaff, B. Mitbender, and D. Webster, "Program Understanding and the Concept Assignment Problem," *Communications of the ACM*, vol. 37, no. 5, 1994.
- [100] J. E. Lighter, *Random House Dictionary of American Slang*, 1st ed. Random House, 1997.
- [101] "Figure of Merit," *Merriam-Webster Dictionary*. [Online]. Available: [http://www.merriam-webster.com/dictionary/figure of merit](http://www.merriam-webster.com/dictionary/figure%20of%20merit).
- [102] B. Boehm, "A spiral model of software development and enhancement," *Computer*, vol. 21, no. 5, pp. 61–72, 1988.
- [103] "Coupling," *American Heritage Dictionary of the English Language*, 2009. [Online]. Available: <http://www.thefreedictionary.com/coupling>.
- [104] D. Halliday, R. Resnick, and J. Walker, *Fundamentals of Physics*, vol. 8th. Wiley, 2008, p. 1136.
- [105] B. Henderson-Sellers, *On the Mathematics of Modelling, Metamodeling, Ontologies and Modelling Languages (Google eBook)*. Springer, 2012, p. 106.
- [106] A. M. Ross and D. E. Hastings, "The Tradespace Exploration Paradigm," *INCOSE*, 2005.

- [107] *Multidisciplinary Design Optimization: State of the Art ; Proceedings of the ICASE NASA Langley Workshop on Multidisciplinary Design Optimization, Hampton, Virginia, March 13 - 16, 1995.* SIAM, 1997, p. 455.
- [108] R. J. Gerrig and P. G. Zimbardo, "Glossary of Psychological Terms," *Psychology and Life*, 2002. [Online]. Available: <http://www.apa.org/research/action/glossary.aspx>.
- [109] J. V. McConnell and D. W. Gorenflo, "The Most Frequently Cited Journal Articles and Authors in Introductory Psychology Textbooks," *Teaching of Psychology*, vol. 18, no. 1, 1991.
- [110] G. a Miller, "The magical number seven, plus or minus two: some limits on our capacity for processing information. 1956.," *Psychological review*, vol. 101, no. 2, pp. 343–52, Apr. 1956.
- [111] E. N. Lorenz, *The essence of chaos*. University of WASHINGTON Press, 1995, p. 227.
- [112] H. Simon, "Autobiography," 1978. [Online]. Available: http://www.nobelprize.org/nobel_prizes/economics/laureates/1978/simon-autobio.html.
- [113] H. A. Simon, G. B. Dantzig, R. Hogarth, C. R. Plott, T. C. Schelling, K. A. Shepsle, R. Thaler, A. Tversky, and B. George, "Decision Making and Problem Solving," *Interfaces*, vol. 17, no. 5, pp. 11–31, 1987.
- [114] H. A. Simon, *The New Science of Management Decision*. Prentice-Hall, 1977.
- [115] G. E. P. Box and N. R. Draper, *Empirical Model-Building and Response Surfaces*. Wiley, 1987, p. 669.
- [116] R. Larson and B. H. Edwards, *Calculus*. Cengage Learning, 2009, p. 1142.
- [117] M. R. Garey and D. S. Johnson, *Computers and Intractability: A Guide to the Theory of NP-Completeness (Series of Books in the Mathematical Sciences)*. W. H. Freeman, 1979, p. 340.
- [118] R. Falck and J. Dankanich, "Optimization of Low-Thrust Spiral Trajectories by Collocation," no. August, pp. 1–17, 2012.
- [119] NASA GRC, "Group Projects: In-Space Propulsion," 2013. [Online]. Available: <http://trajectory.grc.nasa.gov/projects/lowthrust.shtml>.
- [120] L. Kos, T. Polsgrove, R. Hopkins, D. Thomas, and J. Sims, "Overview of the Development for a Suite of Low-Thrust Trajectory Analysis Tools," *AIAA/AAS Astrodynamics Specialist Conference and Exhibit*, Aug. 2006.

- [121] X. Hellin and P. Perola, "Study of Earth-to-Mars Transfers with Low-Thrust Propulsion Project Report," 2011.
- [122] R. W. Humble, G. N. Henry, and W. J. Larson, *Space Propulsion Analysis and Design*, First. The McGraw-Hill Companies, Inc., 1995, pp. 518–519.
- [123] NASA JPL, "Sky Crane," 2013. [Online]. Available: <http://mars.jpl.nasa.gov/msl/mission/technology/in situexploration/edl/skycrane/>.
- [124] C. Doornkamp and V. Ponc, "The universal character of the Mars and Van Krevelen mechanism," *Journal of Molecular Catalysis A: Chemical*, vol. 162, no. 1–2, pp. 19–32, Nov. 2000.
- [125] G. Jacobs and B. H. Davis, "Reverse water-gas shift reaction: steady state isotope switching study of the reverse water-gas shift reaction using in situ DRIFTS and a Pt/ceria catalyst," *Applied Catalysis A: General*, vol. 284, no. 1–2, pp. 31–38, Apr. 2005.
- [126] B. D. & S. Group, "Space Transfer Concepts and Analysis for Exploration Missions."
- [127] W. J. Larson and L. K. Pranke, *Human spaceflight: mission analysis and design*. McGraw-Hill, 2000, p. 1035.
- [128] K. Laurini and J. Connolly, "Altair Lunar Lander Development Status: Enabling Lunar Exploration," *International Astronautics Congress*, 2009.

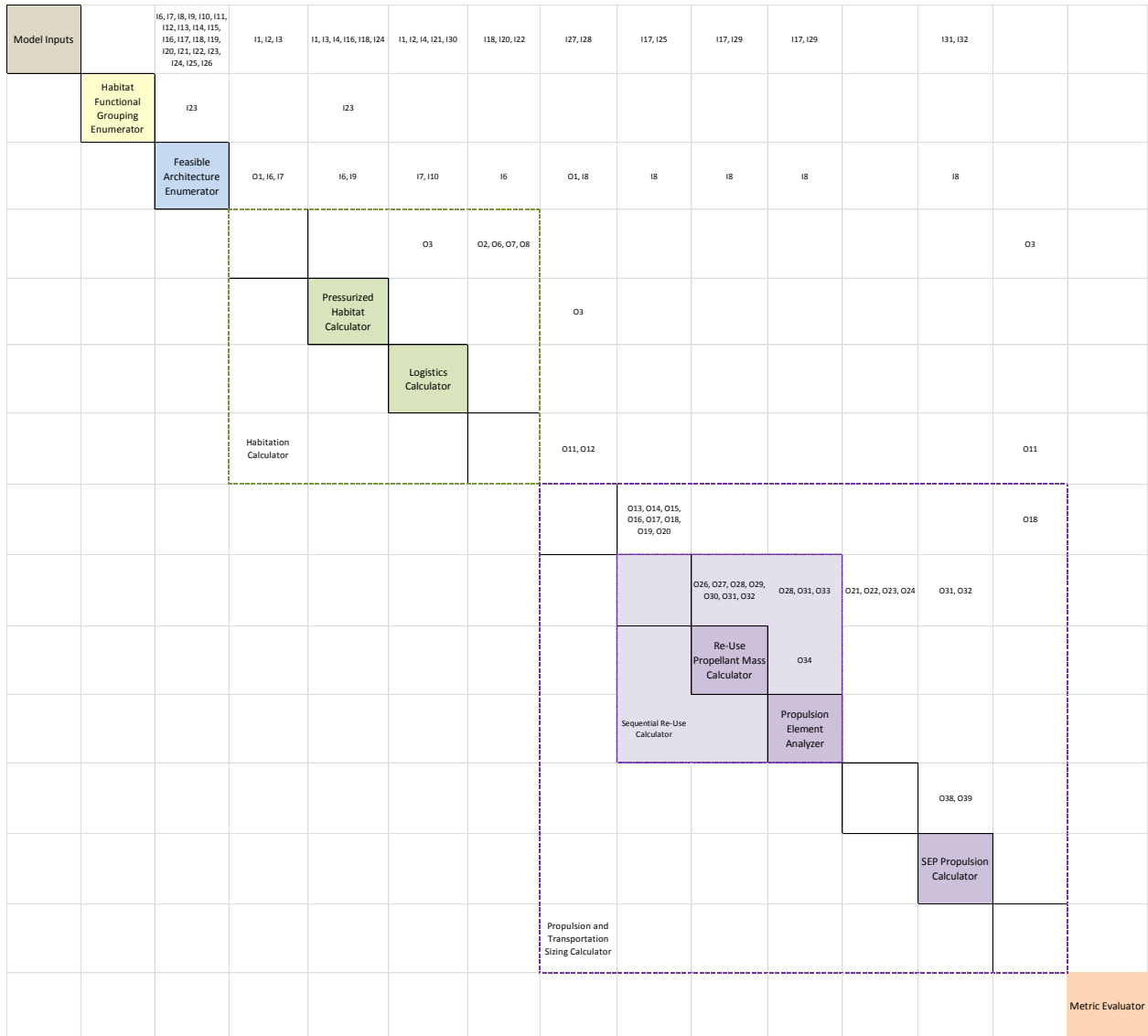
APPENDIX A: Additional HEXANE Information

A-1: Parameter Database

Input/Definition	Input ID	Input Description	Variable Name	Units	Sub-Module	Sub-Module	Module	Output ID	Output Description	Output Name	Units	Parameter Relationship
parameter	11	Number of Crew	num_crew	%				11	Number of Crew	num_crew	%	
parameter	12	Heat shield characteristic (TPS mass per entry mass)	Heat_Shield	kg/kg				12	Heat shield characteristic (TPS mass per entry mass)	Heat_Shield	kg/kg	
parameter	13	Surface static part (percentage of mass on destination surface)	Surf_Static_Pct	%				13	Surface static part (percentage of mass on destination surface)	Surf_Static_Pct	%	
parameter	14	Total consumables mass per person per day	Conm_mss_rate	kg				14	Total consumables mass per person per day	Conm_mss_rate	kg	
parameter	15	Solar collector efficiency	Eff	%				15	Solar collector efficiency	Eff	%	
parameter	16	Habitat elements properties array	Hab_Prop_Array	-				16	Habitat elements properties array	Hab_Prop_Array	-	Taken from InSpace_Master_Excel
parameter	17	Logistics properties array	Log_Prop_Array	-				17	Logistics properties array	Log_Prop_Array	-	Taken from InSpace_Master_Excel
parameter	18	Reduced propulsion properties array	Prop_Array	-				18	Reduced propulsion properties array	Prop_Array	-	Taken from InSpace_Master_Excel
parameter	19	Habitat element regression array	Hab_Reg_Array	-				19	Habitat element regression array	Hab_Reg_Array	-	Taken from InSpace_Master_Excel
parameter	20	Logistics regression array	Log_Reg_Array	-				20	Logistics regression array	Log_Reg_Array	-	Taken from InSpace_Master_Excel
parameter	21	Habitat element regression array	Hab_Reg_Array	-				21	Habitat element regression array	Hab_Reg_Array	-	Taken from InSpace_Master_Excel
parameter	22	Logistics regression array	Log_Reg_Array	-				22	Logistics regression array	Log_Reg_Array	-	Taken from InSpace_Master_Excel
parameter	23	Mission profile degenerator	Mission_Deleg	-				23	Mission profile degenerator	Mission_Deleg	-	Aggregated from input and enumerated properties
parameter	24	Destination surface degenerator	Dest_Deleg	-				24	Destination surface degenerator	Dest_Deleg	-	
parameter	25	Intermediate staging locations list	Inter_Stage	-				25	Intermediate staging locations list	Inter_Stage	-	
parameter	26	Earth return staging locations list	Earth_Stage	-				26	Earth return staging locations list	Earth_Stage	-	
parameter	27	Earth return staging locations list	Earth_Stage	-				27	Earth return staging locations list	Earth_Stage	-	
parameter	28	Duration of stay on destination surface	ISRU	days				28	Duration of stay on destination surface	ISRU	days	
parameter	29	Heat shield characteristic (TPS mass per entry mass)	Heat_Shield	kg/kg				29	Heat shield characteristic (TPS mass per entry mass)	Heat_Shield	kg/kg	
parameter	30	Landing cycle (number of days between possible launches from LEO)	Landing_Cycle	days				30	Landing cycle (number of days between possible launches from LEO)	Landing_Cycle	days	
parameter	31	Habitat set partition allocation	Habitat_Set	kg				31	Habitat set partition allocation	Habitat_Set	kg	
parameter	32	Decayed payload on high energy stack	Dec_Pay	kg				32	Decayed payload on high energy stack	Dec_Pay	kg	
parameter	33	Habitat set partition allocation	Habitat_Set	kg				33	Habitat set partition allocation	Habitat_Set	kg	
parameter	34	Pre-Deployment choice	Predep	-				34	Pre-Deployment choice	Predep	-	
parameter	35	Pre-Deployment choice	Predep	-				35	Pre-Deployment choice	Predep	-	
parameter	36	Pre-Deployment choice	Predep	-				36	Pre-Deployment choice	Predep	-	
parameter	37	Pre-Deployment choice	Predep	-				37	Pre-Deployment choice	Predep	-	
parameter	38	Pre-Deployment choice	Predep	-				38	Pre-Deployment choice	Predep	-	
parameter	39	Pre-Deployment choice	Predep	-				39	Pre-Deployment choice	Predep	-	
parameter	40	Pre-Deployment choice	Predep	-				40	Pre-Deployment choice	Predep	-	
parameter	41	Pre-Deployment choice	Predep	-				41	Pre-Deployment choice	Predep	-	
parameter	42	Pre-Deployment choice	Predep	-				42	Pre-Deployment choice	Predep	-	
parameter	43	Pre-Deployment choice	Predep	-				43	Pre-Deployment choice	Predep	-	
parameter	44	Pre-Deployment choice	Predep	-				44	Pre-Deployment choice	Predep	-	
parameter	45	Pre-Deployment choice	Predep	-				45	Pre-Deployment choice	Predep	-	
parameter	46	Pre-Deployment choice	Predep	-				46	Pre-Deployment choice	Predep	-	
parameter	47	Pre-Deployment choice	Predep	-				47	Pre-Deployment choice	Predep	-	
parameter	48	Pre-Deployment choice	Predep	-				48	Pre-Deployment choice	Predep	-	
parameter	49	Pre-Deployment choice	Predep	-				49	Pre-Deployment choice	Predep	-	
parameter	50	Pre-Deployment choice	Predep	-				50	Pre-Deployment choice	Predep	-	
parameter	51	Pre-Deployment choice	Predep	-				51	Pre-Deployment choice	Predep	-	
parameter	52	Pre-Deployment choice	Predep	-				52	Pre-Deployment choice	Predep	-	
parameter	53	Pre-Deployment choice	Predep	-				53	Pre-Deployment choice	Predep	-	
parameter	54	Pre-Deployment choice	Predep	-				54	Pre-Deployment choice	Predep	-	
parameter	55	Pre-Deployment choice	Predep	-				55	Pre-Deployment choice	Predep	-	
parameter	56	Pre-Deployment choice	Predep	-				56	Pre-Deployment choice	Predep	-	
parameter	57	Pre-Deployment choice	Predep	-				57	Pre-Deployment choice	Predep	-	
parameter	58	Pre-Deployment choice	Predep	-				58	Pre-Deployment choice	Predep	-	
parameter	59	Pre-Deployment choice	Predep	-				59	Pre-Deployment choice	Predep	-	
parameter	60	Pre-Deployment choice	Predep	-				60	Pre-Deployment choice	Predep	-	
parameter	61	Pre-Deployment choice	Predep	-				61	Pre-Deployment choice	Predep	-	
parameter	62	Pre-Deployment choice	Predep	-				62	Pre-Deployment choice	Predep	-	
parameter	63	Pre-Deployment choice	Predep	-				63	Pre-Deployment choice	Predep	-	
parameter	64	Pre-Deployment choice	Predep	-				64	Pre-Deployment choice	Predep	-	
parameter	65	Pre-Deployment choice	Predep	-				65	Pre-Deployment choice	Predep	-	
parameter	66	Pre-Deployment choice	Predep	-				66	Pre-Deployment choice	Predep	-	
parameter	67	Pre-Deployment choice	Predep	-				67	Pre-Deployment choice	Predep	-	
parameter	68	Pre-Deployment choice	Predep	-				68	Pre-Deployment choice	Predep	-	
parameter	69	Pre-Deployment choice	Predep	-				69	Pre-Deployment choice	Predep	-	
parameter	70	Pre-Deployment choice	Predep	-				70	Pre-Deployment choice	Predep	-	
parameter	71	Pre-Deployment choice	Predep	-				71	Pre-Deployment choice	Predep	-	
parameter	72	Pre-Deployment choice	Predep	-				72	Pre-Deployment choice	Predep	-	
parameter	73	Pre-Deployment choice	Predep	-				73	Pre-Deployment choice	Predep	-	
parameter	74	Pre-Deployment choice	Predep	-				74	Pre-Deployment choice	Predep	-	
parameter	75	Pre-Deployment choice	Predep	-				75	Pre-Deployment choice	Predep	-	
parameter	76	Pre-Deployment choice	Predep	-				76	Pre-Deployment choice	Predep	-	
parameter	77	Pre-Deployment choice	Predep	-				77	Pre-Deployment choice	Predep	-	
parameter	78	Pre-Deployment choice	Predep	-				78	Pre-Deployment choice	Predep	-	
parameter	79	Pre-Deployment choice	Predep	-				79	Pre-Deployment choice	Predep	-	
parameter	80	Pre-Deployment choice	Predep	-				80	Pre-Deployment choice	Predep	-	
parameter	81	Pre-Deployment choice	Predep	-				81	Pre-Deployment choice	Predep	-	
parameter	82	Pre-Deployment choice	Predep	-				82	Pre-Deployment choice	Predep	-	
parameter	83	Pre-Deployment choice	Predep	-				83	Pre-Deployment choice	Predep	-	
parameter	84	Pre-Deployment choice	Predep	-				84	Pre-Deployment choice	Predep	-	
parameter	85	Pre-Deployment choice	Predep	-				85	Pre-Deployment choice	Predep	-	
parameter	86	Pre-Deployment choice	Predep	-				86	Pre-Deployment choice	Predep	-	
parameter	87	Pre-Deployment choice	Predep	-				87	Pre-Deployment choice	Predep	-	
parameter	88	Pre-Deployment choice	Predep	-				88	Pre-Deployment choice	Predep	-	
parameter	89	Pre-Deployment choice	Predep	-				89	Pre-Deployment choice	Predep	-	
parameter	90	Pre-Deployment choice	Predep	-				90	Pre-Deployment choice	Predep	-	
parameter	91	Pre-Deployment choice	Predep	-				91	Pre-Deployment choice	Predep	-	
parameter	92	Pre-Deployment choice	Predep	-				92	Pre-Deployment choice	Predep	-	
parameter	93	Pre-Deployment choice	Predep	-				93	Pre-Deployment choice	Predep	-	
parameter	94	Pre-Deployment choice	Predep	-				94	Pre-Deployment choice	Predep	-	
parameter	95	Pre-Deployment choice	Predep	-				95	Pre-Deployment choice	Predep	-	
parameter	96	Pre-Deployment choice	Predep	-				96	Pre-Deployment choice	Predep	-	
parameter	97	Pre-Deployment choice	Predep	-				97	Pre-Deployment choice	Predep	-	
parameter	98	Pre-Deployment choice	Predep	-				98	Pre-Deployment choice	Predep	-	
parameter	99	Pre-Deployment choice	Predep	-				99	Pre-Deployment choice	Predep	-	
parameter	100	Pre-Deployment choice	Predep	-				100	Pre-Deployment choice	Predep	-	
parameter	101	Pre-Deployment choice	Predep	-				101	Pre-Deployment choice	Predep	-	
parameter	102	Pre-Deployment choice	Predep	-				102	Pre-Deployment choice	Predep	-	
parameter	103	Pre-Deployment choice	Predep	-				103	Pre-Deployment choice	Predep	-	
parameter	104	Pre-Deployment choice	Predep	-				104	Pre-Deployment choice	Predep	-	
parameter	105	Pre-Deployment choice	Predep	-				105	Pre-Deployment choice	Predep	-	
parameter	106	Pre-Deployment choice	Predep	-				106	Pre-Deployment choice	Predep	-	
parameter	107	Pre-Deployment choice	Predep	-				107	Pre-Deployment choice	Predep	-	
parameter	108	Pre-Deployment choice	Predep	-				108	Pre-Deployment choice	Predep	-	
parameter	109	Pre-Deployment choice	Predep	-				109	Pre-Deployment choice	Predep	-	
parameter	110	Pre-Deployment choice	Predep	-				110	Pre-Deployment choice	Predep	-	
parameter	111	Pre-Deployment choice	Predep	-				111	Pre-Deployment choice	Predep	-	
parameter	112	Pre-Deployment choice	Predep	-				112	Pre-Deployment choice	Predep	-	
parameter	113	Pre-Deployment choice	Predep	-				113	Pre-Deployment choice	Predep	-	
parameter	114	Pre-Deployment choice	Predep	-				114	Pre-Deployment choice	Predep	-	
parameter	115	Pre-Deployment choice	Predep	-				115	Pre-Deployment choice	Predep	-	
parameter	116	Pre-Deployment choice	Predep	-				116	Pre-Deployment choice	Predep	-	
parameter	117	Pre-Deployment choice	Predep	-				117	Pre-Deployment choice	Predep	-	
parameter	118	Pre-Deployment choice	Predep	-				118	Pre-Deployment choice	Predep	-	
parameter	119	Pre-Deployment choice	Predep	-				119	Pre-Deployment choice	Predep	-	
parameter	120	Pre-Deployment choice	Predep	-				120	Pre-Deployment choice	Predep	-	
parameter	121	Pre-Deployment choice	Predep	-				121	Pre-Deployment choice	Predep	-	
parameter	122	Pre-Deployment choice	Predep	-				122	Pre-Deployment choice	Predep	-	
parameter	123	Pre-Deployment choice	Predep	-				123	Pre-Deployment choice	Predep	-	
parameter	124	Pre-Deployment choice	Predep	-				124	Pre-Deployment choice	Predep	-	
parameter	125	Pre-Deployment choice	Predep	-				125	Pre-Deployment choice	Predep	-	
parameter	126	Pre-Deployment choice	Predep	-				126	Pre-Deployment choice	Predep	-	
parameter	127	Pre-Deployment choice	Predep	-				127	Pre-Deployment choice	Predep	-	
parameter	128	Pre-Deployment choice	Predep	-				128	Pre-Deployment choice	Predep	-	
parameter	129	Pre-Deployment choice	Predep	-				129	Pre-Deployment choice	Predep	-	
parameter	130	Pre-Deployment choice	Predep	-				130	Pre-Deployment choice	Predep	-	
parameter	131	Pre-Deployment choice	Predep	-				131	Pre-Deployment choice	Predep	-</	

01	Array of feasible architectures	Feasible_Arch	-					
02	Habitat element properties array	Habitat_Prop_Arry	-					
03	Number of Crew	num_crew	-					
04	Same parts percentage of total mass	Same_Perc	%					
05	Surface same parts percentage of mass on destination surface	Surf_Same_Perc	%					
06	Number of Crew	num_crew	-					
07	Habitat set partition allocation	Habit_Set	-					
08	Habitat pre-deployment scheme	Habit_Prep	-					
09	Habitat element properties array	Habit_Prop_Arry	-					
10	Habitat element properties array	Habit_Prop_Arry	-					
11	Same parts percentage of total mass on destination surface	Surf_Same_Perc	%					
12	Heat shield characteristic (TPS mass per entry mass)	Heat_Shield	kg/kg					
13	Duration of stay on destination surface	Stay_Dur	days					
14	Total consumables mass per person per day	Con_Mass_Perc	kg					
15	Number of Crew	num_crew	-					
16	Logistics regression array	Log_Reg_Arry	-					
17	Logistics regression array on light energy/stark	Log_Reg_Arry	kg					
18	Logistics regression array	Log_Reg_Arry	kg					
19	Total Consumables Mass Consumption per Day	Con_Mass_Perc	kg/day					
20	Same Parts Percentage of Total Mass	Same_Perc	%					
21	Time of Flight array	TOF_DSM1	days					
22	Habitat mass array	Habit_Mass	kg					
23	Habitat element total volume	Habit_Tot_Vol	m ³					
24	Habitat element properties array	Habit_Prop_Arry	-					
25	Unpressurized logistics volume	Unpress_Log_Vol	m ³					
26	Unpressurized logistics volume	Unpress_Log_Vol	m ³					
27	Logistics mass	Log_Mass	kg					
28	Descended payload on light energy stark	Desc_Pay	kg					
29	Heat shield characteristic (TPS mass per entry mass)	Heat_Shield	kg/kg					
30	Mass of pre-deployed cargo (in addition to habitats or propulsion)	PreDeploy_Cargo	kg					
31	Arrival delta V DSM	dt_Arrival	m/s					
32	Propulsion delta V DSM	dt_Propulsion	m					
33	Array of feasible architectures	Feasible_Arch	-					
34	Dry mass array	Dry_Mass_Arry	kg					
35	Reduced propellant properties array	Prop_Arry	kg					
36	Habitat mass array	Habit_Mass	kg					
37	Non-habitat mass array	NonHabit_Mass	kg					
38	Delta V array for specific architectures	dt_Arrival	m/s					
39	Vector of masses for reaction maneuver	dt_Arrival	m					
40	Vector of propellant mass for each of maneuver	Prop_Mass_Arry	kg					
41	Array determining which transportation elements carry which others	Trans_Carry_Mass	logical					
42	In-Situ Resource Utilization indicator	ISRU	logical					
43	Transportation set partition allocation	Trans_Part	-					
44	Propulsion elements mass array	Prop_Elem_Mass	kg					
45	Range of elements for calculation	range	-					
46	Additional propellant element mass carried by evaluated element	elem_and	kg					
47	Reduced masses array	prop_elem_mass	kg					
48	Initial propellant mass guess	prop_elem_mass	kg					
49	Initial propellant mass guess	prop_elem_mass	kg					
50	Time of flight array in months	TOF_mos	months					
51	Propellant masses	masses	kg					
52	Reduced masses array	prop_elem_mass	kg					
53	Index of 0V maneuvers for propulsion element	elem_idx	-					
54	Reduced propellant mass carried by evaluated element	prop_elem_mass	kg					
55	Initial propellant mass guess	prop_elem_mass	kg					
56	Initial propellant mass guess	prop_elem_mass	kg					
57	Time of flight array in months	TOF_mos	months					
58	Propellant masses	masses	kg					
59	Reduced masses array	prop_elem_mass	kg					
60	Index of 0V maneuvers for propulsion element	elem_idx	-					
61	Reduced propellant mass carried by evaluated element	prop_elem_mass	kg					
62	Initial propellant mass guess	prop_elem_mass	kg					
63	Initial propellant mass guess	prop_elem_mass	kg					
64	Time of flight array in months	TOF_mos	months					
65	Propellant masses	masses	kg					
66	Reduced masses array	prop_elem_mass	kg					
67	Index of 0V maneuvers for propulsion element	elem_idx	-					
68	Reduced propellant mass carried by evaluated element	prop_elem_mass	kg					
69	Initial propellant mass guess	prop_elem_mass	kg					
70	Initial propellant mass guess	prop_elem_mass	kg					
71	Time of flight array in months	TOF_mos	months					
72	Propellant masses	masses	kg					
73	Reduced masses array	prop_elem_mass	kg					
74	Index of 0V maneuvers for propulsion element	elem_idx	-					
75	Reduced propellant mass carried by evaluated element	prop_elem_mass	kg					
76	Initial propellant mass guess	prop_elem_mass	kg					
77	Initial propellant mass guess	prop_elem_mass	kg					
78	Time of flight array in months	TOF_mos	months					
79	Propellant masses	masses	kg					
80	Reduced masses array	prop_elem_mass	kg					
81	Index of 0V maneuvers for propulsion element	elem_idx	-					
82	Reduced propellant mass carried by evaluated element	prop_elem_mass	kg					
83	Initial propellant mass guess	prop_elem_mass	kg					
84	Initial propellant mass guess	prop_elem_mass	kg					
85	Time of flight array in months	TOF_mos	months					
86	Propellant masses	masses	kg					
87	Reduced masses array	prop_elem_mass	kg					
88	Index of 0V maneuvers for propulsion element	elem_idx	-					
89	Reduced propellant mass carried by evaluated element	prop_elem_mass	kg					
90	Initial propellant mass guess	prop_elem_mass	kg					
91	Initial propellant mass guess	prop_elem_mass	kg					
92	Time of flight array in months	TOF_mos	months					
93	Propellant masses	masses	kg					
94	Reduced masses array	prop_elem_mass	kg					
95	Index of 0V maneuvers for propulsion element	elem_idx	-					
96	Reduced propellant mass carried by evaluated element	prop_elem_mass	kg					
97	Initial propellant mass guess	prop_elem_mass	kg					
98	Initial propellant mass guess	prop_elem_mass	kg					
99	Time of flight array in months	TOF_mos	months					
100	Propellant masses	masses	kg					
101	Reduced masses array	prop_elem_mass	kg					
102	Index of 0V maneuvers for propulsion element	elem_idx	-					
103	Reduced propellant mass carried by evaluated element	prop_elem_mass	kg					
104	Initial propellant mass guess	prop_elem_mass	kg					
105	Initial propellant mass guess	prop_elem_mass	kg					
106	Time of flight array in months	TOF_mos	months					
107	Propellant masses	masses	kg					
108	Reduced masses array	prop_elem_mass	kg					
109	Index of 0V maneuvers for propulsion element	elem_idx	-					
110	Reduced propellant mass carried by evaluated element	prop_elem_mass	kg					
111	Initial propellant mass guess	prop_elem_mass	kg					
112	Initial propellant mass guess	prop_elem_mass	kg					
113	Time of flight array in months	TOF_mos	months					
114	Propellant masses	masses	kg					
115	Reduced masses array	prop_elem_mass	kg					
116	Index of 0V maneuvers for propulsion element	elem_idx	-					
117	Reduced propellant mass carried by evaluated element	prop_elem_mass	kg					
118	Initial propellant mass guess	prop_elem_mass	kg					
119	Initial propellant mass guess	prop_elem_mass	kg					
120	Time of flight array in months	TOF_mos	months					
121	Propellant masses	masses	kg					
122	Reduced masses array	prop_elem_mass	kg					
123	Index of 0V maneuvers for propulsion element	elem_idx	-					
124	Reduced propellant mass carried by evaluated element	prop_elem_mass	kg					
125	Initial propellant mass guess	prop_elem_mass	kg					
126	Initial propellant mass guess	prop_elem_mass	kg					
127	Time of flight array in months	TOF_mos	months					
128	Propellant masses	masses	kg					
129	Reduced masses array	prop_elem_mass	kg					
130	Index of 0V maneuvers for propulsion element	elem_idx	-					
131	Reduced propellant mass carried by evaluated element	prop_elem_mass	kg					
132	Initial propellant mass guess	prop_elem_mass	kg					
133	Initial propellant mass guess	prop_elem_mass	kg					
134	Time of flight array in months	TOF_mos	months					
135	Propellant masses	masses	kg					
136	Reduced masses array	prop_elem_mass	kg					
137	Index of 0V maneuvers for propulsion element	elem_idx	-					
138	Reduced propellant mass carried by evaluated element	prop_elem_mass	kg					
139	Initial propellant mass guess	prop_elem_mass	kg					
140	Initial propellant mass guess	prop_elem_mass	kg					
141	Time of flight array in months	TOF_mos	months					
142	Propellant masses	masses	kg					
143	Reduced masses array	prop_elem_mass	kg					
144	Index of 0V maneuvers for propulsion element	elem_idx	-					
145	Reduced propellant mass carried by evaluated element	prop_elem_mass	kg					
146	Initial propellant mass guess	prop_elem_mass	kg					
147	Initial propellant mass guess	prop_elem_mass	kg					
148	Time of flight array in months	TOF_mos	months					
149	Propellant masses	masses	kg					
150	Reduced masses array	prop_elem_mass	kg					
151	Index of 0V maneuvers for propulsion element	elem_idx	-					
152	Reduced propellant mass carried by evaluated element	prop_elem_mass	kg					
153	Initial propellant mass guess	prop_elem_mass	kg					
154	Initial propellant mass guess	prop_elem_mass	kg					
155	Time of flight array in months	TOF_mos	months					
156	Propellant masses	masses	kg					
157	Reduced masses array	prop_elem_mass	kg					
158	Index of 0V maneuvers for propulsion element	elem_idx	-					
159	Reduced propellant mass carried by evaluated element	prop_elem_mass	kg					
160	Initial propellant mass guess	prop_elem_mass	kg					
161	Initial propellant mass guess	prop_elem_mass	kg					
162	Time of flight array in months	TOF_mos	months					
163	Propellant masses	masses	kg					
164	Reduced masses array	prop_elem_mass	kg					
165	Index of 0V maneuvers for propulsion element	elem_idx	-					
166	Reduced propellant mass carried by evaluated element	prop_elem_mass	kg					
167	Initial propellant mass guess	prop_elem_mass	kg					
168	Initial propellant mass guess	prop_elem_mass	kg					
169	Time of flight array in months	TOF_mos	months					
170	Propellant masses	masses	kg					
171	Reduced masses array	prop_elem_mass	kg					
172	Index of 0V maneuvers for propulsion element	elem_idx	-					
173	Reduced propellant mass carried by evaluated element	prop_elem_mass	kg					
174	Initial propellant mass guess	prop_elem_mass	kg					
175	Initial propellant mass guess	prop_elem_mass	kg					
176	Time of flight array in months	TOF_mos	months					
177	Propellant masses	masses	kg					
178	Reduced masses array	prop_elem_mass	kg					
179	Index of 0V maneuvers for propulsion element	elem_idx	-					
180	Reduced propellant mass carried by evaluated element	prop_elem_mass	kg					
181	Initial propellant mass guess	prop_elem_mass	kg					

A-2: Expanded Functional Block Diagram



See the parameter database for information on the parameters, *i.e.* the off-diagonal elements.

A-3: Assumptions List

Category	Assumption	Source	Value
General - Architectural	Destinations are hard bodies (planets, asteroids, and planet satellites)		Moon, Mars, Phobos/Daemos, NEA
	Lagrange points are operational staging locations only		
	All missions are sortie-like (no long-term presence intended), no deployed elements across missions		
	All supplied not needed past any operational staging point are discarded		
	All materials assumed to be capable of launch into LEO (decoupled from launch vehicle architecture)		
	Launch vehicle capacity to LEO		105 mt
General - Parameter	Ground-up calculation growth margin	HAT documentation	30%
	Historical regression parametric modeling growth margin		0%
	Number of crew	HAT documentation, user input	[4]
	Mass of crew		75 kg
	Sizing based on maximum fairing diameter of SLS		7 m
Destination Specific	Available trajectory types		
	Useable intermediate locations	user input	EML1, EML2, SEL1, SEL2
	Surface stay duration	user input	
	Low thrust ΔV	Planar, circular-restricted model	
	Deployed science payload and volume	user input	
Logistics	Spare parts mass fraction for in-space	SpaceNet	10%
	Spare parts mass fraction on destination surface	DRM studies	5%
	Mass of consumables per day per crew	JPL 7.9.07 Model	2.883 kg/crew/day
	Volume-based mass and power regression for pressurized logistics	Orbital Cygnus, ISS MPLM	
	Volume-based mass and power regression for unpressurized logistics	ESP-2, Express Logistics Carrier	
Propulsion - General	No multiple tank staging, except NTR drop tanks		
	Constant dry mass fraction		
	SEP only used for pre-deployed cargo		
Chemical Propulsion	Isp	HAT, NASA	
	Mass fraction	HAT, NASA	
	Propellant boil-off rates	user input, Delta IV stage info.	
	Arrival/Departure ΔVs	various	
Solar Electric Propulsion	Overall specific mass (kg/W)	HAT documentation	0.0394
	Power per module	HAT documentation	43 W
	Propellant	HAT documentation	Xe
	Power conversion efficiency	HAT documentation	99% (direct drive)
	Exit velocity of propellant	Reverse engineered from HAT (estimate)	17 km/s
	Isp	HAT documentation	2000 s
	Single fault tolerance	HAT documentation	
	Structure will be able to withstand acceleration requirements for pre-deployment		
TOF for pre-deployment	Planar, circular-restricted model		
Nuclear Propulsion	nuclear thermal rockets	DRA 5.0	
	Power system with radiation shield mass	DRA 5.0	41.7 mt
	LH2 Propellant with zero boiloff control	DRA 5.0	
	Mass fraction for LH2 tank	DRA 5.0-derived	0.13
	Isp	DRA 5.0	950 s (advanced)
	Thrust	DRA 5.0	25 k-lbf

Habitats - General	7 core functions always performed		launch, Earth outbound, descent, surface stay, ascent, Earth inbound, Earth entry
	two primary trajectories for habitats to be deployed upon		fast/high energy (for crewed stack), slow/low energy/low thrust (pre-deployment)
	when combining functional elements into single formal elements, the total mass is taken to be the largest of the functional masses		
Deep Space Habitat	Volume-based mass regression for DSH based on space station historical data Mass does not include logistics (spare parts, consumables)	HAT documentation, ISS USOS, ISS Destiny, Skylab	regression, 55% total volume is habitable
Launch Vehicle	Orion MPCV		8.6mt
Descent Vehicle	Entry System EDL mass fraction does not include propellant	Samareh and Komar	regression
Surface Habitat	No ISRU for NEAs		
	kg / m ³ / crew mass regression	DRA 5.0, Austere, DRM 3.0, Mars-Oz	35
	TPS mass fraction Surface spare mass	Samareh and Komar	regression 5%
Ascent Vehicle	Even if combined vehicle, always abandon TPS HIDH Volume	NASA HIDH	
Earth Entry Vehicle	Per person mass sizing	Apollo-era US and Russian capsules	regression
	EDL mass fraction	Apollo-era US and Russian capsules	integrated into regression
	If alone, Orion MPCV		8.6mt
Operations	Always use LEO as re-entry staging location Destinations always have an orbital staging location (when available)		
Metrics - Habitat Mass	For habitation forms with more than one habitation function, assign the form the mass of the most massive function		
Metrics - Chemical Propulsion Mass	Prop_Mass*(1+mass_fraction); Not assuming any mass for RCS propulsion (which is assumed in Cycle B)		
Metrics - Chemical Propulsion Volume	Assume volume of Cyro-Stage in HAT Cycle B, scale for propulsion size; change what propulsion mass is used for control / no control. Eventually will need to think about how to scale this for different propellants, but that is not included yet. Also need a better estimate for ascent/landing tanks because this one is not a very good analogy right now--but Cycle B didn't have that.	HAT Cycle B	Volume = $\pi*((7.5/2)^2)*13*(67,782/Mass_Prop)*Mass_Prop [m^3]$
Metrics - SEP Propulsion Volume	Assume volume of single tank from HAT, multiply by number of tanks, assume solar panels volume is negligible in comparison	HAT Cycle B	Volume = num_tanks*pi*(0.5^2)*(3.8) [m^3]
Metrics - NTR Propulsion Volume	Assume size from Mars DRM 5, different sizes if NTR is cargo (i.e. on the "slow" trajectory) or on the "fast" one (i.e. with people)	Mars DRM 5	Volume_cargo= $\pi*((8.9/2)^2)*42.6 [m^3]$ Volume_manned= $\pi*((8.9/2)^2)*72.6 [m^3]$
Metrics - Number of SLS Launches (by Mass)	Assume that propulsion stages + habitation forms will be packed in the most efficient way (i.e. any combination is possible). All segments larger than 105mt are not possible to fit Logistics, cargo, airlock, mobility not accounted for	SLS initial sizing	SLS initial capacity = 105 mt SLS evolved capacity = 130 mt
Metrics - Number of SLS Launches (by Volume)	For habitation forms with more than one habitation function, assign the form the volume of the most massive (i.e. voluminous) function		
	Assume that propulsion stages + habitation forms will be packed in the most efficient way (i.e. any combination is possible). Propulsion stage volume estimated from HAT B dimensions	HAT Cycle B	SLS initial volume = $\pi*((7.5/2)^2)*18 [m^3]$ SLS evolved volume = $\pi*((9.1/2)^2)*30 [m^3]$

A-4: ΔV Matrices

Departure ΔV , maneuver read “from row to column,” units are m/s

			1	2	3	4	5	6	7	8	9	10	11	12	13	14	15	16	17	18	19
KSC	1	x 9500																			
LEO	2	0 x 3100	3150	3230	3230	3150	3910	3400	3600	3600	4100	3714	3714	4214	4272	4272	4272	4772	4772	4208	
EML1	3	750 x 140				248	2520	3400	3600	3600	4100	3714	3714	4214	4272	4272	4272	4772	4772	1249	
EML2	4	350 140 x				152	2500	4000	3600	3600	4100	3714	3714	4214	4272	4272	4272	4772	4772		
SEL1	5	900				300	2500	4000	3600	3600	4100	3714	3714	4214	4272	4272	4272	4772	4772		
SEL2	6	900 400				300	2500	4000	3600	3600	4100	3714	3714	4214	4272	4272	4272	4772	4772		
LLO	7	850 850	632	632	700	700	x 0														
LS	8	2700	2450	2450	2550	2550	1871	x													
NEO (low)	9	147	147	147		147		0													
Phob (1)	10	3500	3500							x											
LMO (1)	11	3500	2115	3500						x	0										
MS (1)	12	6115	6115	6115	6115	6115			4000		x										
Phob (2)	13	4100	4100	4100	4100	4100															
LMO (2)	14	2600	2600	2600	2600	2600								0							
MS (2)	15	6600	6600	6600	6600	6600			4000						4000						
Phob (3)	16	4100	4100	4100	4100	4100															
LMO (3)	17	2600	2600	2600	2600	2600													0		
MS (3)	18	6600	6600	6600	6600	6600			4000									4000			
NEO (high)	19	0	1125																	0	

Arrival ΔV Matrix, read “from row to column,” units are m/s:

		1	2	3	4	5	6	7	8	9	10	11	12	13	14	15	16	17	18	19
KSC	1	x	0																	
LEO	2	0	x	750	350	900	900	850	2000	180	2115	2115	4000	3465	3465	5500	6782	6782	7800	1359
EML1	3	0	3100	x			632	2000	2000	180	2115	2115	4000	3465	3465	5500	6782	6782	7800	1359
EML2	4		3150		x		610	2000	2000		2115	2115	4000	3465	3465	5500	6782	6782	7800	
SER1	5		3230			x		2000	2000		2115	2115	4000	3465	3465	5500	6782	6782	7800	
SER2	6	0	3230				0	2000	3000	2115	2115	4000	3465	3465	5500	6782	6782	7800		
LLO	7	0	3150	248			x	2083												
LS	8						0	x												
NEO (low)	9		3500	300					0											
Phob (1)	10		3500							x										
LMO (1)	11		3500	300	300	300	300				x	625								
MS (1)	12		3500	300	300	300	300				0	x								
Phob (2)	13		3500	300	300	300	300						x							
LMO (2)	14		3500	300	300	300	300					625		x	625					
MS (2)	15		3500	300	300	300	300							0	x					
Phob (3)	16		3500	300	300	300	300									x				
LMO (3)	17		3500	300	300	300	300					625					x			625
MS (3)	18		3500	300	300	300	300											0		x
NEO (high)	19		3500	300																
	0																			

A-5: TOF Matrix

Fast transfer matrix, read “from row to column,” units are days:

		1	2	3	4	5	6	7	8	9	10	11	12	13	14	15	16	17	18	
KSC	1	0																		200
LEO	2	0	3.5	9	15	15	3.5		174		260			180				130		200
EM1	3	3.5	0				3.5		174		256.5			176.5				126.5		200
EM2	4	9		0			3													
SEL1	5	15			0															
SEL2	6	15				0														
LLO	7	3.5	3.5				0	0												
L5	8						0	0												
NEO (low)	9	170	170						0											
Phob	10								0											
LMO	11	260	256.5							0										
MS	12							0												
Phob (2)	13											0								
LMO (2)	14	180	176.5										0	0	0					
MS (2)	15													0	0					
Phob (3)	16														0					
LMO (3)	17	180	176.5														0			
MS (3)	18																	0		
NEO (high)	19	196	196																	0

A-6: Low-Thrust ΔV Estimation Method

The assumption of short duration rocket thrust in comparison with orbital periods around a central body inherent in impulsive ΔV calculations does not hold true for low-thrust maneuvers associated with SEP. Typical modern analysis of low-thrust trajectories involves the use of a numerical integration model to produce high accuracy results [118][119][120]. This is both resource-intensive and heavily dependent on the particular system under analysis. With the reduced fidelity of the model, simplifying assumptions that limit the computational requirements can retain sufficient precision appropriate to the analysis.

For the purposes of the model, it is assumed that the thrust-to-weight ratio of the SEP system remains constant, implying that the power and thruster systems are scaled with the system to retain the consistency. To accomplish this, modular 43kW thrusters are stacked to provide sufficient thrust, while the solar panel systems are expanded to scale with the thruster power requirements. Further discussion of SEP element sizing can be found in Appendix A-12. Calculation of the energetic requirements assumes that the trajectory occurs within a planar circular spiral with the thruster always pointed in a direction tangential to the circle of the current spiral radius.

To determine the total impulse-equivalent energetic requirement, two types of maneuvers are integrated into a single energy requirement. The first increases the radius of the exiting spiral around a central gravitational body, which can be described under the assumptions listed by Equation 4.

Equation 4: Radial Spiral with SEP

$$\Delta v_{SEP\ rad} = \sqrt{\frac{\mu}{r_0} - \frac{\mu}{r_f}}$$

Where

$\Delta v_{SEP\ rad}$ is the energetic requirement for an SEP radius-increasing maneuver

μ is the standard gravitational parameter

r is the radius

The assumptions inherent in this calculation hold true so long as the acceleration due to thrust, a , is much lower than gravitational acceleration. The ratio of these values, which gives a measure of the relative strength of gravity at a given radius, can be expressed as a non-dimensional term, ϵ . The mathematical expression is given in Equation 5.

Equation 5: Non-dimensional Parameter for SEP Spirals

$$\varepsilon = \frac{a}{\mu/r_0^2}$$

When far from the central body, the assumption of small ε breaks down. In order to include escape trajectories for low-thrust systems, the model must be extended to include these large radii. Numerical calculation of a few points allows for the extrapolation of a parametric between ΔV and ε . This relationship, shown in Figure 81, strongly suggests a dependency on the logarithm.

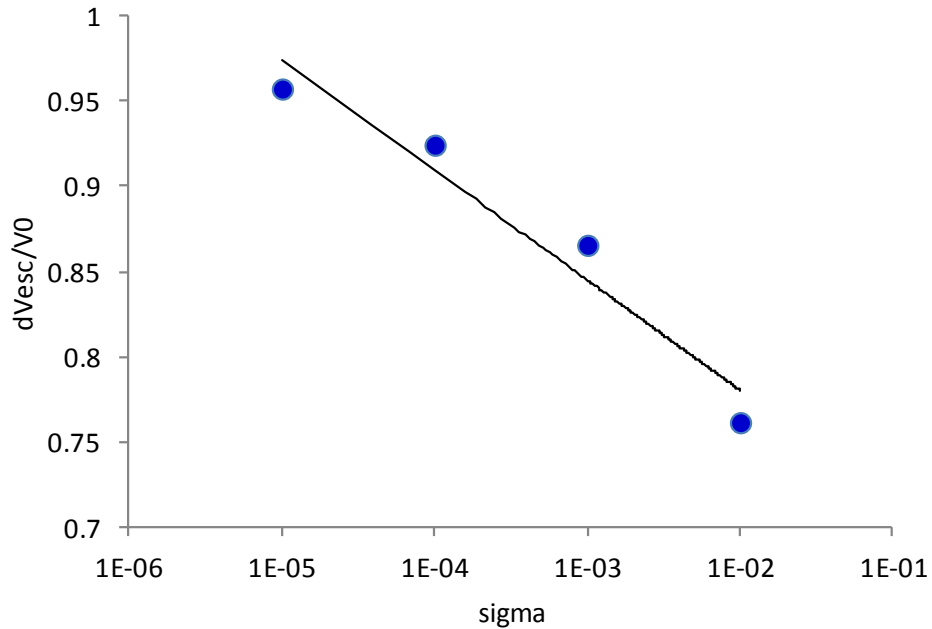


Figure 81: Escape ΔV Parametric for Low-Thrust

The curve fit equation for this parametric is given in Equation 6.

Equation 6: Escape Spiral for SEP

$$\Delta v_{SEP\ esc} = v_0(-.028 \ln \varepsilon + .651)$$

Where

v_0 is the initial orbit velocity

Final ΔV maneuvers for the low-thrust trajectories consist of the aggregate radius-increasing and escape maneuvers. These were validated against reference design missions such as [121]. The matrix of associated energetic requirements can be found in Appendix A-7.

A-7: Low-Thrust ΔV Matrix

Read “from row to column,” units are m/s:

		1	2	3	4	5	6	7	8	9	10	11	12	13	14	15	16	17	18	19
KSC	1	0	0	0	0	0	0	0	0	0	0	0	0	0	0	0	0	0	0	0
LEO	2	0	0: 6557.903	0	0	0	0: 8075.673	0	0	0: 7390	0: 15792.32	0	0	0	0	0	0	0: 15792.32	0	0: 8314
EM1	3	0: 6557.903	0	0	0	0	0: 1517.77	0	0	0	0: 9490.923	0	0	0: 15792.32	0	0	0	0: 15792.32	0	0
EM2	4	0	0	0	0	0	0	0	0	0	0	0	0	0	0	0	0	0	0	0
SEL1	5	0	0	0	0	0	0	0	0	0	0	0	0	0	0	0	0	0	0	0
SEL2	6	0	0	0	0	0	0	0	0	0	0	0	0	0	0	0	0	0	0	0
LLO	7	0: 8075.673	0: 1517.77	0	0	0	0	0	0	0	0	0	0	0	0	0	0	0	0	0
LS	8	0	0	0	0	0	0	0	0	0	0	0	0	0	0	0	0	0	0	0
NEO (low)	9	0	0: 7390	0	0	0	0	0	0	0	0	0	0	0	0	0	0	0	0	0
Phob	10	0	0	0	0	0	0	0	0	0	0	0	0	0	0	0	0	0	0	0
LMO	11	0: 15792.32	0: 9490.923	0	0	0	0	0	0	0	0	0	0	0	0	0	0	0	0	0
MS	12	0	0	0	0	0	0	0	0	0	0	0	0	0	0	0	0	0	0	0
Phob (2)	13	0	0	0	0	0	0	0	0	0	0	0	0	0	0	0	0	0	0	0
LMO (2)	14	0: 15792.32	0: 9490.923	0	0	0	0	0	0	0	0	0	0	0	0	0	0	0	0	0
MS (2)	15	0	0	0	0	0	0	0	0	0	0	0	0	0	0	0	0	0	0	0
Phob (3)	16	0	0	0	0	0	0	0	0	0	0	0	0	0	0	0	0	0	0	0
LMO (3)	17	0: 15792.32	0: 9490.923	0	0	0	0	0	0	0	0	0	0	0	0	0	0	0	0	0
MS (3)	18	0	0	0	0	0	0	0	0	0	0	0	0	0	0	0	0	0	0	0
NEO (high)	19	0	0: 8314	0	0	0	0	0	0	0	0	0	0	0	0	0	0	0	0	0

A-8: Low-Thrust TOF Matrix

Read “from row to column,” units are days:

		1	2	3	4	5	6	7	8	9	10	11	12	13	14	15	16	17	18	19
KSC	1	0	0	0	0	0	0	0	0	0	0	0	0	0	0	0	0	0	0	0
LEO	2	0	0: 151.8033	0	0	0	0: 191.8577	0	0	185	0: 387.7612	0	0	0: 387.7612	0	0	0: 387.7612	0	0	206
EML1	3	0: 151.8033	0	0	0	0	0: 40.05443	0	0	0	0: 236.0165	0	0	0: 236.0165	0	0	0: 236.0165	0	0	0
EML2	4	0	0	0	0	0	0	0	0	0	0	0	0	0	0	0	0	0	0	0
SELL	5	0	0	0	0	0	0	0	0	0	0	0	0	0	0	0	0	0	0	0
SEL2	6	0	0	0	0	0	0	0	0	0	0	0	0	0	0	0	0	0	0	0
LLO	7	0: 191.8577	40.05443	0	0	0	0	0	0	0	0	0	0	0	0	0	0	0	0	0
LS	8	0	0	0	0	0	0	0	0	0	0	0	0	0	0	0	0	0	0	0
NEO (low)	9	0	185	0	0	0	0	0	0	0	0	0	0	0	0	0	0	0	0	0
Phob	10	0	0	0	0	0	0	0	0	0	0	0	0	0	0	0	0	0	0	0
LMO	11	0: 387.7612	236.0165	0	0	0	0	0	0	0	0	0	0	0	0	0	0	0	0	0
MS	12	0	0	0	0	0	0	0	0	0	0	0	0	0	0	0	0	0	0	0
Phob (2)	13	0	0	0	0	0	0	0	0	0	0	0	0	0	0	0	0	0	0	0
LMO (2)	14	0: 387.7612	236.0165	0	0	0	0	0	0	0	0	0	0	0	0	0	0	0	0	0
MS (2)	15	0	0	0	0	0	0	0	0	0	0	0	0	0	0	0	0	0	0	0
Phob (3)	16	0	0	0	0	0	0	0	0	0	0	0	0	0	0	0	0	0	0	0
LMO (3)	17	0: 387.7612	236.0165	0	0	0	0	0	0	0	0	0	0	0	0	0	0	0	0	0
MS (3)	18	0	0	0	0	0	0	0	0	0	0	0	0	0	0	0	0	0	0	0
NEO (high)	19	0	206	0	0	0	0	0	0	0	0	0	0	0	0	0	0	0	0	0

A-9: Matrix Method for Simultaneous Propulsion Element Sizing

A generalized method for simultaneously solving for the sizing of all propulsion elements in a given system was developed by Austin Nicholas and Alex Buck who were both M.I.T. graduate students at the time of development. This method allows for nested propulsion elements by simultaneously solving for all elements using matrix methods. This method is reliant on the assumption of linear dry mass scaling. The generalized method is herein described.

Let the dry mass fraction be described by Equation 7.

Equation 7: Dry Mass Fraction Definition

$$\frac{m_p}{m_{total}} = 1 - \epsilon$$

Where

m_p is the propellant mass

m_{total} is the total mass

ϵ is the dry mass fraction

Let F be the additional flight performance reserve, unusable propellant, and RCS mass. Therefore it is assumed that actual propellant mass scales linearly with required propellant, given a ΔV maneuver. Let a Unique Propulsive Maneuver (UPM) be defined as a sequence of burns performed without a change in mass other than the reaction mass of the propulsion system. Each UPM has a specified payload (L) given a defined architecture, which includes the dry mass and all other mass besides the required propellant (P). The set of UPMs therefore defines a linear system.

Let $\hat{\epsilon}_i$ be defined by Equation 8.

Equation 8: Modified Tsiolkovsky Rocket Equation

$$\Delta V_i = gI_{sp_i} \ln \left(\frac{L_i + (1 + \hat{\epsilon}_i)P_i}{L_i + \hat{\epsilon}_i P_i} \right); \text{ where } \hat{\epsilon}_i = \frac{F_i + \epsilon_i}{1 - \epsilon_i}$$

This formulation has the solution:

Equation 9: Generic Rocket Equation Solution

$$P_i = L_i \frac{-\rho_i}{(1 + \rho_i \hat{\epsilon}_i)}; \text{ where } \rho_i = 1 - e^{\frac{\Delta V_i}{g I_{sp_i}}}$$

This implies that the propellant mass is a linear function of L for a set of parameters, as seen in Equation 10.

Equation 10: Rocket Equation Linear Function

$$P_i = L_i * f(\Delta V_i, I_{sp_i}, \hat{\epsilon}_i) \triangleq L_i C_i$$

This can be arranged in a matrix representation of the linear system formed by the set of UPMs, generically seen in Equation 11.

Equation 11: Linear System Matrix Formulation

$$Ax = b \Rightarrow \begin{bmatrix} 1 & 0 & \cdots & 0 & B_{11} & B_{12} & \cdots & B_{1n} \\ 0 & 1 & \cdots & 0 & B_{21} & B_{22} & \cdots & B_{2n} \\ \vdots & \vdots & \ddots & \vdots & \vdots & \vdots & \ddots & \vdots \\ 0 & 0 & \cdots & 1 & B_{n1} & B_{n2} & \cdots & B_{nn} \\ -C_1 & 0 & \cdots & 0 & 1 & 0 & \cdots & 0 \\ 0 & -C_2 & \cdots & 0 & 0 & 1 & \cdots & 0 \\ \vdots & \vdots & \ddots & \vdots & \vdots & \vdots & \ddots & \vdots \\ 0 & 0 & \cdots & -C_n & 0 & 0 & \cdots & 1 \end{bmatrix} \begin{bmatrix} L_1 \\ L_2 \\ \vdots \\ L_n \\ P_1 \\ P_2 \\ \vdots \\ P_n \end{bmatrix} = \begin{bmatrix} b_1 \\ b_2 \\ \vdots \\ b_n \\ b_{n+1} \\ b_{n+2} \\ \vdots \\ b_{2n} \end{bmatrix}$$

This matrix can be inverted to solve for all L and P values, which can then be used to find the initial and final mass values.

In the case of HEXANE, in order to create the most generic solution, all 10 propulsive maneuvers are taken to be UPMs. Because there is linear scaling and the propulsive elements can be treated as cargo, this generic formulation solves correctly for all nested cases.

A-10: Alternative Iterative Solver for Nested Propulsion Elements

An alternative approach to the matrix method is an iterative solver. This was originally implemented in HEXANE and replaced by the matrix solver for efficiency purposes. Figure 82 summarizes the iterative solver method.

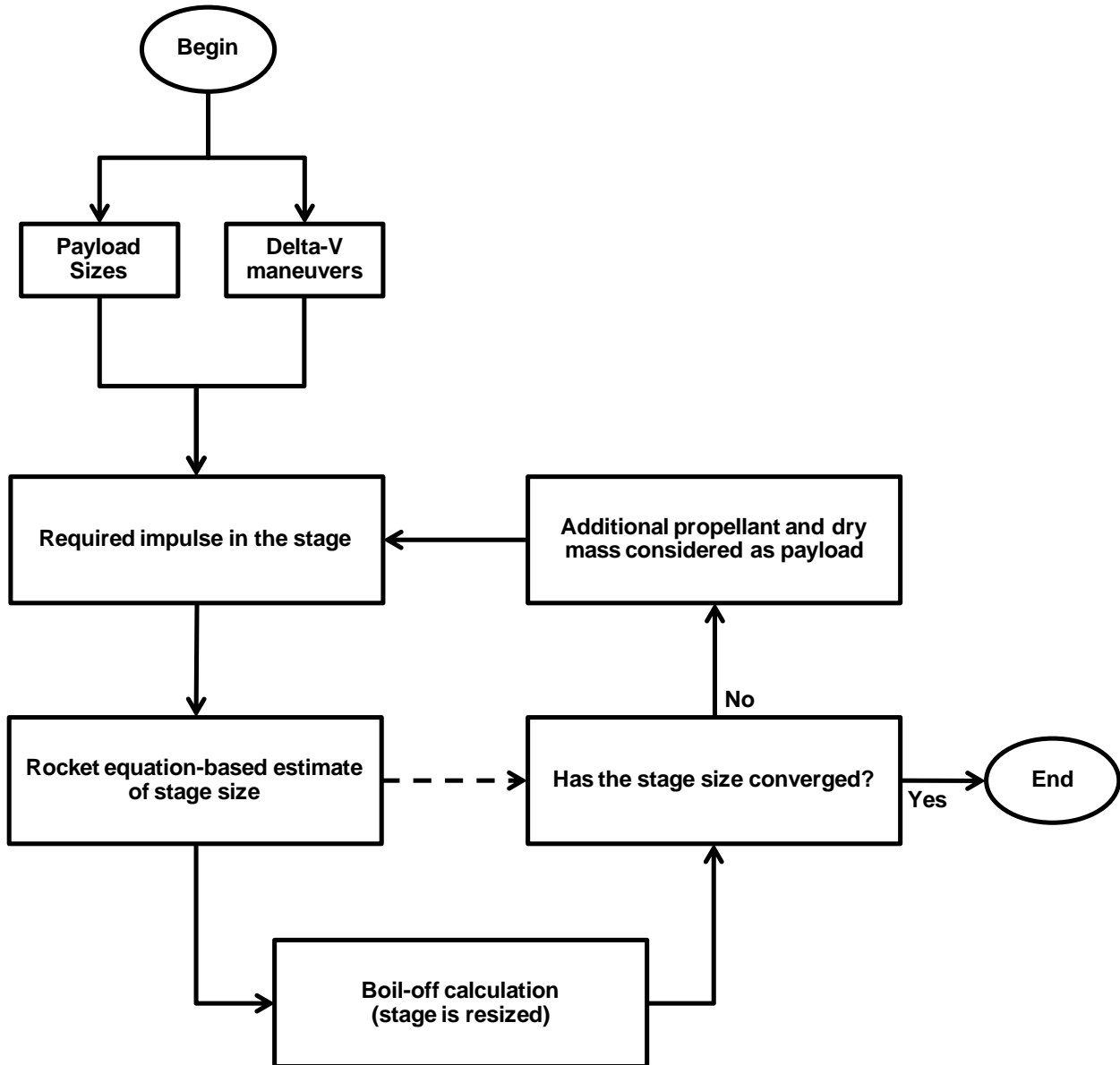


Figure 82: Propulsion Iterative Solver

A-11: Chemical Propulsion Element Sizing Method

Sizing of the high-thrust chemical propulsion stages is primarily reliant on the Tsiolkovsky Rocket Equation, Equation 12. This is reliant on an assumption of impulsive maneuvers.

Equation 12: Tsiolkovsky Rocket Equation

$$\Delta V = gI_{sp} \ln \left(\frac{m_0}{m_f} \right)$$

Where

g is the gravitational constant

I_{sp} is the specific impulse

m_0 is the initial mass of the system

m_f is the final mass of the system

To take into account thruster mass, tank mass, other structural mass, flight performance reserve, boil-off, and ISRU requirements, the initial mass is defined using Equation 13.

Equation 13: Initial Mass Calculation

$$m_0 = (1 + \mu)(1 + F)m_{prop} * e^{r*TOF} + m_{pay}$$

Where

μ is the dry mass fraction

F is the flight performance reserve fraction

r is the propellant boil-off rate

TOF is the time of flight prior to the maneuver

It is assumed that the dry mass fraction, defined by Equation 14, is linear with propellant mass and constant with propellant type. Boil-off rate is assumed to be constant as a fraction of the propellant throughout the mission and therefore follows an exponential decay law. In the case of HEXANE, the flight performance reserve is taken to be 10%.

Equation 14: Propellant Dry Mass Fraction

$$\mu = \frac{m_{dry}}{m_{dry} + m_{prop}}$$

Where

m_{dry} is the propulsion element dry mass, including the thruster, tank, and structure mass

ISRU requires that two additional factors be taken into account. These include the amount of propellant taken from Earth orbit given production of either the fuel or oxidizer in a bi-propellant system and the tank size required to support the operation. The propellant taken from Earth orbit is determined by the propellant's mixture ratio, given in Appendix A-13. Boil-off of this portion of the propellant is also accounted for, but no further details will be given here. Tank sizing is dependent on the coupling between the ascent stage and any other maneuvers as well as the descent tank size. It is assumed that the descent tanks may be re-purposed for use in the ascent stage. Therefore, they are sized by the larger of the propellant requirements for the burns integrated into the descent or ascent stages. If, for example, the ascent stage were coupled with TEI, a large amount of propellant would be manufactured using ISRU, and the ascent stage propellant mass would dominate the descent stage. Therefore, the descent propellant would be carried in an oversized tank prior to landing, at which point it is filled with ascent propellant. Additional tank space required for either the oxidizer or fuel source not taken from the destination environment is also taken into consideration during these calculations.

In the case of NTR, an additional dry mass is added to account for both the large power plant and radiation shield on manned vehicles. The additional dry mass of 41.7mt is taken directly from sizing estimates in DRA 5.0 [17]. The dry mass fraction for NTR therefore only reflects the additional tank and limited structural mass requirements. For staged NTR, only one power plant and shield are assumed, reflecting the concept of drop tanks also discussed in DRA 5.0, therefore limiting the mass impact of NTR technology.

The method for solving for all propulsion stage sizes simultaneously is discussed in Section A-9.

A-12: SEP Element Sizing Method

The general sizing method for low-thrust SEP is based on the framework described in [122]. This work describes a generic method given properties of the low-thrust propulsion mechanism, including the specific mass, specific power, and efficiency characteristics of the power subsystem. The properties assumed for HEXANE come from recent estimates from high-fidelity analysis conducted by NASA HAT [44]. The assumptions drawn from this work are as follows:

$$\beta \text{ (specific mass, kg/W)} = 0.0394$$

$$\eta \text{ (efficiency)} = 0.99 \text{ (direct drive)}$$

I_{sp} (specific impulse) = 2000 s

The first step is to calculate the initial mass of the vehicle, which can be derived using the payload mass fraction equation, Equation 15. This assumes that the required ΔV and TOF are known quantities.

Equation 15: Payload Mass Fraction

$$\frac{m_{pay}}{m_i} = e^{-\frac{\Delta V}{V_e}} - \left(1 - e^{-\frac{\Delta V}{V_e}}\right) * \left(\frac{\beta V_e^2}{2\eta TOF}\right)$$

$$V_e = g * I_{sp}$$

Where

m_{pay} is the payload mass

m_i is the initial mass of the system

g is the gravitational constant

TOF is the time of flight, directly related to the thrust duration

From here, the required propellant mass can be calculated using Equation 16.

Equation 16: Low-Thrust Propellant Mass

$$m_{prop} = m_i \left(1 - e^{-\frac{\Delta V}{V_e}}\right)$$

The inert mass of the system can then be calculated with Equation 17.

Equation 17: Low-Thrust Inert Mass

$$m_{inert} = \frac{\beta V_e^2 m_{prop}}{2\eta TOF}$$

From this, the power requirements can be calculated from Equation 18.

Equation 18: Low-Thrust Power Requirements

$$m_{inert} = \beta P_s$$

The necessary mass knowledge is therefore known from the initial mass, inert mass, propellant mass, and payload mass. Additional knowledge regarding the power subsystem is also known following the calculation in Equation 18. Assuming a modular thruster power of 43 kW, the total number of thrusters is also output given the power requirements. Additionally, SEP propulsion elements may be staged in the case of multiple pre-deployment points. Calculation of these masses is accomplished in a similar fashion to the high-thrust chemical propulsion stages with use of an iterative solver. The final propulsion element mass is first calculated and added to the payload mass of the first, assuming consistency in the thruster system and therefore only additional tank and propellant mass.

A-13: Propellant Data

Table 40: Propellant Data

Propellant	Boil-Off Control	I_{sp} (s)	Boil-off Rate (%/mo.)	Dry Mass Fraction (μ)	Inverse Fuel Mixture Ratio
LOX/LH ₂	No	465	9.2000	0.1525	0.207
LOX/LH ₂	Yes	465	0.0833	0.2922	0.207
LOX/CH ₄	No	369	7.2000	0.1300	0.059
LOX/CH ₄	Yes	369	0	0.2600	0.059
NTO/MMH	No	324	0	0.1000	0.422
NTR	Yes	950	0.5000	0.2300	N/A

Propellant	Boil-Off Control	I_{sp} (s)	Boil-Off Rate (%/mo.)	Efficiency (%)	Power/Module (kW)
SEP	No	2000	0	99	43

A-14: Aerocapture Shield Sizing and EDL Response Surface

For the purposes of HEXANE, ablative shield sizing comes in three forms. The first is associated with re-entry capsule mass sizing, whose parametric can be found in Appendix A-16. In this case, the habitat is sized to include the ablative heat shield. The second case applies to aerocapture shield sizing, and it is taken to be a constant mass fraction of the total mass being slowed by ablative aerocapture. The third ablative shield sizing method deals exclusively with large EDL systems and is taken from [53].

Ablative braking maneuvers have been successfully completed using the Mars atmosphere for payloads of up to several hundred kilograms [123]. However, the assets associated with manned exploration missions are likely to be massed on the order of several metric tons. Recent studies have shown that rigid aeroshell systems using Phenolic Impregnated Carbon Ablators (PICA) are capable of providing sufficient stability and survivability of systems of up to 300 m³ in volume and 110 mt in mass [53][75]. The elements analyzed within HEXANE are considered to be within these limits, and therefore it is assumed that the capability for ablative braking with these elements is feasible.

Under the assumption of feasibility, the method of sizing ablative aerocapture shields is assumed to be applicable. Based on [47], large masses using atmospheric aerocapture are assumed to have an additional 15% mass penalty to account for the shielding and TPS required. This applies for both Mars and Earth aerocapture systems.

The third method for ablative shield sizing utilizes the work in [53] directly for sizing large EDL systems. Large systems are considered to be >5mt. For smaller payloads <5mt, the shielding and TPS mass is assumed to be ~30% of the payload mass. The large payload method is based more specifically on the work using rigid mid-L/D aeroshells, which is based on the dual-use Ares V shroud. There are six sub-components involved in the model: structure, acoustic blanket, separation mechanism, body flaps, and TPS. These sub-components' masses are dependent on the following assumptions:

- Aeroshell diameter is 10m (Ares V shroud)
- Aero heat load is 345 MJ/m²
- Entry heat load is 130 MJ/m²
- Maximum dynamic pressure is 11 kPa
- Maximum lateral deceleration is 2.96 Earth g's
- Maximum axial deceleration is 0.41 Earth g's

The process is as follows:

1. Length is calculated assuming a 10m outer diameter and 7m inner diameter, given total volume requirements from habitat sizing and mass density estimates for payload
2. Surface area is computed assuming a cylindrical aeroshell with semi-domed caps
3. Acoustic blanket mass is calculated assuming 6.28 kg per square meter of internal surface area
4. TPS mass is calculated assuming 9.80 kg per square meter of internal surface area
5. 2000 kg is added for avionics and flaps
6. Separation mechanism mass is calculated assuming that it is 10% of the sum of the acoustic

blanket, TPS, and avionics and flaps mass

7. Structural mass is determined using Equation 19
8. Total mass is the summation of the blanket, TPS, avionics, flaps, separation mechanism, and structural mass elements.

Equation 19: EDL Structural Mass Sizing

$$m_{struc} = 1.25 * \left(a_{surf} \exp \left(-1.5774462 + \ln(m_{TPS} + m_{blanket} + m_{flaps} + m_{avionics}) * 0.58278956 + \ln(d) * -0.8533078 + \ln(l) * 0.65239167 + p_{dyn,m} * (-0.00765) + decel_{lat,m}(0.133) + decel_{ax,m}(-0.00748) \right) \right)$$

Where

a_{surf} is the internal surface area

m_{TPS} is the TPS mass

$m_{blanket}$ is the thermal blanket mass

m_{flaps} is the flaps mass

$m_{avionics}$ is the avionics mass

d is the external diameter of the aeroshell

l is the length of the aeroshell

$p_{dyn,m}$ is the maximum dynamic pressure

$decel_{lat,m}$ is the maximum lateral deceleration

$decel_{ax,m}$ is the maximum axial deceleration

Although not implemented in this model, a more integrated method for sizing both the ablative shielding system and propulsion elements is presented in [53]. The associated response surface is shown in Table 41. This was not implemented in order to retain the separation between the habitation and propulsion elements necessary for the remainder of the analysis.

Table 41: SRP Response Surface with No Pre-Entry Jettison

β for y1	β for y2	β for y3	β for y4	β for y5	β for y6	β for y7	β for y8	β for y9	β for y10	Coeff.
18142.37359	9548.288	25691.98	19757.3	18142.3	10559.41	7038.234	544.665	8590.715	64315.78	1
-130.7168504	-85.8375	813.7455	894.3086	869.2857	951.2568	-108.069	26.09754	-81.1023	-1079.74	x1
-12.60424068	-5.94664	-17.3243	-13.4013	-12.6042	-3.85025	-8.37556	-0.3784	-5.59554	-53.2636	x2
-1378.494491	-546.768	-1831.68	-1459.54	-1378.48	-839.607	-497.493	-41.3846	-514.276	-8431.26	x3
-32.38618099	-19.0341	-49.2018	-34.6706	-32.386	-13.0252	-18.3885	-0.97229	-17.9032	-110.949	x4
-38.32795655	1479.21	1454.016	1462.53	-38.3283	-28.9669	-8.21073	-1.15069	27.01717	-59.639	x5
-11.02482642	-19.9648	-15.9654	-12.5419	-11.0248	-8.23006	-2.46375	-0.33098	-18.8651	-17.3876	x6
-9.92472471	-17.6546	-25.4733	-11.2881	-9.92476	-6.37774	-3.24906	-0.29796	-16.667	-32.2847	x7
0.560947888	0.100297	0.644629	0.586438	0.560947	0.075128	0.468978	0.016841	0.094319	0.830519	x1*x2
26.00705727	4.732423	29.96714	27.19382	26.00706	19.51139	5.714891	0.780779	4.450543	371.8767	x1*x3
0.479789289	0.120392	0.585101	0.503716	0.479789	0.429774	0.035611	0.014404	0.113226	0.760405	x1*x4
5.15E-07	0.086319	0.00746	0.002376	1.34E-06	9.46E-07	3.58E-07	4.04E-08	0.084023	2.44E-06	x1*x5
3.81E-06	0.680435	0.045628	0.04173	8.39E-06	5.90E-06	2.24E-06	2.52E-07	0.64	1.52E-05	x1*x6
0.0488	0.688417	0.718697	0.092743	0.0488	0.024	0.0233	0.00147	0.647565	0.106	x1*x7
0.78	0.153247	0.909538	0.816042	0.78	0.345	0.411	0.0234	0.144091	5.99	x2*x3
0.01	0.003597	0.013252	0.010562	0.01	0.00678	0.00291	0.0003	0.003383	0.0164	x2*x4
4.40E-07	0.00149	0.000127	5.14E-05	9.68E-07	6.80E-07	2.58E-07	2.91E-08	0.001441	1.75E-06	x2*x5
6.60E-09	0.00989	0.000663	0.000607	1.72E-08	1.21E-08	4.59E-09	5.17E-10	0.009304	3.12E-08	x2*x6
0.00245	0.0103	0.0124	0.00316	0.00245	0.00187	0.0005	7.35E-05	0.00969	0.00604	x2*x7
3.99	1.756882	5.6	4.24	3.99	3.05	0.825	0.12	1.65227	9.8	x3*x4
7.15E-05	0.077598	0.00667	0.00295	0.000157	0.000111	4.20E-05	4.72E-06	0.074902	0.000285	x3*x5
1.07E-06	0.482	0.0323	0.029561	2.80E-06	1.97E-06	7.46E-07	8.41E-08	0.453	5.08E-06	x3*x6
0.156354937	0.50819	0.647852	0.192935	0.156361	0.106261	0.045406	0.004694	0.478036	0.255812	x3*x7
3.01E-06	0.003642	0.000274	0.000198	6.62E-06	4.66E-06	1.77E-06	1.99E-07	0.00346	1.20E-05	x4*x5
4.52E-08	0.008118	0.000547	0.000499	1.18E-07	8.30E-08	3.14E-08	3.54E-09	0.007636	2.14E-07	x4*x6
0.02	0.011511	0.030766	0.021445	0.02	0.00868	0.0108	0.000602	0.010828	0.164	x4*x7
0.0413	0.660801	0.123033	0.082297	0.0413	0.0201	0.02	0.00124	0.622504	0.0896	x5*x6
5.15E-08	0.623	0.602	0.0383	1.34E-07	9.46E-08	3.58E-08	4.03E-09	0.586	2.44E-07	x5*x7
3.81E-07	0.022192	0.00625	0.00128	8.39E-07	5.90E-07	2.24E-07	2.52E-08	0.020957	1.52E-06	x6*x7
0.079	0.036214	0.093438	0.0824	0.079	0.0714	0.00525	0.00237	0.035518	0.139	x1**2
0.00537	0.000952	0.00614	0.005616	0.00537	0.000892	0.00432	0.000161	0.000895	0.00789	x2**2
33.9	6.745954	38.90495	35.50517	33.9	26.1	6.76	1.02	6.337443	284	x3**2
-0.029	-0.00324	-0.03278	-0.03024	-0.029	-0.0598	0.0316	-0.00087	-0.00305	-0.0409	x4**2
0.587197393	0.1232	0.67371	0.613818	0.587185	0.457683	0.111874	0.017628	0.116992	0.881866	x5**2
0.0652	0.022617	0.0756	0.0689	0.0652	0.0509	0.0124	0.00196	0.021289	0.098	x6**2
0.00587	0.010002	0.015287	0.006648	0.00587	0.00458	0.00112	0.000176	0.009447	0.00882	x7**2

Where

x1 is payload

x2 is terminal descent ΔV

x3 is initial T/W

x4 is area ratio

x5 is aeroshell mass

x6 is aerocapture apoapsis correction ΔV

x7 is descent orbit insertion ΔV

y1 is SRP initial mass

y2 is aeroshell initial mass

y3 is stack mass at arrival

y4 is stack mass at entry

y5 is stack mass at terminal descent

y6 is stack mass at landing

y7 is SRP propellant mass

y8 is SRP RCS propellant mass

y9 is aeroshell RCS propellant mass

y10 is SRP thrust per engine

A-15: ISRU

For the purposes of HEXANE, it is assumed that methane and oxygen can be extracted *in-situ* on both the moon and Mars. For both locations, it is assumed that the necessary hydrogen is brought from Earth for all reactions. ISRU is not assumed to be possible for NEA missions due to the lack of information about asteroid composition and the feasibility constraints of trying to extract and convert asteroid materials.

In the case of Mars, the pure oxygen is assumed to be extracted by dissociating CO_2 taken from the Martian atmosphere. This is a highly energetic process, requiring a large power plant. For methane production, a Sabatier reaction [124] is combined with the reverse water gas-shift reaction [125] to create methane, carbon monoxide, and water in the following reaction:



This scheme affords a mass leveraging of 18:1 when the hydrogen is transported from Earth. It is not assumed that the water byproduct is used to supplement surface water supplies for the astronauts. The power plant is assumed to have a fixed mass of 9300kg for both a 30kWe fission

plant and ISRU equipment. If not using ISRU, a 20kWe fission plant is assumed for surface power with a mass of 6800kg.

On the lunar surface, oxygen and methane can be produced by extracting volatiles from the lunar regolith. The extraction process would produce carbon monoxide and carbon dioxide, along with trace amounts of methane. The Sabatier reaction can then be used to create additional methane. The extraction of volatiles from regolith is also extremely energy intensive, as is the dissociation of carbon monoxide, meaning that lunar ISRU also requires a large power plant. A fixed mass of 15,100kg is assumed for a 50kWe fission plant. Without ISRU for missions over 21 days, a 40kWe fission plant is assumed with a mass of 8800kg.

A-16: Habitat Sizing Parametrics

As discussed in Section 2.5, HEXANE relies on parametric relationships in order to size habitat elements. [50] and [126] showed that there are, in fact, multiple regimes of sizing that should be used, depending on the environment and length of time spent in a habitat. Long duration deep space habitats are sized more for comfort than short duration entry vehicles, for example. This is not only because the amount of volume that is necessary for comfort is dependent on duration but also because the comfort level allowable is much different.

The parametrics themselves also had to be based on different sources, given the amount of information that exists from a combination of real programs and detailed point designs. Almost all of the operational environments required either one or two independent parametric relationships to be established. For the launch environment, the Orion MPCV is assumed to be used in all cases, modified to launch without a heat shield with a total mass of 6400kg. For the deep space habitats, two parametrics were established. For flight durations greater than 10 days, the regression shown in Figure 21 couples with the mass sizing regression in Figure 20 to size the DSH. For flight durations less than 10 days, a regression established from Mercury, Gemini, and Apollo spacecraft is used, shown in Equation 20.

Equation 20: Short Duration DSH Regression

$$vol_{total} = 7.7478 * \ln(n_{crew}) + 0.7119$$

This is once again coupled with the regression from Figure 20 to establish the habitat mass. A switch may also be triggered to use the MPCV without a heat shield in place of this parametric.

Descent and ascent follow the same volume sizing parametric. Unlike the remainder of the parametrics, these rely on the suggested habitable volumes from the NASA HIDH. In both cases, each crew member is assumed to be assigned one sitting location for ascent and/or descent,

requiring 1.7 m³ per crew, as shown in Figure 83 [52]. In addition, the vehicle is assumed to have an area assigned for suit donning and egress with a suit donned. This is assumed to be a single volume for both, requiring 6.35 m³ of habitable volume, taken from Figure 84. Habitable volume is assumed to be approximately 55% of the total volume [127]. This volume is then used to size the vehicles. Heat shields are added through a separate process for the descent vehicle.

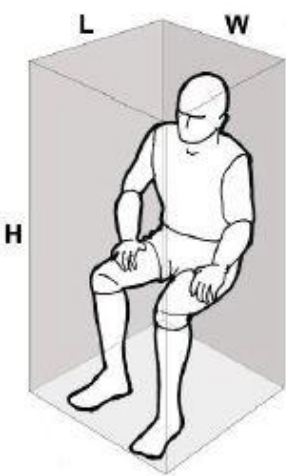
Figures of Human Body Postures and Volumes	Applicable Functions	Dimensions (m)		Volume (m ³)
	Body waste management facilities, ascent and descent, spacecraft duty station	H	1.52	1.70
		L	0.91	
		W	1.23	

Figure 83: HIDH Sitting Volume

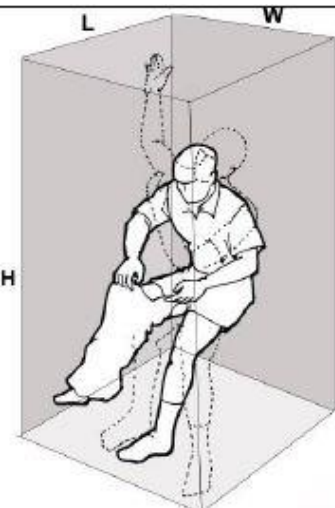
Figures of Human Body Postures and Volumes	Applicable Functions	Dimensions (m)		Volume (m ³)
	Dressing (don and doff), EVA suiting area	H	2.20	6.35
		L	1.45	
		W	1.99	

Figure 84: HIDH Suit Donning Volume

Surface habitats for Mars missions are parametrically sized from a set of point designs. Each point design was built component-up, giving much more accurate results for the total vehicle mass. These point designs were taken from DRA 5.0, Mars-Oz, and Austere [17–19]. For DRA 5.0, two habitats were designed, both of which were used for the regression. The data is shown in Table 42.

Table 42: Mars Surface Habitat Regression Data

Historical Reference	# Crew	Volume (m³)	Volume/crew	Landed Mass (kg)
DRA 5.0 type 1	4	197.73	49.4325	12975
DRA 5.0 type 2	4	154	38.5	12280
MARS-OZ	4	210	52.5	19300
Caltech Study	5	143.25	28.65	18120

It was found that the most consistent measure across these point designs was the mass per volume*crew. This was found to be 21.2 on average, with a covariance of 18.21%. Figure 21 is used to determine the volume, while the above-described relationship is used to find the mass of the habitat.

For short duration lunar missions, a regression used during the Constellation program sizing of the Altair lander is used [128]. That parametric is represented in Equation 21.

Equation 21: Altair Lunar Lander Parametric

$$mass_{total} = 244.55 * vol_{total} + 103.57$$

Volume is sized assuming the need for 1.5m³ of habitable volume per crew member. The habitable volume is once again assumed to be 55% of the total volume. It should also here be noted that the surface habitat is also sized to include spare parts on the surface and consumables for the surface mission duration.

The ascent stage is sized in the same manner as the descent stage, with the exception of the addition of a heat shield. The return DSH is also sized in the same manner as the outbound DSH. The Earth re-entry vehicle is also assumed to be the Orion MPCV with a heat shield, having a total mass of 8600kg.

A-17: Logistics Sizing Parametric

Currently, the logistics sizing mechanism for HEXANE is a fixed linear regression based on the number of crew. The regression is based on the ISS Multi-Purpose Logistics Module (MPLM),

which follows the simple relationship shown in Equation 22.

Equation 22: MPLM-based Logistics Regression

$$Volume_{unpressurized} = 5 * num_{crew}$$

$$Volume_{pressurized} = 15 * num_{crew}$$

The total volume requirements are a combination of pressurized and unpressurized requirements, with units in m^3 . Pressurized logistics require increased volume due to the structural requirements for pressurization. Useable volume for storage is much less than the total volume, the latter of which is given by Equation 22.

Mass of logistics are given by a combination of the containment mass, which combines the volume from the above equation with the regression for mass given for habitats in Figure 20. This applies given that the logistics require very similar hard-walled structures to the habitat structures and given that they are much smaller in total volume requirements, thus having a small impact on the overall mass.

Logistics also include two other mass sources: spares and consumables. Spares are calculated as a percentage of the habitat masses, with different percentages for in-space and surface operations. The baseline for in-space operations is 10%, with 5% for surface operations [127]. Consumables are based on the 2007 JPL consumables calculator. Each person is assumed to require 2.886 kg of consumables per day. This and the spares percentages are inputs to the model that may be altered via the Excel front end.

APPENDIX B: Lunar and NEA HEXANE Results

B-1: Lunar Results

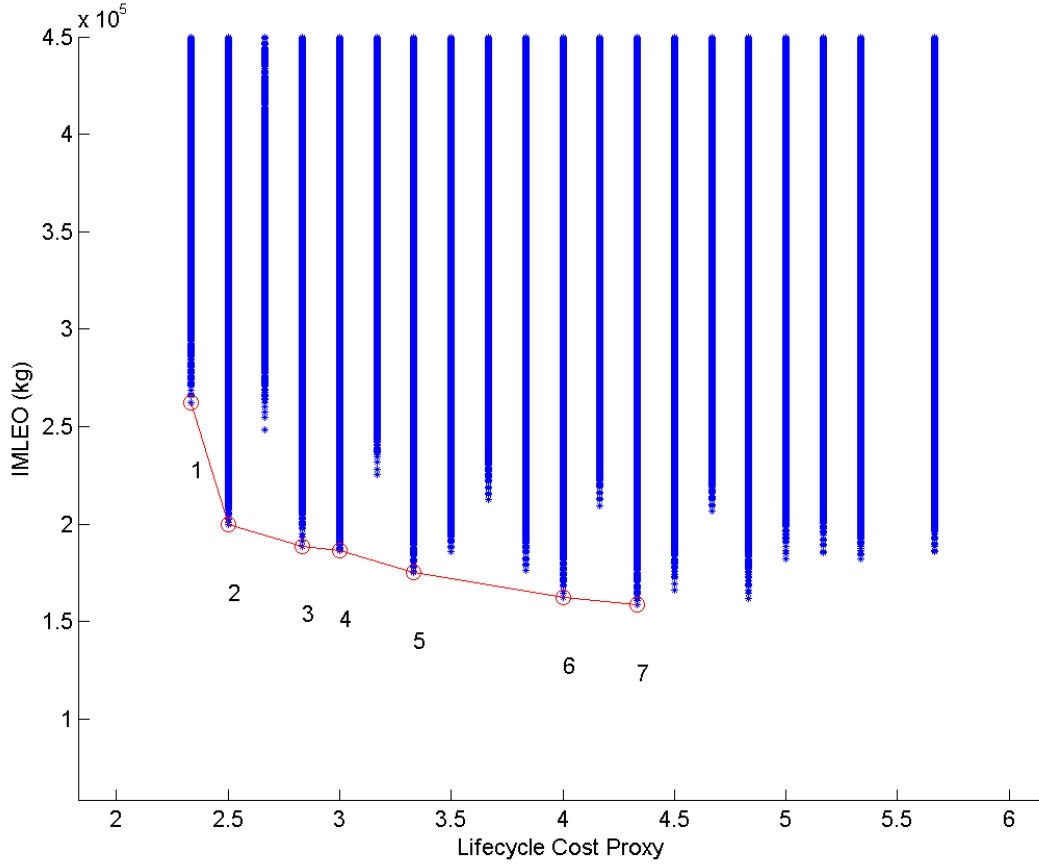


Figure 85: Lunar Tradespace

Table 43: Lunar Non-Dominated Architecture Properties

	IMLEO (kg)	LCC	SEP	Aerocapture	Boil-Off	ISRU
Arch. 1	262410	2.333	Yes	No	No	No
Arch. 2	199760	2.500	Yes	No	No	No
Arch. 3	188840	2.833	Yes	Yes	No	No
Arch. 4	186290	3.000	Yes	No	Yes	No
Arch. 5	174990	3.333	Yes	Yes	Yes	No
Arch. 6	162180	4.000	Yes	No	Yes	Yes
Arch. 7	158560	4.333	Yes	Yes	Yes	Yes

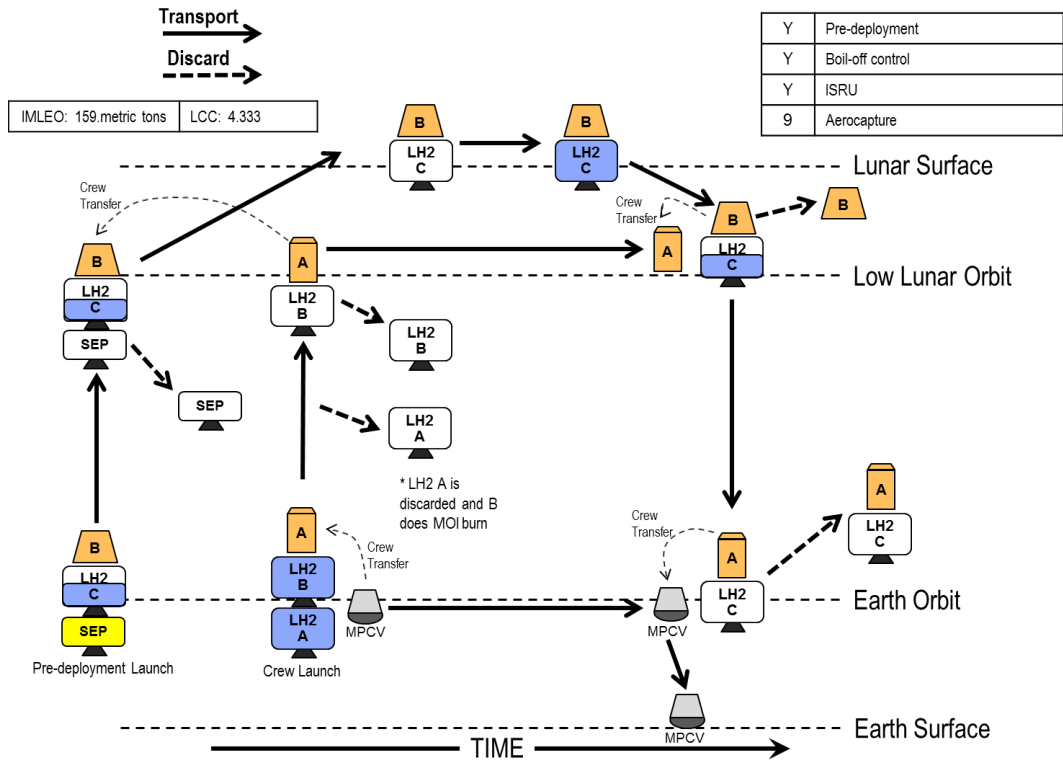


Figure 86: Lunar Minimum IMLEO BAT Chart

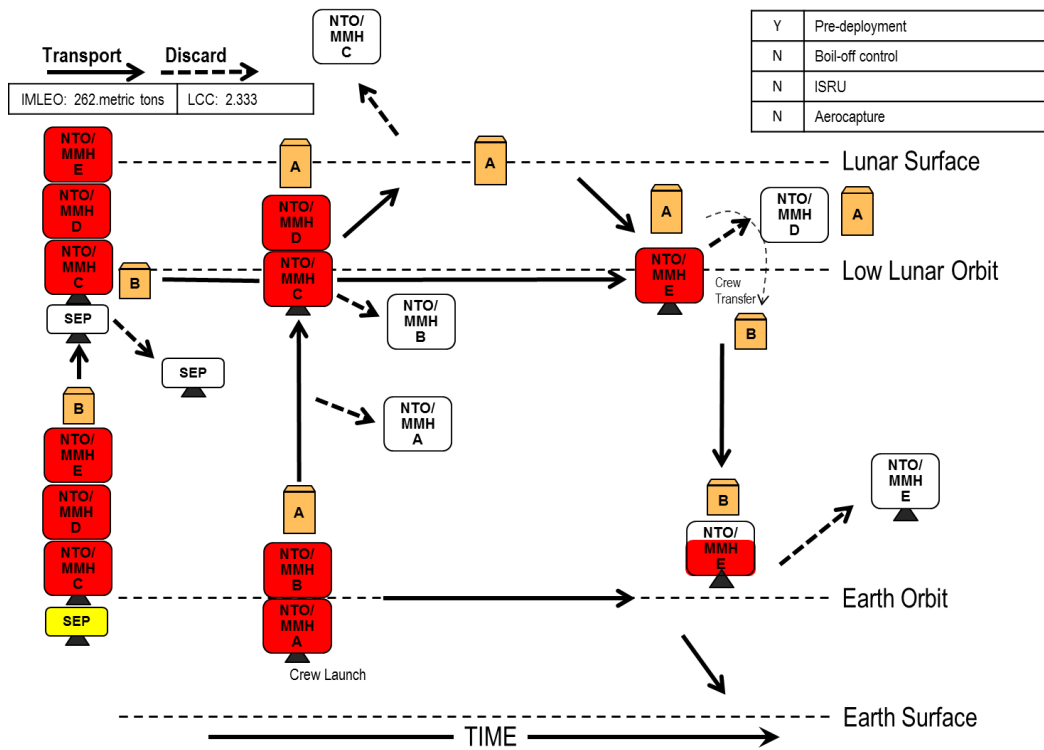


Figure 87: Lunar Minimum LCC BAT Chart

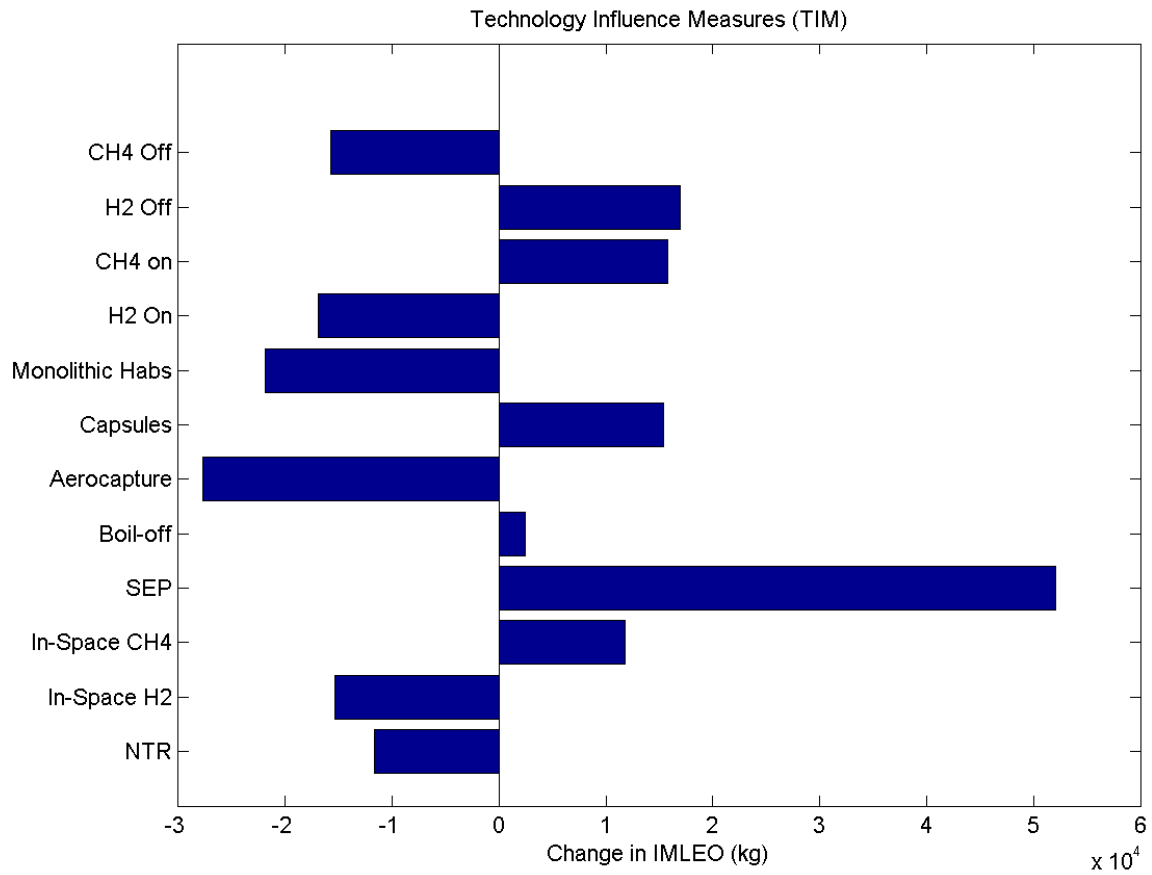


Figure 88: Lunar Feature TIM Chart

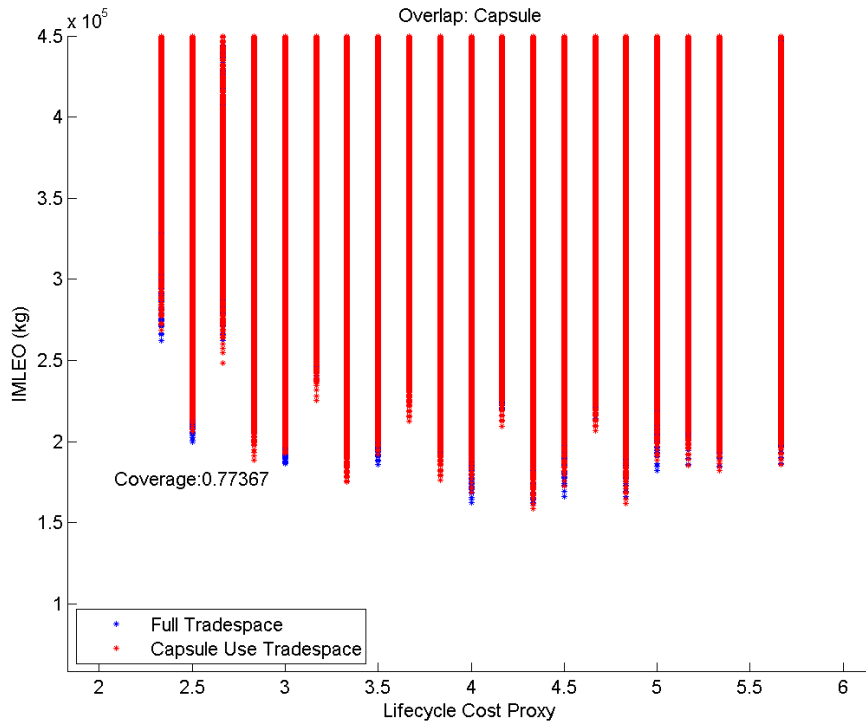


Figure 89: Lunar Capsule Tradespace Coverage

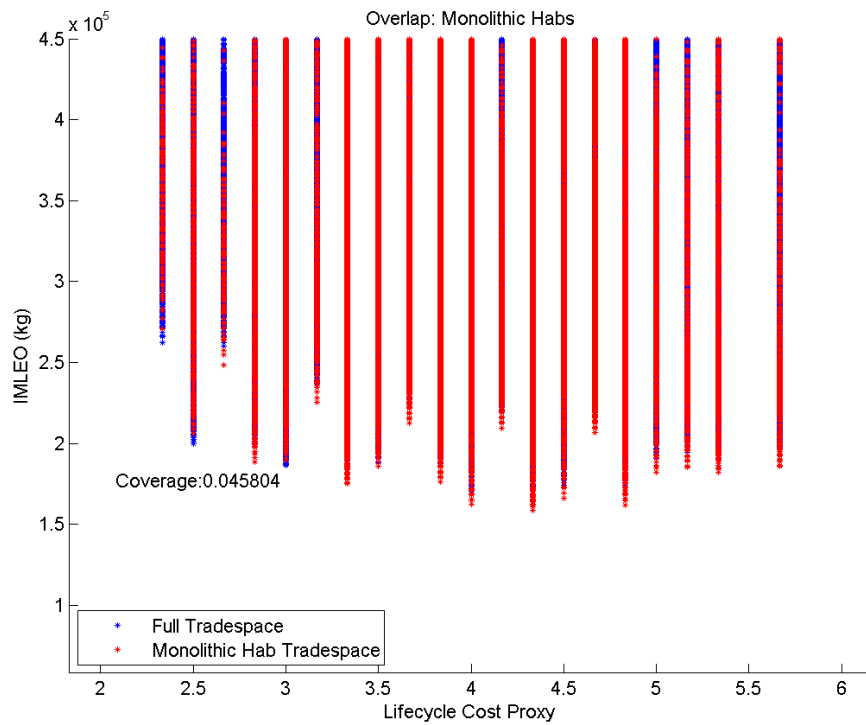


Figure 90: Lunar Semi-Monolithic Habitat Coverage

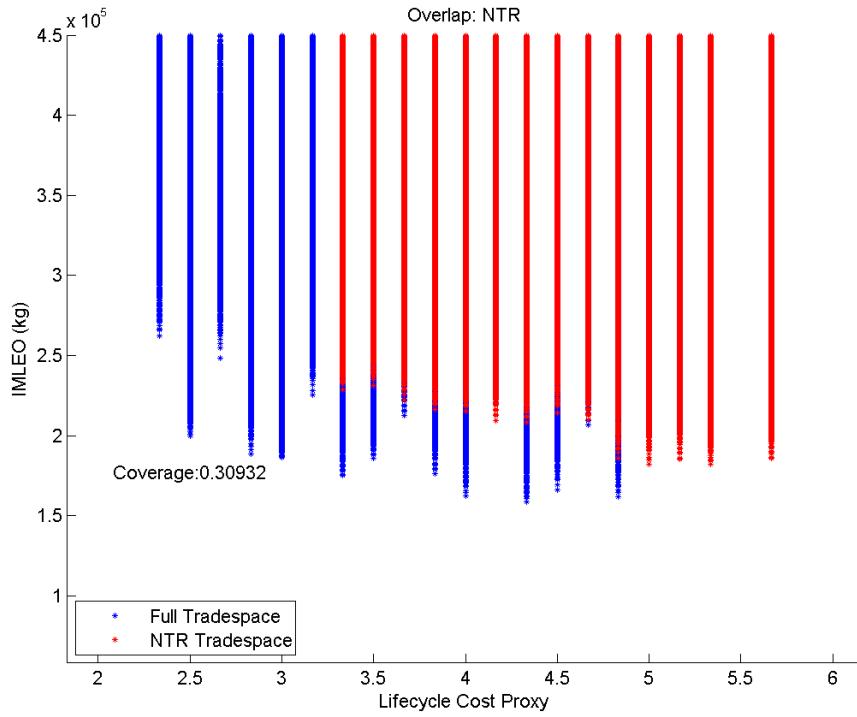


Figure 91: Lunar NTR Coverage

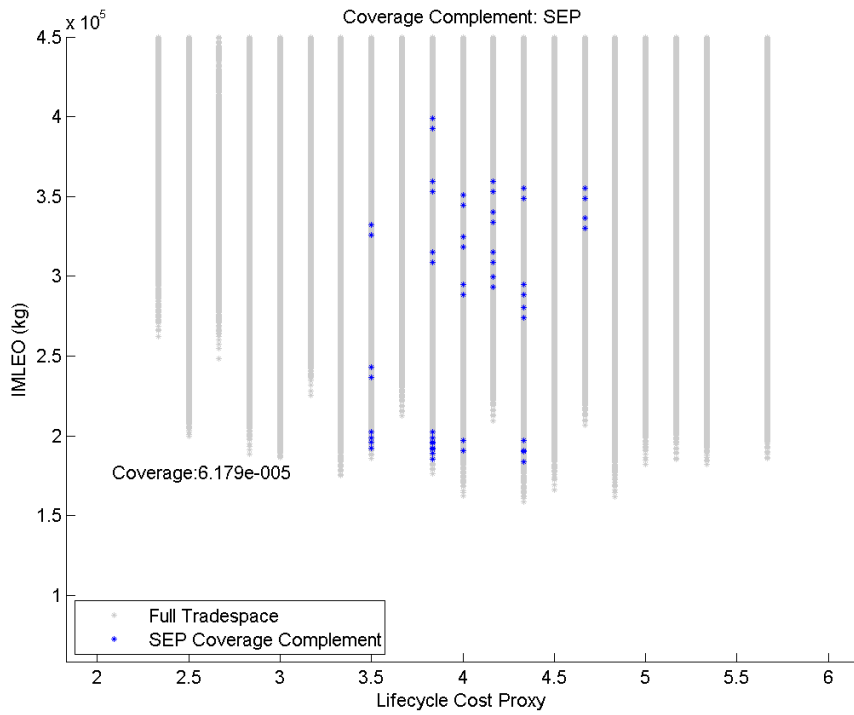


Figure 92: Lunar SEP Pre-Deployment Coverage Complement

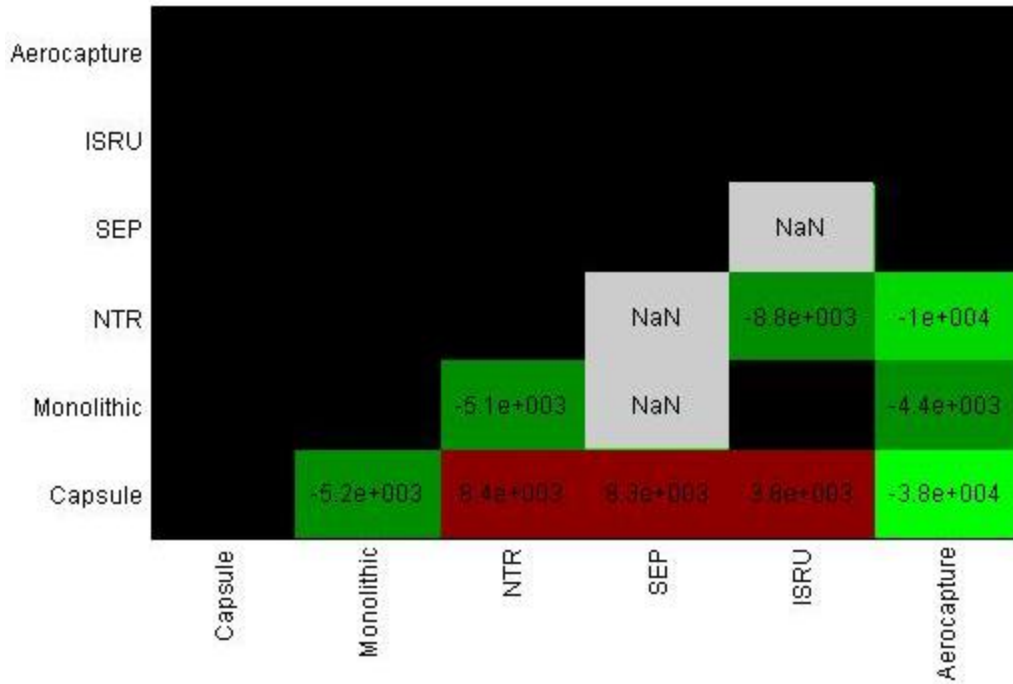


Figure 93: Lunar Feature TCIM

B-2: Low-Energy NEA Results

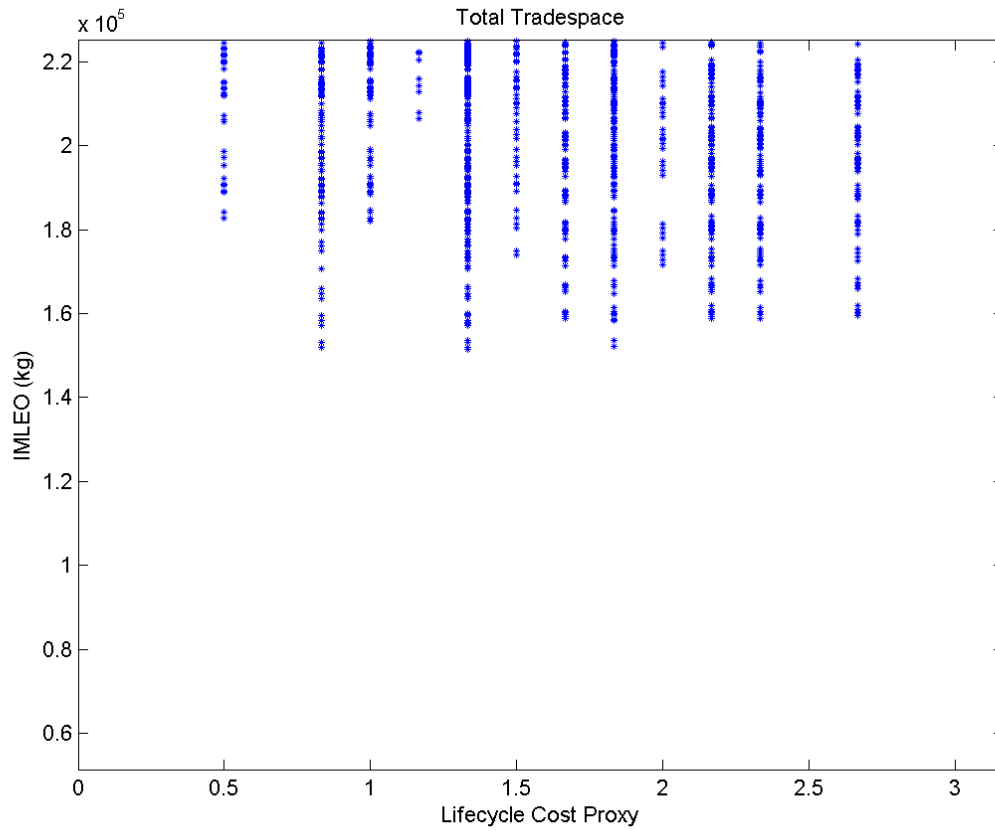


Figure 94: Low-Energy NEA Tradespace

Table 44: Low-Energy NEA Non-Dominated Architecture Properties

	IMLEO (kg)	LCC	SEP	Aerocapture	Boil-Off
Arch. 1	182760	0.500	Yes	No	No
Arch. 2	152020	0.833	Yes	Yes	No
Arch. 3	151400	1.333	Yes	Yes	Yes

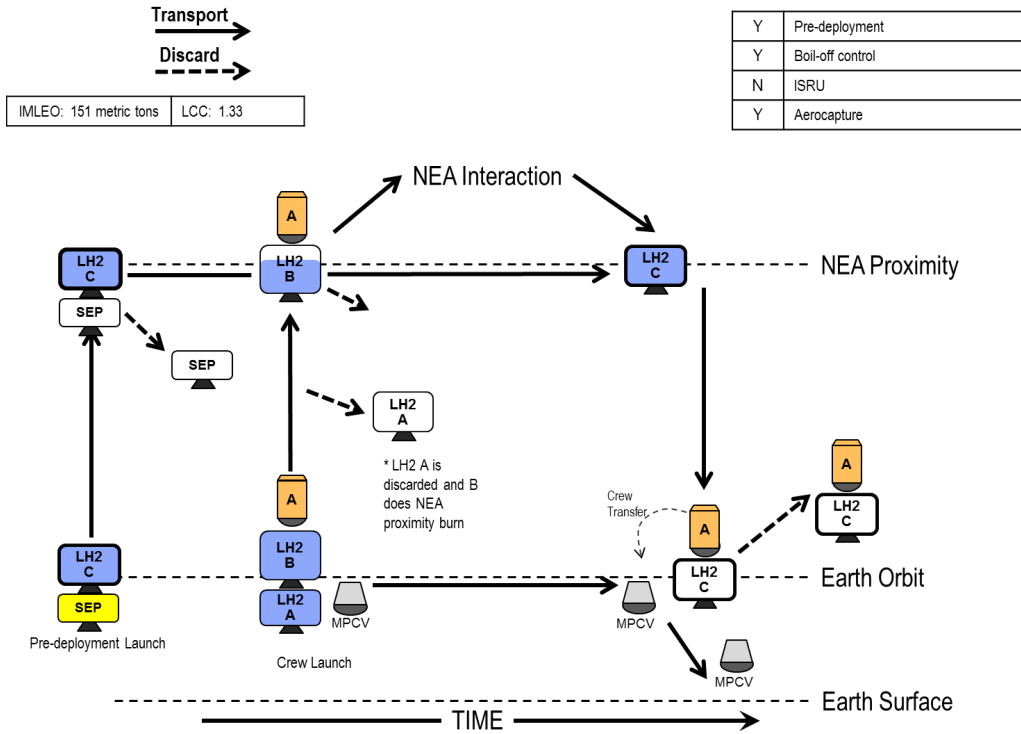


Figure 95: Low-Energy NEA Minimum IMLEO BAT Chart

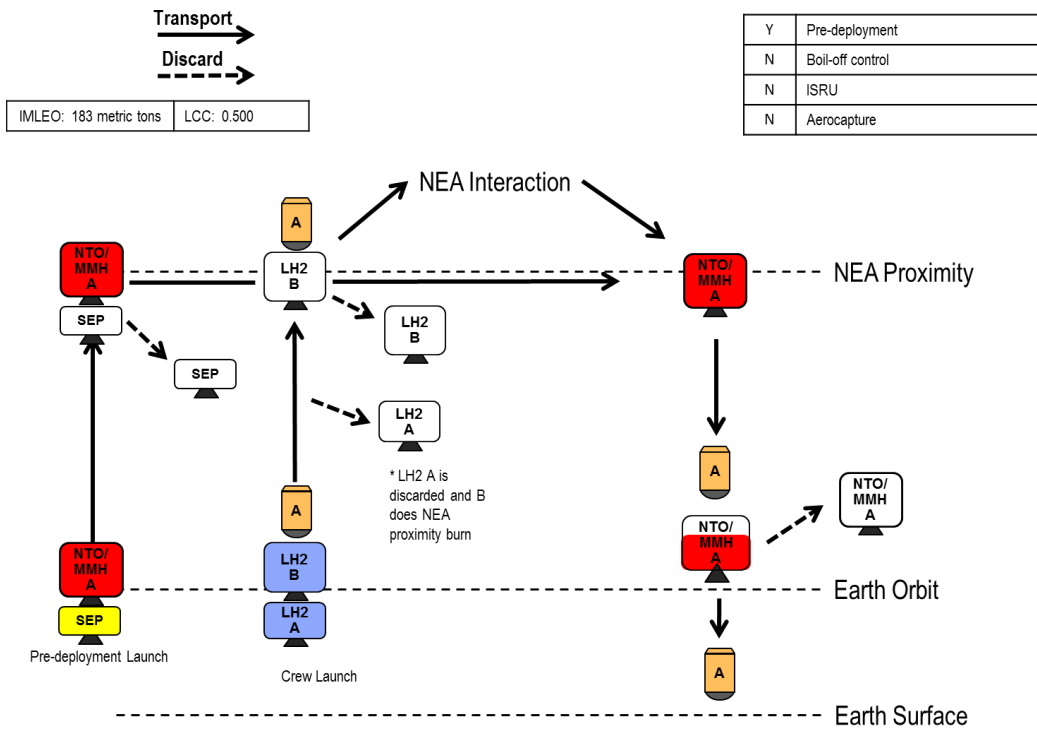


Figure 96: Low-Energy NEA Minimum LCC BAT Chart

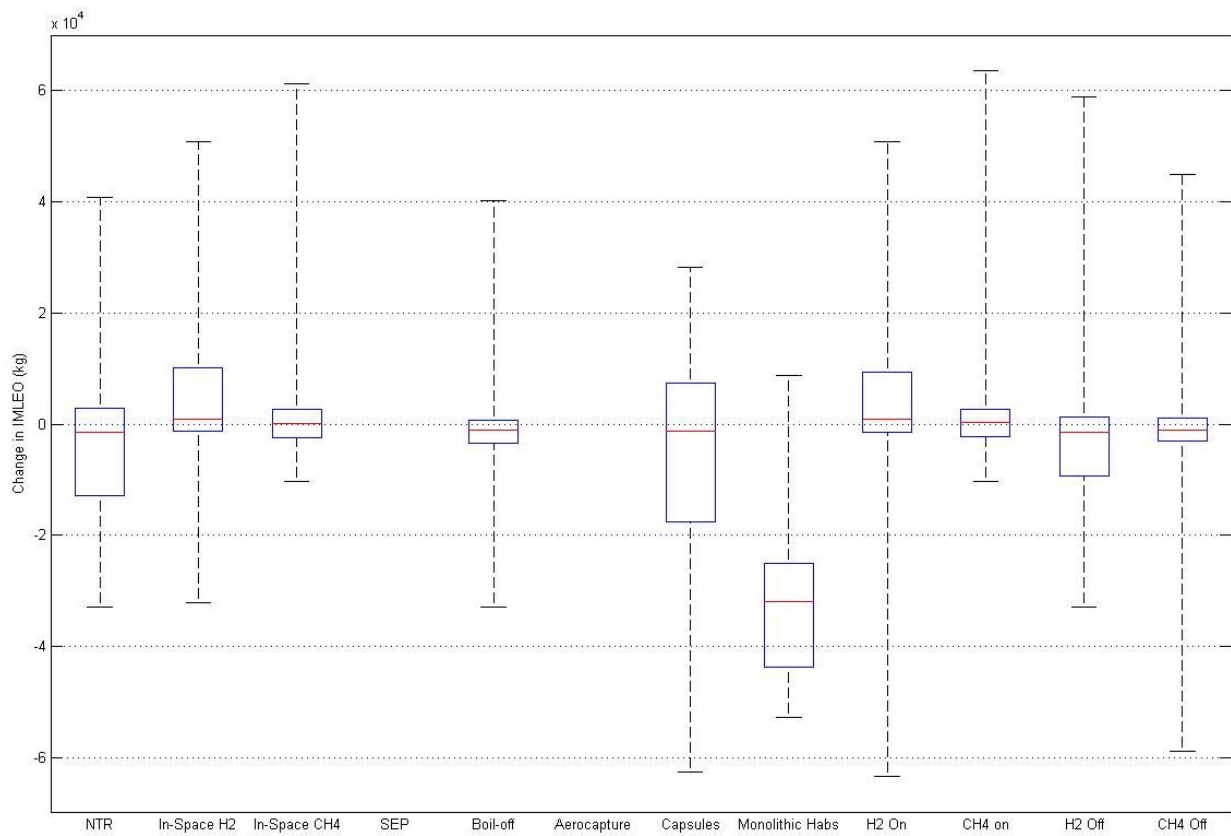


Figure 97: Low-Energy NEA Feature Switch Box Plots

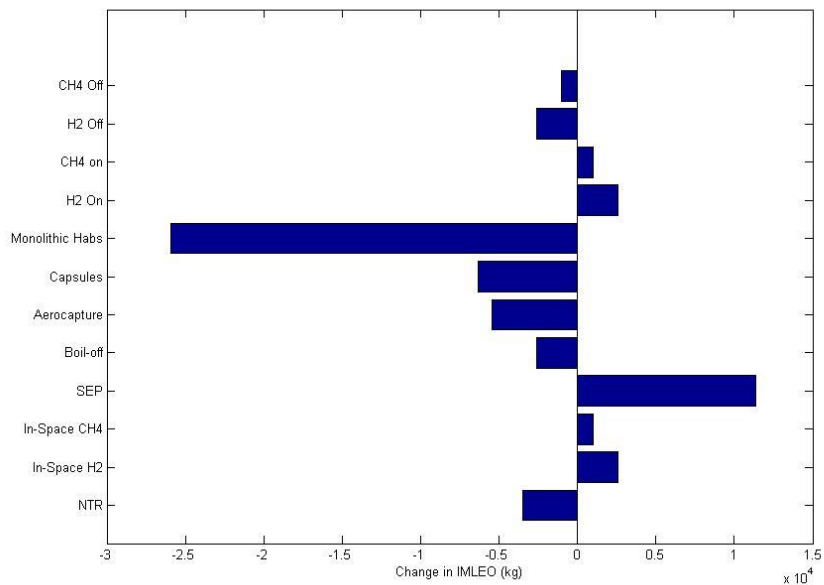


Figure 98: Low-Energy NEA Feature TIM Chart

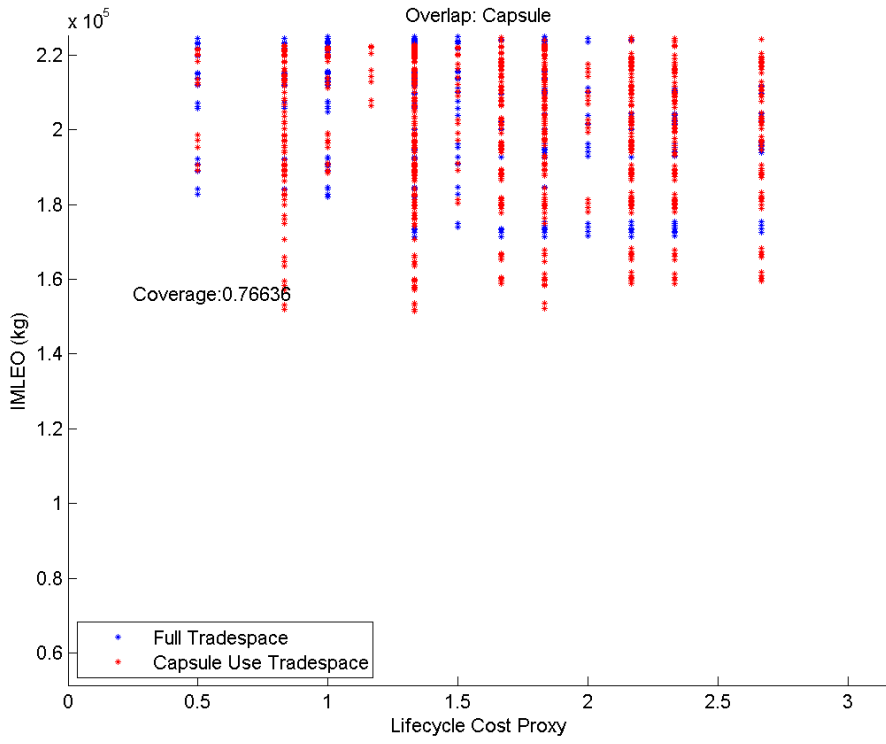


Figure 99: Low-Energy NEA Capsule Tradespace Coverage

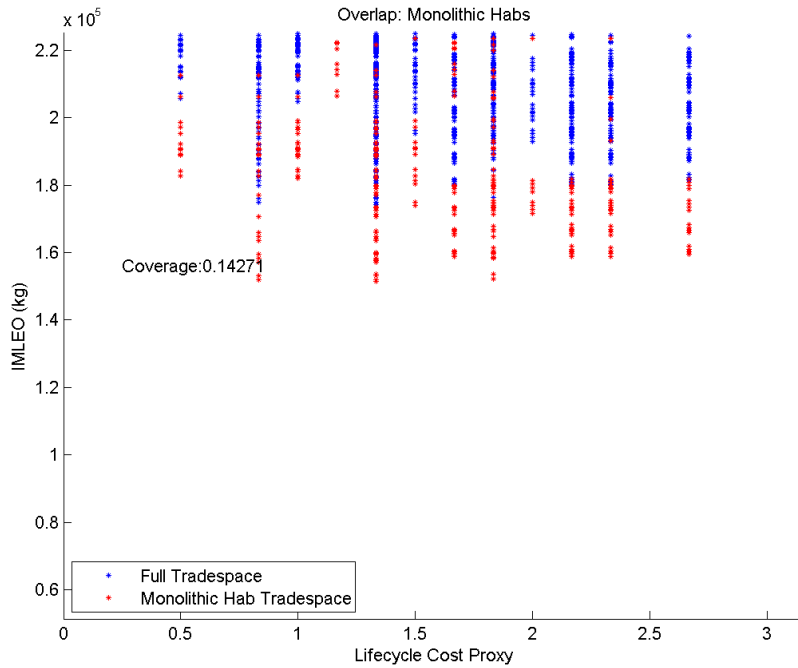


Figure 100: Low-Energy NEA Semi-Monolithic Habitat Coverage

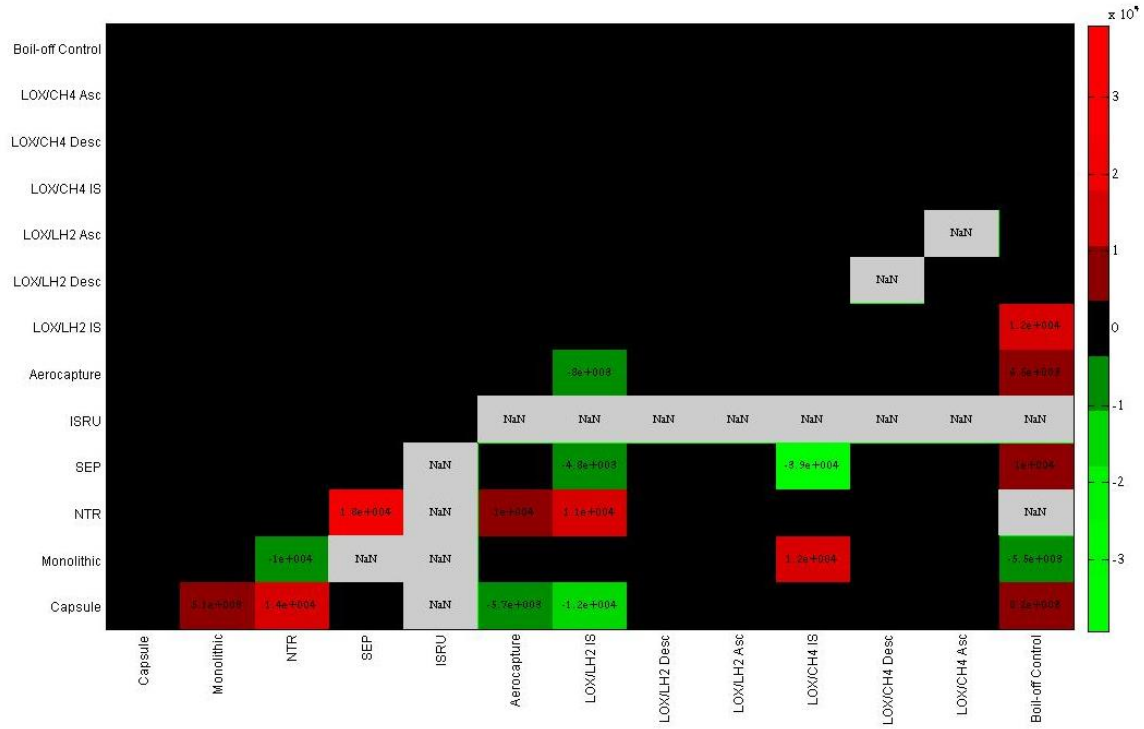


Figure 101: Low-Energy NEA TCIM

B-3: High Energy NEA Results

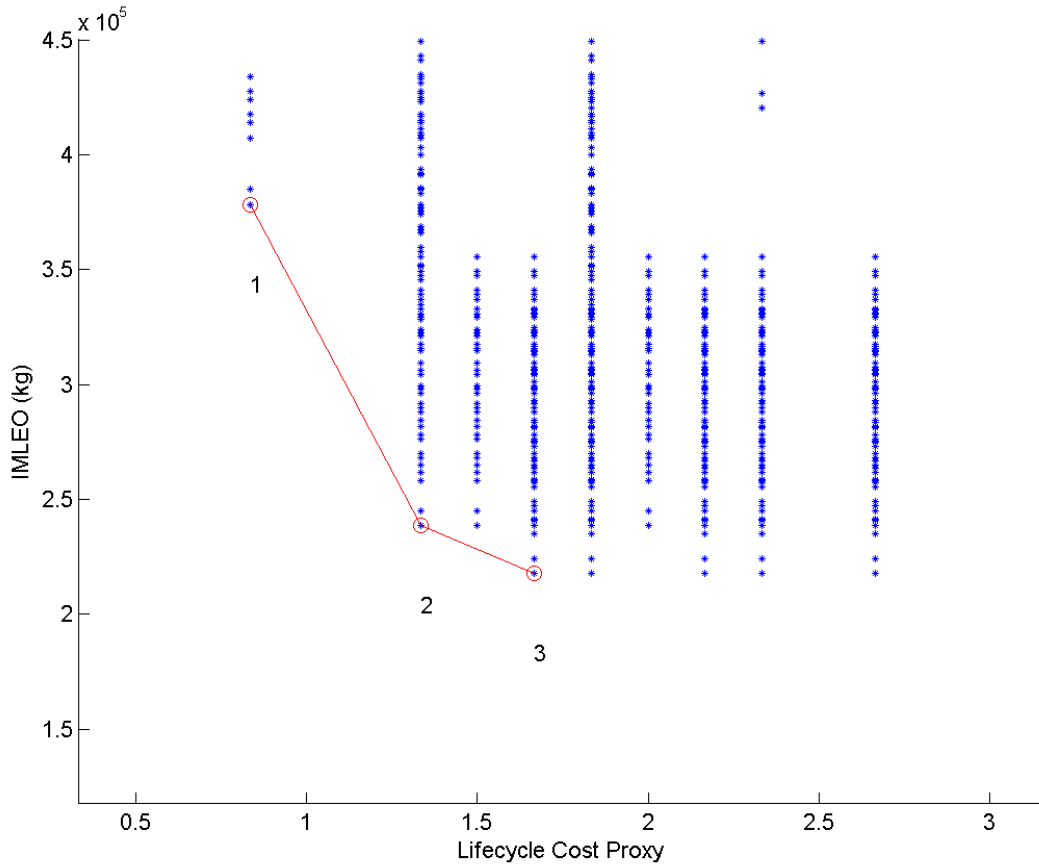


Figure 102: High-Energy NEA Tradespace

Table 45: High-Energy NEA Non-Dominated Architecture Features

	IMLEO (kg)	LCC	SEP	Aerocapture	Boil-Off
Arch. 1	378400	0.833	No	Yes	No
Arch. 2	238580	1.333	Yes	No	Yes
Arch. 3	217850	1.667	Yes	Yes	Yes

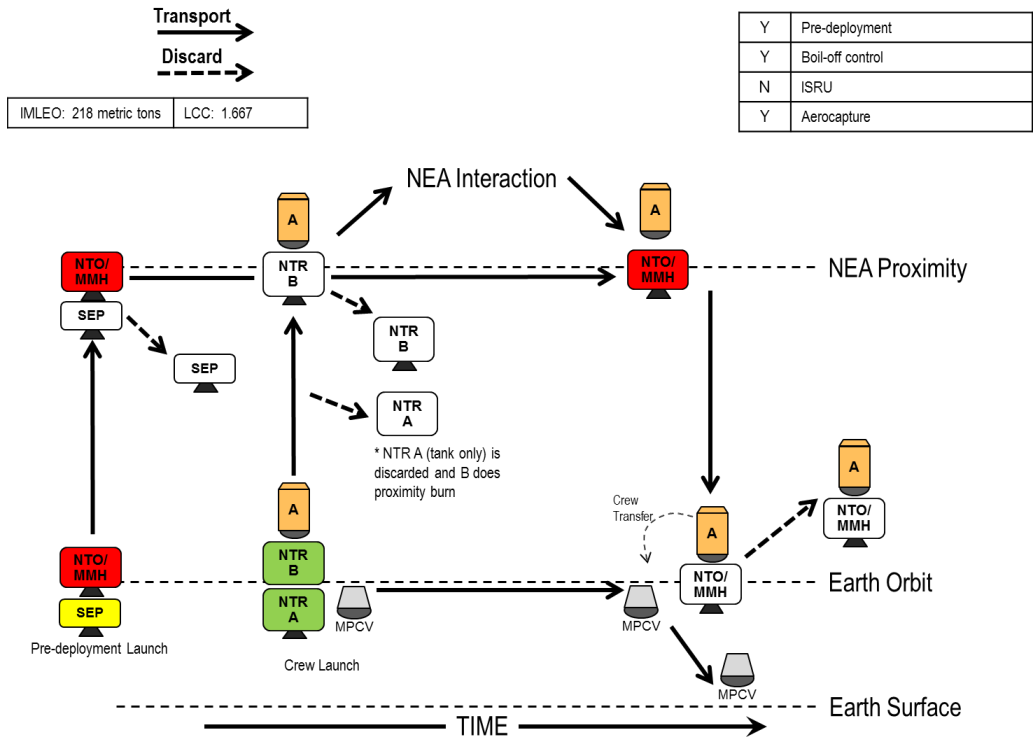


Figure 103: High-Energy NEA Minimum IMLEO BAT Chart

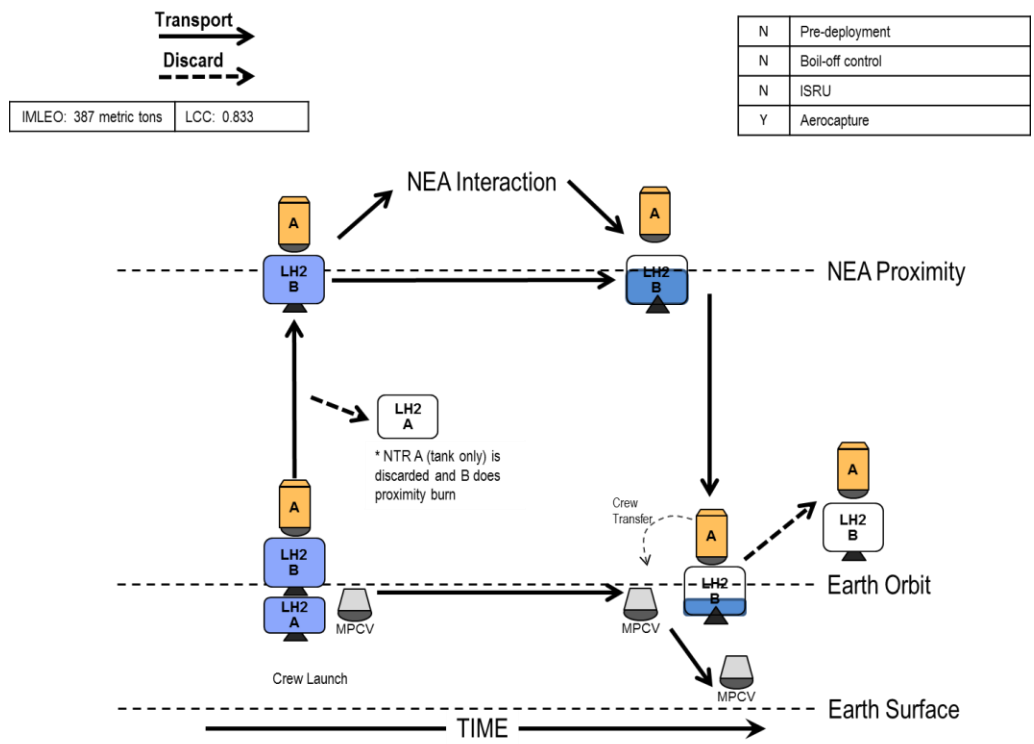


Figure 104: High-Energy NEA Minimum LCC BAT Chart

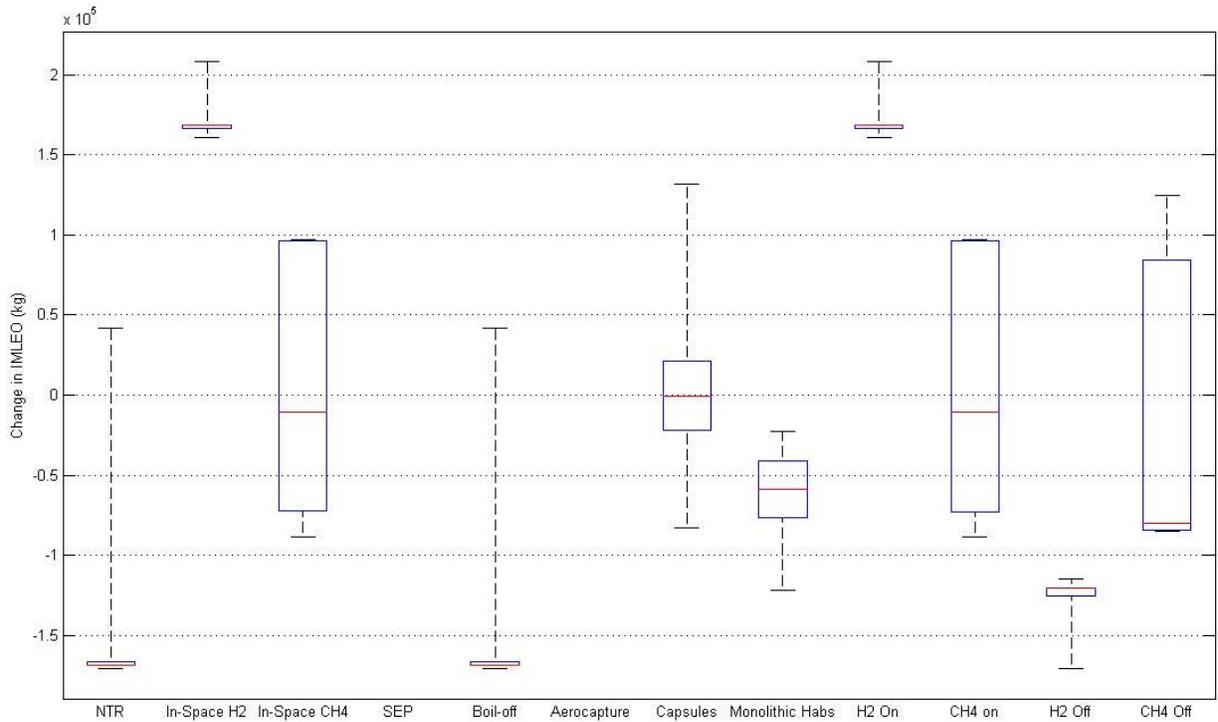


Figure 105: High-Energy NEA Feature Switch Box Plots

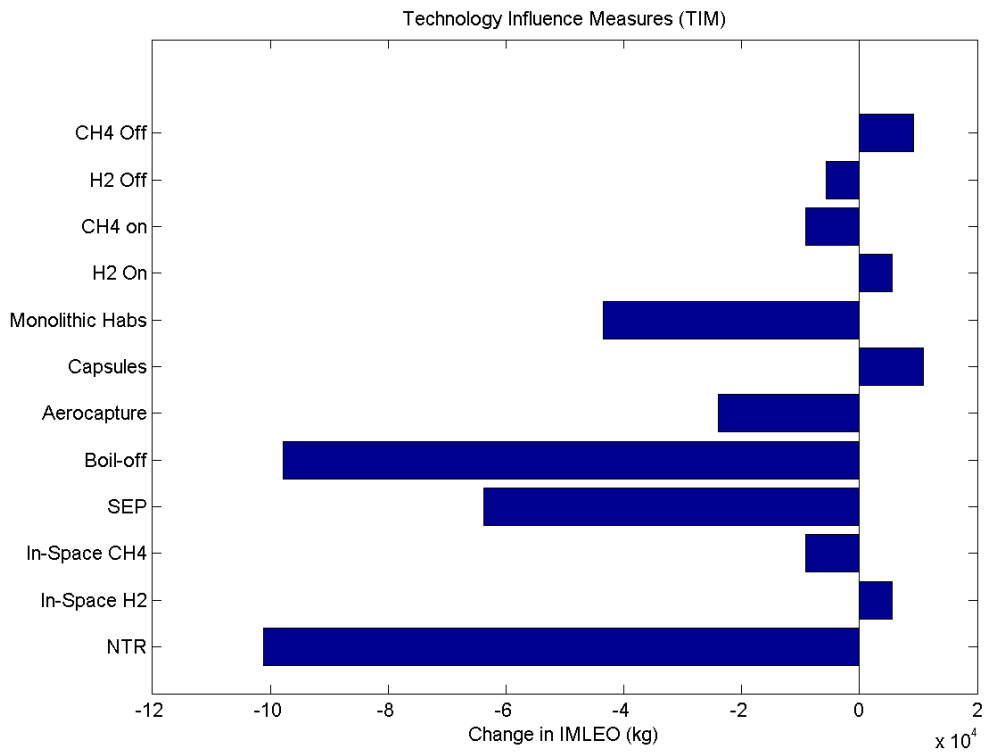


Figure 106: High-Energy NEA Feature TIM Chart

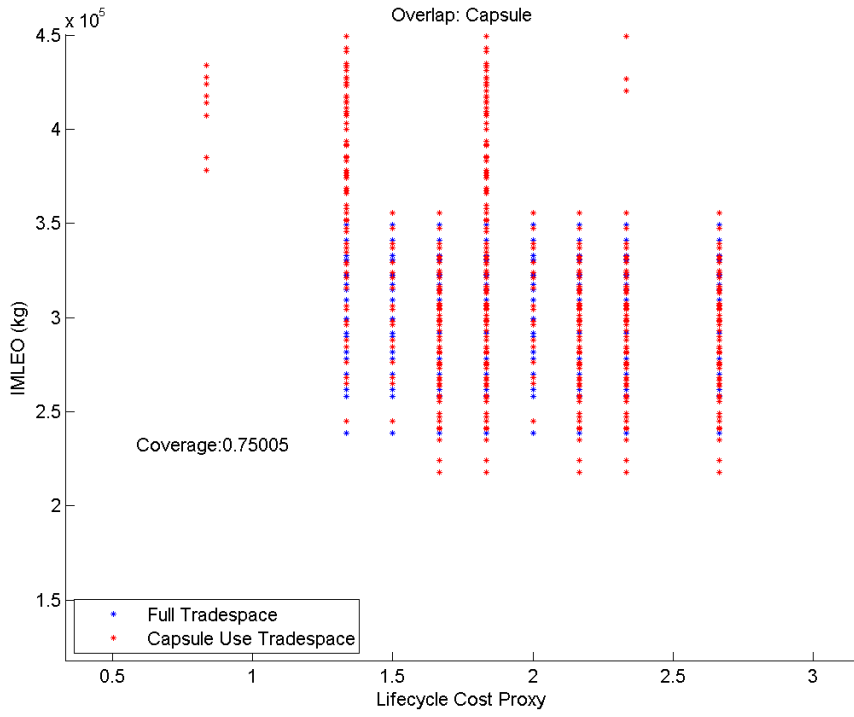


Figure 107: High-Energy NEA Capsule Coverage

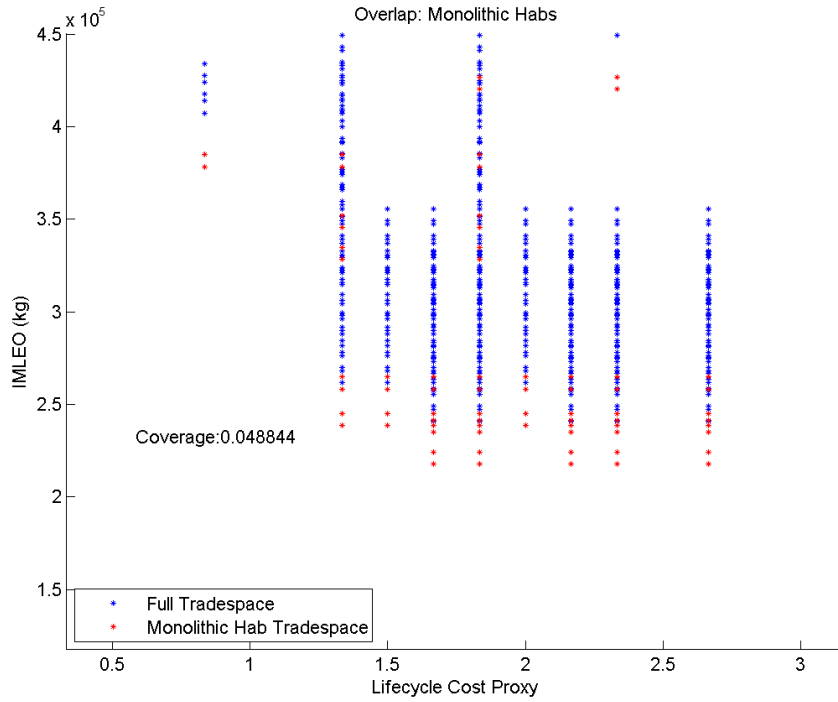


Figure 108: High-Energy NEA Semi-Monolithic Habitat Coverage

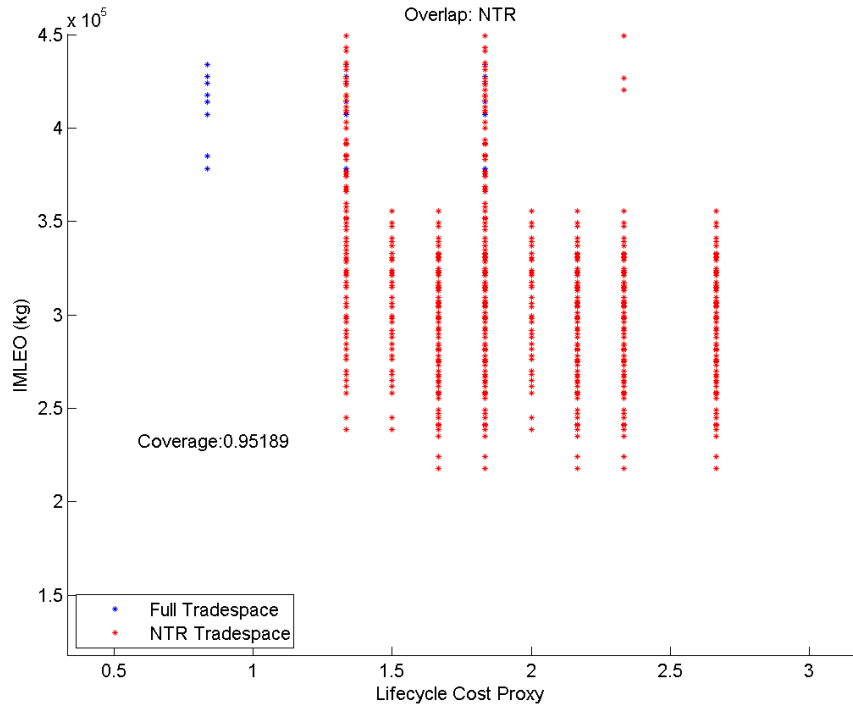


Figure 109: High-Energy NEA NTR Coverage

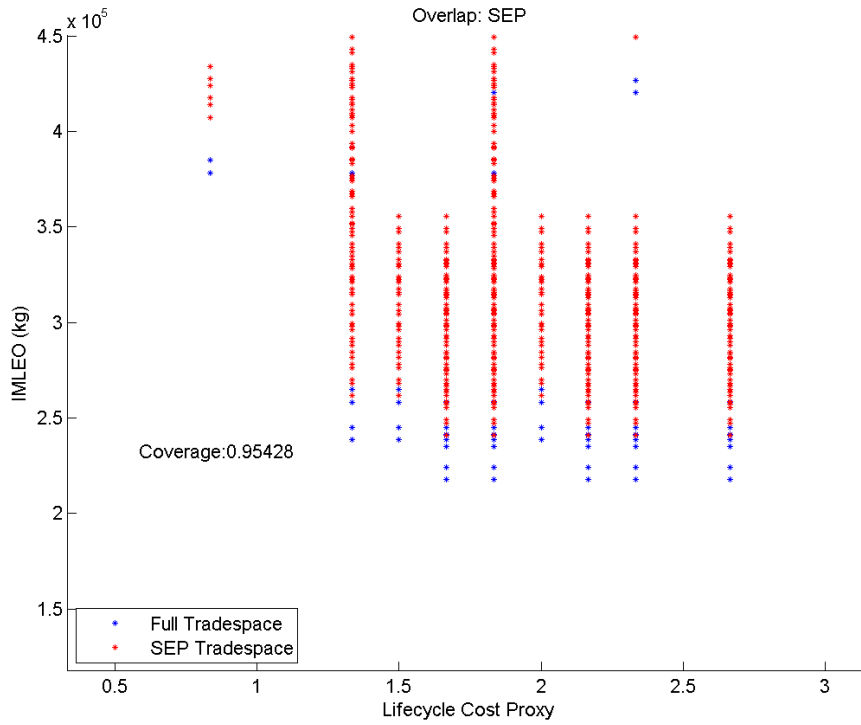


Figure 110: High-Energy NEA SEP Pre-Deployment Coverage

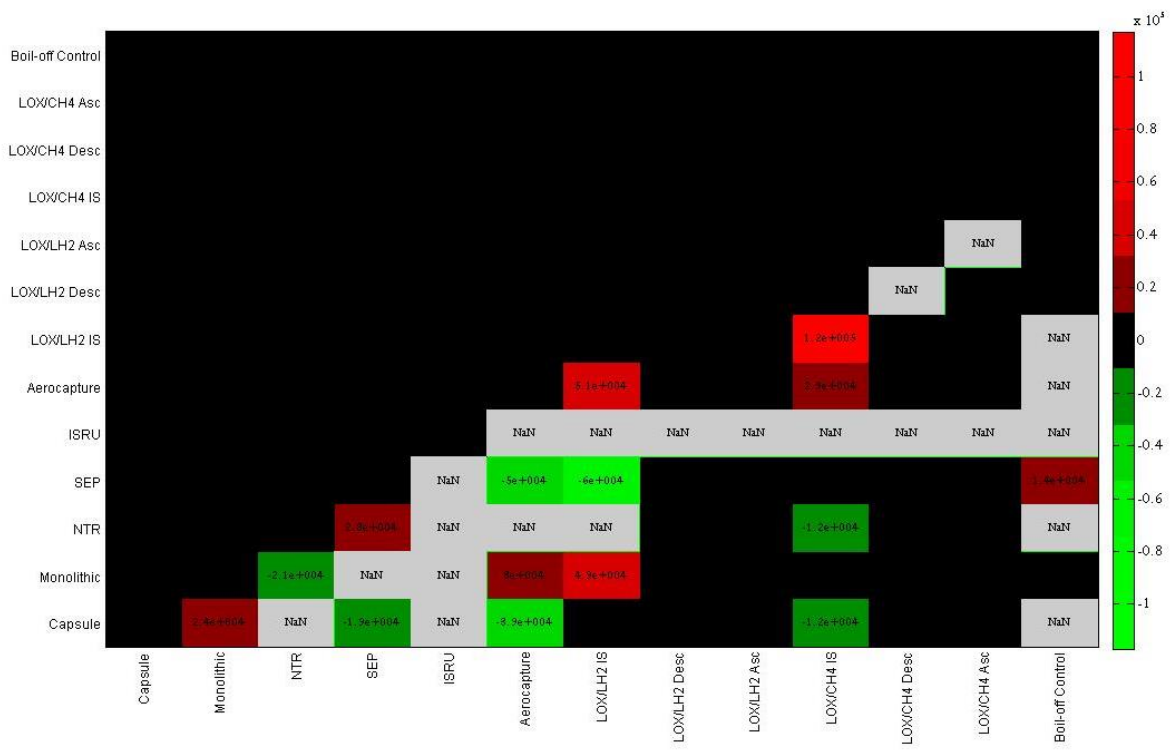


Figure 111: High-Energy NEA Feature TCIM